MANUFACTURING OF HUMAN MESENCHYMAL STEM CELLS: THE ANALYTICAL CHALLENGES

Emma Neale-Edwards, BSc (Hons), MSc

Thesis submitted to Loughborough University for the degree of Doctor of Philosophy

May 2018

Abstract

It has been repeatedly proven that cell therapies can address many current unmet clinical treatment needs and also improve on current treatment options for various diseases, from neurological disorders to bone repair (Rosset et al. 2014; Corey et al. 2017). Though the potential of cell therapies has been demonstrated at a relatively small scale, the realisation of bringing cell based treatments to a larger market is hindered by the complexity of the product along with safety concerned and high production cost. Safety concerns can be informed with more in-depth analytical analysis of the product, however this in turn increase the costs involved in producing a cell therapy (Davie et al. 2012). Consequently the cost of analytical techniques also needs to be reduced, to address this need the area of microfluidic based bioanalytics holds much promise (Titmarsh et al. 2014).

The culturing of human mesenchymal stem cells (hMSC) was used as a proof of concept model to demonstrate where improved bioanalytical and bioassay methods could be utilised in the production of cell therapies. Cells from four donors were cultured under three different oxygen environments and the conditioned medium assessed for pro-angiogenic capabilities using a tube formation bioassay and a proportion of the cytokine secretome profile measured using Luminex technology.

Thorough secretome analysis it was shown that predicting cytokine levels based solely on the donor was not possible as the handling of the cells also had an influence on the secretome profile. The donor expression profiles did not behave in the same manner across all oxygen environments, for example in some donors IL-8 levels increased per cell at lower oxygen where as other donors showed a decrease per cell. While the tube formation assay showed some differences between donors in pro-angiogenic capabilities it also highlights the challenges with interpreting large data sets.

The feasibility of using a microcapillary film (MCF) based enzyme-linked immunosorbent assay (ELISA) to detected two relevant cytokines, IL-8 and hepatocyte growth factor (HGF) was investigated. Following on from this work the development of a combined MCF ELISA assay with hMSC cell culture to produce a fully closed cell screening system was initiated. It was shown that it was feasible to

measure IL-8 and HGF using the MCF ELISA platform but further work would need to be done to make the system more compatible with the manufacturing environment. In order to adapt the MCF to also be an hMSC culture platform the first challenge was to functionalise the Fluorinated Ethylene Propylene (FEP) surface of the MCF. It was concluded that a poly (vinyl- alcohol) (PVA) and gelatin mixture produced a homogenous coating to which a consistent level of hMSC would attach. This work was carried out on a flat surface; therefore steps were taken to adapt this knowledge into the MCF, while there was evidence of hMSCs present inside the MCF more work will need to be done to bring this concept to an established platform.

Acknowledgements

I would first like to thank Loughborough University graduate school and the Centre of Doctoral training for giving me the opportunity to undertake the PhD program. I would also like to the Centre of Biological Engineering where I have been based for the majority of the PhD program, not only was I privileged to work in such a fantastic facility but I also worked with some amazing and talented researchers during my time there. I would also like to thank Dr Karen Coopman and Dr Nuno Reis for supervising this PhD. Dr Coopman has also acted as a fantastic role model and mentor providing many words of wisdom and emotional support during this turbulent journey and has played a significant role in shaping my future.

The support and guidance I have received from the professors, lectures, post-doctoral researchers and support staff with in the Centre of Biological Engineering has shaped the researcher I have become today and for that I will be forever grateful. In particular I am deeply grateful to Dr Andrew Picken and Dr Petra Hanga for making time to mentor me and being there through my whole journey. Jennifer Bowdrey who not only supported me with my laboratory work but was there for me whenever I needed her and has continued to be there even after I have left. Dr Katie Glen and Dr Elizabeth Radcliff who along with Dr Coopman have been excellent female role models for me as young female researcher at the beginning of my career.

A massive thank you to my fellow PhD students with whom I have shared the ups and downs of this PhD journey, we have celebrated the highs together and picked each other up off the floor during the lows. In particular my work hubby Dr Alex Chan, Preeti Holland, Matthew Worrallo, Maaria Ginai and Katherine Pitrolino this experience has bonded us forever and I hope we will be lifelong friends.

I would like to thank my friends and family who have all been so understanding during this time. Jamy, the gang and little Luca who have put a smile on my face and listened to me when I have needed it most and continue to do so.

This journey may never have started if it was not for the most important person in my life, my husband, Daniel Ratzinger. With the stress and the pressure a PhD brings with it we have come through stronger as a couple, I am very lucky to have you by my side.

Papers and presentations

In process

Neale-Edwards, E.C., Crooper, P., Coopman, K., Reis, N.M., Surface Functionalization of FEP-Teflon® for Adhesion and Growth of Human Mesenchymal Stem Cells.

Poster representations

2nd-3rd June 2016, Bioprocessing of Advanced Cellular Therapies Congress, London, UK

Oral presentations

8th July 2016, Regenerative Medicine conference, Manchester, United Kingdom: *Assay Development for the Scale up of Cell Therapy Manufacturing*

Table of Contents

Table of Figures

Table of Tables

List of abbreviations

aFGF	Acidic fibroblast growth factor
ANOVA	Analysis of variance
ATMPs	Advanced therapy medicinal products
CBER	Center for biologics evaluation and research
CQA	Critical quality attributes
CTP	Cell therapy products
ECM	Extracellular matrix
ECs	Endothelial cells
ELISA	Enzyme-linked immunosorbent assay
EMA	European medicines agency
EVOH	Ethylene vinyl alcohol
FACS	Fluorescence-activated cell sorting
FBS	Fetal bovine serum
FDA	Food and drug administration
FEP	Fluorinated ethylene propylene
FGF	Fibroblast growth factor
FGF-Basic	Basic fibroblast growth factor
GMP	Good manufacturing practice
GVHD	Graft verses host diseases
hESC	Human embryonic stem cells
HGF	Hepatocyte growth factor
hHSC	Human hematopoietic stem cells

hMSC	Human mesenchymal stem cell
hRPE	Human retinal pigment epithelium
HRP	Horseradish peroxidase
HUVECs	Human umbilical vein endothelial cells
IGF-1R	Insulin-like growth factor 1 receptor
IL-8	Interleukin 8
iPSC	Induced pluripotent stem cells
LOD	Limit of detection
MCF	Microcapillary film
MFD	Microcapillary flow disc
MOA	Mode of action
PAT	Process analytical technology
PBS	Phosphate buffered saline
PDGF	Platelet-derived growth factor
PIGF	Placental growth factor
PVA	Poly (vinyl alcohol)
RPE	Retinal pigment epithelium
SCs	Stalk cells
TCs	Tip cells
TGF-β	Transforming growth factor beta
UK	United Kingdom
US	United States
UV	Ultra violet
VEGF	Vascular endothelial growth factor

WC   Whole cells

1 Introduction

1.1 Introduction

There is an ever increasing demand for new clinical treatment options resulting in the healthcare industry needing to continually develop safe, effective and affordable therapies (FDA 2004). Manufacturers, scientists and engineers are looking to regenerative medicine to provide more permanent solutions to these challenges, and reduce the reliance of healthcare systems on long term or lifetime drug treatment regimes. Regenerative medicine includes tissue engineering, gene therapy, stem cell treatments, and cellular products, all of which are of great clinical importance and hold much promise for the future of healthcare (Halme & Kessler 2006; Trounson et al. 2011). Within this work, cell therapies, in particular human mesenchymal stem cell (hMSC) therapies, and the challenges of bringing them to the healthcare market are examined from the perspective of satisfying regulatory requirements, ensuring product quality and product safety during the expansion phase for the production of cell therapies. Cell based assays and bioanalytical technologies are particularly important in the development of cell therapies and overcoming challenges unique to this field. Treatments predominantly involve administering live cells into a patient, thus it is essential that the identity, quality and function of the cells is fully established before delivery (Bravery et al. 2013; Carlos Polanco et al. 2013). From a cost-effective manufacturing perspective, the function of the cells needs to be determined not only in early upstream isolation and culture, but continuously monitored throughout every processing stage up to delivery. There are also treatments using cell therapy products (CTP) whereby a mixed or single population of cell type(s) produce a complex cocktail of biomolecules which can be used as the therapy (Ranganath et al. 2012). Being able to characterise the product that will be administered to a patient is a critical parameter in therapeutic safety, that requires the use of bioassays and bioanalytical techniques (Gronthos 2003; Ocampo et al. 2007).

Bioanalytics refers to the methods used to quantify drugs, drug metabolites and biomarkers (Food and Drug Administration 2013). The field utilizes a number of different platforms including chromatography, mass spectrometry, enzyme mediated

assays, genetic analysis and electrophoretic techniques. In contrast, bioassays are methods used to analyse the effect of a product, drug or cell therapy on a population of cultured cells (Ma et al. 2015). Combining methods within the two fields would create powerful tools that enable safe, efficacious cell therapies to be brought to the market and would help reduce the cost and risk associated with cell therapies and scalable production (Scheper et al. 1999; Brindley et al. 2011).

The work presented here identifies some of the challenges facing the regenerative medicine industry in taking hMSC therapies to the clinic and develops methods to begin addressing these. For example, there are many conditions for which hMSCs are being used as a treatment; these range from autoimmune disease to restoring neurological functions and re-establishing blood supplies in damaged or implanted tissues. Therefor there is a need to establish if every population of cells identified as hMSCs can effectively treat such a range of pathophysiologies. While improvements in process control can counteract some of these issues of cell expansion the manufacturing environment may need to adapt a more responsive approach to the hMSC behaviour during culture. To provide increased flexibility and responsiveness within the manufacturing of hMSC, more rapid and at line or online bioanalytics and bioassays need to be developed. In the first instance it must be established where these methods are required, what and where the changes in hMSC functionality are, including protein secretion, and what are the parameters the culture needs to meet. Once these parameters have been established, the field of microfluidics can meet the need of more rapid bioanalytical methods. Microfluidics reduces the scale at which standard bioanalytical testing is carried out, this not only reduces the time and cost of product analysis but has also been shown to improve sensitivity in some devices (Xiong et al. 2014).

2 Literature Review

2.1 Regenerative medicine

With the increasing demands placed on healthcare attributed to the rising and aging population classic pharmaceutical and surgical treatment approaches have a limit (World Health Organization 2015). Chronic conditions such as diabetes require a lifetime of medication, which is costly to a healthcare system as well as the disease having wider socio-economic implications such as loss of work days due to associated illnesses (Jonsson 1998; Tunceli et al. 2005; Dall et al 2008). There are also many conditions for which there are limited or no existing treatment which amounts to a lower quality of life or end of life for the patient. Fortunately, with the expanding field of regenerative medicine, scientists and clinicians are exploring and developing new treatment options with long-term efficacy as an alternative to a lifetime of medication (Fodor et al. 2003; George 2011). There is a lot of different terminology used for these treatments, though regulatory bodies refer to them as human cell-based medicinal products (European Medicines Agency 2008). Regenerative medicine comprises of tissue engineering, gene therapy, cell therapy and stem-cell based therapy (Kellathur & Lou 2012; Pfeifer & Verma 2003; Mason et al. 2011). The main objective of these treatments is to use the cells to restore normal function to the affected organ or tissue minimising or completely omitting the long term reliance on medication and improving the quality of life (Mason & Dunnill 2008). The concept of restoring bodily function is not new. Transplanting living cells from either within the same patient (e.g. skin grafts) or from a donor into a recipient (e.g. bone marrow transplants, blood infusion, organ transplants) are common practice in the healthcare field. The main challenge with donor transplants is that the demand for donated tissue is greater than the supply (Kirouac & Zandstra 2008) with many patients dying while on the waiting list (Dutkowski et al. 2015). There are also genetic diseases which can only be managed as opposed to cured, even with tissue replacement and long-term medication the only way to completely cure is to target the underlying cause using gene therapy.

Gene therapies comprise of recombinant nucleic acids being administered to a human in order to have a therapeutic effect. This can include inserting a new nucleic acid

sequence, deleting, repairing or replacing a nucleic acid sequence, the cells can be modified *in vivo* or *ex vivo* and the transplanted into the patient (Wirth et al. 2013). The currently used application of gene therapy is the treatment of individuals with genetic disease such as Huntington's disease (Wild & Tabrizi 2014) and muscular dystrophies (Bengtsson et al. 2016). Based on data from The Journal of Gene Medicine's, Gene Therapy Clinical Trials Worldwide website (http://www.wiley.co.uk/genmed/clinical) 1178 gene therapy clinical trials have been granted approval worldwide in the past 10 years (2006- August 2016) and the total number of gene therapy clinical trials that have been granted approval worldwide is 2409. Of 2409 approved trials 91 to phase III (i.e. 3.9% of the total), only 3 to phase IV and a mere 0.1% have been marketed. In comparison the Food and Drug Administration (FDA) approved 108 novel drugs between 2014-2016 alone (FDA 2014; FDA 2015; FDA 2016). A challenge of gene therapies is the delivering of the recombinant sequence to the cells, there are the standard efficacy issues which are recognised in the molecular biology area but there are also important safety concerns. Many gene therapies use viral vectors as a delivery mechanism which is preferable as viruses are more efficient at delivering the nucleic acids; there are concerns about being able to control the viral vector. Incidences such as patients suffering from Leukaemia following treatment with a retroviral vector, although the treatment was successful (Yi et al. 2005).

While gene therapies can treat disease with genetic defects they cannot help where whole organs or tissues need to be replaced. This is the remit of tissue engineering and cell therapies. Tissue engineering focusing on growing whole tissues *in vitro* which may be formed of more than one cell type and require a structure similar or the same to the tissue it is replacing. There is also a demand for tissue engineering to provide human models for research use with the long-term goal to replace or reduce the use of animals in drug testing. By having a tissue model which is made from human cells the model is also more relevant to the end user of the drug or treatment which has historically been a criticism of using animal models in the development of treatments for humans (Holmes et al. 2009). Animal models have different physiology and genetic to humans, therefore data collected based on animal models may not always be applicable to humans. In addition to the relevance of animal models there are also the ethical concerns as studies may induce pain and suffering to the animal

subjects, and the premature termination of life (Levy 2012). With the great potential of regenerative medicine there is still no routine treatment using stem cells (Badylak & Rosenthal 2017), the barriers to market include cost, safety concerns and feasibility of treating large patient numbers.

2.2 Cell Therapies

The use of human cells to replace or repair damaged or diseased tissue provides treatment options for conditions ranging from cancers (Jorgensen et al. 2003; Lipowska-Bhalla et al. 2012), neurodegenerative diseases (Lindvall et al. 2004; Oh & Choo 2006) and autoimmune diseases (Jorgensen et al. 2003; Corcione et al. 2006; Gieseke et al. 2010) to full organ replacement (Sharma et al. 2010). As the field has advanced it has become clear that a multidisciplinary approach is required. The complexity of the treatments, controlling and understanding the interactions of the cell therapy *in vivo* coupled with providing a robust supply chain meets this need (Badylak & Rosenthal 2017). For example, cells are not only used as physical replacements of damaged tissue but their mode of action (MOA) may instead be to control and enhance innate biological processes to treat disease. This takes advantage of a normal behaviour for a cell type (e.g. secretion of particular proteins) and applies the behaviour to a different tissue of disease. Human mesenchymal stem cells (hMSCs) are a prime example as they have been shown to not only be used in whole cell replacements therapies but also to invoke or regulate a number of biological processes discussed in Section2.6.1.

Broadly, cell therapies can be split into autologous or allogenic treatments and can represent various stages of cell linage commitment (Jones et al. 2012). Human embryonic stem cells (hESC) and induced pluripotent stem cells (iPSC) have unlimited self-renewal capacity and are pluripotent meaning they have the capacity to differentiate down any of the linage pathways (Takahashi et al. 2007). Multipotent stem cells have a more limited differentiation and self-renewal capacity compared to pluripotent stem cells. Multipotent stem cells include human hematopoietic stem cells (hHSC) and hMSCs. Any cell type found in the human body can, at least theoretically, be used for an autologous cell therapy. Due to the source and nature of hESC, treatments using from this cell type will always be allogenic.

Autologous therapies have a minimal risk of invoking an immune reactions to the treatment as the treatment uses the patients' own cells as the starting product thus it should not be required for the patient to take immune suppression medication (Bang et al. 2005). The use of autologous treatments can be limit due to the diseased state of the patient, for example if a patient has bladder disease healthy cell must be available to extract and there is also a risk of the disease reoccurring by using a cell population from a tissue which has already been diseased (Atala et al. 2006). Thus, all treatment options need to be explored including careful consideration of the tissue source and cell type for autologous therapies. The tissue source and cell type are not mutually exclusive for example hMSCs have been extracted from bone marrow, dental pulp and adipose tissue (Barry & Murphy 2004; Collart-Dutilleul et al. 2014). The removal of patients' teeth to extract hMSCs is not ideal as adult teeth do not self-renew, however it may not be in the best interest of the patient to undergo a bone marrow aspirate procedure. These factors need to be considered when developing sustainable cell therapy treatments.

The use of undifferentiated cells provides a greater number of treatment options but gives rise to more functional and safety concerns compared to treatments using differentiated cells. These concerns are mostly related to the use of iPS and hESC but some issues are also applicable to multipotent stem cells. Tumorgenesis is a major hurdle for pluripotent cell therapies, resulting in the use of undifferentiated iPS or hESC directly as a treatment unsafe (Lee et al. 2013). Subsequently pluripotent, and in some cases multipotent stem cells, need to be directed down a differentiation pathway *ex vivo* to produce the cell type required for the intended treatment. Stem cell differentiation *in vitro* can be achieved by using biochemical signalling and some work has suggested mechanical stimulation can also instigate differentiation (Toma et al. 2001; Reilly 2010). From a treatment perspective, the cells administered need to be characterised to be able to quantify how much of the cell population are the intended cell type required for the treatment.

A branch of cell therapies which is gaining momentum within the field is the development of cell therapy products (CTP). CTP use the protein molecules or exosomes produced by cells as a treatment as opposed to treating a patient with whole cells (WC), this overcomes some of the previously mentioned issues in terms of safety and characterisation of WCs. One of the mechanisms by which cell therapies

are shown to work is though stimulating the body's innate signalling cascades to heal and regrow damaged tissue. The MOA of the molecules produced by the cells may invoke different responses depending on which tissue type the CTP is administered to. For example, hMSCs are being used to regulate immune responses in patients with graft versus host diseases (GVHD) and for tissue ischemia (Yañez et al. 2006; Russo et al. 2014). The possibility of invoking the same *in vivo* response by culturing the cell *in vitro* and administering the enriched culture medium negates the WC safety issue, however this treatment may need to be administered multiple times if the MOA in not self-sustained. The CTP would also need to be screened for adverse effects as with any standard pharmaceutical drug but would provide a more complex cocktail of molecules which would simplify a treatment as opposed to artificially making the same molecule cocktail. Characterisation of a cell therapy medicinal product including WC and CTP a regulatory requirement is part of the regulatory frame work governing the use of cell therapies in the clinic (Pellegrini et al. 2014).

The area of regenerative medicine and cell therapies holds much promise, but the question needs to be asked as to what the barriers are in bringing these treatments into the main stream healthcare systems around the world. In each branch of regenerative medicine there are some common challenges. Most importantly safety, which is the reason for the development of detailed regulatory frameworks (Pearce et al. 2014). Many of the cell based treatments developed have been established on a small scale; therefore in order to meet the demand of these treatments there is the challenge of scaling up these treatments with a robust, reliable and cost effective manufacturing process while meeting the requirements of a fit for human use product (Hambor J.E 2012). There is a clear requirement for the standardisation of these processes. The FDA gave their perspective on this, highlighting the amount of diversity seen between clinical trial application for MSC therapies. Most notably the diversity in cell source, culturing methods and lack of continuity in bioactivity characterisation (Mendicino et al. 2014). The concept of personalised medicine also needs to be taken into consideration when discussing standardisation of cell therapies. Personalised medicine is a term used to decided tailoring a treatment or therapy to the patient needs as opposed to solely the disease (Vogenberg et al. 2010). However classic pharmaceuticals and biologics are still manufactured to a specific standard, but the combination of products, dosage and dosing regimens can be tailored to a specific

patient. Cell therapies are more complex and therefore the process of standardising them may need to be more adaptive, by which the patients physiological state dictates the standards a cell therapy needs to meet. In order to overcome these barriers there is a key need to have the infrastructure to support these challenges and to take a more multidisciplinary approach to achieve progress. In the United Kingdom (UK) for example the government funded Cell and Gene Therapy Catapult was formed to help support the commercialisation of cell and gene therapies (Gardner & Webster 2017). The Cell and Gene Therapy Catapult is therefore able to provide not only support to researchers and companies in the area of regenerative medicine but is also able to facilitate harmonisation within the field.

2.3 Cell therapy manufacturing

The principal objectives of cell therapies and CTP are to deliver improved and long term treatments which are safe, well defined and efficacious in a timely manner, ensuring they have been fully tested for quality, quantity and potency (Goldring et al. 2011; Rayment & Williams 2010; Carmen et al. 2012). These tasks are even more challenging when dealing with such a complex material as live human cells and defining CTP. With demands of up to 10^9 cells/dose there are challenges in maintaining quality and quantity of the cell product in scale up environment (Ratcliffe et al. 2011; Simaria et al. 2014). As briefly mentioned, within cell therapies the starting material can be a matured cell source such as chondrocytes used in cartilage regeneration (Bhosale et al. 2007), or stem cells which have to potential to be directed into certain cell types depending on the type of stem cell and multi-lineage potential (Pittenger 1999; Baharvand et al. 2008; Yu et al. 2012). As the treatment options can potentially be autologous or allogenic, the different combinations of autologous or allogenic and differentiated or undifferentiated cells present, independently, some unique challenges.

2.3.1 Autologous vs allogeneic cell therapies

From an immune system perspective, autologous cells have an advantage over allogenic cells; however, this limits the source of starting material and makes the material more precious, as cells can only be obtained from the patient who is receiving the end product. In turn it becomes even more paramount to have an

efficient and reliable scale up/scale out process as there is minimal room for error because of the finite and usually minimal amount of starting material. For example a 10ml bone marrow aspirate was required for an hMSC treatment for osteonecrosis, from this aspirate and after a two week culture period 2×10^6 hMSCs were harvested (Zhao et al. 2012). This issue can also be further compounded if the starting material has limited self-renewal capacity as it therefore needs to be determined if it is possible to achieve the cell numbers required for a treatment from the starting material. hMSCs are known to have a limited renewal capacity for example it has been shown that hMSCs from the bone marrow enter senescence after 7 passages tough this varies depending on tissue source and patient age (Lu et al. 2006). Other studies demand higher cell numbers which require a stable supply of cells such as a hMSC treatment for Crohn's disease which required $1-2 \times 10^6$ cells/kg body weight and each patient (10 patients in total) required two infusions 7 days apart (Duijvestein et al. 2010). Determining renewal capacity of a cell type or population is also an issue for other cell types, there is some debate regarding the extent of the self-renewal capacity of hematopoietic stem cells as much variation has been seen within this cell type (Eaves 2015). This presents some challenges as growth characterisation is a regulatory requirement (British Standards Institution 2011) .Pluripotent stem cells such as hESC (Oh & Choo 2006), have the potential to differentiate into multiple cell types and a greater self-renewal capacity so consequently they are of great interest from a manufacturing perspective as from one starting product, in theory, multiple end products can be manufactured (Unger et al. 2008). In practice this manufacturing pathway and the route to market is exceptionally complicated in fact the first trial involving hESC was halted due to strategic issues as opposed to concerns regarding product safety (Whiting et al. 2015).

From a classic manufacturing perceptive all parts of the process need to be controlled and any process variation accounted for, however due to the inherent biological variation of cells and stem cells a new set of challenges arises particularly in terms of defining input material and end product (Ratcliffe et al. 2011). Good manufacturing practice (GMP) needs to be adhered to when producing a product that will be administered to a patient. This increases the overall cost of a product but is designed to ensure product safety and quality (Unger et al. 2008). Autologous cell therapies require segregated manufacturing processes for patient specific treatments, at no stage

can cells for multiple sources mix or use the same equipment without sterilisation in between as per GMP requirements. While from an immunogenicity perspective autologous cells have less risk, the cost of manufacturing an autologous treatment is greater per unit and there is no room for error in the process which brings into question how sustainable they are on an open market.

2.3.2 Regulatory considerations

As with all healthcare products manufacturing and over all approval of cell therapies, also referred to as human cell based medicinal products, is governed by a regulatory framework, which is recognised, along with development costs, as being the major barriers to market (Plagnol et al. 2009). The European Medicines Agency (EMA) which sets, in conjunction with individual countries' regulatory bodies, the regulatory requirements for cell therapies within Europe refers to all therapies involving cells as somatic cell therapy medicinal products and falls under the advanced therapy medicinal products (ATMPs) remit (Maciulaitis et al. 2012). The FDA, which is the regulatory body in the United States, has the Centre for Biologics Evaluation and Research (CBER) which regulates cellular therapy products and like the EMA is also includes gene therapy medicines, tissue engineered medicines and devices that are transplanted into the body with cells (Center for Biologics Evaluation and Research 1998). The regulatory framework needs to account for the extra safety concerns which are not normally present with classic chemical or biological pharmaceuticals. In particular with pluripotent stem cells, including the risk of tumour formation *in vivo* (Abad et al. 2013), and in the case of iPS cells the use of viruses to alter the genes carries a risk of uncontrolled genetic modifications leading to cancers (Reisman & Adams 2014). There has been criticism toward the regulatory bodies, most notably the FDA for not providing stricter regulatory definitions on cell therapies, in particular the ambiguity in the regulation of autologous treatments. The use of human cells as a treatment is placed into a 361 category or a 351 category. Products in the 351 are more closely regulated by the FDA as the cells are manipulated to a greater degree, such as *ex vivo* mixing of cell populations, administration on a scaffold or containing different genetic material to the recipient (Preti 2005; Knoepfler 2015). The 361 products include autologous cells that are being used for the same or similar physiological function and have only been minimally manipulated, which under

current FDA guidelines, requires minimal vetting and are not subject to the same regulatory approvals as a 351 product (Knoepfler 2015; Fox 2008).

Minimal manipulation includes processes such as separating CD34+ hematopoietic progenitor cells from peripheral blood progenitor cells and cryopreservation of cells or tissues (Preti 2005). The indistinctness within the 361 FDA regulations has led to the opening of clinics which offer patients cell therapies and making unfounded claims (Turner 2015), some on these unregulated clinics have resulted in patients becoming blind from one such cell based treatment (Ledford 2016). This demonstrates the need for not only tighter regulation on all cell-based therapies but also a better understanding of even minimally manipulated autologous cells which are considered "safe". The impact of unsafe treatments on the reputation of cell therapies also needs to be considered as bad press can negatively impact research funding and companies willing to invest into the area if it is thought patients are less likely to adopt the treatments. The complexities of cell-based therapies are considered to be the reason behind this apparent lack of specificity in the regulatory frame work. As the field is continually evolving and more knowledge about stem cell and cell behaviour is coming to light it can be a challenge for regulatory bodies to sustain the formation of new guidelines at the same rate (Fox 2008). It is important to establish the impact of *ex vivo* manipulations on a cell population including the harvesting of the cells, storage of the cells (where needed), culture conditions of the cells and the administration methods of WC or CTP.

Within a manufacturing setting there needs to be a defined process. The starting material and the end product need to be defined as per quality parameters, from a safety point of view the end product and its behaviour *in vivo* is the most critical. From a manufacturing aspect, in terms of efficiency and therefore cost, a defined process is required. Determining that the starting material will form the required end product and being able to monitor the process are highly important (Carpenter et al. 2009).The term critical quality attributes (CQA) of a product refers to a physical, chemical, biological, or microbiological property or characteristic, and needs to be within an appropriate limit, range, or distribution to ensure the desired product quality (Ich 2009). CQA are determined by the MOA of a product which is the pathways through which a product achieves its intended therapeutic effect (Food and Drug Administration, HHS 2005). The EMA states within regulation (EC) No 1394/2007

"When products are based on viable cells or tissues, the pharmacological, immunological or metabolic action should be considered as the principal mode of action".

One of the challenges when manufacturing CTP and WC is ensuring that the product will still invoke the MOA and maintain CQA, this includes identity, purity, potency and safety of the product (Carmen et al. 2012). As previously discussed pluripotent stem cells can differentiate into multiple cell types, therefore identifying the cell types present in the manufacturing process of pluripotent stem cells is one of the first challenges due to the heterogeneity of the population. If in the regulatory approval, it is stated that only differentiated cells will be administered to a patient then analysis needs to be carried out to determine the homogeneity of the population. For example, current clinical trials using hESC derived retinal pigment epithelium (RPE) cells for the treatment of acute wet age related macular degeneration in the first instance determine successful hESC differentiation and maturation based on pigmental changes and a cluster formation with cobblestone morphology. Though the cells may look like RPE cells subsequent testing including karyotyping, staining for hRPE markers, functional analysis included phagocytosis says, fluorescence-activated cell sorting (FACS), genetic analysis, FACS labelling for undifferentiated hESCs and testing for pathogen contamination is required. In this particular instance >99 % of the cell population fulfilled the RPE identification criteria and >90 % viable cells were transplanted into the patient (Song et al. 2015). It can be argued that it only takes a few cells to be unintentionally transplanted and a tumour may form. The advantage with this treatment is that the retina can be easily visually monitored, and any adverse effects seen and treated.

CTPs differ in terms of safety as the cells themselves are not being administered, however the potency and purity of the product needs to be assessed and from a manufacturing perspective continuous monitoring of any adverse effects during manufacturing is paramount (Food and Drug Administration 2008; Unger et al. 2008). Within the cell therapy manufacturing space there is a constant demand in very stage of the process for product monitoring and analysing. The FDA among other stakeholders identified that the more widely adopted offline process measurements used in pharmaceutical manufacturing were impacting production quality and efficiencies (Read et al. 2010). Within the pharmaceutical industry, the FDA

promoted the concept of process analytical technology (PAT) in 2004 in order to encourage innovation for the development of at-line, in-line and on-line measurement systems. The measurements could be physical, biological or chemical but the overall aim is for the measurements to improve process control and optimisation (FDA 2004). One of the key elements in manufacturing is reducing the sample to result window, particularly in processes that involve an active biological environment (Scheper et al. 1999), which is highly applicable to in stem cell manufacturing where cells can intentionally or unintentionally differentiate or de-differentiate. It is also important as cell culture environments as factors such as temperature, oxygen concentration, pH and growth medium are consistently shown to impact on cell growth and behaviour (Chen et al. 2014; Kagawa et al. 2016; Heathman et al. 2016).

2.3.3 Manufacturing scale

Some clinician-led autologous treatments currently in clinical trials are manufactured at a smaller scale and use a scale out approach as opposed to scale up. This method is not seen as being financially viable for the larger biopharmaceutical industry, and may not meet the market demand (Hourd et al. 2014). In order to produce the number of cells required for a treatment and quality testing, bioreactor systems are commonly used in the scale up of cell manufacturing. Bioreactors types include stirred tank reactors (Kirouac & Zandstra 2008; Rafiq et al. 2013), roller bottles, packed bed reactors (Palomares & Ramírez 2009; Brandwein et al. 2012). Bioreactors are also being used to replicate 3D *in vivo* environments for tissue engineering such bone constructs on scaffolds (Viateau et al. 2014). There are added challenges in the scale up of adherent cells such as hMSC to achieve the required level of cell growth. Though work is being carried out to successfully culture viable adherent cells in aggregates (Bartosh et al. 2010), most hMSC cultures require the cells to be attached to a functional surface. The use of microcarriers in stirred tank bioreactors provides a greater surface area per volume unit compared to the standard monolayer culture methods such a stacked T-flasks (Rafiq et al. 2013). The surface to which the cells are adhered, the seeding and harvesting methods and the forces the cells are exposed to during culture have also been shown to impact on cell viability (Curran et al. 2005; Heathman et al. 2016). Given the number of variables that can occur during the scale up processes, online system monitoring is of paramount importance to insure the

product will meet the quality standards required and to have as much continuous information as possible regarding the culture environment the cells are exposed to. Within the bioreactor system it is standard to have sensors constantly monitoring temperature, carbon dioxide levels, dissolved oxygen concentration and pH. Factors which as previously mentioned impact cell behaviour. However, given the complexities of cells simply measuring these parameters is not sufficient to determine how the cells are behaving and coping within the culture environment. Other measurements are usually taken which includes cell viability, cell surface marker analysis using flow cytometry, genetic profiling and protein analysis, however these methods are often carried out offline (Astori et al. 2010; Pal et al. 2012). Allogenic therapies are seen as more sustainable on terms to reaching a bigger market with and off the shelf product as opposed to a personalised autologous treatment.

2.4 Bioanalytics for Cell Therapy Manufacturing

Whether it is meeting regulatory requirements for release criteria or forming part of the manufacturing process, culturing cells for human use requires extensive testing and monitoring. The tests used need to need justified and related to the MOA and CQA of the cell-based treatment. It is possible to perform basic monitoring of gases and some metabolites online, but these measurements do not give an entire over view of the cells behaviour. Offline monitoring of product potency in the form of bioanalytical testing is therefore necessary but there is an need for test that reduce the time gap between sampling and date output of bioanalytical test (Scheper et al. 1999). The complex challenges of cell therapy manufacturing alone and the high level of testing required to meet regulatory standards drives the need for bioanalytics within the cell therapy manufacturing and processing environments (Lim et al. 2007). Bioanalytics specific to hMSC are discussed further in section 2.6.

The uses of bioanalytical methods are fundamental in the discovery and manufacturing processes of drug and biologics. Bioanalytics, also referred to as bioanalysis, originated due to the need to measure drug levels in biological fluids as part of the evolving science of toxicology. The emerging field of pharmacokinetics in the 1930s coupled with new drug development fuelled the need for high specificity analysis methods (Hill 2009). The field utilizes a number of different platforms including chromatography, mass spectrometry, enzyme mediated assays and

electrophoretic techniques. There is some debate regarding the use of the term bioanalytics/bioanalysis when referring to the determination of purity and identity of a product. Ritter (2011) argues that the term bioanalytics is often used wrongly as an overarching term for all analytics including bioassays.

In this work bioassays refer to the testing of the biological response to a treatment at a cellular level and are often used to determine the potency of a product i.e. the effect of a product on the cell population. Bioanalytics refers to the measurement of a discreet molecule or compound such as a protein or metabolites. Bioanalytical methods are used across many areas of research and manufacturing including drug development, biotherapeutics, biomaterial development, quality system monitoring and diagnostics (Romanyshyn et al. 2000; Whitmire et al. 2011; Zhang et al. 2016). Classic small molecule and even biotherapeutics (proteins including antibodies) are relatively simple to characterise as opposed to cell therapies. In general, the manufacturing processes are well defined, robust and reliable and it is proven in the development phase that certain manufacturing parameters will consistently produce an intended product (Li et al. 2010). This results in more straight-forward monitoring of the product, quality checks and batch release criteria. Bioanalytical methods used include immunoassays, flow cytometry, genetic analysis, electrophoreses, spectrometry methods and chromatographic methods which detect protein expression, characterisation of proteins, mRNA expression profiles, cell surface markers and the presence of metabolites (Findlay et al. 2000; Romanyshyn et al. 2000; Harkness et al. 2008; Carlos Polanco et al. 2013). Flow cytometry is of particular interest in the cell therapy field as it is a common method for characterising and sorting (FACS) cell types based on cell surface markers also known as cluster of differentiation (CD) markers (Kiel et al. 2005; Rasini et al. 2013). Immunoassays also are able to provide information on the proteins a cell population is secreting i*n vitro,* proteins such as cytokines are the major conduit through which cells communicate with the microenvironment and with each other (Turner et al. 2014). Immunoassays are capable of extracting a molecule of interest from a complex matrix (Ohno et al. 2008) they amplify the signal from these molecules through a number of mechanisms which result in a detectable signal that is proportional to the quantity of the molecule (Wild 2013).

A limitation of flow cytometry and immunoassay methods is that prior knowledge is needed to be able to screen for specific CD markers or proteins. Flow cytometry utilises CD markers using fluorescently conjugated CD marker specific antibodies. As with most antibody related analytical test there is the risk of nonspecific binding, while this can be reduced through the use of blocking buffers background fluorescence is an artefact which needs to be compensated for during data analysis (Andersen et al. 2016). Different cell types also express on or more of the same CD markers; therefore, a panel of CD markers specific to a cell type must be screened for. Due to this issue negative testing is also required to prove the absence of a cell type in a population, for instance to separate undifferentiated hESC from a differentiated cell type (Pruszak et al. 2007). There are new markers and cell types regularly being identified consequently field is continuously re-evaluating the CD marker panels, expression levels and the impact on the function of the cell population (Diaz-Romero et al. 2005; Carlos Polanco et al. 2013)

Again, this is a disadvantage of manufacturing such a complex product which carry out 100s or processes within the cell unit while communicating and reacting to the culture environment, it is not possible to gain a full picture of cell behaviour based on a minimal number of analytical tests. Thus, a wider panel of bioanalytical tests need to be carried out and at multiple stages in the manufacturing process (Figure:1).

Cell source
- Autologous /Allogeneic?
- Direct from donor/ cell bank?
- Cryopreserved?
- Cell sorting (CD marker identification)
- Pathogen screening
- Viability

Up stream processing
- Pre screening
- Predicting behaviour in a scale up system
- Cell population behaviour (growth rate, biochemical finger print etc.)
- Quality of input material

Scale Up/ Scale Out
- Process monitoring
- Feeding
- Online, near online and offline monitoring of culture.
- Compliance to pre determine culture parameters

Down stream processing/fill and finish
- Cell numbers achieved?
- Viability, purity, potency and identity?
- Harvesting and purification of product
- Potency and safety of product
- Fill and finish for delivery to patient

Release criteria
- Product specification
- Defined release limits
- Satisfying regulatory bodies by ensuring product meeting the release criteria specifications

Administration to patient

Figure:1 Summary of a cell therapy manufacturing process. The green text boxes refer to information that need to be determined and the pink text boxes process requirements which need to be satisfied.

Figure:1 shows a simplified summary of the manufacturing process and identifies in the pink text boxes some of the areas where bioanalytics and in some case bioassays are required. In basic terms the starting material needs to be characterised, screened for infectious agents and the cell behaviour assessed prior to committing to an expensive and time-consuming scale up process. The methods used and the criteria the cells will need to meet will depend on the cell source and the treatment type. This is decided during the process development period. The scale up/scale out system needs to be monitored during the culture period. For instance, if unexpected events occur such as an accelerated growth rate, feeding regimes may have to be altered to avoid batch loss. Post expansion the cells need to be harvested and unwanted

contaminants such as cell debris or microcarriers removed and the final product tested when purified. The final product also needs to be tested for potency and to test for adverse effects such as impurities which could invoke an immune response. How to supply the product to the patient is also a factor which could impact product quality. Cryopreservation is a favoured method to preserve cells but there is evidence that there is a negative impact on cell quality (Xu et al. 2012; Coopman & Medcalf 2014). The number of tests required for one product run adds to the cost of the overall manufacturing process and requires samples of the product for testing. With destructive testing methods used, more tests mean more of the product is lost in quality control, reducing that available for treatment. This is particularly challenging for autologous treatment. There is also the additional time delays from the time the samples are taken to obtaining the results, many of the methods used at the research level in cell therapy are not optimal for large scale manufacturing (Scheper et al. 1999; Vojinović et al. 2006). As cell behaviour is difficult to predict during culture it is even more paramount, compared to classic pharmaceutical manufacturing, to be able to have continues feedback of the system and to reduce the test to result time frame would enable a more flexible and proactive approach to cell therapy manufacturing. Cost coupled with regulatory hurdles are some of the biggest barriers to a cell therapy reaching the market (Plagnol et al. 2009). It is unlikely regulatory requirements will ease for cell therapies, the product needs to be deemed safe and effective, and as there are so many elements where a cell therapy can fail to meet these requirements a panel of bioassays and bioanalytical tests will be required to determine with product quality.

2.5 Microfluidic-based Bioanalytics

With such extensive demands on bioanalytics within the cell therapy industry the area of microfluidic bioanalytics aims to satisfy these demands. Microfluidics is based on fluid handling and manipulation between 10^{-9} to 10^{-18} litre scale (Whitesides 2006). Microfluidic based platforms can help to address some of the hurdles encountered in cell manufacturing and at the fundamental research level, firstly by minimising quantities of reagents and cells used, thereby reducing costs. Secondly by reducing the scale of an assay it may be possible to improve assay sensitivity due to the unique microenvironment (Pihl et al. 2005). Finally, the speed of the assay is often quick

compared to standard bioanalytical assays. For example, many core analytical tests such as flow cytometry require many manual handling steps and long incubation steps. Due to the scale and geometries in microfluidic devices it is possible to carry out multiple steps in one system and reduce incubation times. All these factors allow the biomanufacturing field to have continuous process monitoring capabilities (Karle et al. 2016).

A number of assays have already been translated from macro to micro scale and exploited the benefits of micro scale assays. The majority of microfluidic platforms are 'lab-on-a-chip' style devices; these allow for a high level of control with low reagent and sample volume requirements (Whitesides 2006). Barbulovic-Nad et al. (2008) used a planar array of electrodes in combination with droplets of reagents to increase the sensitivity of a live/dead cytotoxicity assay (calcein AM and ethidium homodimer-1) by ~20 fold compared to the standard microtiter plate. Reverse transcription polymerase chain reaction (RT-PCR) assays are also a focus of scaling down the reaction size with the aim of achieving rapid and reliable results for the point of care (POC) diagnostics market. Verdoy et al. (2012) developed salmonella POC detection chip that incorporated the time-consuming sample preparation steps and reduced the analytical test time to 35mins; this is considerably quicker compared to the well plate assay which, depending on reagents requires 1.5-2hrs. Chang et al. (2006) combined microfluidic PCR chips with digital technology, utilising electro-wetting-on-dielectric (EWOD) and moving reagent droplets along micro channels via hydrophilic/hydrophobic generated tension gradients. The authors focused on amplification of Dengue II virus and report a reduction in consumable costs and amplification time compared to larger scale assays (Chang et al. 2006). Lab-on-a-chip devices have been able to analyse microscopically down to the single cell level. Cells which are culture in micro wells under separate conditions can be stimulated with biochemicals and the response analysed, this platform accommodates a high number of cells in the same device with low reagent costs (Gupta et al. 2010). Being able to identify a single rogue or undifferentiated cells within a population is important for treatments using iPS or hESC, as previously mentioned these cells can results in tumour formations (Abad et al. 2013). Some organ-on-a-chip concept use chambers on a microfluidic chip which contain the cell populations that form a tissue or organ. The chambers are continuously perfused, and,

using finely controlled channels between the chambers, the aim is to be able to mimic the *in vivo* physiological functions of the organ or tissue *in vitro* (Bhatia & Ingber 2014). Through using organ-on-a-chip platform tissue responses to pharmaceuticals, integration of stem cell derived tissues within the platform can be analysed as well as being able to test the cellular products such as protein production after exposure to specific conditions. These platforms can also help identify the impact of single rogue or undifferentiated cells within a system. There are application for this technology within drug research, particularly as organs-on-chips could be a realistic replacement of animal testing, or at least be able to reduce the use of animals in line with government and ethical body initiatives (Huh et al. 2012). In the remit of personalised medicine organs-on-a-chip would be highly functional in terms of using a patient's own cells and being able to analyse drug responses. Similar work to this has been carried out in microarray formats, however these are not able to replicate the fluidic dynamics of the *in vivo* system which lab-on-a-chip devices can (Xu et al. 2011).

Cells being cultured inside microfluidic devices and be analysed using a number of techniques for example in-cell Westerns. In-cell Westerns adapt standard immunohistochemistry staining of proteins inside cells coupled with a laser scanner detection method. The short distance between the cells inside a microfluidic device and the lasers reduces the level of environmental interface which improves the sensitivity of the method and enables successful quantitation of the proteins. (Paguirigan et al. 2010). It has also been shown that it is possible to carry out analytics at the nanolitre scale using electrode array for cell based assays (Barbulovic-Nad et al. 2008). Toriello et al. (2008) developed an integrated single cell gene expression analysis which is able to capture a single cell and amplify the mRNA using pumps that operate at the nanolitre scale. The amplified product is then analyses using microcapillary electrophoreses that is integrated into the same system (Toriello et al. 2008) Microfluidic applications for analysing cell products are also another focus within the field, with a demand for POC and easy to use tests are of particular interest (Myers & Lee 2008). Developments so far include paper-based microfluidics, where micro-channels are patterned onto the paper using a wax printing and cutting method. This platform has been used for immunoassay bioanalytics but is struggling to compete with the level of sensitivity achieved by conventional bench top

immunoassays (Martinez 2011). Novo et al. (2014) integrated a photodiode based optical detection system with a microcapillary system that could carry out sequential fluid flow function in order to carry out a chemiluminescence ELISA spot assay. The whole system could be contained in a 5.5cm x 15.2cm x 3.3cm box, and the assay could be carried out in 15mins achieving a LOD of ~2nM.

There are some challenges when using microfluidic devices to perform measurements, assays or culturing live cells such as maintaining the optimal environment. Bubble formation in microfluidics is a common issue (Gao et al. 2012; Young & Beebe 2010), and though the issue is often debated within the cell culture field, bubbles are thought to harm cells when they burst due to hydrodynamic shock damaging the cells (Hu et al. 2011). The cells produced during the manufacturing process need to be consistent or at the very least any variation introduced due to the manufacturing processes needs to be accounted for in terms of safety and functionality

A challenge in using optical detection of absorbance in microfluidic devices is the reduction in the light path length which in turn reduces the sensitivity (Mogensen & Kutter 2009). This is based on the Beer-Lambert law where by absorbance is directly proportional to the light path length (Strafford 1936; Vila-Planas et al. 2011), the shorter the light path the more sensitive the value is to issue such as poor mixing and contaminants.

2.6 Bioanalytics and hMSCs

2.6.1 Clinical applications using hMSCs

While there are many cell types being used in clinical trials, hMSCs are of great interest for cell therapy applications due to their multilineage potential (Figure 2) ability to be expanded *in vitro* and the minimally invasive techniques used to obtain aspirates of them from within bone marrow (Caplan & Bruder 2001). Dental pulp, adipose tissue, Wharton's jelly and umbilical cords have also been used as sources of hMSCs (Yañez et al. 2006; Collart-Dutilleul et al. 2014; Chen et al. 2015). There is also evidence that hMSCs are an immunoprivileged or immunoevasive cell type whereby they do not express antigen stimulating surface markers which trigger an immune response leading to issuers of immunogenicity and immunotoxicity (Caplan

& Bruder 2001; Goldring et al. 2011; Shin et al. 2017). A minimal criteria for defining hMSCs is that they are paslstic adherant, can differiantate down the adipocytes, chondrocytes and osteoblasts lineages and express CD105, CD73 and CD90, but lack the expression of CD45, CD34, CD14, CD79a and HLA-DR (Dominici et al. 2006; Rasini et al. 2013).
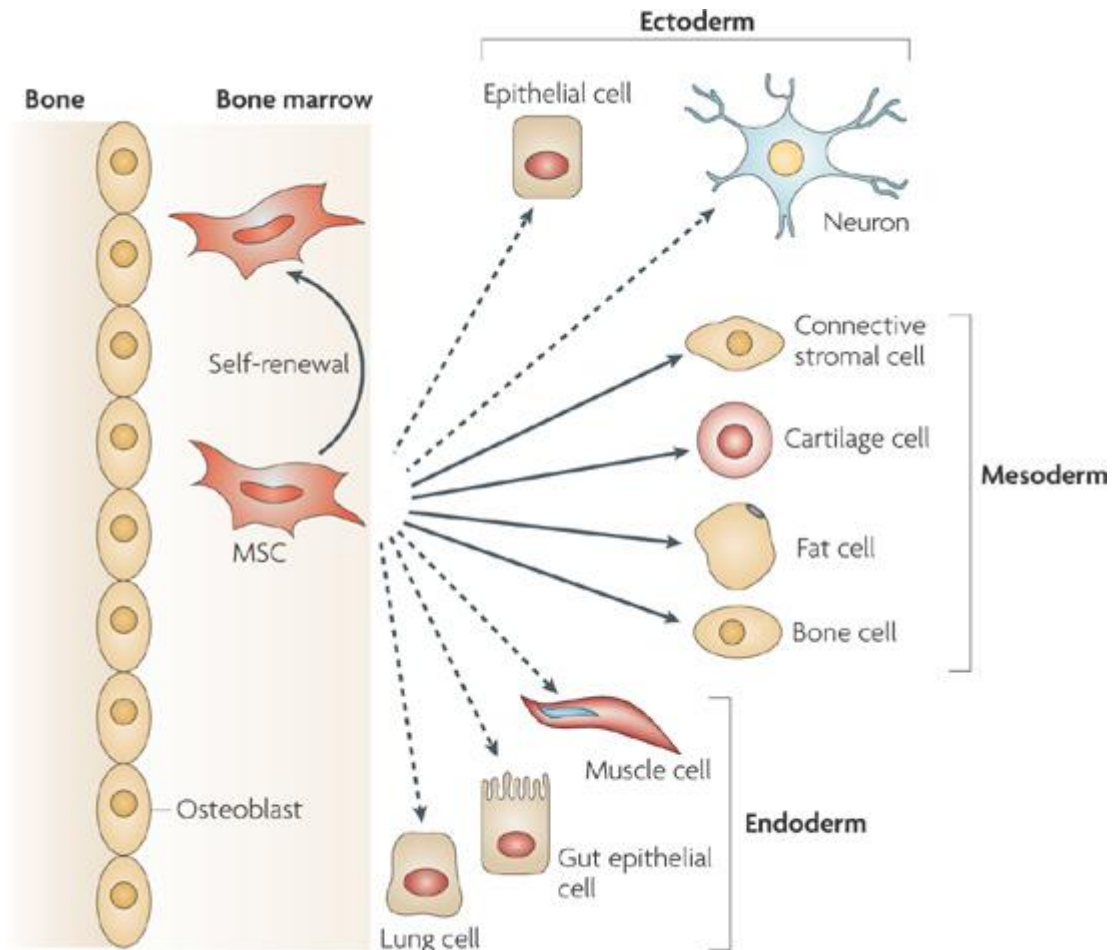
Figure 2 Bone marrow derived hMSCs differentiation pathways. Cells types which hMSCs have been shown to differentiate to under specific biochemical (*in vitro*) and physiological (*in* vivo) conditions (Uccelli et al. 2008).

The paracrine properties of hMSCs are becoming of increasing interest, these properties are not included with it characterisation criteria of hMSCs. The paracrine properties of hMSCs have been used for treatments such as graft-versus-host disease (GVHD). In autoimmune diseases hMSCs are shown to supresses the immune system through multiple pathways including direct cell to cell contact with T-cells and

secretion of cytokines which among other mechanisms seem to supress dendritic cell migration and expression of CCR7 on T-lymphocytes which results in dendritic cells from maturing. Maturation and migration of dendritic cells is a key mechanism in acute GVHD (Li et al. 2008). The challenge as with many biological processes is that though a cause and effect can be seen. In the example of GVHD treatment with hMSC *in vitro* and *in vivo* has been shown to dampen the immune response, all the exact molecular mechanisms remain elusive. Some signalling pathways have been extensively studied and are widely accepted such as cytokines hepatocyte growth factor (HGF) and transforming growth factor beta (TGF-β) have been shown to be involved in signalling to supress T-cell proliferation. These cytokines are also expressed by hMSCs and therefore are considered to be some of the mechanisms by which hMSCs regulate immune responses (Dorronsoro et al. 2013). Other conditions which use hMSCs as a treatment include ischemic stroke (Bang et al. 2005), cardiac tissue recovery after damage (Windmolders et al. 2014) and neurodegenerative diseases (Kim et al. 2013).

Though a wide variety of hMSC-based treatments are being investigated at the laboratory bench level not all have advanced as far as clinical trials. In the United States of America, as of March 2017, 704 were registered in that were either completed or on going. The most treated clinical conditions include 82 trials for using hMSCs to heal wounds and injuries, digestive system diseases, most notably liver conditions for which there are 73 trials registered and there are 43 trials registered for diabetes mellitus (ClinicalTrials.gov 2017). Translating laboratory research into the clinical has been highlighted as a particular problem in the UK and Europe (Plagnol et al. 2009) In 2015 there were 58 registered clinical trials that are using hMSCs within the European Union (European Medicines Agency 2015) based on data from 2017 this figure now stands at 74 (European Medicines Agency 2017). These values indicate that, as noted by Plagnol et al. (2009), the European industry, including the UK, is lagging behind the United States in terms of bringing hMSC treatments to fruition. As mentioned in Sections 2.1 and 2.2 there are many hurdles to bring a cell therapy to the clinical trial stage and to the wider market.

2.6.2 Utilising hMSC conditioned medium

Many of the clinical trials use the cells to either replace tissue or modulate biological process. However, the use of condition medium as a form of CTP for a treatment option are also being investigated (Kwon et al. 2014a). Using medium in which hMSC have been cultured and expressed CTPs such as complex paracrine factors and exosomes which invoke behaviours *in vivo* including immunomodulation, negate the issue of administering a live cell product to a patient (Baraniak & McDevitt 2010; Anderson et al. 2016). With the use of hMSCs in clinical trials and the cell type becoming a realistic and established treatment option the demand is increase for cost effective, rapid and sensitive assays which can qualify the product for the healthcare market. There is also the additional challenge that hMSCs are used for multiple clinical conditions which exploit different properties of hMSCs. As mentioned previously of particular importance are assays that characterise cells, measuring the products ability to carry out the intended mode of action, measurements of adverse effects and potency assays, there for the analytics need to be aligned with the specifics mode of treatment, while also ensuring no adverse effects occur. For example when using hMSCs to supress T-cell and B-cell activity in an autoimmune system disorder such as GVHD (Ma et al. 1998; Gieseke et al. 2010), hMSCs properties such as promotion of angiogenesis would be an adverse side effect. Consequently, it is difficult to justify the commonly used hMSC characterisation criteria which is routinely cited as the focus of so many treatments are the utilisation of discrete aspects of hMSC behaviour. Functionality of an hMSC population for a specific treatment cannot be determined based on the existing characterisation criteria. Cell characterisation in general revolves around the quantification of cell types that are present in a population based on CD surface markers which the cells display. A minimal criteria for hMSC characterisation was defined by ISCT (Dominici et al. 2006), following on from this paper a working proposal was published highlighting the need for characterising the immunoregulatory function of hMSC (Krampera et al. 2013). To distinguish between other cell types hMSCs must be plastic adherent when cultured under standard conditions and differentiate down the adipocyte, chondrocyte and osteocyte linages. They must also be positive for CD90, CD73 and CD105; and the hMSCs must also lack the expression on haematopoietic stem cell markers in order to be deemed hMSCs (Dominici et al. 2006; Chan et al. 2013; Rasini et al.

2013). However, given the range of treatment applications the hMSCs are being harnessed for the question of how relevant the characterisation criteria really are needs to be asked.

2.6.3 Clinical need for improved product characterisation

Clinical trial NCT00447460 is an example of a clinical trial using hMSCs which were characterised based on the ISCT guidelines. The trial involved 18 patients being treated for GVHD with hMSC donated by family members or by a haploid match. Originally there were 28 patients in the trial, 4 responded to standard medication prior to treatment, the hMSC for 1 patient failed to expand and 5 died before they could receive the treatment. This alone demonstrates the need for a faster pipeline of cell therapies, patient death while waiting for the product to be manufactured is unacceptable but at this stage unavoidable. Of the 18 patients treated with an hMSC infusion 10 had refractory or relapsed acute graft-versus-host disease GVHD and 8 had chronic GVHD. Only 1 patient from each group had a complete response to the treatment 3 chromic patients and 6 refractory or relapsed acute had a partial response and the rest had no response (Pérez-Simon et al. 2011). Besides the hMSC used in this trial being characterised according to the ISCT guidelines a tissue match between donor and recipient was also carried out but no further testing. The hMSCs were not tested to see if they had the ability to invoke the level of immune suppression required to modulate GVHD. The cells were administered into patients whose tissue was being damaged by the grafts immune response, hMSC survival and function within a pathophysiological environment (e.g. pro-inflammatory) was not assessed. When trials using hMSCs are not as successful as intended it can harm funding and licensing for subsequent trials, therefore more needs to be carried out in determining the hMSCs from a selected donor are suitable for the patient and the disease requiring treatment.

The current release criteria require a minimum of 70% cell viability, viability does not automatically equate to functionality. The issue of limited release criteria and lack of functional testing at the point of release caused the death of four paediatric bone marrow recipients at Great Ormond Street hospital in 2013. Prior to transplantation the cell viability was deemed acceptable but after an investigation into the deaths it was determined that the cells transplanted where not functional and could not mature

once administered to the patient (Morgenstern et al. 2017) The cryopreservation processes was thought to have not been effective though the same process had been used for ten years, this not only demonstrates the urgent need for more in-depth testing post thaw and prior to transplant but also that process monitoring (in this instance cryopreservation) needs to be continuous (Morgenstern et al. 2016). For these reasons, surrogate potency assays have become more of a focus within cell therapies. Potency assays provide a quantitative measure of a cell or cells biological activity which is biologically relevant to the end therapeutic need. Potency assay are more in the remit of bioassays as opposed to bioanalytics in terms of a product or cell population us applied to cells and the effect of the product on the cells is measured (Bravery et al. 2013). Potency assays *in vitro* are not a new concept, they have been used to test microbial responses to antibiotics (Jones et al. 2008) and for testing drug toxicity on hepatocytes (Xu et al. 2008). However, as previously mentioned in Section 2.5 these models are often not fully representative of the spatial interactions which occur *in vivo* though this is being addresses using lab-on-a-chip and other methods (Vernetti et al. 2017).

For hMSC potency assays the cells or conditioned medium need to be applied to assays which represent the intended mode of action and/or assays to screen for adverse effects as per regulatory guideline (Food and Drug Administration 2008). However this is further complicated as not all mode of actions are defined or can be assessed within one test and regulatory bodies do not state defined release criteria for this assays (Galipeau et al. 2016). There are some angiogenesis assays which have been reported and are applicable to hMSC functional analysis, this is discussed further in Section 2.8. Potency assays are not just important to determine the potency of the cells from a particular donor but also to ascertain the impact of manufacturing processes such as cryopreservation, cell culture conditions and even the administration method on the product potency (Spellman et al. 2011). This raises the same issue as other bioanalytical measurements, in that potency assays could also cause a bottleneck in the manufacturing process due to the time taken for them to be carried out.

2.6.3.1 Cytokine detection

As many of the mechanisms through which hMSCs exert their immuno-suppressive and pro-angiogenic (see section 2.8) MOA is through the secretion of cytokines

measuring cytokine levels and relating the values back to the potency of the hMSCs on a biological process would be a powerful tool. The most common based method for specific protein identification and measurement is the enzyme-linked immunosorbent assay (ELISA). The ELISA was developed as a safer and more stable replacement of radioimmunoassays, the technique was first published by 2 independent research groups in 1971 (Engvall & Perlmann 1971; Van Weemen & Schuurs 1971). ELISAs use protein specific antibodies to capture a target protein then amplify the protein directly or indirectly using colorimetric or fluorescent methods so a signal can be detected (Andreasson et al. 2015). ELISA technology has rapidly advanced since 1971 but many of the assays still utilise horseradish peroxidase (HRP) as the substrate converting enzyme to produce a measurable colour was used in the first papers published. There are different configurations of the ELISA assay (Figure 3) and the type of assay which is used depends on the application and the available reagents. ELISAs are completely reliant on the antibodies available and the quality of the antibodies. For instance, if there is only one antibody available for a specific antigen then a competitive ELISA must be used. Factors such as the purity of the sample and anticipated concentration of target antigen also influence the type of ELISA most suitable (Cox et al. 2004; Moises & Schäferling 2009).
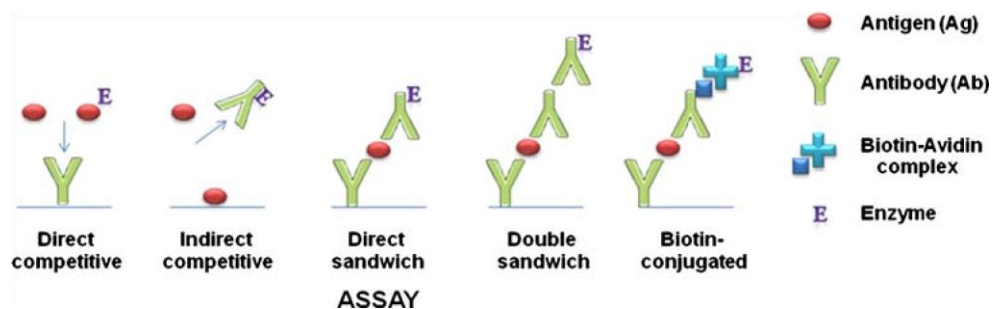
Figure 3: Summary of ELISA assay types (Moises & Schäferling 2009), these are most of the basic principles of ELISA assay but the platform in which they are carried out can vary depending on the test need including using a fluorophore detection system for multiplex ELISAs.

While antibody technology and substrate sensitivity has improved, challenges remain in terms of reducing the cost of the assays. As a panel of ELISA would be needed to be carried out to determine the multiple cytokine levels though which hMSCs invoke many of their paracrine effect, cost per assay becomes an influential factor. Cost of

reagents, length of time per assay and requirements for technically trained operators are issue which need to be addressed. Methods used to address these issues include multiplexing assays. The Luminex platform (Pham et al. 2014) is one of the most popular immunoassay multiplex platforms, however as discussed in Chapter 4 there are still some limitations. Therefore, researchers are looking towards the field of microfluidics to find methods which will ideally improve all aspects of ELISA.

2.6.3.2 Microfluidic ELISA

ELISA are a focus of the microfluidic field, whereby the aim is to reduce the total assay time and costs with equal to or improved sensitivity and/or specify through reducing the scale. Standard ELISAs, such as the commonly used sandwich ELISA, have been translated into a variety of lab-on-a-chip formats while improving the detection methods. Detection methods in ELISA are mostly image based, detecting colour intensity changes in either illuminances, absorbance or fluorescence. Therefore, the sensitivity of the detection equipment is very important as it needs to be able to accurately distinguish between concentrations with only a few femtograms or picograms difference. Many of the lab-on-a-chip devices are fabricated from polydimethylsiloxane (PDMS), a soft polymer in which micro-wells and channels can be moulded and has excellent optical clarity allowing for sensitive optical detection (Schneider et al. 2009). An important parameter used to determine the performance of an ELISA platform if the limit of detection (LOD), the LOD is the lowest amount of analyte that can be detected and distinguished from background noise (Findlay et al. 2000).

Devices developed to date include a femtomolar scale micro well-patterned PDMS chip (Figure 4) designed by Wang et al (2013) (Wang, Zhang, Dreher & Zeng 2013) which contains over 100 wells per chamber and has an integrated-on chip pump system which allows for programmable, controlled fluid handling and excellent mixing. The chip is able to detect insulin-like growth factor 1 receptor (IGF-1R) with a limit of detection (LOD) of 0.0035pg/ml and a detection range of 0.1pg/ml to 1000pg/ml, the LOD was calculated from the value of blank signal plus three standard deviations. This assay was compared to 6 commercially available kits; the most sensitive of the commercial platforms had a LOD of 6 pg/ml the highest LOD was 250pg/ml showing this platform is much more sensitive. While the

detection range is smaller for the microfluidic chip compared to the commercial kits which can detect up to 6000pg/ml-20000pg/ml it is not a draw back as samples can be diluted. This chip is also more focused on the detection of low abundance proteins, within the cell therapy manufacturing field this would be more applicable for contaminates such as virus capsid proteins. At the laboratory research level being able to detect protein which using standard kits would not be identified may give greater insight into signalling mechanisms.
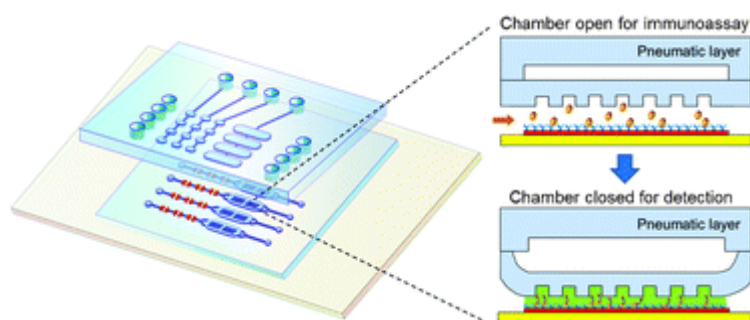
Figure 4: Micro well patterned PDMS chip developed by Wang et al. (2013). Micro wells and micro channels were formed in PDMS on top of a glass slide. The chambers are opened for carrying out the assay and closed during detection which forces liquid into the wells and allow for a concentrated and focused image of the well to be taken.

While the data presented on the femtomolar scale micro well-patterned PDMS chip holds a lot of promise, the authors did not comment on the failure rate of the device and the potential to mass manufacture such an intricate system to a high quality while still providing a cost-effective assay to the market. These questions are important to consider when looking at the commercial market.

Ellinas et al. (2017) used a sandwich ELISA carried out on magnetic beads in a microfluidic device approach. The use of magnetic beads as the solid phase for capture antibody immobilisation is the principle of the Luminex MAGPIX platform (Baker et al. 2012), but this is carried out in a 96 well plate format which still requires higher reagent volumes and longer incubation times compared to what has been seen in microfluidic platforms. The micro-bead platform used a 3-way valve mechanism to deliver wash buffer or reagents to an inlet port which was in turn connected to the bead containing chamber. This simplifies the fluid handling compared to pipetting and aspirating reagents in to microtiter plate wells. Washing, fluid addition and

removal from the chamber were carried out when a magnet was applied to the chamber to prevent any loss of magnetic beads and there for the ELISA reaction. One of the negatives for this assay platform is the detection technology, 3 methods were investigated including using an epifluorescence microscope and a custom-made spectrophotometer based biosensor (Ellinas et al. 2017). These pieces of kit are bulky and are not fully integrate able with the microfluidic chip.

While many of the microfluidic devices achieve a more rapid and, in terms or reagent use, are more cost-effective ELISA tests compared to the standard micro well plate test the devices themselves are intricate and are not straight forward to manufacture. Many also require the use of external pumping system and bulky detection equipment which can increase the cost and prevent or complicate the integration into a manufacturing process. From a manufacturing industry perspective, the ELISA must be fit for purpose and fully validated with the intended use in mind, Figure 5 gives an overview of factors which need to be considered and processes which need to be undertaken to achieve this. One of the key aspects of assay validation is the robustness, repeatability and influence on operator effects. The microfluidic assay must be easy to use and reliable. Assay failure could be detrimental to a batch run when only a small amount of sample is available, and/or there is a short time frame in which the measurements can be carried out.

Immunoassay Critical Success Factors
sensitivity, throughput, dynamic range, reagent cost, etc.

Acquire Reagents
antibodies, analyte, standards, sample matrices,
control samples, labels and substrates

Instrument Testing
calibration, performance testing, linearity

Assay "Proof of Concept" Experiments
Establish preliminary assay parameters, reagent suitability
and matrix compatibility. Signal-to-noise, data analysis models
consult immunoassay expert

Assay Optimization
Select factors to be optimized, determine matrix effects,
construct precision profiles, consult a statistician

Assay Validation
robustness, day-to-day effects, scale up, automation, reproducibility,
operator effects, % recovery analysis

Method Documentation (SOP) and Implementation

Figure 5: Flow chart out lining the development, optimization and validation of immune

2.7 The microcapillary film

The microcapillary film (MCF) is a recently developed microfluidic platform with hollow capillaries embedded within it, invented by Hallmark et al. (2005). The MCF (Figure 6) is produced using a melt extruded method which is not only low cost, but it allows flexibility in terms of the number of embedded capillaries and the diameter of the capillaries. As a result, many applications for the MCF have been developed including a plastic microcapillary flow disc (MFD) reactor. The MFD has been utilised for a continuous flow reaction system for organic synthesis which is capable of withstanding high temperatures and pressures (Hornung. et al. 2007). The MCF can be manufactured from several different polymers, including ethylene vinyl alcohol (EVOH). EVOH creates capillary walls within the MCF that are porous, creating the options to use the MCF for membrane applications such as filtration and membrane bioreactors (Bonyadi & Mackley 2012). However, one of the more relevant applications for cell therapy manufacturing is the use of the MCF for immunoassays.
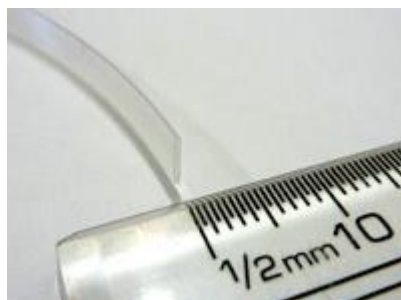
Figure 6: Image of the MCF (Hallmark et al. 2005)

To date ELISA have been developed for prostate serum antigen the cytokines IL-1β, IL-6, IL-12p70 and TNFα in fluorinated ethylene propylene (FEP)-based MCF (Barbosa et al. 2014; Castanheira et al. 2015). The method of carrying out such an MCF ELISA is explained in detail in Chapter 4 but in brief, a long length of MCF is coated with capture antibody and then blocked. The MCF is then cut into small strips and placed in a multi-syringe aspirator. All subsequent ELISA steps including wash, target protein incubation, and detection steps are carried out by aspirating fluids into the MCF. Detection is either carried out using a flatbed scanner or a smart phone depending on the format of the assay (Barbosa et al. 2014; Castanheira et al. 2015). The assays can be completed in less than 15 mins post addition of the sample and thus

far have been aimed at the point-of-care and in-field diagnostics market. With the cell therapy manufacturing field needing a platform such as the MCF ELISA examining the feasibility of its use for relevant cytokine detection is a logical step (Chapter 4). There is also value in exploring the possibility of combining cell culture (in this case hMSCs) with the technology of the MCF ELISA, to be able to detect cytokines production within the same device (Chapter 5). Using the MCF for adherent cell culture applications the suitability of the surface needs to be examined, the practicability of administering hMSC into the MCF and the methods used to analyse the cells inside the MCF.

2.7.1 Surface Chemistry of Fluorinated Ethylene Propylene

FEP is a copolymer of hexafluoropropylene and tetrafluoroethylene it has similar properties as poly (tetrafluoroethylene) (PTFE) and a refractive index of 1.338 (Sahlin et al. 2002). The refractive index of FEP is close to that of water which is 1.3325, making FEP an ideal material to manufacture products from which required optical interrogation. Fluorocarbon polymers are inert and hydrophobic; this is due to the fluorine carbon bond (F-C) resulting in an overall low surface energy (Kozlov et al. 2003; Griesser et al. 1991; Shoichet & McCarthy 1991). Hydrophobic surfaces, which are a benefit for antibody immobilisation due to hydrophobic interactions are, however difficult to block effectively resulting in issues with nonspecific binding. This is something which needs to be addresses effectively when using the MCF as an ELISA platform (Eteshola & Leckband 2001).

The hydrophobicity of FEP has been determined using contact angle measurements, values reported are over 110° (113.8° ± 0.19 (D Li & Neumann 1992), 117° (Coupe & Wei Chen 2001) and 115° (Shoichet & McCarthy 1991)). It has been reported that surface roughness can increase the hydrophobicity of fluoropolymers and that adding roughness can be achieve in many ways including simply stretching a film made from the polymer (Ma & Hill 2006). Contact angle measurements are predominantly calculated based on Young's equation (Figure 7), however this equation assumes a droplet is being measured on a perfectly smooth ridged surface, on which a maximum contact angle of 120° can be measured (Xu & Wang 2010). However, by combining chemical composition and surface roughness larger contact angles can be achieve. Wenzel and Cassie equation takes into account the roughness of the surface and

chemical composition of the surface which is being measured (Figure 7). The variation in contact angle of FEP reported in the literature could be due to the manufacturing process when making the FEP samples that were tested, irregularities in the measurement methods, or calculation of the contact angle.

Young's Eq.

$$\cos\theta = \frac{\gamma_{sg} - \gamma_{sl}}{\gamma_{gl}}$$

$\gamma_{sg}, \gamma_{sl}, \gamma_{gl}$: the interfacial free energies per unit area of solid-gas, solid-liquid and gas-liquid interfaces, respectively

Wenzel's Eq.

$$\cos\theta' = r\frac{\gamma_{sg} - \gamma_{sl}}{\gamma_{gl}} = r\cos\theta$$

$$r = \frac{Real\ Sa}{Apparent\ Sa}$$

Cassie's Eq.

$$\cos\theta' = f\cos\theta + (1-f)\cos 180°$$
$$= f\cos\theta + f - 1$$

f : Area fraction of solid surface
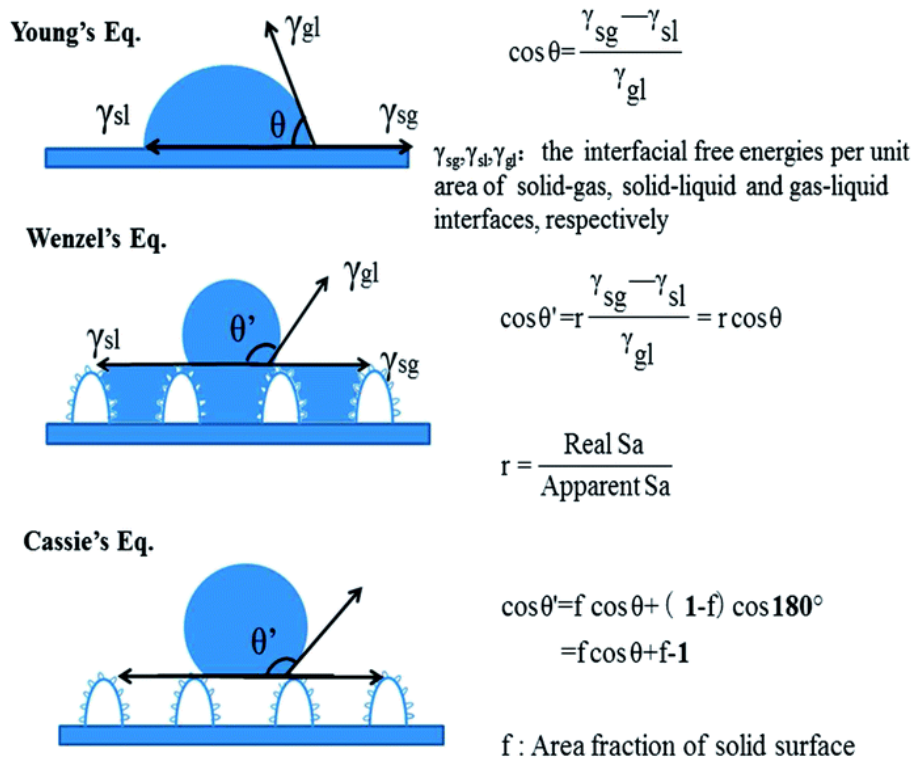
Figure 7: Young, Wenzel and Cassie models for calculating contact angle based on the roughness of the surface (Zhan et al. 2014).

While for many applications chemical inertness and hydrophobicity are required, for cell attachment fluoropolymers are not an optimal surface, this is thought to be due to the low surface energy and lack of functional groups (Griesser et al. 1991; Shoichet & T. J. McCarthy 1991). There are multiple elements that need to be considered when developing a cell culture-based platform made from FEP. The desired properties of FEP such as the optical clarity and robustness of the fluoropolymer need to be maintained after functionalization. The functionalization process must produce a homogenous coating equal or better than current methods used to culture the cell type of interest, for hMSCs this is standard tissue culture plastic. It is always desirable for the functionalization process to be as inexpensive and as easy to carry out as possible, options have been presented that can satisfy these requirements. Once the FEP surface has been functionalised it may need to be further optimised in order for cells to adhere

and proliferate but any further steps need to comply as much as possible with these requirements When modifying FEP for cell attachment the surface energy must be increased, essentially reducing the hydrophobicity, but there must be the correct functional groups that are optimal for the adhesion of the required cell type(s). The extra cellular matrix (ECM) is formed of macromolecules which provided structural support to which cells can adhere it also provided functional cues through the cells physical interaction with the ECM and spatial relationship to other cells (Liu Tsang et al. 2007). Therefore, the ECM plays a critical role in cell function and survival *in vivo*; the requirements for cells to adhere to the ECM *in vivo* need to be considered when culturing hMSC *in vitro*.

2.7.2 Current Modification Methods of FEP

Due to the inertness of FEP, modification of the surface chemistry is most commonly achieved either by absorption or using high energy processes to break carbon-fluorine bonds and exchange the fluorine atoms with more reactive functional molecules such as hydroxyl groups. There are many reasons for the surface of FEP to be modified; these include improving wettability, increasing adhesion and biocompatibility (Kozlov & McCarthy 2004). For example, Ranieri et al (1995) utilized a radiofrequency glow discharge (RFGD) method when modifying FEP for neuronal cell attachment. Once the surface was modified with hydroxyl groups, laminin derived oligopeptides were introduced to the surface, a region of the peptide reacted with the hydroxyl group via a nucleophilic substitution reaction resulting in the peptide being immobilized on the FEP surface (Ranieri et al. 1995). This method enabled successful neuronal attachment, but it limited by the lack of control over the fluorine/hydroxyl group exchange which can result in a heterogeneous surface modification. RFGD can also not effectively be applied to FEP surface that difficulty to access such as the inside of a microcapillary tube.

There are a number of polymers which have been investigated to coat fluoropolymers and other hydrophobic materials in order to functionalize the surface. Poly-L-Lysine (PLL) and Poly-D-Lysine (PLD) are common coatings used to coat tissue culture plastic to promote cell attachment and growth (Harnett et al. 2007; Qian & Saltzman 2004; Mazia 1975; Quirk et al. 2001). PLL promotes cell adhesion through non-specific electrostatic interactions of the polycation with the negative charges of the

cell membrane (Quirk et al. 2001; Harnett et al. 2007). It has also been shown that PLL is able to absorb onto FEP under certain conditions (Shoichet & T. J. McCarthy 1991). Shoichet & McCarthy (1991) showed that PLL could absorb onto the FEP surface but only if a high enough molecular weight and when the PLL polymer is used at approximately pH11. At pH11, the PLL is thought to form a α-helix this structure along with the decrease in interfacial free energy drives the absorption of PPL to FEP (Shoichet & McCarthy 1991).

Poly-vinyl alcohol (PVA) has been shown to be absorbed from aqueous solution on to hydrophobic surfaces and successfully reduce the hydrophobicity of the surface (Kozlov & McCarthy 2004). PVA is unusual as it is both an atactic and semi crystalline polymer, properties which are thought to be why it can be absorbed onto hydrophobic surface. PVA contains reactive hydroxyl groups which results in similar surface chemistry as (John P. Ranieri et al. 1995) in terms of reactive functional groups.

Exactly how the absorption of PVA onto a hydrophobic surface is driven is still unclear but due to PVA having atactic and semi crystalline properties it is thought the process at the aqueous/sold interface is hydrophobic interaction driven resulting in absorption/crystallization of PVA at the aqueous/solid surface (Kozlov & McCarthy 2004). Kozlov et al. (2003) have stated that the molecular weight and degree of hydrolysis have been shown to have an effect. Kozlov et al. (2003) have shown that a higher molarity of PVA solution results in a thicker layer of coating, the outcome of which is a greater reduction of contact angle. The absorption capacity of a hydrophobic surface has been shown to plateau at 24h hours and no de-absorption of the subsequent PVA layer occurred after fourteen days in water (Coupe & Wei Chen 2001; Kozlov & McCarthy 2004). PVA has been shown to be irreversibly absorbed onto FEP after 96hrs (Wei Chen 2003). Though Kozlov et al. (2003) did investigate the effect of molecular weight on PVA absorption other studies did not justify the use of specific molecular weights for example Wei Chen (2003) only uses PVA with a molecular weight of 108,000.

PVA has been shown to absorb onto FEP but there is also evidence that PVA is not an optimal polymer for cell attachment. While FEP is too hydrophobic, PVA is considered too hydrophilic for cell attachment (Liu et al. 2009) and has been

presented to not support the adhesion and growth of a number of cell types (Zajaczkowski et al. 2003). The surface characteristics required for cell adhesion does vary depending on cell type (Rosso et al. 2004; Harnett et al. 2007; Trappmann et al. 2012) but for hMSCs there are no specific studies to show how well hMSCs adhere to and expand on PVA.

PVA is used to make hydrogels and electro spun scaffolds as it is a biocompatible and porous polymer that can mimic some of the *in vivo* architecture of the human body (Zajaczkowski et al. 2003; Song et al. 2012). To be able to overcome the inability for cells to adhere directly to PVA, studies have either mixed (ECM) mimicking macromolecules with the PVA in aqueous solution or functionalised the PVA surface with ECM proteins (Liu et al. 2009; Zajaczkowski et al. 2003; Song et al. 2012). Gelatin is a commonly used tissue culture coating; it is denatured collagen and is there for cheaper and easy to use than the structurally integral collagen (Paguirigan & Beebe 2006).

2.8 Angiogenesis, bioassays and hMSCs

There are many physiological processes which hMSC can influence with in the body through paracrine effects, immunomodulation has been previously discussed. There are conditions which require the processes of angiogenesis to be stimulated or controlled such as post ischemic injury and there are reports that hMSC may be able to accomplish this (Russo et al. 2014). Angiogenesis is the formation of new blood vessels that sprouting from existing blood vessels, blood vessels are critical for supplying oxygen and nutrients to cells and tissues, as well as removing cellular waste (Nakatsu et al. 2003; Ishak et al. 2014). The actual process of angiogenesis is a multi-step and tightly controlled biological procedure through pro- and anti-angiogenic factors that involve the endothelial cells (ECs) which, form the parent vessel, being stimulated to sprout and form new vasculature (Nakatsu et al. 2003). Angiogenesis is vital for tissue survival, however angiogenesis can also be damaging to tissues when not tightly regulated which is part of the pathophysiology of tumour formation (Walsh 2007). Activating and controlling angiogenesis has several potential therapeutic applications ranging from restoring blood supply to damaging tissue *in vivo* to forming new vasculature in tissue engineered products. Angiogenesis is such a critical process and though the process and be studied extensively the complexity and

involvement of multiple dependant and independent factors mean information in the field is continuously being updated (Richarz et al. 2017).

Fundamentally angiogenesis progresses when the ECs are stimulated and some of the ECs lining the blood vessel act as tip cells (TCs), the TCs react to gradients of signalling molecules within the microenvironment via filopodial extensions (Herbert & Stainier 2011). Filopodials are thin extensions of the plasma membrane which contain a high proportion of actin (Mattila & Lappalainen 2008), via filopodial sensing migration of the TCs can be guided (Gerhardt et al. 2003). As the TCs migrate into the interstitial space they are trailed by other ECs that have been stimulated to become stalk cells (SCs), SCs maintain the connection between the parent vessel and the sprouting vessel. The process of elongation and migration of the TCs and SCs is halted when the TCs make contact with other ECs and the mechanisms of anastomosis are initiated (Gerhardt et al. 2003). A summary of this process can be seen in Figure 8 which has been minimally adapted from Francavilla et al. (2009).
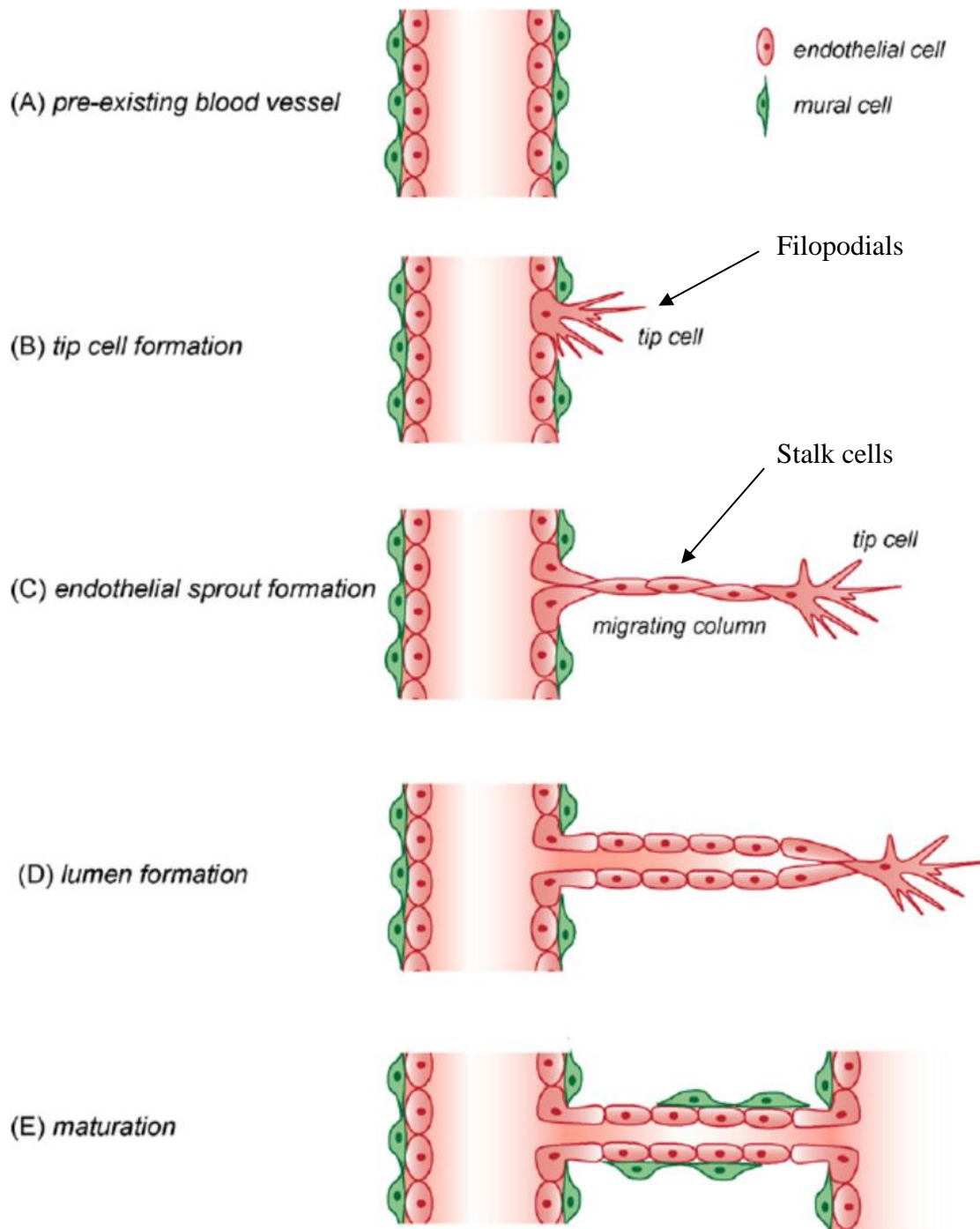
Figure 8 The process of EC activity during angiogenesis (Francavilla et al. 2009)

There are many factors which have been shown to play a role in positively or negatively regulating angiogenesis through intracellular communication. These include but are not limited to; angiogenin, angiopoietins, fibroblast growth factors (FGFs), hepatocyte Growth Factor (HGF), IL-8, platelet derived growth factor (PDGF), placental growth factor (PIGF), TGF-β, Vascular endothelial growth factors (VEGFs), endostatin, IL-12 and platelet factor 4. Signalling pathways such as the

notch signalling pathway also play a role in the regulation of angiogenesis via ligand-receptor binding. (Rehman & Wang 2006). Ligands and receptors expressed on the surface of the cells allow signals to be exchanged between neighbouring cells, this signals can be modulated and thus control the fate of the cell (Ahmed & Bicknell 2009).

Direct cell-cell interactions have a function within angiogenesis, however, hMSC are thought to primarily have an effect on angiogenesis due to the aforementioned secreted factors. VEGFs are part of the PDGF family, the VEGF family of cytokines and receptors play a key role in angiogenesis (Shibuya 2009). Five isoforms of VEGF, VEGF-A, B, C, D and E, have been identified, VEGF-A has been shown to play the key role in the regulation of angiogenesis(Shibuya 2011; Herbert & Stainier 2011). Many publications when using the term VEGF are referring to VEGF-A specifically. VEGF-A binds and activates two tyrosine kinase receptors, VEGFR-1 [Flt (Fms-like tyrosine kinase)-1] and VEGFR-2 [KDR (kinase insert domain receptor) (Shibuya 2009). VEGF-A has been shown to have a higher binding affinity to the VEGFR-1 receptor however the strength of the tyrosine kinase activity is greater via the VEGFR-2 receptor, triggering of the tyrosine kinase activates downstream signal transduction mechanisms that regulates ECs migration and proliferation and the initiation of the filopodial formation (Cross & Claesson-Welsh 2001) VEGF is the main cytokine investigated when developing strategies to target angiogenesis in tumour formation and therefore preventing the tumour from growing and surviving (Chuang et al. 2014).It was originally thought the VEGF receptors were only found on the surface on ECs making VEGF an ideal target to inhibit in order to supress tumour growth, however evidence is being found that other stromal cells also express these receptors (Duffy et al. 2013).

The proliferative effect of VEGF-A occurs in SCs, proliferation of the SCs is dependent on the concentration of VEGF-A, however TCs also respond to VEGF-A, but this response is gradient dependant (Herbert & Stainier 2011). FGFs have been shown to have an important role in angiogenesis, within the FGF family 22 ligands and 4 receptors have been identified (Presta et al. 2005; Yancopoulos et al. 2000; Ornitz et al. 1996). There are a number of mechanisms through which FGFs invoke angiogenesis these are primarily by stimulating tyrosine kinase receptors, heparan-sulfate proteoglycans, and integrins which are present on the surface of the

endothelial cells lining blood vessels (Presta et al. 2005). Acidic FGF (aFGF, also known as heparin binding growth factor 1 or endothelial cell growth factor) and FGF basic (also known as bFGF or heparin binding growth factor 2) are thought to be of particular importance for angiogenesis (Chen & Forough 2006; Ornitz & Itoh 2015).

Both VEGFs and FGFs can stimulate the endothelial cells to secrete molecules such as proteases such as metalloproteinases which in turn degrade the surrounding ECM (Herron et al. 1986). This then provides a region where the TCs can invade (Presta et al. 2005). There is also thought to be cross talk between FGFs and VEGFs, although the exact mechanisms are not fully understood (Presta et al. 2005). Work by (Murakami et al. 2011) provides strong evidence that the maintenance of the VEGFR-2 receptor independent on FGF via the activation of transcription factors, as VEGFR-2 has been shown to be the strong activator of the tyrosine kinase pathways deactivation of this receptor results in a reduction of the effect of VEGF-A. Therefore, successful initiation and speed of angiogenesis is not solely dependent on the levels of VEGF-A but also FGF. In fact too much VEGF-A would result in over vascularisation of tissues which is why VEGFR-1 receptors function is so important as it is able to act as a sink for excess VEGF-A without producing such a strong intracellular signal (Lieu et al. 2011).

While VEGFs and FGFs play key roles in initiation of angiogenesis, other factors are also involved in the recruitment of ECs to the newly forming vessel and the maintenance of the vessel. IL-8 is a member of the chemokine family and is a key factor in capillary tube organisation (Li et al. 2003). IL-8 binds to CXCR1 and CXCR2 receptors which can be found on ECs cells, CXCR1 and CXCR2 are G-coupled protein receptors (Heidemann et al. 2003a). Li et al. (2003) have shown the ECs cultured in IL-8 spiked medium has a higher proliferation rate and that when IL-8 activity is blocked in a tube formation assay capillary like structures fail to form. It should be noted that the tube/branch formation assay used in this work was only imaged after 6hrs therefore it cannot be determined if capillaries were formed and then degraded due to the absence of IL-8 activity.

PDGF is another cytokine involved in angiogenesis, however it does not have a direct action ECs to form new vessels, instead it up regulates VEGF, and in conjunction with VEGF and FGF-basic aid the recruitment of other cell types to mature the newly

formed vascular structure (Raica & Cimpean 2010). It has been demonstrated that PDGF-AA specifically dominates the VEGF regulation in angiogenesis, making PDGF-AA an essential autocrine regulator of VEGF and therefore angiogenesis (Shikada et al. 2005).

HGF, also known as Scatter Factor, is considered to be a potent mitogen. VEGF and HGF have been shown to activate distinctly separate signalling pathways but when combine both factors create a potent proliferative effect on ECs through the up regulation of a number of other growth factors and receptors (Gerritsen et al. 2003; Gerritsen 2005).

2.8.1 Angiogenesis bioassays

To study angiogenesis at the research level there are a variety of *in vivo* and *in vitro* bioassays. The *in vivo* assays involve the uses of animal models which are costly, time consuming and subject to ethical regulation, therefore relevant *in vitro* bioassays are more commonly used (Bischel et al. 2013). Many of the bioassays carried out *in vitro* need to replicate *in vivo* angiogenesis events involving ECs where factors such as ECM need to be considered. *In vivo* ECs are in contact on the basal (non luminal) surface with a thin, highly specialized ECM: the basement membrane. This matrix forms a continuous sleeve around the endothelial cells, and maintains the tube-like structures of the blood vessels. (Arnaoutova et al. 2009).The branch formation assay is one of the most popular surrogate angiogenesis assays used, measures the ECs ability to form capillary like structures. When carrying out the branch formation assay the ECM needs to be recreated *in vitro* usually by coating a microtiter plate with basement membrane proteins such as matirgel and Geltrex (Kleinman & Martin 2005). Coating the microtiter plate out manually the surface smoothness can be inconsistent which impacts the quality of the image however whether it impacts the function of the assay has not been established, but this is something which needs to be taken into consideration. In a branch formation assay disintegration of the ECM to prepare space for ECs to migrate into doesn't occur as the cells are in a single cell suspension. Post attachment to the ECM it is the motility, elongation of SCs and the maintenance of the structure which can be studied using the branch formation assay(Arnaoutova et al. 2009).

The angiogenesis assay is a useful tool to measure hMSC potency on ECs *in vitro.* While it could be used as a screening tool for hMSC cell donors to determine if the cells will function to the required level, it is not the optimal assay to be carried out in parallel with the hMSC scale up culture. Many of the measurements are taken between 4-8hrs after hMSC conditioned medium has been applied (Donovan et al. 2001; Lehman et al. 2012). Within this time the expression profile may have change in the cell culture which many have a different angiogenic effect.

2.8.2 hMSC cytokines relevant to angiogenesis

Many of the cytokines involved in angiogenesis have be shown to be secreted by hMSC, hypoxia has also been shown to improve the levels of angiogenic cytokines, it is well established in tumour angiogenesis that the process of established a blood supply in stimulated by the hypoxic tumour environment (Neufeld & Kessler 2006) Five cytokines know to have a functional role in angiogenesis have been proposed to be further investigated in this work, in terms of optimal combined potency are; vascular endothelial growth factor A (VEGF-A), basic fibroblast growth factor (bFGF), hepatocyte growth factor (HGF), platelet-derived growth factor (PDGF-BB) and Interleukin 8 (IL-8) /CXCL8 (Heidemann et al. 2003b; Kaga et al. 2012; Boomsma & Geenen 2012; Kwon et al. 2014b). IL-6 is also often analysed in experiments relating to angiogenesis. It is a multifunctional cytokine involved in immune regulation, haematopoiesis and inflammation (Fan et al. 2008). Although it is relevant to the angiogenesis work due to its multiple functions it lacks a strong single association to angiogenesis when in a multi-tissue environment (Tran & Damaser 2014).

Findings from a few studies detailed below are an example of the lack of continuity in the area of cytokine induced angiogenesis research. The culture methods vary in seeding density, FBS concentration and length of conditioning time, as well as the detection methods. Some of these issues have been highlighted by Ranganath et al. (2012), hypoxic preconditioning effects are also not well understood as well as being able to optimize the effect of hypoxia in terms of optimal cytokine secretion for an optimal duration. A number of methods have been used to determine the levels of cytokines secreted by hMSCs for angiogenesis applications in a variety of culture conditions. The methods used include antibody arrays, gene expression and ELISAs.

Kinnaird et al. (2004) conducted a broad-spectrum analysis of the cytokine coding genes that are expressed by hMSCs using the Affymetrix GeneChip platform. ELISAs were also carried out to determine the secretion levels of VEGF, bFGF, IL-6, PIGF and MCP-1. hMSCs were cultured for 72hrs in normoxic (20% oxygen) or hypoxic (1% oxygen) conditions, but seeding density was not stated. For the GeneChip array 8μg of total RNA was used to synthesize cDNA, HGF and PDGF showed no significant increase in hypoxic conditions (a >1.5 fold change was considered significant). However, VEGF-A gene expression increased 2.47 fold in hypoxic conditions compared to normoxic and bFGF showed a 1.62 fold increase, IL-8 results were not reported. The ELISAs were carried out using hMSC conditioned medium which was collected after 24hrs of culture. After collection the cells were lysed and total protein concentration determined, ELISA values were corrected for total cell protein. Five cytokines including VEGF, bFGF, and IL-6 were measured using sandwich ELISA kits from R&D systems. The reported level of VEGF-A, bFGF, and IL-6 secretion for normoxic and hypoxic (1% oxygen) are summarised in Table 1. The increase levels of cytokine detected corresponds to the gene expression results (IL-6 had a 2.26 fold increase in hypoxic conditions).

Table 1 Summary of VEGF, bFGF and IL-6 cultured under normoxic and hypoxic conditions from work carried out by Kinnaird et al. (2004).

Cytokine	Normoxic (pg/ml)	Hypoxic (1% O_2) (pg/ml)
VEGF	375	698
bFGF	2320	3970
IL-6	3885	7665

Kagiwada et al. (2008) investigated hMSC VEGF production *in vitro* and *in vivo* using both ELISA and an Angiogenesis Antibody Array I (RayBiotech, Norcross, GA, USA). Results for the array were based on presence/absence of spots or intensity. ELISAs were used to determine *in vitro* VEGF secretion over 9 passages (P2-P10) from 3 different donors. Cells we seeded at P2 with a density of 4×10^5 cells/100mm

culture dish, culture medium was collected after 3 days, and the cells we then passaged and reseeded at the same density. The procedure was repeated until P10. VEGF secretion levels across all passages and donors ranged from $300pg/ml/10^6$cells to $850pg/ml/10^6$cells. To measure VEGF production *in vivo* hMSCs were seeded on to hydroxyapatite discs at passage 2 with a density of $2.5x10^5$ cells/disk. The disks were implanted into the backs of mice and harvested after two or four week. VEGF production was estimated by grinding down the implants and separating the supernatant, the supernatants were then used for ELISA assays. The VEGF levels after 2 weeks' implantation were 49.4 ± 3.81 pg/implant and 43.9 ± 6.08 pg/ implant at 4 weeks.

Park et al. (2009) cultured hMSCs under standard culture conditions at a density of $2x10^3/cm^2$ cells, cells and medium were collected and the early 3rd passage. The culture medium was diluted either 4 or 20-fold and then applied to Human Cytokine Arrays VI and VII (Ray Biotech Inc, Norcross, GA), detection was by enhanced chemiluminescence captured on X-ray film. Semi- quantification was conducted using the average gray-scale of the positive control and negative controls to normalise. Expression levels were reported as average intensity: PDGF-BB as 6.5, HGF as 21.9, IL-8 as 112.5 and bFGF 10.5. The paper reported array intensities of 60.3 and 26.9 for VEGFB and VEGFD respectively but did not report finding from VEGF-A which is considered the most influential and most studied form of VEGF in angiogenesis (Lehman et al. 2012). The study does not provided fully quantitative data

Kwon et al. (2014) used hMSCs from a number of donors at passage 5 and seeded them at $1.6x10^6$ cells in 1 T-175 (density of $9.1x10^3/cm^2$), the cells were cultured in DMEM completed with 10%FBS. To condition the medium after 24hrs the cells were washes with PBS and the medium was replaced with DMEM containing 1% FBS and incubated for 72hrs. The conditioned medium was then tested for the presence of seven growth factors and cytokines Including VEGF, HGF, IL-6 and PDGF-AA. The level of VEGF measured ranges from 336.1 ± 11.1 (pg/ml) to 428.2 ± 30.1 (pg/ml), PDGF-AA was 2.5 ± 0.8 (pg/ml) to 3.1 ± 1.1 (pg/ml), HGF 169.7 ± 18.0 (pg/ml) to 283.5 ± 26.6 and IL-6 28.0 ± 0.7 (pg/ml) to 71.0 ± 2.7 (pg/ml).

It is difficult to draw direct comparisons from these studies, each used different culture containers, densities and detection methods. It highlights a more wide spread issue in the field that it is not always possible to draw conclusions based on work from multiple research groups, therefore conclusions can only be specific to a small subset of experimental parameters which may not be applicable to commercial applications. There is also significant number of cytokines that are produced by hMSCs with up to 120 being identified (Park et al. 2009) yet not all will have a significant role in angiogenesis. The aforementioned studies look at a number of cytokines know to be secreted by hMSCs and play a role in inducing angiogenesis however the studies have only chosen a small number of cytokines for example Kwon et al. (2014) only looked at PDGF-AA but PDGF-BB and PDGF-AB which have been shown to have a role in angiogenesis (Yancopoulos et al. 2000; Boomsma & Geenen 2012; Vertelov et al. 2013). It has been determined that IL-8 has an angiogenic effect (Petzelbauer et al. 1995; Heidemann et al. 2003b) and is secreted hMSCs (Park et al. 2009) but it is not as well reported in the area of hMSC induced angiogenesis as VEGF. It is a large undertaken to define the CQA needed in an hMSC population to induce the MOA required, the task is complicated as the full angiogenesis mechanisms are not completely defined.

Looking at cytokine detection form the perspective of hMSC manufacturing the sample preparation methods and relevance need to be considered. For example in the work carried out by Kinnaird et al. (2004) the cells were lysed to determine cytokine levels, intracellular cytokine production is not relevant when using CTP or analysing how much hMSC produce as the cytokines need to be secreted in order to invoke an effect. Extra sample preparation steps also increase the time taken for analysis and maybe a hurdle to online or inline product analysis.

Bioanalytical methods need to improve in order for more cell therapy products to satisfy safety and regulatory requirements, successfully bringing much needed treatments to the market. The issues which have been mostly spoken about in the cell therapies context are also applicable to the wider regenerative medicine field. Microfluidics is a promising filed which can address many of the cost and time challenges associated with currently used bioanalytical methods. However, as many of these devices intricate devices are at the research stage it is yet to be determined if the devices can be reliably and cost effectively manufactured. As cytokine expression

is a key element of hMSCs regulating biological processes immunoassays are of particular importance in the bioanalytics needed for hMSC. Bioassay give a greater insight into physiological effects of hMSC, angiogenesis is the main bioassay focus of this review. As it is not feasible to run a bioassay inline or online with the cell manufacturing process they could be used to determine the cytokine panel and respective ranges needed to achieve a specific level of angiogenesis. The cytokines could then be measured in parallel to the culture process using rapid microfluidic detection methods such as the MCF ELISA, giving close to real time values. Real time values enable a more reactive manufacturing process; if the levels of cytokines are not being reached the manufacturing process can be ended saving time and money. From another perspective if a donor cell population reach the required values more rapidly than anticipated the treatment can be administered to the patient sooner.

2.9 Aims and objectives

The aim of this work was to examine the culture conditions of hMSCs and the effect of the culture environment on the promotion of angiogenesis by using a surrogate *in vitro* bioassay. This work aimed to identify the challenges of studying this therapeutic application and proposes the utilisation of microfluidics to overcome these challenges.

2.9.1 Objectives

- Determine the impact on the secretome profile of five cytokines when culturing hMSCs from four donors at three different atmospheric oxygen concentrations and cultured over 3 passages by analysing the conditioned culture medium.

- Improving the amount of data obtained when analysing hMSCs functionality in relation to angiogenesis using an *in vitro* bioassay and assessing the challenges of using this assay.

- Assess the levels of relevant pro-angiogenic cytokines present in the conditioned medium used in the bioassay. Determine the relationship between these levels and the data obtained from the angiogenesis bioassay.

- Evaluate the feasibility of using a microcapillary film (MCF) based enzyme-linked immunosorbent assay (ELISA) for the detection of the cytokines previously measured.

- Adapt the MCF to facilitate the culturing of hMSCs with a view to develop an all in one pre-screening tool for hMSC function or a hMSC based assay.

- Identify the overarching issues of culturing hMSCs to be used in cell therapies through a review of the literature and lessons learnt during the experimental studies of hMSC.

2.9.2 Hypothesis

Hypothesis 1: The hMSCs secretome profiles of VEGF-A, bFGF, HGF, PDGF-BB IL-8 /CXCL8 exhibited the same trends under three different atmospheric oxygen concentrations independent of the cell donor.

Hypothesis 2: Translating a plate-based ELISA assay into an MCF based microfluidic platform reduces the time between the addition of sample to result.

Hypothesis 3: The surface of FEP can be modified to improve the culture of viable hMCS.

3 Manufacturing of hMSCs for pro-angiogenic therapies

3.1 Introduction

With the use of hMSCs for promoting angiogenesis in diseased tissue and engineered tissue further knowledge is required to understand the consistency of hMSC behaviour between donor populations. Angiogenesis activity is accelerated in oxygen environments below normal physiological levels. A condition which tumour formation takes advantage of (Krock et al. 2011), but which is also looking to be exploited in the development of new therapies. Most hMSC culturing methods are carried out at atmospheric oxygen conditions however this is not truly representative of the oxygen levels the cell are exposed to *in vivo* as dissolved physiological oxygen concentration is less than the atmosphere (Rosová et al. 2008). Work has been carried out in the area of hMSC preconditioning at lower oxygen levels to improve hMSC performance for a variety of treatments including treating ischemia through promoting angiogenesis (Mirotsou et al. 2011), however little has been done identifying the challenges of bring consistent hMSC treatments to market. This Chapter explores the variation between four hMSC lines obtained from four different donors over three passages cultured in 3 different oxygen environments atmospheric, 5% oxygen and 2% oxygen. This study also examines the methods used to determine the angiogenic capacity of hMSCs via the application of an angiogenesis bioassay. While hMSC are the cell type used many of the lessons learnt are applicable to other cell types and bioassay in terms of the methods used to obtain samples for analysis, the handling of the samples and the analysis of the data. The donor variation is investigated from the point of view of hMSCs promoting angiogenesis via cytokine production. There is a plethora of research aiming to ascertain the paracrine effects of hMSCs on a number of biological processes including immune regulation, neurogenesis and angiogenesis (Doorn et al. 2012; Bang et al. 2005; Liang et al. 2014). The mechanisms involved in processes such as angiogenesis are complex involving feedback mechanisms, other cell types and signal cascades (as mentioned in Chapter 2, Section 2.8), therefore there is yet no single indicator that an hMSC line will invoke the required signalling for successful angiogenesis. There is

more than likely a combination of factors which need to be measured in order to have a truly reliable and predictable profile.

As discussed in the literature review (Section 2.6.1) there are several hMSC based treatments currently in trials being used to treat patients with a variety of conditions including those with cardiac tissue damage induced by myocardial infarction where the hMSCs ability to stimulate angiogenesis is believed to be a key factor in its MOA. However success has varied (Suna Wang et al. 2015) which may be due to a number of reasons including that many of the treatments use autologous hMSC and therefore the starting material is not consistent in every treatment. The response of the patients' cells *in vivo* to the cytokine stimulation may vary between patients with some patients requiring higher concentrations of some cytokines compared to others. The variation of patient response to the same treatment has given rise to the concept of precision medicine, where by treatments need to be tailored to the individual not to the majority (Collins & Varmus 2015). There is currently only defining criteria for hMSC cell identity (Rasini et al. 2013) but not criteria for a hMSC cell line that will guarantee the promotion, to the required level, of angiogenesis *in vivo*. Consequently, pre-screening hMSC should be a requirement and data obtained for the individual donors regarding the secretome profile of the hMSC line also collected. As well as donor variation the impact of cell treatment post thaw and atmospheric culture conditions were also investigated. The impact of cold shock during the cryopreservation of cells has been shown to effect the growth rate recovery time posy thaw (Xu et al. 2012), therefore it is important to determine if this also effects the cells ability to secrete cytokines. There is evidence that by reducing the atmospheric oxygen levels during hMSC cell culture cell growth and stability increases (Estrada et al. 2012). In cancers angiogenesis is stimulated by the hypoxic conditions, hMSC have also been shown to increase the production of some cytokines most notably VEGF in hypoxic conditions (Potier et al. 2007). Thus culturing of hMSC in lower oxygen environments is not only relevant to mimic physiological conditions but the environment may also enhance the angiogenic potential of the cells. Post thaw recovery and controlling culture conditions are central features of cell therapy manufacturing, therefore any improvements or adverse effects of these processes needs to be established, including whether those effects are donor specific or a constant affect across all lines.

Five cytokines PDGF-AA, FGF-basic, IL-8, VEGF and HGF; that have been shown to be involved in angiogenesis and have been previously shown to be produced by hMSCs (Boomsma & Geenen 2012; Bronckaers et al. 2014) were screened for in hMSC conditioned medium using Luminex technology. Four different hMSC donor lines were used to produce conditioned medium. As hypoxia has also been shown to increase the levels of proangiogenic cytokines (Potier et al. 2007), therefore all four hMSC lines we cultured in 2% oxygen, 5% oxygen environments and compared to controls cultured at atmospheric oxygen levels. The 5% atmospheric oxygen environment is also considered to be more relevant as a hypoxic chamber was not available the cultures were carried out in an oxygen level controlled incubator Investigating the effects of hypoxia provides important information on the cell behaviour from a manufacturing point of view and a treatment point of view. From a manufacturing perspective controlling the oxygen levels could be a low cost method of increasing cytokine yield when manufacturing hMSC, however the yield from the system as a whole needs to be considered. While reducing oxygen levels in the manufacturing system could increase the per cell yield, this gain could be counteracted with a reduction in cell growth. Physiological oxygen levels depending on the tissue type can range from 1-11% (Carreau et al. 2011), therefore, if hMSCs are administered directly as a treatment the secretome profile at lower oxygen levels in important. When administering hMSC to a tissue that requires improved vasculature the oxygen environment of that tissue is below normal physiological oxygen levels as the tissue is usually ischemic (Suna Wang et al. 2015; Anderson et al. 2016)hence differences in branch formation and cytokine secretions across a range of oxygen concentrations needs to be investigated.

Conditioned medium samples were run on an *in vitro* HUVEC based branch formation assay (also called tube formation assay) to determine the angiogenic effects of the conditioned medium (Arnaoutova et al. 2009). The branch formation assay allows many of the processes of angiogenesis to be studied as a whole as opposed to individual steps these processes include cell adhesion, migration, alignment which result in overall branch formation followed by degradation of the branches which is an indicator of protease activity. The branches form capillary like network and are therefore an indicator on how well the conditioned medium/lines will perform *in vivo*, all though true *in Vivo* performance is only truly known when live animal studies

have been conducted. The branch formation assay has been used is tandem with *in Vivo* animal studies and is considered to be a realistic representation of *in Vivo* activity (Donovan et al. 2001; Lehman et al. 2012).

This Chapter aims to determine the PDGF-AA, FGF-basic, IL-8, VEGF and HGF secretome profile in four hMSC lines (M2, M3 M6 and Rooster); in standard culture conditions compared to 2% and 5% oxygen culture conditions. Fresh medium was added to the cells on day 3 of culture and conditioned for 48hrs. Using conditioned medium from hMSCs is a cost effective method of delivering paracrine factors to a patient. This approach negates the regulatory and safety hurdles of delivering live cells to a patient and has a simpler route to market compared to live cells, as biologics are a common pharmaceutical treatment. Therefore the experimental protocol was designed to reflect a realistic treatment option, but insight into live hMSC treatments was also gained. The age of the cells is also being investigated to determine if potency changes as the passage number increases and impact of post thaw recovery. The impact of lower oxygen levels on the secretome profile and variation at lower atmospheric oxygen levels across all three passages compared to standard oxygen conditions is also examined.

3.2 Materials and Methods

3.2.1 Materials

Low glucose Dulbecco's Modified Eagle Medium (DMEM), phosphate buffer saline (PBS) Bone marrow derived human Mesenchymal stem cells (hMSCs), ultra glutamine 200mM were purchased form Lonza (Slough, UK). Fetal Bovine Serum (FBS), Trypsin 0.25% (1X) Solution with 0.1% EDTA, human Umbilical Vein Endothelial cells (HUVECs), Medium 200PRF, Low Serum Growth Supplement, Geltrex lactose dehydrogenase elevating virus -free reduced growth factor basement Membrane Matrix, Trypsin/Neutralising Solution and Suramin, hexasodium salt StemPro osteogenesis, adipogenesis and chondrogenesis differentiation medium kits were procured from ThermoFisher Scientific (Paisley, UK). NucleoCounter® NC-3000 and Via1-Cassett were obtained from Chemometec (Allerod, Denmark). A Galaxy 107R CO_2 incubator with oxygen sensor was purchased from Eppendorf UK Limited (Stevenage, UK). Silver nitrate solution (2.5% solution) naphtol AS-MX

phosphate alkaline solution, Fast Violet B salt grade III, Oil Red O powder, Alcian blue powder; fixation buffer (4% para-formaldehyde), 0.1 N Hydrochloric Acid (HCl), and 99% isopropanol were brought from Sigma (Dorset, UK). Luminex assay kits (LXSAHM-05) with analytes: CXCL8/IL-8 (BR18) FGF basic (BR47) HGF (BR66) PDGF-AA (BR56) VEGF (BR26) purchased from Bio-Techne, (Abingdon, UK). Biostation CT was manufactured by Nikon Instruments Europe and Nikon CL Quant software (Amsterdam, Netherlands). CD73 (PE-Cy7), CD90 (APC), CD105 (PE) and HLA-DR (FITC) antibody conjugates were purchased from BD Biosciences (UK).

3.2.2 Cell Culture

Human mesenchymal stem cells were cultured in low glucose DMEM supplemented with ultra-glutamine 2nM and 10% v/v fetal bovine serum (FBS). Cells were seeded in T25 flasks at a density of 5000 cells/cm^2 and cultured in 5mls medium for five days with a medium change on day three. Cell cultured was carried out at 37°C, 5% carbon dioxide with 95% humidity and either 2%, 5% or atmospheric oxygen levels. At separate times two vials for each line were thawed, each vials was divided between 8 T25 flasks, 4 flasks from one vial were cultured at 5% oxygen and the other 4 flasks from the same vials cultured under atmospheric oxygen as the control condition. This process was repeated for the second vial and the experimental condition was 2% oxygen.

Cell passage was undertaken on day five; all medium was aspirated and placed in a sterile centrifuge branch then frozen for later use. The flask gently washed with PBS added at a volume 0.2ml/cm^2 then aspirated. Cells were detached using trypsin 0.25% (1X) solution with 0.1% EDTA at a volume of 0.04ml/cm^2, the cells were incubated with the trypsin solution at 37°C for 3-5mins; detachment was checked visually using an inverted light microscope. The trypsin was inactivated by quenching with the cell culture medium. The cell suspension was aspirated into a centrifuge branch; 0.5ml removed to an eppendorf branch for cell counting. The centrifuge branch was centrifuged at 220g for 5 minutes, the supernatant aspirated away and the cell pellet re-suspended in the culture medium. Cells were seeded on a new surface at a density of 5x10^3/cm^2 with a culture medium volume of 0.2ml/cm^2.
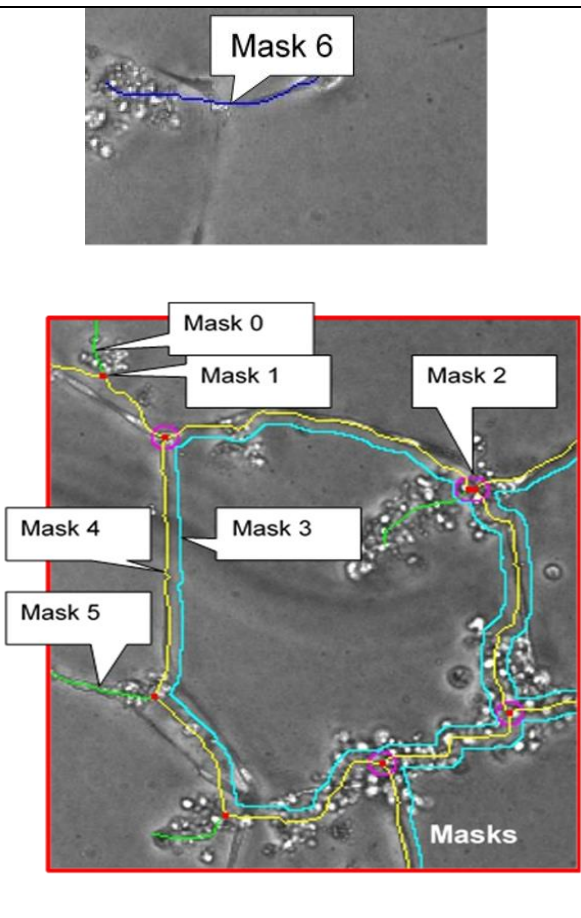
Cells from four donors were cultured in this work labelled M2, M3, M6 and Rooster, these were internal cell donor labels.

3.2.3 Branch formation assay

Geltrex was treated as per manufactures instructions, 95µl was used per well to coat wells in a 24 well plate, then placed in an incubator for 30mins at 37°C. The previously collected hMSC medium was thawed in a water bath at 37 ^{o}C. Containers were inverted for mixing and 1ml of conditioned hMSC medium was added to each well and placed in incubator at 37°C. HUVEC cells were seeded in a T75 at a density of $2.5x10^3$/cm^2, cultured in M-200 supplemented with LSGS till 80% confluent under standard conditions of 37°C, 5% carbon dioxide with 95% humidity and atmospheric oxygen levels. Medium was changed after 24hrs then every 48hrs till 80% confluence was reached. Passage was carried out by aspirating medium then washing cells with PBS. 0.01% EDTA at a volume of 0.047ml/cm^2 was added and the cells incubated at room temperature for 3mins, detachment was checked visually using an inverted light microscope. Trypsin was quenched with 3mls trypsin neutralizer solution the flask was further washed with 3mls trypsin neutralizer solution. A 0.5ml sample was taken for cell counting and the cell suspension was centrifuged at 200g for 7 minutes. Liquid was aspirated from the cell pellet and the pellet was resuspended to a concentration of $5.5x10^5$/ml, 100µl of cell suspension was added to each well containing conditioned medium in the 24 well plates. Positive controls used 1ml fresh DMEM and negative controls were 1ml fresh DMEM with 10µl Suramin. The plate was then put into the Biostation CT and a 7 mmx7 mm area at 4x magnification of each well was imaged using a phase contrast setting every 20 minutes for 24 hours. Branch length and node formation was determined by image analysis using Nikon CL Quant software. The software processing and data out puts are summarised in Table 2. The image processing recipe which was custom developed for the CL Quant software. The software provides 5 data out puts, in this work the count which is the number of branches (referred to as lines by the software) between two nodes were used in the data analysis. The mean branch length of the branches between two nodes was also used. Though total branch length would also have been informative image quality issue arose in the lower oxygen concentrations. Debris within the wells resulted in poor image quality and there for the software was falsely reporting nodes

and extra branch length. By using branches which were connected to two nodes the data was more reliable. The optimisation of this assay including seeding density and optimal surface coating was carried out in conjunction with Alexander Chan (Chan 2016).

Table 2: Branch formation assay image processing methodology in Nikon CL Quant software.

Mask	Output data	
Mask0: Tubes connecting to one node point or two node points	Count(Mask4)	
Mask1: Node points	Mean of Ph-Mask 4 Line length	
Mask2: Node points connecting to more than 3 "Mask4" tubes	Number of nodes(Mask1)	
Mask3: Closed tube	Total of Ph-Mask 0 Line length	
Mask4: Tubes connecting to two node points	Total of Ph-Mask 4 line length	
Mask5: Tubes connecting to one node point		
Mask6: Tubes connecting to no node point		

3.2.4 Luminex analysis

A multiplex five cytokine panel analysis was carried out as per manufactures instruction. 50µl of sample was added per well, and each well was analysed for PDGF-AA, FGF-basic, IL-8, VEGF and HGF quantities.

3.2.5 Differentiation assays

Differentiation assays were carried out using StemPro kits purchased from ThermoFisher Scientific (Paisley, UK). The kits contained a basal medium (adipocyte differentiation basal medium and osteocyte/chondrocyte differentiation basal medium) which was completed with either an adipogenesis supplement, osteogenesis supplement or chondrogenesis supplement. The manufacturer does not provide further details regarding specific molecular components found in the medium or supplements.

3.2.5.1 Adipogenesis

The hMSCs were seeded in a 12 well plate at a density of $2.5x10^3$ cells/cm^2, with 2mls completed DMEM. After 24hrs the DMEM was aspirated and 2mls adipogenesis differentiation medium was added to each well. Cells were culture for 21 days with differentiation media changes every 3 days. After 21days cultures were fixed by washing 3 times with PBS, 1ml fixation buffer was added to each well and incubated for 30mins at room temperature. The wells were then washed three times with PBS. Cells were stained by adding 1ml of a 1.8mg/ml working solution of Oil Red O to each well and incubated at room temperature for 5mins. Oil Red O is a fat-soluble dye which statins lipids present in adipocytes (Nunnari et al. 1989). Wells were then washed with deionised water until the water ran clear imaged under a light microscope.

3.2.5.2 Osteogenesis

Cells were seeded in a 12 well plate at a density of $2.5x10^3$ cells/cm^2, with 2mls completed DMEM. After 24hrs the DMEM was aspirated and 2mls osteogenesis differentiation medium was added to each well. Cells were culture for 21 days with differentiation media changes every 3 days. After 21days cultures were stained for alkaline phosphatase using a 4% v/v solution of naphtol AS-MX phosphate alkaline solution in Fast Violet B salts, alkaline phosphates is indicative to osteoblasts (Addison et al. 2007). Sliver nitrate staining was used to show the presence of insoluble calcium phosphate salts which is indictive of bone tissue (Schmitt et al. 2008). Cell cultures were fixed by washing 3 times with PBS, 1ml fixation buffer was added to each well and incubated for 30mins at room temperature. The wells were then washed 3 times with PBS. Cells were stained first with 1ml of a 4% v/v solution of naphtol AS-MX phosphate alkaline solution in Fast Violet B salts

solution, the plate was incubated in the dark for 45mins and then washed 3 times with deionised water. 1ml of 2.5% silver nitrate solution was added to each well and incubated at room temperature under UV for 30mins. The cells were washed in deionised water 3 times then imaged under a light microscope.

3.2.5.3 Chondrogenesis

Post cell count and centrifugation cells were resuspended at 1×10^7 cells/ml. 5 x 5μL droplets of concentrated cell suspension were pipetted per well of a 12 well plate in order to form micro masses. The plate was then placed in the incubator at 37°C, 5% carbon dioxide with 95% humidity for 1-2hrs. Without disturbing the micro-masses 1ml of warmed chondrogenesis differentiation medium was added to each well. Cells were cultured for 21 days with differentiation media changes every 3 days. The cultures were then stained for the presence of glycosaminoglycans using alcian blue, glycosaminoglycans are indicative though not exclusive to cartilage (Mallinger et al. 1986). Micro-masses were then fixed by washing 3 times with PBS; 1 ml fixation buffer was added to each well and incubated for 30mins at room temperature. Micro-masses were stained with a filtered solution of 1%wt/vol of alcian blue (powder) in 0.1N HCl, 2 mls was added to each well and incubated at room temperature for 1hr. The solution was aspirated, and the micro masses washed with 0.1N HCl solution 3 times with 1 mL/well and then 2 times with deionised water. The micro masses were then imaged under a light microscope.

3.2.6 Flow cytometry analysis

In a 96 conical clear well plate hMSCs were seeded at a density of 2×10^5 cells/well, the plate was centrifuged for 5 min at 250g to obtain cell pellets in wells. The supernatant was aspirated and each pellet resuspended in 200 µl staining buffer, the plate was briefly vortexed and centrifuged for 5 min at 250g and the supernatant aspirated. 0.5µl of anti-human fluorescently tagged CD73, CD90, CD105 and HLA-DR antibodies (see Table 3 for details) were added directly to cell pellets, the cell pellets were then resuspended and an additional 50 µl staining buffer was added to each well. The cells were incubated with the antibodies for 30 minutes in the dark at room temperature. The plate was then centrifuged at 250g for 5 min and the supernatant aspirated. The antibody cell pellet was washed x2 with 200 µl of staining buffer, then resuspended in 200 µl of staining buffer. Cells were analysed using a 4-

colour panel on the FACS Jazz. This protocol is based on a paper published by Chan et al. (2013).

Table 3: Detail of antibody-fluorophore conjugates and respective emissions spectra used in flow cytometry analysis of hMSCs.

CD Antibody	Fluorophore conjugate	Excitation max	Emission max
CD73	PE-Cy7	496 nm	785 nm
CD90	APC	650 nm	660 nm
CD105	PE	496 nm	578 nm
HLA-DR	FITC	494 nm	520 nm

3.2.7 Statistical analysis

Evaluation of cytokine data and branch formation assay data was carried out using GraphPad Prism 7 purchased from GraphPad Software (California, US).

3.3 Results and Discussion

3.3.1 Characterisation of hMSC lines

The minimum criteria for characterising hMSC according to Rasini et al. (2013) is based on the ability for the cells to adhere to tissue culture plastic, the ability for the cells to differentiate down the adipocyte, osteocyte and chondrocyte linages and to display certain phenotypic markers while being negative for surface markers associated with other cells. In this work CD90, CD73 and CD105 are used as positive phenotypic markers and HLA-DR negative (Chan et al. 2013). The four donor cell populations used in this work were first characterised after growth in standard control conditions at passage P2 and P3.
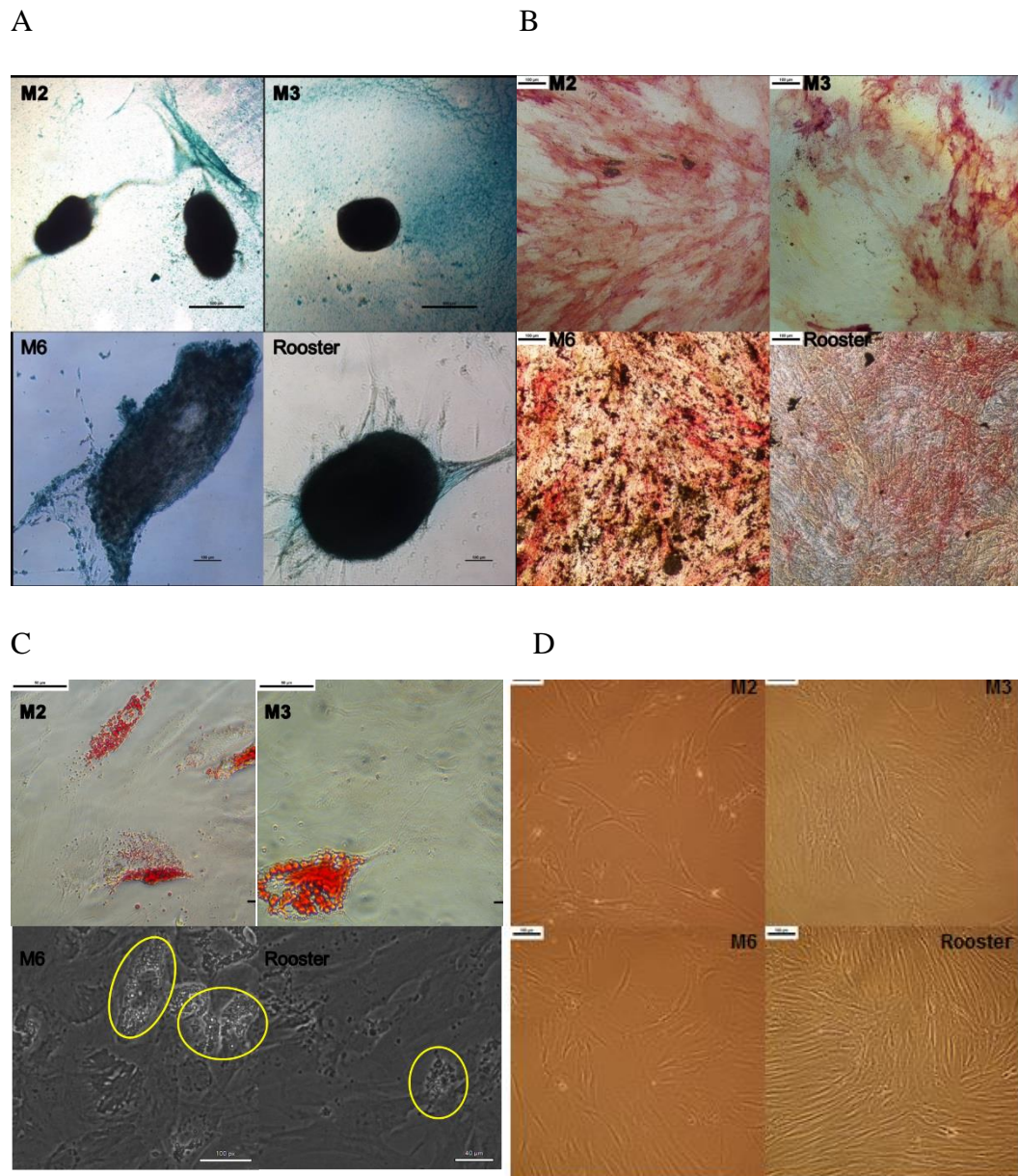
Figure 9 Histology of differentiated lines taken in phase contrast. A) Chondrocytes stained with alcian blue, scale bar 500µm B) Osteocytes stained with Fast Violet B Salt with 4 % (v/v) naphthol AS-MX phosphate alkaline solution, scale bar 100µm C) Adipocytes, M2 and M3 stained with Oil Red O, M6 and Rooster lines are imaged in phase contrast unstained, scale bar 100µm. Yellow circles highlight the lipid vacuoles. Each image is representative of 3 wells (n=3) D) Control hMSC lines plastic adherence at P2 imaged on day 6 under standard cell culture conditions. Imaged in phase contrast with 100µm, scale bar. Images representative of n=3.

Table 4 Flow cytometry analysis of M2, M3, M6 and Rooster donors. All four cell lines were positive for CD105 (PE) and CD90 (APC) and negative for HLA-DR (FITC). Over all there were some equipment issues which affected the quality of the results subsequently the results for CD73 (PE-Cy5) are unclear. This is discussed further in the chapter.
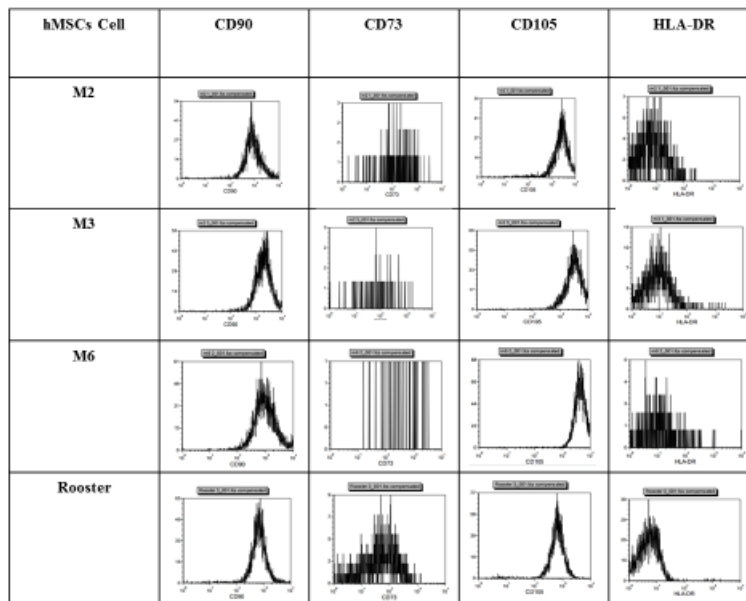
M2, M3, M6 and Rooster lines demonstrate tissue culture plastic adhere (Figure 9D), the cell cultures *in vitro* display the fibroblast spindle like morphology that is commonly referred to the literature as the typical morphological traits of hMSCs (Gebhardt et al. 2003; Ullah et al. 2013). After 6 days in culture the rooster line achieves full confluence compared to M2, M3 and M6 lines, giving an early indication that there may be a difference in growth rates between lines. The four lines are all able to differentiate down the adipocyte, chondrocyte and osteocyte lineages (Figure 9). All four lines formed microspheres and stained positive for alcian blue (Figure 9 A) which confirms the presence of cartilage proteoglycans (Ullah et al. 2012). Alkaline phosphatase staining (red) was positive in all lines when under osteogenic differentiation conditions (Figure 9 B). The M6 line produced more areas that stained positive for mineralisation (black) compared to the M2, M3 and Rooster lines. M2, M3, M6 and Rooster lines all show under phase contrast lipid

vesicle formation, the M2 and M3 cultures were stained with Oil Red O which has been taken up by the lipid vesicles (Figure 9 C). One of the challenges of histological analysis of hMSC differentiation is the method is difficult to accurately quantify. Consequently, while one donor line maybe more efficient at differentiation it can only be determined whether or not the cells are capable of differentiating and are therefore the starting material can be classified as hMSCs.

Some of the data presented in Table 4 is not very clear; this was due to issues with the voltage while the measurement was taken however all four cell lines were positive for CD90, CD73 and CD105 and HLA-DR negative. Due to the voltage issues it was not possible to fullly quantify the population percentage which displayed the aforementioned markers. The cell lines analysed in the work have been used by other researchers from the same facility. Some of this work has been published which further supports the premise that these cell populations are hMSCs (Chan et al. 2013; Rafiq et al. 2013; Heathman et al. 2016; Rafiq et al. 2018).

While the M2, M3 M6 and Rooster donors meet the minimal criteria (Dominici et al. 2006) for hMSC identification, it is not possible to assume that all four donors are completely identical. Some differences have already been shown in levels of confluence achieved in the same culture period (Figure 9 D), and level of mineralisation when differentiated down the osteogenic lineage (Figure 9 B). Variation of the population doubling times (PDT) between lines and passage numbers can be seen in Figure 6. The Rooster line had the fastest PDT at passage 2 (~0.5 days) this concurs with evidence (Figure 9 D) that the line is fast growing over 5 days compared to M2, M3 and M6. At P2 M2, M3 and M6 have a PDT of less than 2 days in all culture conditions, in the M6 line a PDT of ～2 days is maintained across all three passages. The PDT of P3 2% oxygen significantly increases ($P<0.05$) in the M2 and M3 lines with PDT in excess of 6 days. In the M3 line at P4 the atmospheric oxygen control for the 5% oxygen PDT also significantly increases compared to P3. Differences can also be seen between the controls in M2 and M3 at P4, in the M2 line (Figure 10A) PDT for the 2% control remains below 2 days, however in the 5% control the PDT increase to over 2 days. PDT is important from a manufacturing perspective as higher yields can be achieved in a shorter time therefore decreasing costs (Davie, et al 2012). When considering the possible reasons for this variation between the controls three main factors need to be considered, the control cells were

thawed from separate vials, at separate times therefore did the thawing processes cause cell damage and thus an increase in PDT. The M2 and M3 lines were cultured at the same time in the same incubator; during P4 the incubator environment could have been compromised resulting in a decreased growth rate. The cells were also passaged at the same time, if there was an issue with the NucleoCounter the potential errors in counting would result in inconsistent seeding density, seeding density has been shown to be an influence in cell growth rate (Thomas et al. 2007).

When examining the *in vitro* growth rates of other cell types such as hESC and iPSC, high growth rates are not automatically assumed to be a positive attribute. Enhancement of hESC and iPSC proliferation rates *in vitro* has been shown to be linked to changes in the cells karyotype and an indication of tumorigenicity, this is thought to be more of a safety issue in pluripotent stem cells but multipotent stem cells such as hMSCs are also susceptible (Knoepfler 2009). From a manufacturing standpoint the rate of cell proliferation must also be balanced with consistency between batches.

Figure 10: Population doubling times in days of M2 (A), M3(B), M6 (C) and Rooster (D) lines cultured in 2% or 5% atmospheric oxygen compared to a control cultured in 20% atmospheric oxygen. Mean values and standard deviation of n=4 are shown Two-way ANOVA was performed, significant differences (P = ≤ 0.05) were seen indicated by *.

3.3.2 Secretome profile of hMSC lines

A number of factors are being investigated when looking at the secretome profile of the four hMSC lines, firstly the difference between each line for each of the five cytokines (PDGF, FGF-B, IL-8, VEGF and HGF), secondly does the oxygen level affect the cytokine production, and thirdly does the passage number and therefore the age of the cells affect cytokine production.

Figure 11: PDGF secretome profile of M2 (A), M3(B), M6 (C) and Rooster (D) lines cultured in 2% or 5% atmospheric oxygen compared to a control cultured in 20% atmospheric oxygen. Samples were collected after 48hr of conditioning with the hMSCs which were on day 5 of culturing. Expression quantities calculated per cell based on the per ml value divided by the cell number at the end of the passage, n=4 and standard deviated is shown

Across all four lines and all three passages PDGF expression does not exceed more than 0.3fg/cell (Figure 11). It is difficult to draw direct quantitative comparisons from the literature however PDGF expression has been reported as being lower compared to other cytokines in the same sample, Kwon et al. (2014) reported PDGF production

between 2.5pg/ml-3.1pg/ml, no per cell values were given but cells we cultured at a higher density of 1.6×10^6 in T175 flasks.

From a cryopreservation recovery aspect, the M2 and M3 show an increase in PDGF production after the first passage in all four experimental conditions. The M6 and Rooster lines show PDGF production at P2 across all four conditions, but in both incidences the 5% oxygen and respective control does not produce PDGF within the detectable range at P3 and P4. The greatest amount produced was in the M3 cells line, in all culture conditions and passages PDGF was detected P4 20% Oxygen (5% oxygen control) had the highest amount with 0.2275 ±0.0737 fg/cell. The same culture condition also had a significantly higher PDT in Figure 10, however P4 2% oxygen had a higher PDT so a direct relationship between longer PDT and increase PDGF production cannot be theorised. The M2 line produced the PDGF in all condition apart from P2 2% oxygen, however in the P3 and P4 conditions PDGF is detected and increases further in P4 producing the highest amount (0.0675 ±0.02 fg/cell) for the M2 conditions. Interestingly some differences between the 20% oxygen control conditions can be seen, particularly in the M6 and Rooster lines where no PDGF was detected in the 5% oxygen control but was detected in the 2% oxygen control. PDGF-AA has been reported to have a proliferative effect (Doorn et al. 2012), it has also been shown to regulate VEGF expression at an autocrine level (Shikada et al. 2005). However the minimal concentration of PDGF required to induce a biological response has not been determined, it is also not the sole cytokine to have a proliferative effect FGFs have also should to hold similar properties (Doorn et al. 2012).
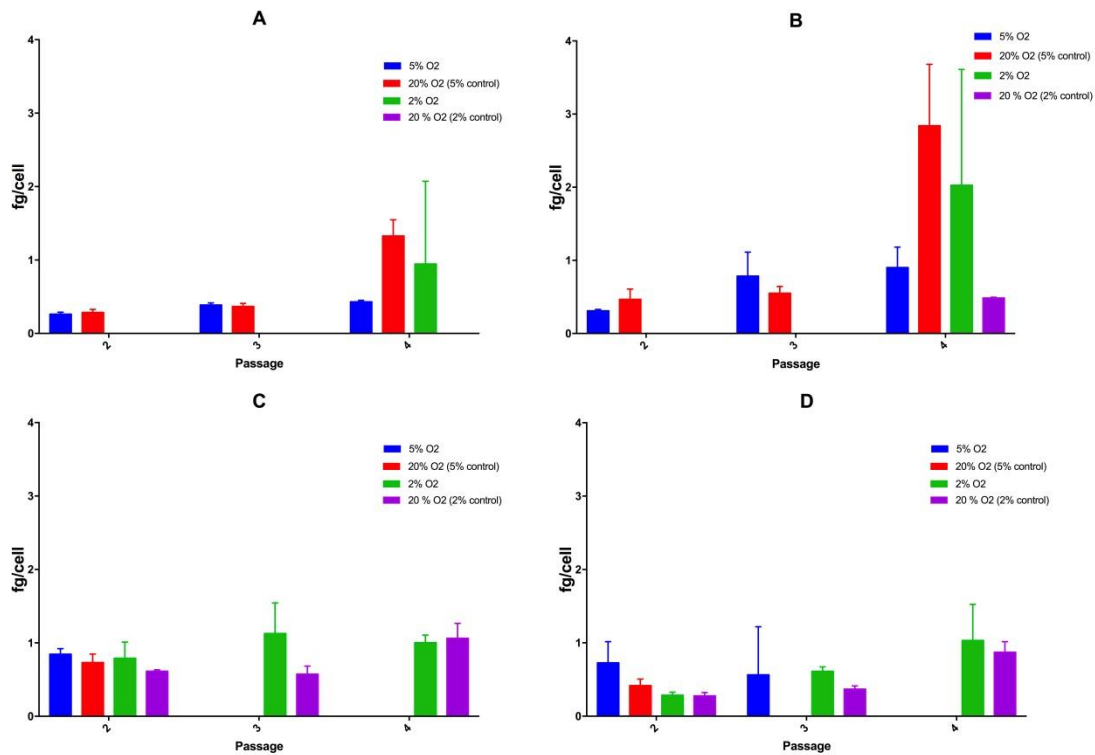
Figure 12: FGF basic secretome profile of M2 (A), M3(B), M6 (C) and Rooster (D) lines cultured in 2% or 5% atmospheric oxygen compared to a control cultured in 20% atmospheric oxygen. Samples were collected after 48hr of conditioning with the hMSCs which were on day 5 of culturing. Expression quantities calculated per cell based on the per ml value divided by the cell number at the end of the passage, n=4 standard deviated is shown

In Figure 12 the production of FGF-basic cytokine is at a larger scale compared to PDGF which was detected at the 10ths of a femtogram level (Figure 11). The secretome profile of M6 and Rooster lines are similar as PDGF, FGF is detected in P2 across all four culture conditions, but in P3 and P4 the levels are not detectable for the 5% oxygen and the respective control. In the M2 line 5% oxygen, 20% oxygen (5% oxygen control) conditions FGF-basic is produced at all three passages, levels at P2 and P3 are similar for each condition but at P4 the level rises to over 1fg/cell for the FGF-basic in the control condition compared to the lower oxygen condition at 5% oxygen (Figure 12). Interestingly at P4 the 2% oxygen culture condition has a 0.95 ± 1.12 fg/cell FGF-basic production. This behaviour is also seen in the M3 line, no FGF-basic is detected at P2 and P3 in the 2% oxygen culture condition and the 20% control, but at P4 in both the 2% oxygen and the corresponding 20% oxygen

control FGF-basic levels of 2.027±1.581 fg/cell and 0.485±0.1 fg/cell respectively are shown. The disparity between the controls in the M2 and M3 in both PDGF and FGF-basic could be attributed to the fact they were cultured at different times or from separate vials, damage in thawing, drop in culture temperature or changes in CO_2 levels (Xu et al. 2012). The profiles of the M6 and Rooster line FGF-basic production follow a similar pattern as the PDGF production with the exception that in the Rooster line 5% oxygen at P3 is producing FGF-basic but not PDGF (Figure 11). At 5% oxygen in the P3 passage all four lines produce FGF-basic and in the corresponding control the values are either similar (M2) or greater (M6 and Rooster), only in M3 P3 is the control value higher 2.84±0.84 fg/cell compared to 0.90±0.28 fg/cell, but both the control and experimental condition have higher standard deviations. The situation changes in M2 P3 where the 5% oxygen condition produces more FGF-basic (0.43±0.02 fg/cell) compared to the 20% control (1.33±0.22 fg/cell). By P4 in the M2 and M3 lines the 20% oxygen control is producing more FGF-basic compared to the corresponding 5% oxygen samples. Overall for the M6 and Rooster lines the 2% oxygen condition produces either similar amount or greater amounts of FGF-basic compared to the control which would indicate that when cultured in 2% atmospheric oxygen FGF-basic expression can be upregulated, the difference is most notable at P3. The 2% condition also shows a delayed recovery and FGF-basic expression at P4 in the M2 and M3 lines, this delay maybe not be a consistent trait of the lines in 2% oxygen due to the disparity between the 20% oxygen controls however it is interesting that FGF basic secretion recovers better in the 2% oxygen condition compared to the respective control.
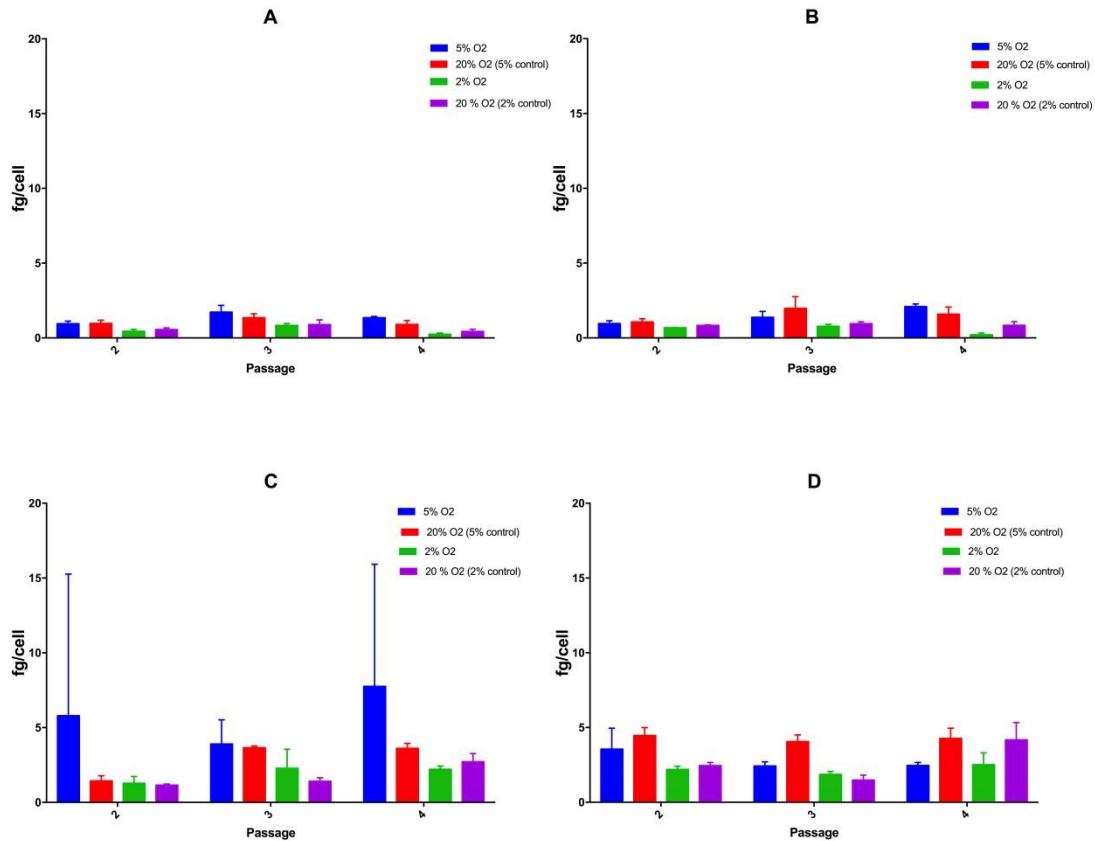
Figure 13: IL-8 secretome profile of M2 (A), M3(B), M6 (C) and Rooster (D) lines cultured in 2% or 5% atmospheric oxygen compared to a control cultured in 20% atmospheric oxygen. Samples were collected after 48hr of conditioning with the hMSCs which were on day 5 of culturing. Expression quantities calculated per cell based on the per ml value divided by the cell number at the end of the passage, n=4 standard deviated is shown.

IL-8 is produced by every cell hMSC line, in all oxygen culture conditions across all three passages (Figure 13), the per cell quantities are higher than PDGF and in some conditions higher that FGF-basic with levels in M6 and Roster around 5 fg/cell. The disparity between the 20% controls seen with the PDGF and FGF-basic cytokines can still be seen within the M2 and M3 conditions though all controls in are producing IL-8. In the M2 and M3 line IL-8 production does not exceed 2.5 fg/cell; in the 2% p4 condition IL-8 production is the lowest at 0.25±0.08 fg/cell in the M2 line and 0.21±0.12 fg/cell in the M3 line. The highest amount of IL-8 produced was in the M6 line in 5% oxygen at P4 with a value of 7.75 fg/cell and a large standard deviation of ±8.17 fg/cell. At P3 IL-8 production was similar between the 5% condition and the

parallel control. In the M6 P2 and P4 the 20% control was less than the 5% condition. In the Rooster line the parallel control for the 5% oxygen condition produced the highest amount of IL-8 across all three passages. Differences can be seen between the two 20% oxygen controls at P2 and P3; but at P4 the 2% oxygen control has a value of 4.190±1.151fg/cell and the 5% oxygen control a value of 4.273±0.684fg/cell. Overall based on the data in Figure 13 the 5% oxygen condition stimulates the expression of IL-8 more than at 2% in M2, M3 and M6 cell lines.
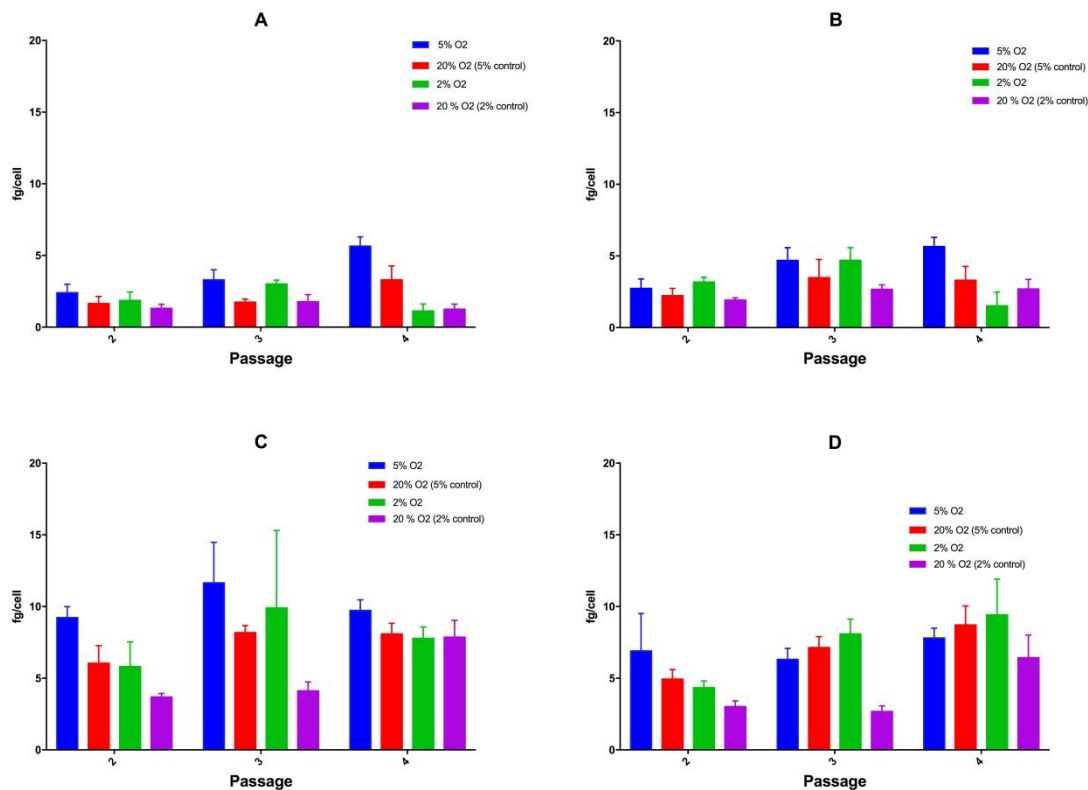
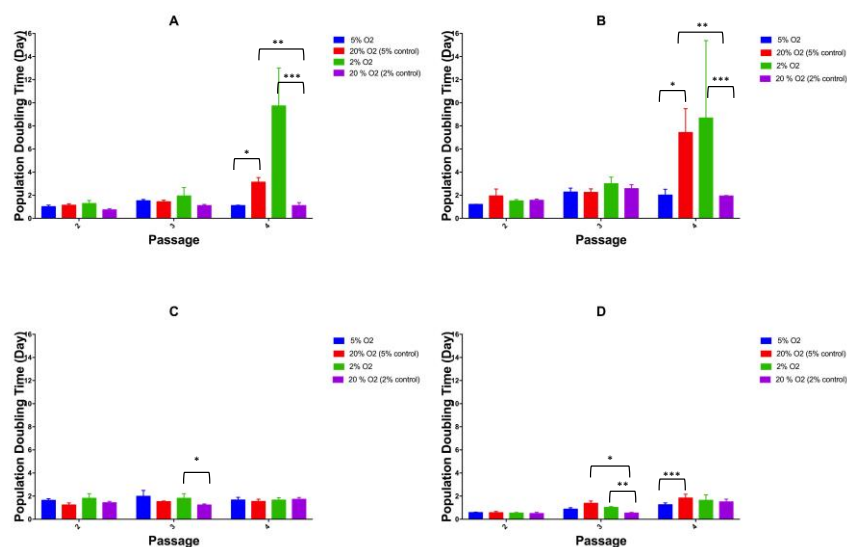Figure 14: VEGF secretome profile of M2 (A), M3(B), M6 (C) and Rooster (D) lines cultured in 2% or 5% atmospheric oxygen compared to a control cultured in 20% atmospheric oxygen. Samples were collected after 48hr of conditioning with the hMSCs which were on day 5 of culturing. Expression quantities calculated per cell based on the per ml value divided by the cell number at the end of the passage, n=4 standard deviated is shown.

VEGF is produced by every cell hMSC line, in all oxygen culture conditions across all three passages. In the M2, M3 and M6 lines the highest amounts of VEGF are produced in the 5% oxygen environments based on the mean values. The M6 line produced the most overall P2 9.23±0.76 fg/cell, P3 11.65±2.83 fg/cell and P4

9.73±0.75 fg/cell. The ability for VEGF production to be induced by hypoxia is mention in numerous papers (Jin et al. 2002; Yancopoulos et al. 2000) so it is therefore not surprising that in most of the 2% and 5% conditions more VEGF in detected compared to the equivalent controls. The M3 P4 2% condition is the only condition where more VEGF is detected in the control compared to the lower oxygen environment. In the M2 and M6 P4 conditions for 2% oxygen similar levels of VEGF are produced by the control and experimental condition. In the majority of conditions for the M6 and Rooster cells lines fg/cell values between 5 and 10 have been detected compared to the M2 and M3 conditions where few conditions exceed the 5fg/cell production level.
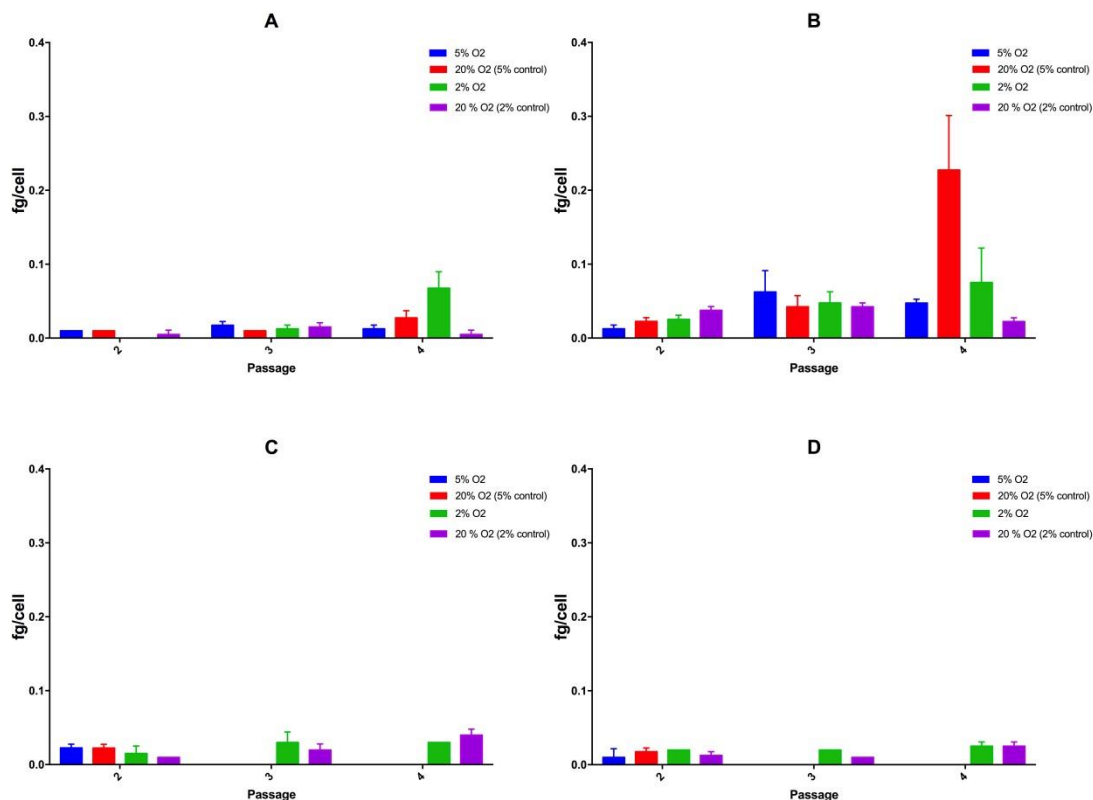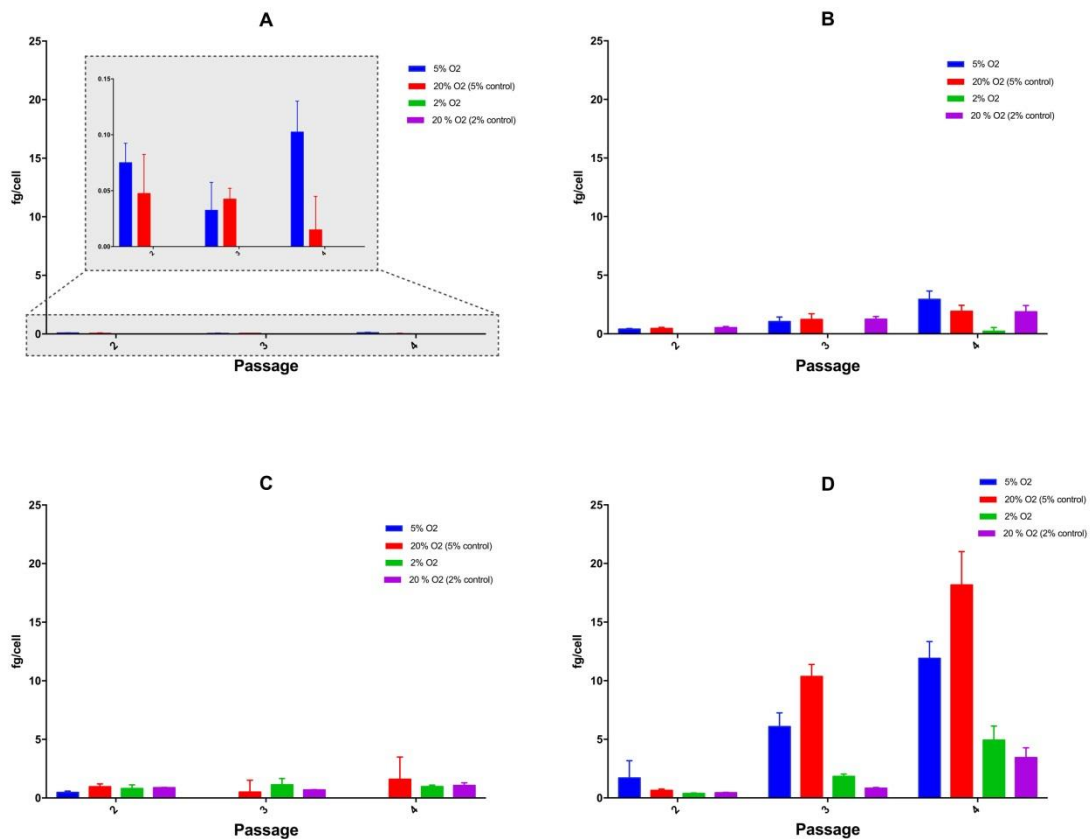

Figure 15: HGF secretome profile of M2 (A), M3(B), M6 (C) and Rooster (D) lines cultured in 2% or 5% atmospheric oxygen compared to a control cultured in 20% atmospheric oxygen. Samples were collected after 48hr of conditioning with the hMSCs which were on day 5 of culturing. Expression quantities calculated per cell based on the per ml value divided by the cell number at the end of the passage, n=4 standard deviated is shown.
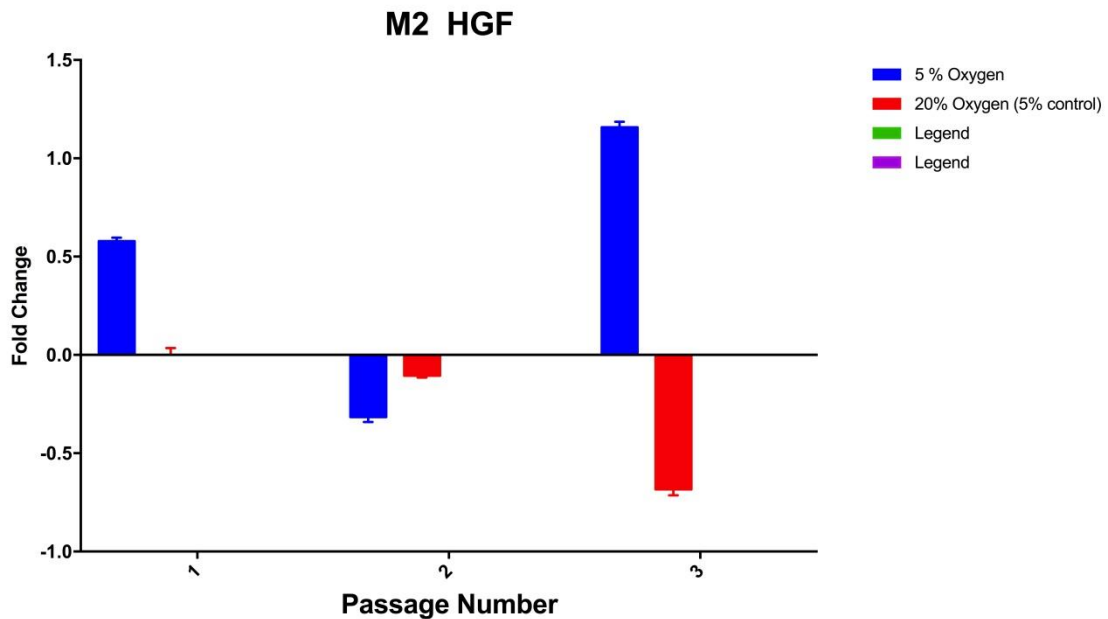
Figure 16: M2 HGF secretome fold difference compared to P2 20% oxygen control. n=4 standard deviated is shown.

The rooster line produces the greatest amount of HGF with a peak value of 18.17 ± 2.69 fg/cell at P4 20% oxygen (5% oxygen control). A positive increase in the amount of HGF produced can be seen going from P2 through to P4 in all four conditions of the Rooster line (Figure 15). At P2 the 5% oxygen condition produces the most HGF but in P3 and P4 the corresponding 20% oxygen control produces the most HGF (P3= 10.36 ± 1.02 fg/cell and P4 18.17 ± 2.69 fg/cell). As seen previously there is variation between the 20% controls with the P3 and P4 2% oxygen control producing 0.83 ± 0.06 fg/cell and 3.44 ± 0.84 fg/cell respectively. Much lower levels of HGF are produced by the M6 and M3 lines, in the M3 line only a small amount of HGF is produced in the 2% P4 condition. In the M6 line only at P3 5% is HGF produced, but HGF is detected though all passages at 2%.Based on the graph in Figure 15 it seems that only at P4 in 5% oxygen HGF is produced, however as shown in Figure 16 small quantities of HGF is produced in the 5% oxygen condition and the parallel control across all three passages. No HGF was detected in the 2% condition and the parallel control. When examining the fold difference of the M2 line HGF production in relation to the P2 20% control value the control decreases with

increasing passage number. The 5% oxygen condition fluctuates initially having ～ 0.5 fold more than the P2 control but in P3 the amount of HGF is lower than the P2 20% oxygen control. At P4 the HGF level recovers to be over 1 fold greater than P2 20% oxygen control. This could indicate that the cells have recovered from cryopreservation and are now responding to the environmental stimulus.
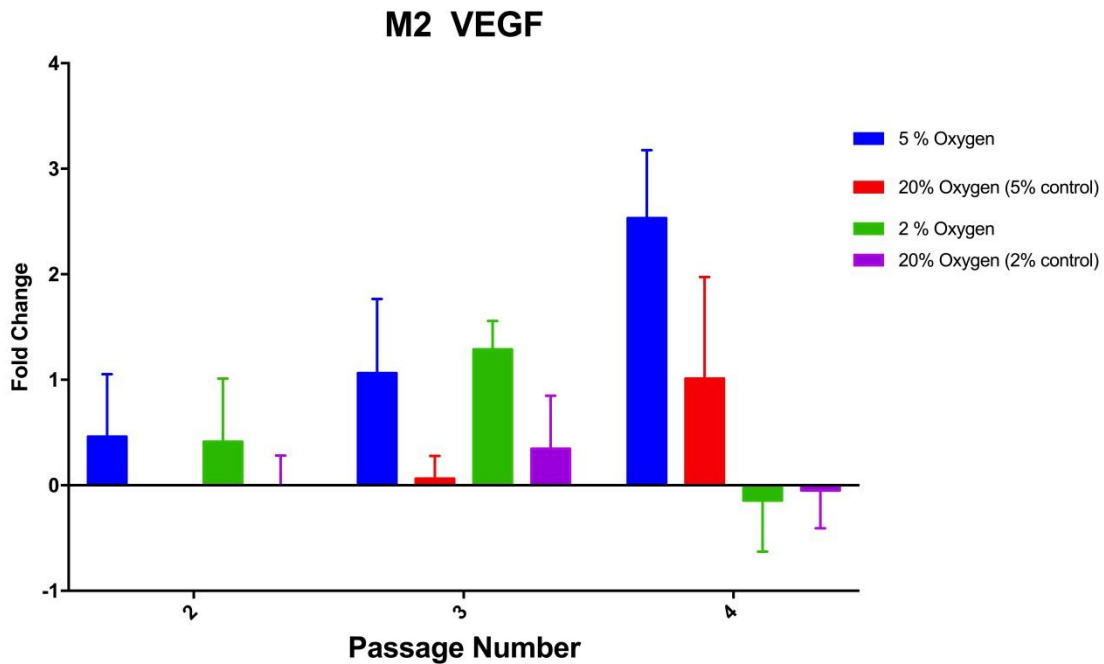
Figure 17: fold difference of M2 VEGF secreatome comparing expression levels to the respective P2 20% oxygen control.

The data from Figure 11 to Figure 15 shows that there is not one line that consistently produces the most or the least of every cytokine analysed, showing that just because one cytokine is produced in a high amount by a specific line the line will not produce all cytokines to high quantities. For example, Rooster cells produced more HGF (Figure 15) than the M2 cells but under certain conditions M2 cells are capable of producing more PGDF than the Roosters (Figure 11) One of the issues to be further investigated is the variation in cytokine levels between the two 20% oxygen controls. For example, in Figure 14 the M2 line the 5% oxygen control is producing more VEGF that the 2% oxygen control. When examined further (Figure 17) it can be seen that the differences are not proportional within the conditions, the two controls were thawed from different vials which suggests there could be some variation introduced by the handling of the cells. This is seen again in the HGF secretome profile (Figure

15) as no HGF is detected in the 2% oxygen control, interestingly despite the variation in controls the 2% P4 oxygen condition produces the most PDGF in the M2 line, which suggests that this line is capable of being primed using lower oxygen concentrations on increase PDGF. The differences between secretome profiles indicates that for treatments that utilises hMSCs for their paracrine properties a 'one cell donor source fits all' approach may not produce the desired effect. Consequently, further investigation into the physiological behaviour of the hMSC line secretome profile needs to be investigated.

Protein degradation needs to be discussed; the conditioned medium samples were treated consistently in terms of the number of freeze thaw cycles they were subjected to. However, if the rates at which each cell line produces the cytokines varies, the cytokines for some cell lines may be exposed to the culture conditions for longer, and therefore potential factors which may cause protein degradation. For example hMSCs have been shown to produce proteases (Hematti & Keating 2013), the production degradation profile of hMSCs has not been extensively investigated in terms of hoe long secreted proteins retain integrity while in cell culture. It also needs to be noted that the pH of the cell culture conditions was not tightly monitored, the standard DMEM buffer systems was in each cell culture system but no adjustments were made for the lower oxygen conditions. Subsequently proteins with a structure that is influenced by pH may have be adversely affected in these culture conditions. In this incidence it was not feasible to run the conditioned medium samples on the Luminex plate immediately necessitating the need for freezing the sample. Due to the sample numbers and the volume of medium in which the cells were being cultured it was not cost effective to take samples at shorter time points in order to investigate protein degradation and establish a secretion degradation profile. This highlights a limitation of the Luminex assay when being used in a manufacturing setting, specifically in terms of the cost as one plate is £525 on which 41 samples can be run in duplicate and in terms of time scale, either 41 samples need to be ready to be run at the same time or samples are put through a freeze thaw cycle, which my compromise sample integrity.

3.3.3 Branch formation assay *in vitro*

Using an *in vitro* branch formation assay the pro-angiogenic *in vitro* effect of the hMSC conditioned medium analysed in Section 3.3.2 can be determined. The branch formation assay or tube formation assay as it is also called has been used by multiple research groups to determine angiogenic properties of various solutions on endothelia cells (Arnaoutova et al. 2009). Normally the assay is imaged at discreet time points however in this methodology the assays were imaged every 15-20mins. The region selected for imaging is also, in previous studies, subject to operator bias, using the Biostation the area and position imaged in the wells were predefined and automated. By using a more extensive imaging procedure with multiple time points the graphs created have tightly packed error bars horizontality which results in difficult to read graphs. Therefore, examples of graphs containing the respective error bars can be seen in Appendix 1. The graphs display the average branch length between two nodes, also known as branch junctions. During the assay branches are constantly being formed and reformed into longer branches, this creates an irregular graph as the images are so frequent small changes are plotted. The branch formation assay analyses images and calculates the total length of branch of nodes, the number and the average branch length between two nodes (Section 3.2.3). The decision was made to only plot the average branch length as the software will include debris or scratches in the total branch length, by only including branches between two nodes the false measurements are not included.

A

B
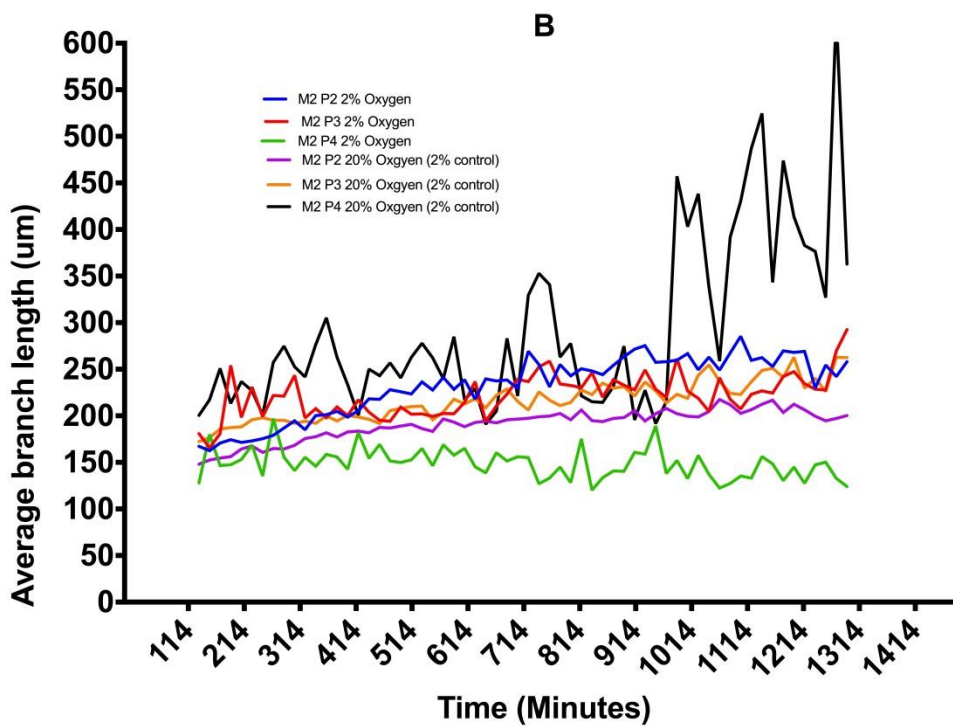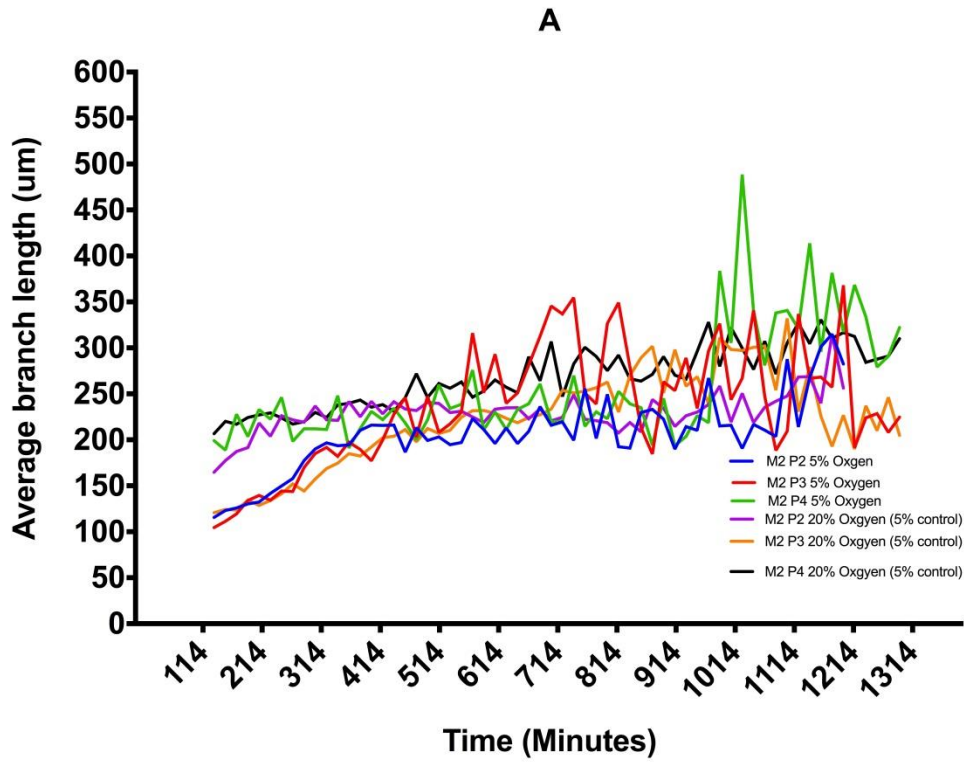
Figure 18: M2 Average branch length for the 2% oxygen Vs 20% controls (A) and the 5% oxygen vs 20% control (B), over 3 passages. n=4

In the M2 2% oxygen condition displayed in Figure 18 the condition with the longest average branch length that increases over time is the P4 20% control. The P4 2% oxygen condition produced the shortest average branch length; at no time point did the mean average branch length exceed 200µm. Of particular interest the difference between the 20% controls, at the beginning of the assay the 5% control has a lower average tube length (under 150um) compared to the 2% oxygen control. This disparity could be linked to the differences seen in the M2 cytokine expression profiles (Figure 11-Figure 15).

Previous luminex data show cytokine production based on a per cell value, however as shown in Figure 10 the number of cells per flask varied due to different PDT therefore the amount of cytokines the branch formation assay contained varies. Table 1 shows the cytokine levels the HUVEC cells are exposed to during the assay notably there is a higher amount of VEGF and IL-8 in the control compared to the 2% condition.

Table 5 Cytokine expression profile mean values and standard deviation in pg of M2 P4 2% oxygen and M2 P4 20% oxygen, corresponding to average branch length profile Figure 18 A. n=4

Cytokine	M2 P4 2%	SD	M2 P4 20% (control)	SD
PDGF	0.89	0.022	0.52	0.006
FGF-basic	0.31	1.128	Below LOD	
Il-8	1.07	0.079	49.26	0.147
VEGF	0.75	0.484	142.43	0.358
HGF	Below LOD		Below LOD	
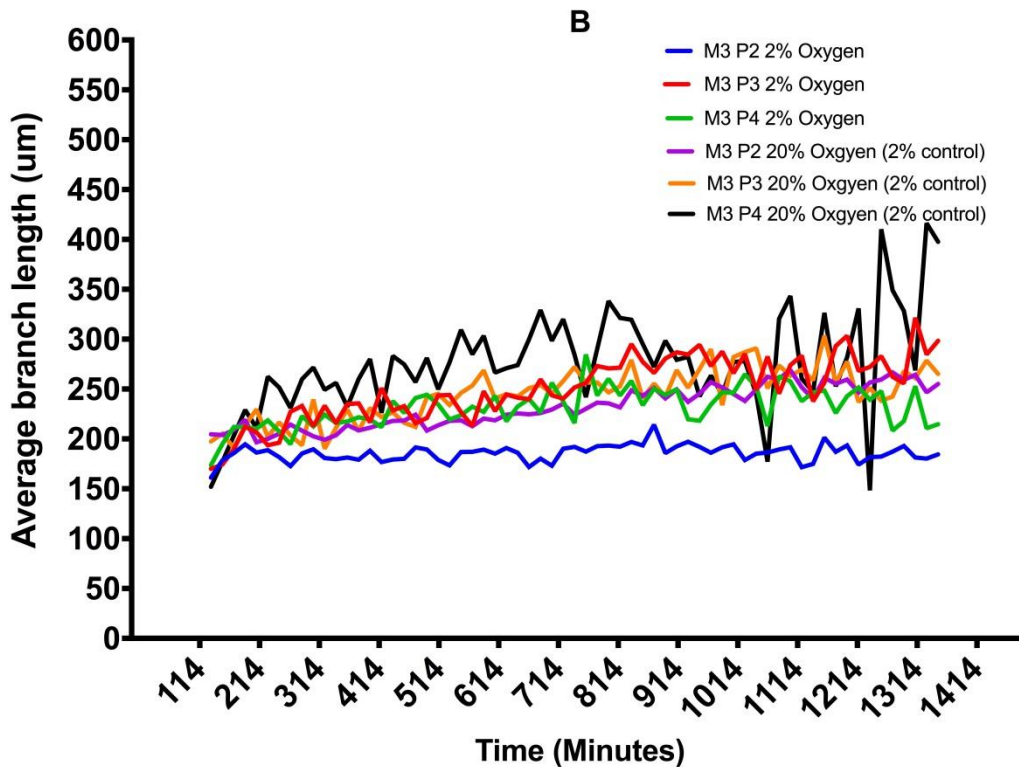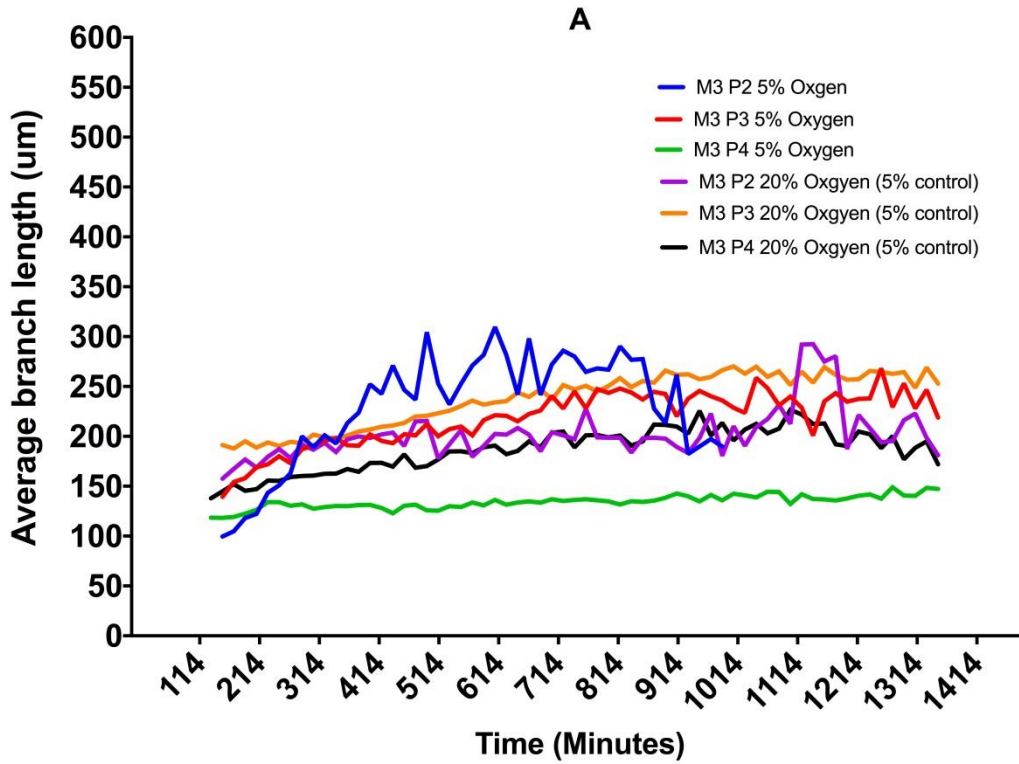
Figure 19: M3 Average branch length for the 5% oxygen Vs 20% controls (A) and the 2% oxygen Vs 20% control (B), over 3 passages. n=3

A

B
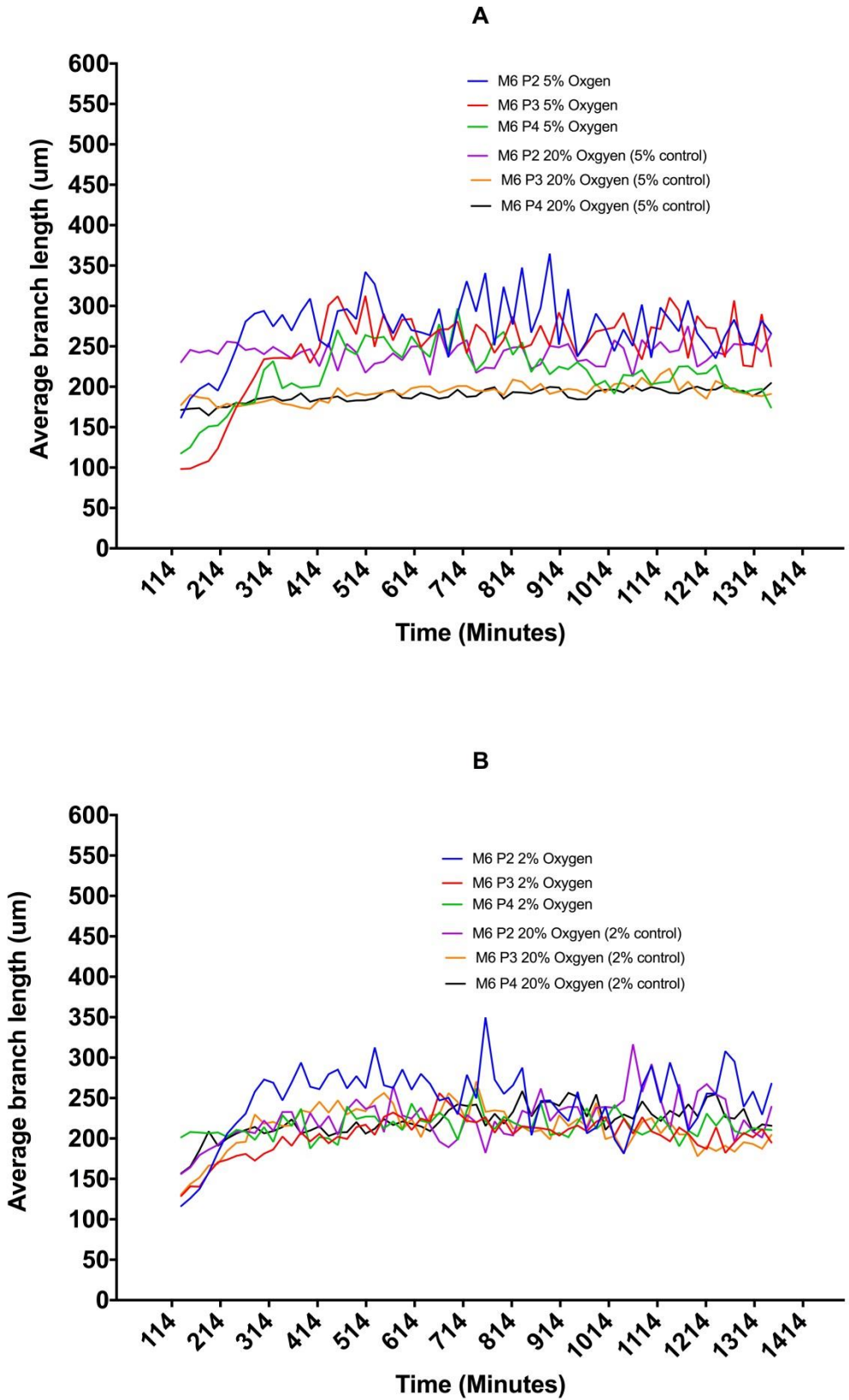
Figure 20: M6 Average branch length for the 5% oxygen vs 20% controls (A) and the 2% oxygen vs 20% control (B), over 3 passages. n=3
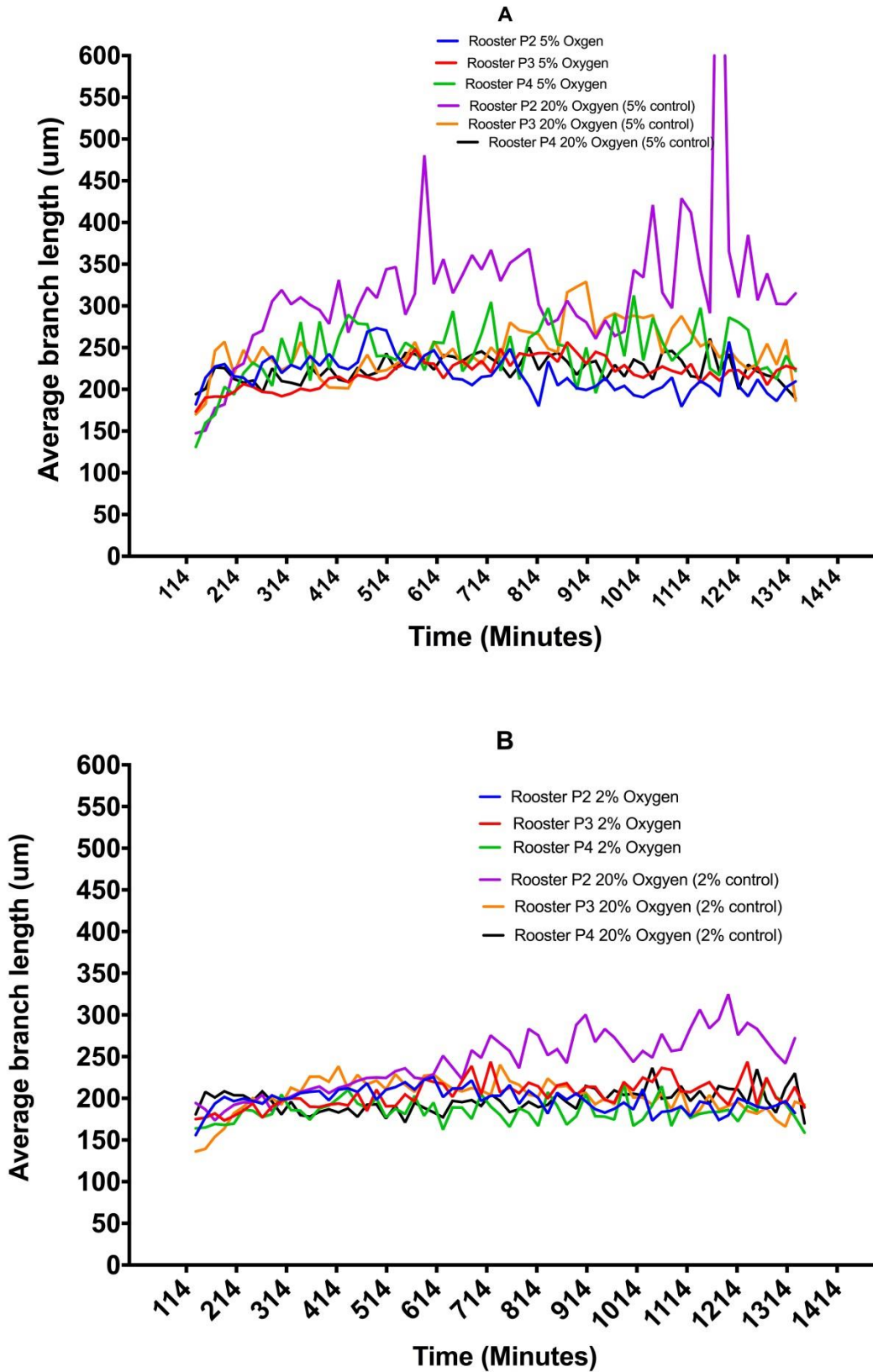
Figure 21: Rooster Average branch length for the 5% oxygen vs 20% controls (A) and the 2% oxygen Vs 20% control (B), over 3 passages. n=3

The average branch length in Figure 21 A and B show there is little distinction between the experimental conditions, in both data sets only the P2 20% oxygen control is more distinct from the other data sets. In Figure 21A the longest average branch length is in the P2 20% control which reaches the 300-400µm length with two time point exceeding 450µm length: the shorter average branch length can be seen in the P2 5% oxygen control. Table 6 shows the average cytokine levels in each well of the angiogenesis assay. The values in this context would initially indicate that longer average tube length is not directly relates to VEGF concentrations as in the 20% condition there is less VEGF compared to the 5% condition. Just based on the data in Table 6 it would indicate that higher levels of PDGF, IL-8 and HGF or lower levels of FGF-basic and VEGF are important for longer average branch length. However this is just a snap shot of the data and the standard deviations are also indicating sources of variation, therefore this data would need to be analysed in greater detail, in terms of assaying for a wider panel of cytokines.

Table 6: Cytokine expression profile mean values and standard deviation in pg/ml of Rooster P2 5% oxygen and Rooster P2 20% oxygen, corresponding to average branch length profile Figure 21 A. n=4

Cytokine	Rooster P2 5%	SD	Rooster P2 20% (control)	SD
PDGF	2.52	2.91	3.61	0.58
FGF-basic	156.53	66.60	92.49	12.11
Il-8	245.89	11.86	291.94	7.72
VEGF	776.81	38.83	596.18	16.54
HGF	1182.47	44.39	1244.40	83.27

The data form the Rooster P2 20% (oxygen control) and the corresponding P2 5% culture conditions was further analysed to the individual replicate level in order to further understand the variation in the data.

Based on the data in Figure 21, in both A and B, the P2 Rooster 20% control results in the longest average branch length; in A after 314min the average branch length in over 250nm for the rest of the duration of the assay with a spike at 1314mins of over 600 nm. In B the average branch length does not exceed 259nm until after 614mins, the average branch lengths between 250nm-350nm are then maintained for the duration of the assay. Examining Figure 21 A further the P2 5% oxygen conditions results in the shortest branch length as it reduces after 814 compared to the other conditions. Table 6 displays the mean cytokine values which the assays contain. For both the 20% and 5% conditions PDGF quantities are low in comparison to the four other cytokines. In the 20% oxygen condition there is 46.05pg more Il-8 and 61.93pg more HGF however there is actually 64.04 pg less FGF-basic and 180.63pg less VEGF in the better performing 20% condition which is interesting as VEGF is considered to be a key cytokine for angiogenesis (Rosano et al. 2012; Neufeld & Kessler 2006). The data presented in Figure 21 and Table 6 are an average of four repeats, the standard deviations of cytokine expression (Table 6) are large which indicates that each individual replicate contained a varying quantity of all five cytokines. The data is deconstructed further to the individual replicates data.
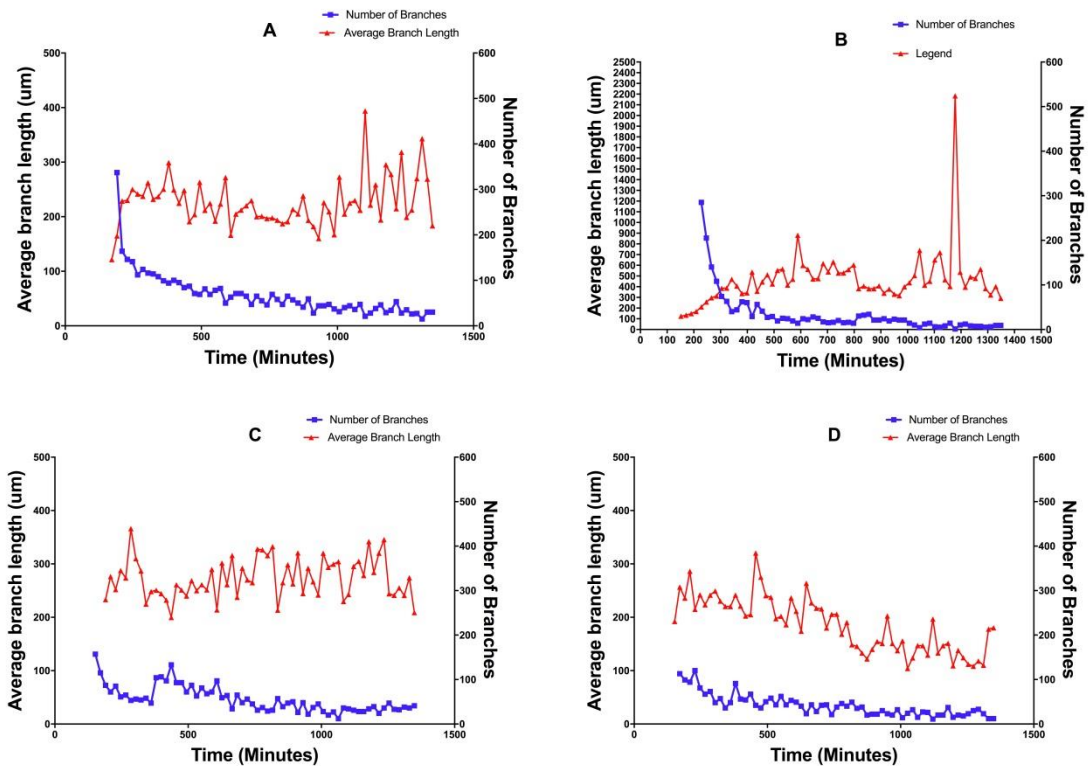
Figure 22: Rooster P2 20% oxygen (5% oxygen control), A, B, C and D are individual repeats, the mean of which is in Figure 21 A. The average branch length (µm) and corresponding number of branches are displayed for each repeat on the same graph. It should be noted the graph scale for replicate B is higher in order to accommodate all the data points.

Figure 22 and Table 7 are a breakdown of the individual replicates (A, B, C and D) shown in Figure 21 A and Table 6 for the P2 20% oxygen condition. The number of branches decreases over the duration of the branch formation assay as shown in Figure 22, degradation of the branches is expected due to protease activity (Lehman et al. 2012). Repeats A and B have a higher number of shorter branches in the early phase of the assay (between 200-300 minutes), examining the cytokine levels in these repeats the only commonality is they have a lower FGF-basic concentration with 82pg in the assay (Table 7), though this is not conclusive evidence that low FGF-basic levels produce shorter branches in the early phase. The spike seen at 1314min in Figure 21A P2 20% oxygen control can be attributed to replicate B; this data point demonstrates the need for detailed data analysis.

Table 7: Corresponding cytokine values for each repeat of Rooster P2 20% oxygen (5% oxygen control) (Figure 22)

Cytokine	A	B	C	D
PDGF	3.53	3.84	4.8	3.61
FGF-basic	82	82	102.97	102.97
Il-8	805.13	1115.39	1244.95	874
VEGF	930.56	1140.59	1355.19	1006.25
HGF	115.39	142.88	191.75	128.18

Replicate C has the highest levels of all 5 cytokines, while C maintains an average branch length between 200nm and 400nm throughout the duration of the assay it does not reach the above 400nm that are seen in replicate B. Replicate B produces the longest average branch length during the assay run time yet there is no reason for this which can be conclusively related to the cytokine levels.
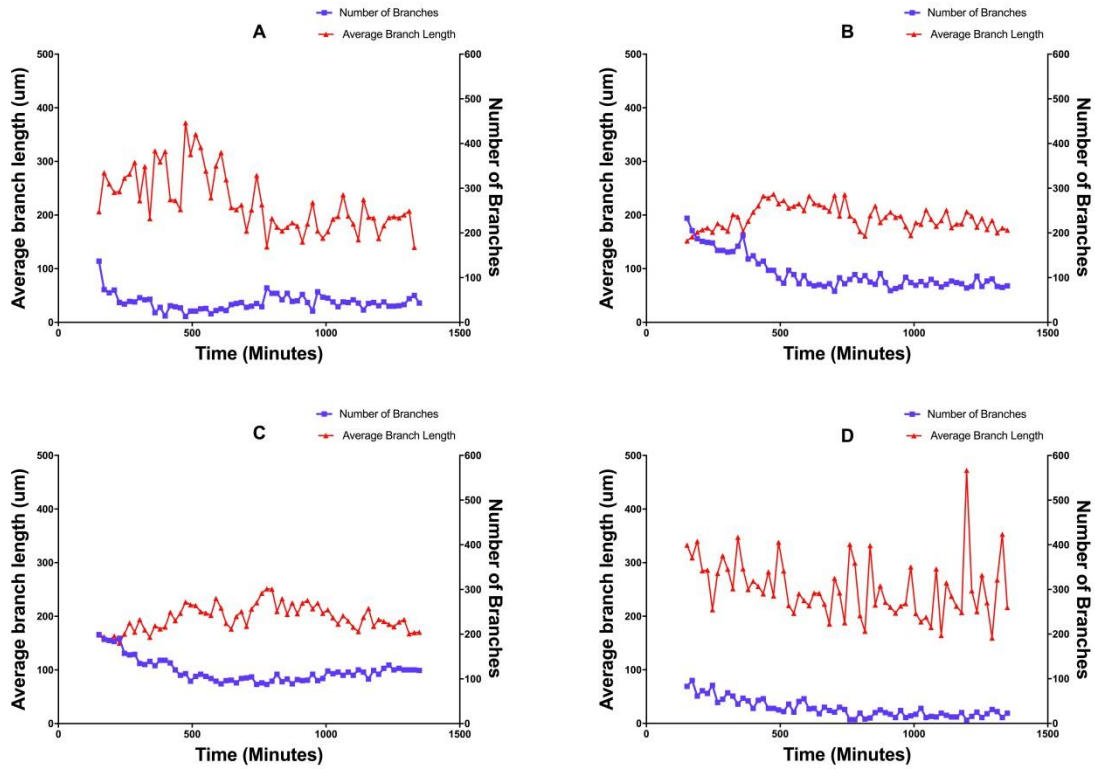
Figure 23: Rooster P2 5% oxygen, A, B, C and D are individual repeats, the mean of which is in Figure 21. The average branch length (µm) and corresponding number of branches are displayed for each repeat on the same graph.

Table 8: Corresponding cytokine values for each repeat of Rooster P2 5% oxygen (Figure 23).

Cytokine	A	B	C	D
PDGF	5	5.08	Below LOD	Below LOD
FGF-basic	106.08	93.06	202.43	224.55
Il-8	1016.64	952.73	495.4	538.17
VEGF	1932.1	1864.61	980.72	1066.03
HGF	97.2	85.75	609.51	693.07

3.4 Conclusions

This Chapter looks at several aspects of using hMSCs as a cell therapy ranging from methods used in determining the fundamental biological effect of hMSC on angiogenesis to identifying key areas for improvement during the processing of a hMSC treatment. Cells from four donors were cultured in lower than atmospheric oxygen conditions over three passages. Due to the complex nature of cells, in this case hMSCs, there are always some common challenges relating to the impact of culture methodology and environmental conditions. The standard 20% oxygen culturing condition controls showed variation in population doubling times and secretome profile (Section 3.3.1and Section 3.3.2). This is therefore indicating that despite the cells being from the same donor and cryopreserved at the same time the recovery processing steps of the vials are also important. This highlights that without tight controls and a rigours cell recovery methodology it cannot be assumed that all cells from the same donor and at the same passage will behave the same. Further work into vial to vial variation would need to be conducted. Alternatively, in a manufacturing setting, early indications in the upstream processing that a batch/vial of cells would not meet defined criteria would mean the run could be halted sooner resulting in time and money being saved.

The Rooster line under standard culturing conditions showed the shortest population doubling time and produces the highest amount of HGF. PDGF and FGF-basic. In Figure 11 A and Figure 12 A the production of PGDF and FGF-basic was greatest at P4 2% compared to the P4 20% control. While the issue of variation between controls has been discussed, the question arises does the M2 line produce more PDGF and FGF-basic at lower 2% or does the production of this recover quicker post thaw at this oxygen level? This would need to be investigated with further repeats but based on Figure 22 and Table 7 FGF-basic may potentially have an impact on initial rate of branch formation. Reducing the lag time between dosage and response of treated tissue is important in conditions where rapid restoration of the bloody supply is critical in order to retain organ/tissue function.

Though no direct trend between cytokine levels and average branch length can be deduced, it needs to be acknowledged that only 5 cytokines have been analysed in this work. The complex control of angiogenesis involves physical stimulus and many

more cytokines such as angiogenin, angiopoietin and placental growth factor (Bronckaers et al. 2014). While a strong relationship between a single cytokine and average branch length cannot be determined, the cytokine data may be applicable for other hMSC paracrine actions. IL-8 is known to have a pro migratory effect on epithelia cells, and its role in wound healing is being investigated (Guo & Dipietro 2010).

Overall this data presents the case that not all hMSC lines will have the same effect on angiogenesis and do not exhibit the same cytokine secretome profiles in standard culture conditions or in lower oxygen culturing conditions. Therefore hypothesis 1 that the hMSCs secretome profiles of VEGF-A, bFGF, HGF, PDGF-BB IL-8 /CXCL8 exhibited the same trends under three different atmospheric oxygen concentrations independent of the cell donor (Chapter 2, Section 3.2) must be rejected. It cannot be assumed that a high amount of VEGF will automatically mean a longer branch formation which in this instance is the presumed surrogate for average capillary length. Based on the data presented in Figure 18, Figure 21, Figure 22 and Figure 23 there appears to be no obvious link between cytokine secretome profiles, which were analysed, and average branch length. This is reflective of the complexity of angiogenesis that one single cytokine is most likely to not be the single biomarker for a good level of angiogenesis. In this instance the cytokine panel should be expanded to include other angiogenesis related cytokines, however given the number of variables which need to be controlled when conducting protein analysis, this would be an extensive and expensive undertaking.

4 Miniaturised ELISA tool for rapid cytokine quantitation of hMSC manufacturing

4.1 Introduction

With the increasing cost and complex nature of a cell therapy treatments there is a need for low cost and rapid bioanalytical technologies (Konstantinidis et al. 2013). The demand for affordable, high throughput, accurate, sensitive and rapid bioanalytical tests is increasing not just in the cell therapy market but also in point of care, precision medicine and drug monitoring trials (Heinzelmann 2016). As examined in Chapter 2 a bioanalytical method must be relevant to the product in terms of identity and/or potency. Alternatively, the method can be used to detect any adverse effect which compromises the safety and/or integrity of the product. For example given that cells are usually cultured at 37°C and temperature increases lead to protein degradation (Chi et al. 2003). During the manufacturing hMSCs for their paracrine properties rapid analysis of the secretome is important in order to ensure the require expression profile is being achieved (Chapter 3). Therefore, reducing the sample to result time is critical when dealing with a dynamic environment such as stirred-tank bioreactors when scaling up cell production.

ELISA-based technologies, including direct ELISAs, sandwich ELISAs and ELISA spot arrays are common methods for protein detection and quantification. There are many platforms which use the fundamental principle of an ELISA assay and in this work three of the platforms were used; the Luminex assay, the standard 96 well plate assay and a novel microfluidic based platform. Current 96 well plate formats are time intensive, some methods having incubations time totalling 3hrs after the addition of the sample. While magnetic Luminex screening assays can analyse multiple analytes simultaneously there are still 3.5hrs of incubations post sample addition. Microfludic ELISA platforms being developed to address many of the limitations of well plate platforms as discussed in Chapter 2. Previous work carried out by Barbosa et al. (2014) used a microfluidic based platform to produce a rapid yet sensitive method

to quantify prostate serum antigen levels. This method used a microcapillary film (MCF), which contained 10 parallel capillaries each with a ～200μm diameter Figure 24. Each MCF is then connected to a syringe via a multi-syringe aspirator (MSA) which is able to hold up to 8 syringes in parallel. This device enables 8 samples to be analysed at the same time and in each strip of MCF there are 10 replicates. Using the MCF device time intensive wash steps are removed as fluid handling is simplified by aspirating waste fluid into the syringe from the side of the MCF connected to the device while concurrently aspirating in new reagents of wash buffer from the unconnected end of the MCF. Due to the high surface area to volume ratio of the MCF incubation times can also be reduced in the ELISA assay as the time for antibody diffusion and adsorption of antibodies and substrates is faster than in the well plate. Further work on cytokine detection has been carried out by Castanheira et al. (2015), whereby in a singleplex format human IL-12 could be detected to concentrations as low as 2pg/ml. Multiplexed ELISA assays using the MCF platform have also been demonstrated, overall the assay times for cytokine detection have been shown to be as fast as 17mins post sample addition (Castanheira et al. 2015).
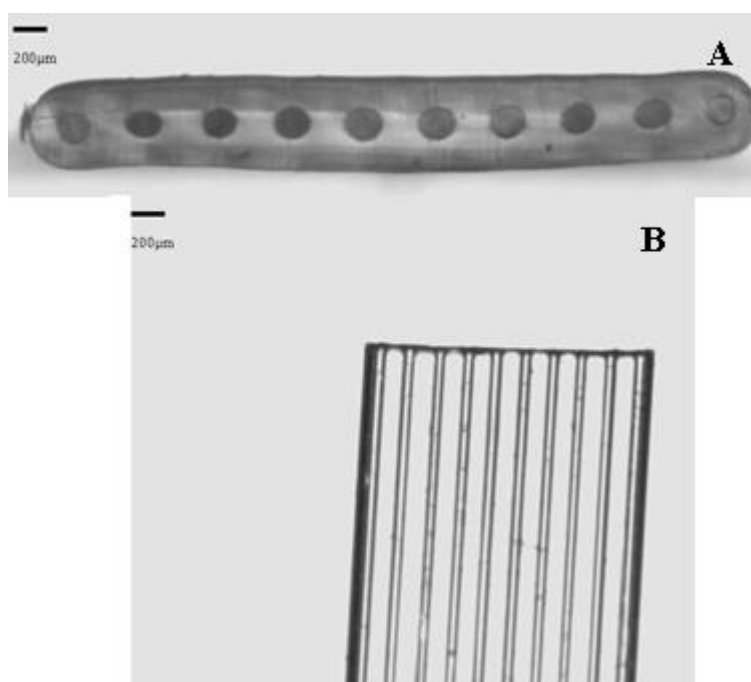
Figure 24: Images of the MCF containing 10 capillaries with a ～200μm diameter A) cross sectional image B) Image of an empty MCF from above.

The MCF ELISA platform was patented in 2011 (Edwards et al. 2011) and entered the commercial arena as part of the company Capillary Film Technology Ltd (CFT). The work on the MCF platform and the commercial focus on CFT has been around the point of care market. This is reflected in the choice of equipment, flatbed scanners and smart phone cameras, used for detection which are low cost and easy to use (Barbosa et al. 2014; Castanheira et al. 2015; Barbosa et al. 2015). While the benefit of rapid ELISA tests for point of care diagnostics is clear, there is also the scope for the platform to be utilised within the protein and cell therapy manufacturing sector. In Chapter 3 the cost and time constraints, in terms of the potential number of analytes needed to be quantified, and the constant monitoring of cell cultures was discussed. There are also the additional complexities of biological variation between cell sources and cell behaviour during culture in terms of different growth rates and the need for cytokine production rates to be effectively modelled thus there is a clear requirement for faster analytics which could be fulfilled by the MCF ELISA platform. A simplified version of the cell therapy manufacturing process for hMSCs (though the process is currently similar for most adherent cell types) can be seen in Figure 25, the role of the MCF would vary depending on the end product requirements. For example, if a whole cell product was required then the initial selection of cells to enter the expansion phase would be important. Being able to have near real-time feedback in the cell culture environment reduces the risk of batch failure and consequently increased costs as well as market supply issues. Though this work is looking at the application of hMSC to promote angiogenesis the application of the MCF ELISA can work in any therapeutic area where cytokine expression is a critical parameter. If the multiple cellular products, which in this case is the cytokine production for hMSCs, needs to be monitored at various stages of the production process then there would be multiple roles for the MCF platform.
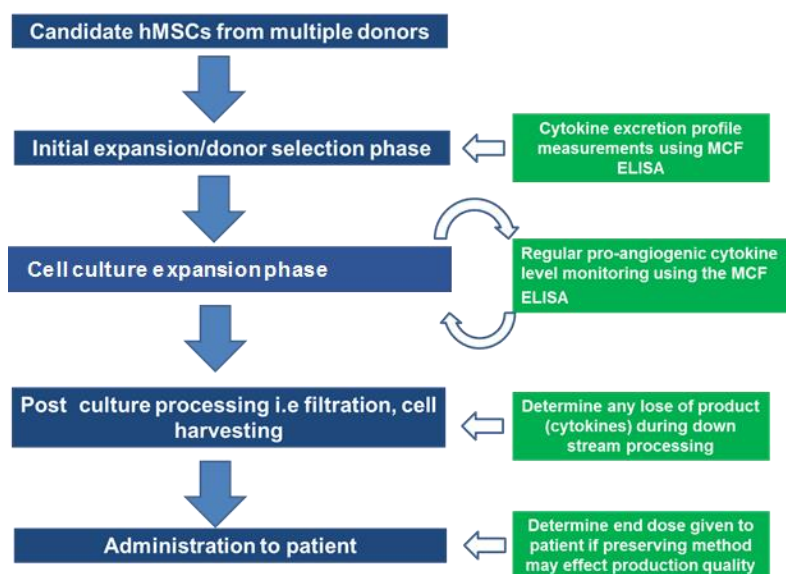
Figure 25 Manufacturing of hMSCs. A simplified schematic indicating the stages where the MCF ELISA platform could be utilised

The aim of this work was to determine the feasibility of using the MCF ELISA platform for the detection of IL-8 and HGF cytokines while ensuring the reliability, robustness and time efficiency required for the manufacturing environment. In the case of the IL-8 assay the limits of detection and coefficient of variation will be compared to a commercially available 96 well plate kit and the magnetic Luminex screening assay used in Chapter 3. Pre-validated commercially available antibody pairs with protocols for making up the standards were used to translate into the MCF ELISA platform.

4.2 Materials and Methods

4.2.1 Materials

Human IL-8 ELISA Ready-SET-Go, human IL-8 recombinant protein was purchased from eBioscience, (Hartfield,UK). Human Il-8 cytoset, high sensitivity strep-HRP was obtained from ThermoFisher Scientific, (Paisley, UK). Human HGF monoclonal antibody (clone24516), human HGF biotinylated affinity purified polyclonal with analytes: CXCL8/IL-8 (BR18) FGF basic (BR47) HGF (BR66) PDGF-AA (BR56) VEGF (BR26) were purchased from Bio-Techne, (Abingdon, UK). Fetal bovine

serum [Origin: E.U. Approved (South American)] were from Invitrogen Gibco now ThermoFisher Scientific, (Paisley, UK). The Bio-Plex MAGPIX System, and Bio-Plex Manager software were purchased from Bio-Rad Laboratories Ltd (Watford, Hertfordshire, UK). Micro capillary film (MCF), 10 capillaries each with a ～200µm diameter (Figure 24) was produced by Lamina Dielectrics Ltd (Billingshurts, West Sussex, UK). MAGPIX multiplex reader was purchased from Bio-Rad Laboratories Ltd, (Hertfordshire, UK). Phosphate buffered saline (PBS) was obtained from Lonza (Slough, UK). SIGMAFAST o-phenylenediamine dihydrochloride (OPD), urea hydrogen peroxide/buffer tablet and Tween-20 were purchased from Sigma (Dorset, UK). HP Scanjet G4050 Photo Scanner with built-in transparent materials adaptor was purchased from Amazon (Slough, UK). Chip vortexer with plate holder platform was obtained from Agilent Technologies LDA UK Limited (Stockport, UK).

4.2.2 96 well plate ELISA

The 96 well plate ELISA was carried out as per manufactures instructions, the coating was reconstituted to 1µg/ml; 100µl was added to each well of a 96 well flat-bottomed plate which was then incubated over night at 4°C. Coating antibody was aspirated and the wells washed 4 times with 400µl wash buffer. 300µl of blocking buffer (provided as part of the IL-8 cytoset, individual components not specified) was added to each well and incubated for 1hr at room temperature, assay buffer was then aspirated and 100µl of sample or known standard added to designated wells. 50µl of 0.04µg/ml detection antibody was added to each well and the plate was incubated at room temperature on a chip vortexer with a plate holder platform set at 700 rpm for 2hrs. After incubation the liquid was aspirated, and the plate washed 5 times with 300µl wash buffer, then 100µl of streptavidin diluted to 1/2500 was added to each well and incubated for 30mins at room temperature on a chip vortexer with a plate holder platform set at 700 rpm. The liquid was aspirated, and the plate washed 5 times with 300µl wash buffer, 100µl of tetramethylbenzidine (TMB) substrate (provided as part of the IL-8 cytoset) and incubated for 30mins at room temperature on a chip vortexer with a plate holder platform set at 700 rpm. 100µl of stop solution was added to each well and absorbance was measured at 450nm within 30mins of the stop solution being added.

4.2.3 Luminex Assay

Standards were reconstituted as per manufacturer's instructions; 6 standards were made in a 3-fold dilution series. Microparticles were mixed and diluted in 5ml of RD2-1 diluent; 50µl of mixture was added to each well flowed by 50µl of sample or standard which was added to designated wells. The plate was then covered with a foil plate sealer and incubated for 2hrs at room temperature on a horizontal orbital shaker set at 800rpm. Using a magnetic plate holder removal of reagents and wash buffer was done by securing the plate in the magnetic plate holder, after resting in the holder for 1min liquid was removed by inverting the plate. Post sample incubation the plate was washed 3 times and 50µl of diluted biotin antibody cocktail was added to each well. The plate was covered with a foil plate sealer and incubated for 1hr at room temperature on a horizontal orbital shaker set at 800rpm. The plate was washed 3 times and 50µl of dilute streptavidin-PE was added to each well the plate was covered with a foil plate sealer and incubated for 30mins at room temperature on a horizontal orbital shaker set at 800rpm. Post-incubation the plate was washed 3 times with wash buffer; particles were resuspended in 100µl of wash buffer and placed on the shaker for 2mins.The plate was then immediately read using a MAGPIX multiplex reader and the data analysed using Bio-Plex Manager Software.

4.2.4 MCF ELISA

The MCF ELISA was carried out by following the SOP- Microcapillary film operational procedure – Multi-Syringe Device: Singleplex Sandwich ELISA Standard Curve produced by Capillary Film Technology (Appendix 2). A solution of coating antibody was prepared to the required concentration using PBS as the diluent. The coating antibody solution was aspirated into a 30cm long piece of MCF (Figure 24) by using a 2cm long piece of tubing to interface one end to the MCF with a 5ml syringe, liquid was taken up by releasing the syringe ensuring all capillaries were filled.

The piece of MCF was placed inside a sealable plastic bag which contained a tissue moistened with water and then incubated inside the humid environment for 2hrs. Post incubation blocking solution was then aspirated into the MCF; the MCF was placed

back in the moist environment and incubated for 2hrs. Post-incubation the MCF was washed with wash buffer using the same aspirating technique.

Figure 26: MCF strips, each 3cm in length in the rubber connector strip (Capillary Film Technology 2014).

The MCF was cut into 3cm strips and, using PBS with 0.01% tween as lubricant 8 strips were inserted into a rubber connector strip which forms part of the MSA (Figure 26). The rubber strips were then inserted into a plastic holder which was then connected to syringes and the MSA (Figure 27).
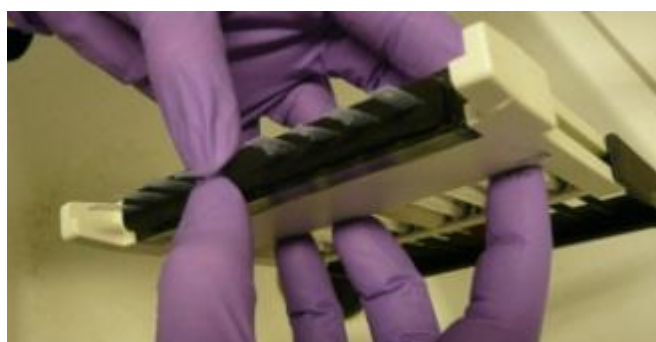
Figure 27: MCF strips in the rubber connector strip inserted into the MSA (Capillary Film Technology 2014).

The MCF strips were filled with PBS until all capillaries were full and no air bubbles could be seen. 150µl of standards or sample were pipetted into wells of a custom designed plate which can hold the MSA while the MCF strips are dipped into the wells. The knob on the MSA was rotated 6 times (Figure 28), which aspirated 78µl of solution from each well.

Figure 28: Turning of the MSA knob while the MCF strips are inserted into reagent wells (Capillary Film Technology 2014).

The standards or samples were incubated for 30mins at room temperature. 150µl of wash buffer was added to the next row of corresponding wells and the solution was aspirated into the MCF post incubation. Biotinylated antibody solution was made to the required concentration, 140µl was added to each well and aspirated into the MCF; this was incubated for 10min at room temperature and then washed once. A solution of streptavidin was made to a concentration 1µg/ml and added to each well, and incubated for 10mins at room temperature, post incubation the MCF was washed 3 times. A solution of 4mg/ml OPD was made and 150µl added to each well, this was aspirated and the MSA placed on a flatbed scanner for measurements. Image analysis was conducted on the scanned images using imageJ software. The RGB images (Figure 29C) were split into the red, green and blue channels, only the blue channel (Figure 29B) was used for the analysis. A $6mm^2$ area was selected and overlaid successively on each of the 8 strips. A grayscale profile (Figure 29C) for each strip was produced and the peak heights measured, each peak corresponds to one capillary.
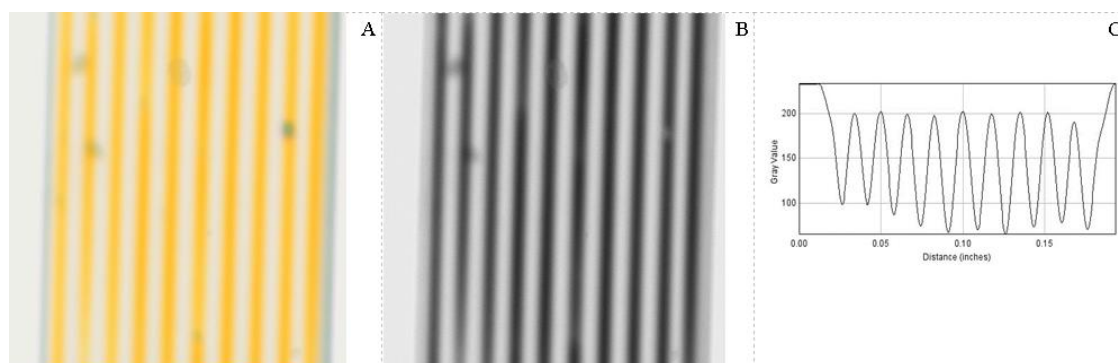
Figure 29: Image processing steps conducted in ImageJ. Converted substrate can be seen in all 10 capillaries (A), the image is split into the red, green and blue channels.

Only the blue channel is used for analyses (B). A grey scale profile in produced by the software (C) from which the peak heights are measured, and the absorbance calculated.

The absorbance is proportional to the concentration of analyte the greater the amount of analyte, the greater about of substrate is converted, producing a higher concentration of colour which in turn causes more light from the flatbed scanner to be absorbed. From the peak high was absorbance determined by:

$$"Abs" = -\log(I/I\text{o})$$

(Equation 1)

Where I is the absorbed light and I_o the transmitted light.

A standard response curve using known concentrations was developed from which unknown sample concentrations can be calculated.

4.2.5 Model fitting

With all three ELISA platforms used in this work a standard curve also referred to as a calibration curve is required from which the unknown sample values can be calculated. In both the Lumiex and standard 96-well plate ELISA methods a serial dilution of known standards are run on every plate. With the MCF ELISA known standards are used in the development and validation processes, when running samples known concentrations are inserted into runs, as due to the capacity of the MSA it is not possible to formulate a full standard curve on every run. In order to insure the accuracy of the standard curve an appropriate mathematical curve fit model must be used (Herman et al. 2008). In this work the 4 parameter logistic regression model (4PL) was used for the 96 well plate and the MCF platforms, the 5 parameter logistic regression model (5PL) was used for the Luminex assay. The 4PL model was calculated using Microsoft Excel software, the 5PL model was fitted within the Lumiex software. The 4PL model, as with all regression models, aims to achieve the smallest weighted sum of squared errors (SSE) through adjusting the 4 parameters on

the curve(Gottschalk & Dunn 2005). The 4 parameters are the minimum response (A), the maximum response (D), the inflection of the curve (C) and the degree of the slope (B), the equation is (Findlay & Dillard 2007):

$$Y = \left(\frac{A - D}{1 + \left(\left(\frac{X}{C} \right)^B \right)} \right) + D$$

(Equation 2)

The 5PL model includes the same parameters in the 4PL model but takes into account the asymmetry of data by adding a fifth parameter (G) which controls the degree of asymmetry of the curve and for asymmetric data sets results in a better curve fit (Gottschalk & Dunn 2005), the calculation is (Findlay & Dillard 2007):

$$Y = \left(\frac{A - D}{\left(\left(1 + \left(\frac{X}{C} \right)^B \right) \right)^G} \right) + D$$

(Equation 3)

Assessing the quality of the curve fit is also required, in this work the SSE value which is referred to as residual variance has been used in the 5PL model. The SSE calculates how far away the actual data points are to the curve of best fit, therefore calculating the quality of the standard curve. The smaller the SSE value the better the fit. If the curve fitting model is a poor fit to the true data, this cannot be compensated for; if the model is deemed a poor fit then the choice of model must be re-examined (Wild 2013).

4.3 Work flow of ELISA Methods

The three ELISA platforms used in this work have a number of advantages and disadvantages between the platforms in terms of cost, capacity, work flow and time. There are also the technical limitations to consider in terms of test accuracy, reliability and sensitivity. The ELISA platform selected needs to be fit for purpose;

the requirements of a research laboratory may be different to a manufacturing facility, therefore the role the ELISA platform needs to fulfil must be considered. Across all three platforms the reagent requirements are similar (Figure 30). The 3 platforms used the sandwich assay method which requires a capture and detection antibody. It is widely reported that antibody behaviour, in terms of binding affinity and cross reactivity, can be influenced by the preparation method of the antibodies, the surface to which the capture antibody is immobilised and the buffer reagents used (Butler et al. 1992; Dmitriev et al. 2013; Tarakanova et al. 2015; Cohn et al. 2015). The structure of an antibody is critical to its performance, therefore any factors such as pH, which change the structure of the antibody, in particular the binding site, or conformational changes which occur while the antibody is immobilised on a solid surface, could result in loss of function (Butler et al. 1992; Tarakanova et al. 2015).

In this work the antibody pairs (capture antibody and detection antibody) were sourced from a commercial company whom had validated the compatibility of the antibody pairs and optimised the reagent conditions in terms of buffer pH and concentration required for the 96 well plate formats.
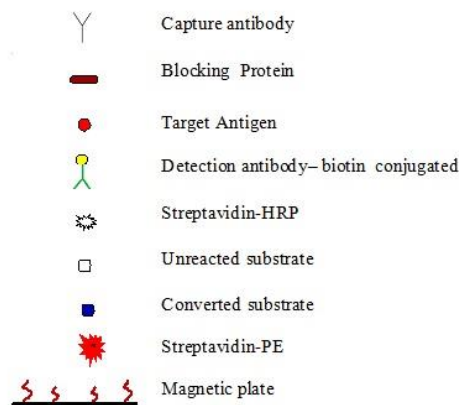
Figure 30: Key reagents of ELISA assays, the utilisation of these reagent varries between the ELISA platform. The 96 well plate ELISA (Figure 31) and the MCF ELISA (Figure 33) utilise a colourimetric based format where by a substrated is converted using streptavidin HPR, which results in colour formation. The formation of colour is directly proptional to the concentration of analyte. The Luminex platform (Figure 32) uses a fluorescent detection method in this incidence streptavidin conjugated to PE.

The commonly used 96 well plate ELISA platform consists of 6 incubation steps including capture antibody immobilisation, blocking reagents, detection reagents, and samples, with repeated wash steps in between (Figure 30 and Figure 31). From a liquid handling perspective, the assay is straightforward and requires basic skills to carry out; it is a series of pipetting steps and washing steps, but the time required to carry out the steps is considerable. In addition to the long incubation times outlined in Figure 31 when running the plate manually the repeated reagent pipetting and washing increases length of time it takes to perform the assay. There is scope to utilise automatic liquid handling robots in order to reduce the labour intensiveness of the manual pipetting (Kong et al. 2012) however this does not overcome the incubation time requirements. Post-sample addition 4hrs of incubations are required in this example, though incubation times are also influenced by antibody performance, in this instance incubation times were determined by the manufacturers protocol. In the 96-well plate colorimetric format it is only possible to detect one analyte per well which limits the throughput of the assay, and in situations where samples are precious and require multiple analytes to be measured it is not an optimal system. A multiwell plate reader is used to determine absorption levels in each well; the run time on a plate reader is relatively short ～5mins however from the absorption values need to be converted into concentrations. This is done by creating a standard curve using serial dilutions of known concentrations of analyte. The standard curve also needs to be fitted to a regression model to calculate fit and confidence in the values.

Immobilisation of capture antibody – 12-18hrs (over night) at 4°C

Wash x1

Blocking of plate – 1hr at room temperature

Incubation with sample/standards – 2hrs at room temperature

Wash x3

Incubation with biotinylated detection antibody – 1hr room temperature

Wash x3

Incubation with streptavidin-HRP – 30mins room temperature

Wash x3

Addition of TMB substrate – 30mins incubation at room temperature

Addition of stop solution – absorbance measured within 30mins

Figure 31: Flow diagram of the 96 well plate ELISA format. Images are representative of 1 well of a 96 well plate, image components are explained in Figure 30. This work flow requires a minimum of 17hrs of incubations and 9 washes. One analyte can be detected per well using this format.

The Luminex platform addresses some of the limitations of the 96 well ELISA platform. The capture antibodies are immobilized on colour coded beads which can to distinguished from one another within the same well allowing multiple analytes can be measured in one well. This reduces the amount of sample required for analysis, and is consequently more time efficient. In the context of this work for the amount of data the Luminex has produced in 1 plate 5 standard 96-well ELISA plates would have been needed. Over all incubation times in a Luminex plate are also reduced from ～17hrs to ～3.5hrs (Figure 31 and Figure 32), this is attributed to the beads being pre-coated with the capture antibody, and no blocking step being required. While it is possible to buy pre-coated 96-well plates these cost more and do not have the added benefit of multiplexing which the Luminex platform has. Though the costs can vary in terms of reagents and labour verses the amount of data obtainable per plate the Luminex platform is considered to be overall more cost effective (Wild 2013). From a manufacturing of a cell therapy perspective the Luminex platform is not perfectly compatible. As discussed in chapter 2 section 2.8 reducing the sample to result time is critical in such a dynamic growth environment, once the sample has been added to the Luminex plate there is still 3.5hr or incubations on top of which there are also 9 wash steps in total, and the plate can take more than 20mins to run on the machine (run time is dependent on the number of analytes being detected per well). Though, as with the standard 96-well plate format there is the scope to investigate the use of automatic liquid handling machines in tandem with the Luminex platform. The current 3.5hrs incubation times could still be seen as a time delay from obtaining results. Measuring all the wells on the plate takes more time that the plate reader used in the 96 well pate formats. For a 5-cytokine panel, the run time is ～1hr, however there is the added advantage that all the analysis is carried out in the Bio-Plex Manager Software including the 5PL model fitting. The Luminex plate has the capacity to analyse 41 samples per plate when allowing for each sample to be run in duplicate. Wells on the 96 well plate also need to be allocated for analyte standards and a matrix normalising control which is required for every plate run.
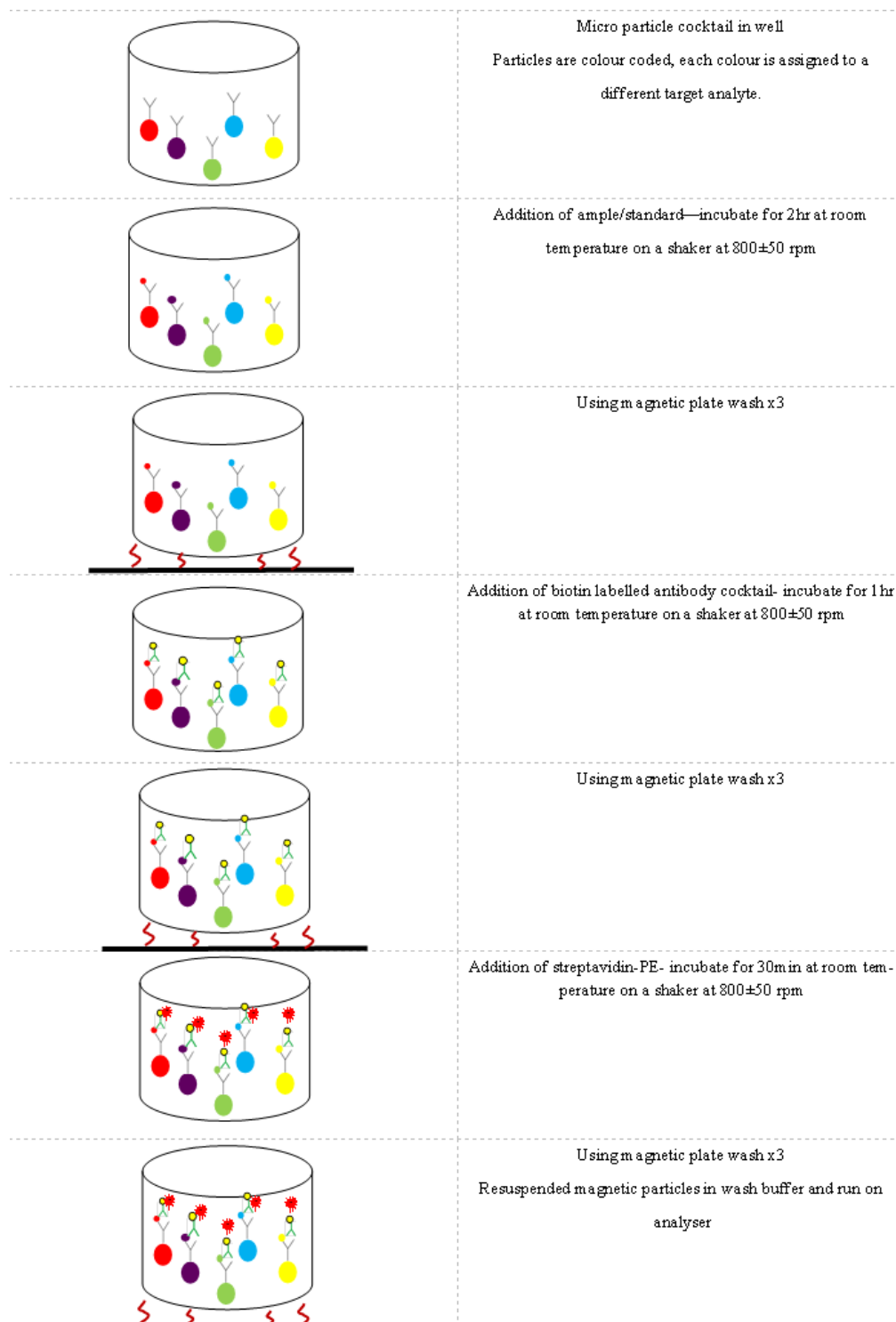
Figure 32: Flow diagram of the Luminex assay format. Images are representative of 1 well of a 96 well plate image components are explained in Figure 30. This platform requires 3.5hrs incubation and 9 wash steps, in this instance 5 analytes can be quantified per well.

The MCF ELISA format addresses the issue of long incubation times, post addition of the sample incubation times can total 50min or less (Barbosa et al. 2014), and due to the use of the MSA washing is carried out by rotating a knob 6 times as opposed to pipetting and aspirating which also reduces the time needed to carry out the washing steps.
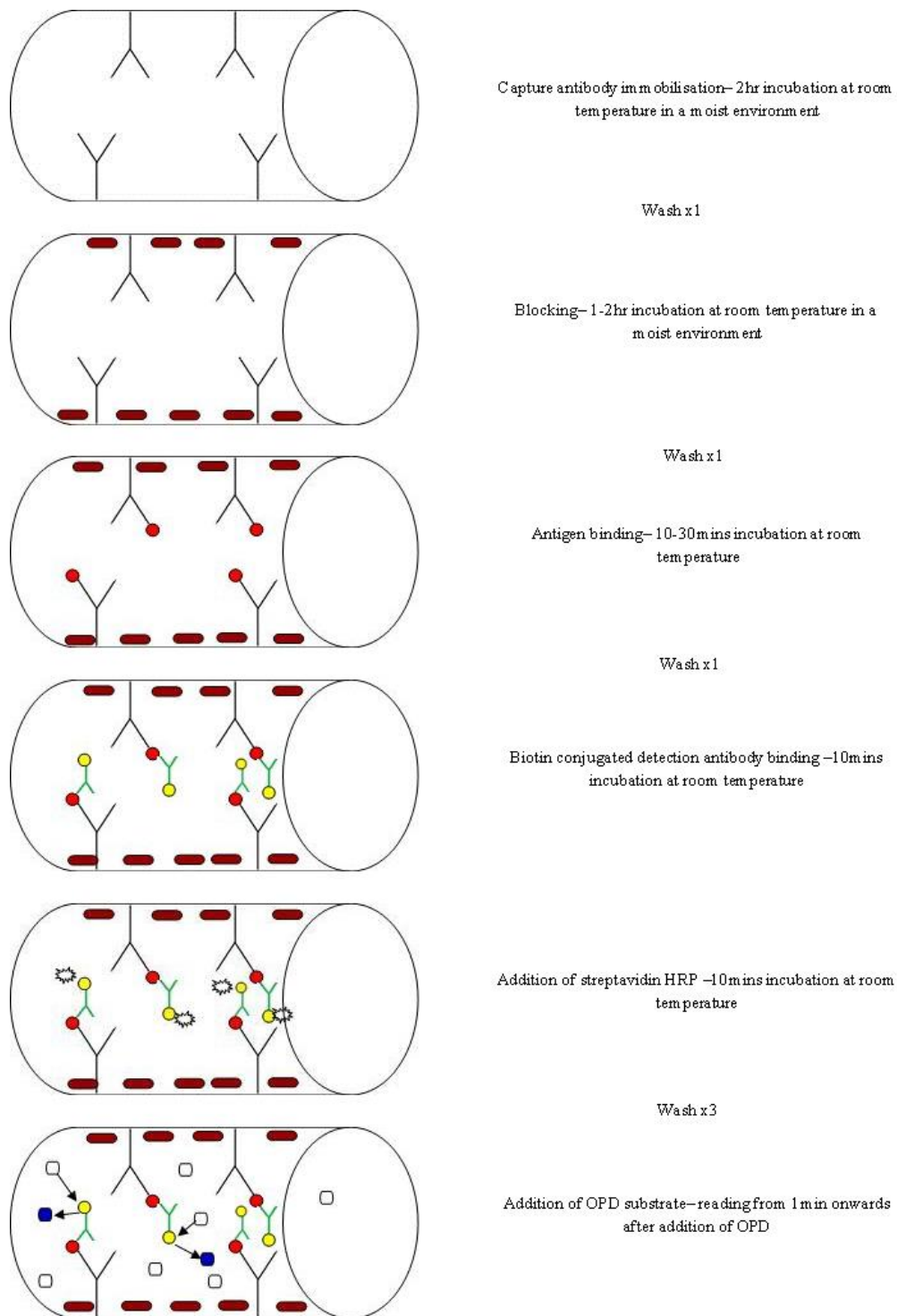
Figure 33: Flow diagram of the MCF ELISA formant. Images are representative of 10 capillaries image components are explained in Figure 30. The MCF ELISA requires 3.5hrs in incubation steps (excluding OPD incubation time) and 6 wash steps, post sample addition an image can be obtained within 32mins; however the image requires further analysis using imageJ software in order to calculate the absorption. One analyte can be detected per strip

4.4 Results and Discussion

4.4.1 Magnetic Luminex Screen Assay- IL-8 standard curve

The most important steps when developing an immunoassay is the validation and calibration. Every commercial kits require standards with a known concentration to be run on every plate in order to formulate a calibration curve from which unknown concentrations can be calculated. In this work the Luminex platform comprises of magnetic beads pre-coated with antibodies specific for one of the target analytes (Figure 32). Each well on the 96 well plate contained 50µl mixture of magnetic beads for all 5 target analytes, fresh culture medium was used as the control sample against which the results were normalised.
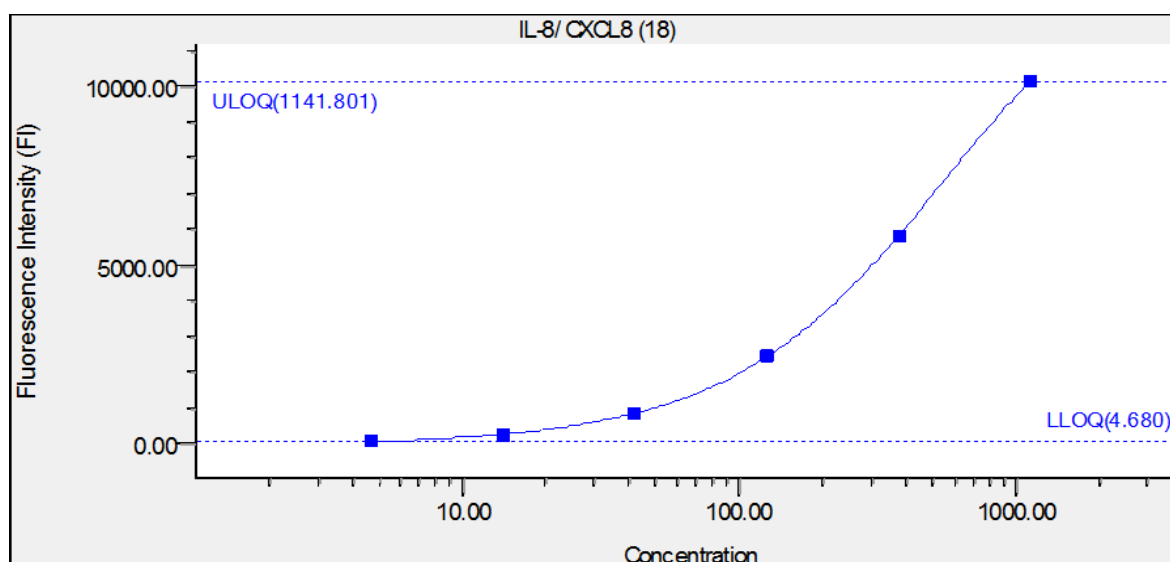
Figure 34: Standard curve for IL-8 analyte produced using Bio-Plex Manage Software. Values were formulated from standards in a five panel magnetic Luminex screening assay and calculated within the Bio-Plex Manage Software. A 1 in 3 serial dilution was carried out 5 times resulting in standard concentrations of 1140pg/ml 380pg/ml, 126.67pg/ml, 42.22pg/ml, 14.07 pg/ml and 4.69 pg/ml. The standards were carried out in duplicate and then fitted to the 5PL model. From the standard curve the Bio-Plex Manager Software calculated the upper limit of quantitation (ULOQ) at 1141.801pg/ml and a lower limit of quantitation (LLOQ) which was 4.68pg/ml. A residual variance value of 0.0944was

calculated deeming the curve a good fit

The Luminex assay has an upper limit of detection/quantitation (ULOQ) of 1144.619pg/ml and a lower limit of 4.649pg/ml for IL-8. Previously reported values hMSC IL-8 secretion lie within these limits, based on the data produced in chapter 3. However, given the disparity of hMSCs culturing methods discussed in chapter 2 section 1.8.2 dilutions of sample maybe required. For example Potier et al. (2007) reported 780±390 pg/ml IL-8 secreted by hMSCs cultured in hypoxic condtions and 440±230 pg/ml in normoxic conditions, accounting for the standard deviation of the quantities produced in the hypoxic conditions exceeds the ULOQ for this Luminex assay.

4.4.2 96 well plate based IL-8 ELISA standard curve
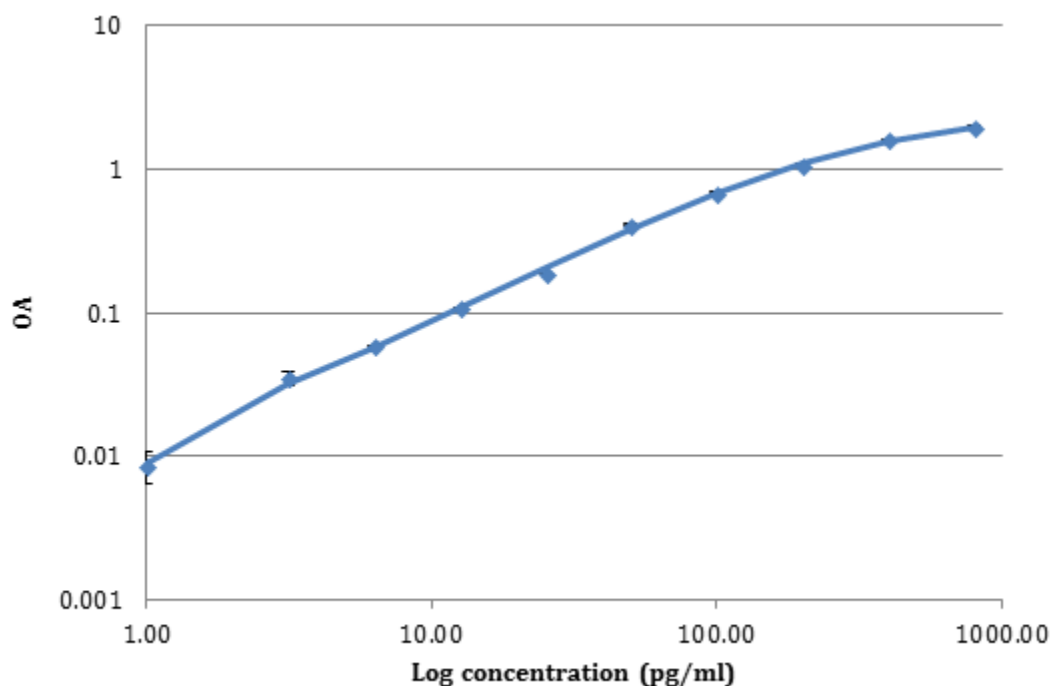
Figure 35: IL-8 Standard curve produced from a standard 96 well plate ELISA following manufacturers' instructions. Results were fitted to the 4PL model. Standard concentrations were 800pg/ml, 400pg/ml, 200pg/ml, 100pg/ml, 50pg/ml, 25pg/ml, 12.5pg/ml and 0pg/ml. r^2= 0.99973, LOD=0.698088pg/ml, CV 0pg/ml 24.96% (n=3)

4.4.3 MCF IL-8 ELISA

Sensitivity of an ELISA assay can be determined by how much signal is produced when no analyte is present in the assay, the lowest concentration detectable should not fall within 3 standard deviations of the mean of the absorbance value when no analyte is present (Wild 2013). One of the parameters that can help improve the sensitivity of an ELISA assay is the selection of a good blocking buffer. Blocking buffers prevent the non-specific binding of detection antibody and are applied to the ELISA system after the capture antibody has bound to the surface. In commercial kits such as the one used in this work the manufacturers offer the kits with all the recommended buffers to use in a well plate format. Blocking buffers generally contain some form of protein(s) and the effectiveness of blocking buffers will vary depending on the surface chemistry of the solid surface they are binding to, consequently as the MCF is made of FEP the surface chemistry will be different to polystyrene. Figure 36 shows 4 different blocking buffers trialled in the IL-8 MCF ELISA assay but without the presence of any analyte.
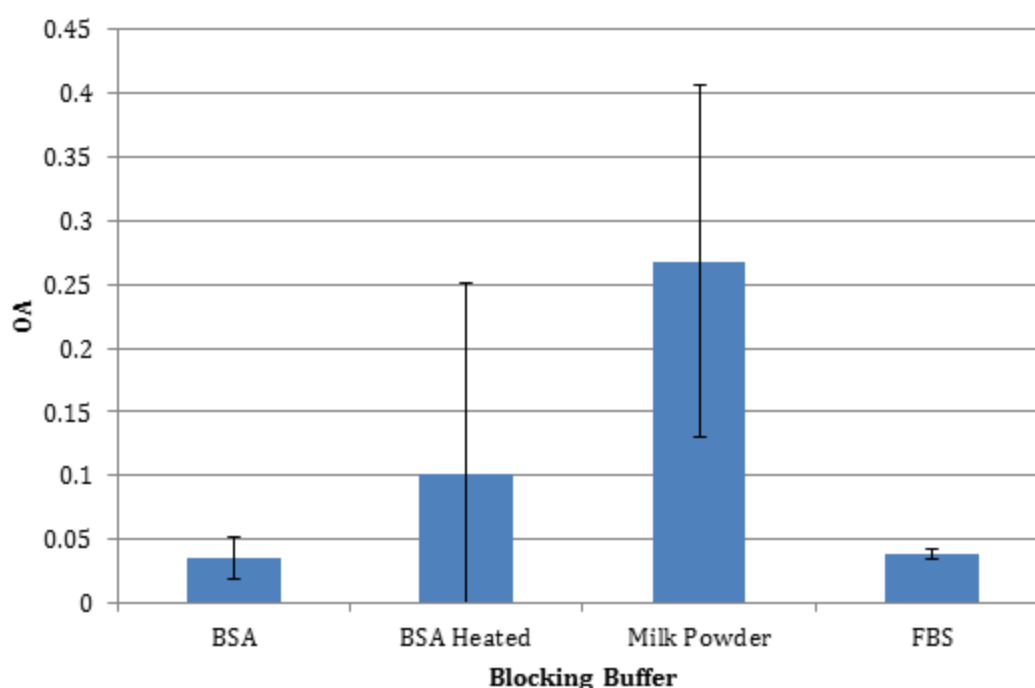
Figure 36: determining optimal blocking buffer to produce the least back ground absorbance in the MCF. Data from 5min incubation with OPD (n=3-10)

In Figure 36 the highest signal is seen with the milk powder blocking solution which has an absorbance above 0.25 and a standard deviation of 0.14. while BSA heated had a lower mean absorbance value compared to the milk powder the standard deviation was greater at 0.15. BSA had the lowest mean absorbance value of 0.04, FBS had a slightly high signal of 0.039 however FBS had a smaller standard deviation of 0.005 compared to BSA with 0.016. FBS was selected as the best blocking buffer for the subsequent MCF ELISA runs.

In standard colorimetric ELISAs the substrate is incubated with the conjugated immobilized enzyme and after a period of time usually optimized by the manufacturer a stop solution is added to prevent any further enzymatic reaction. This format is not possible with the MCF ELISA as addition of new reagents such as the stop solution requires the aspiration of the previous reagents, this would essentially result in the substrate (in this case OPD) being washed away and therefore removing the required coloured product. In the case of the MCF ELISA the strips must be scanned while the enzymatic reaction is occurring, therefore an optimal window of time needs to be determined in which an accurate set of data can be obtained. In the development phase the MCF strips are continuously scanned with the purpose of capture as many time points as possible.
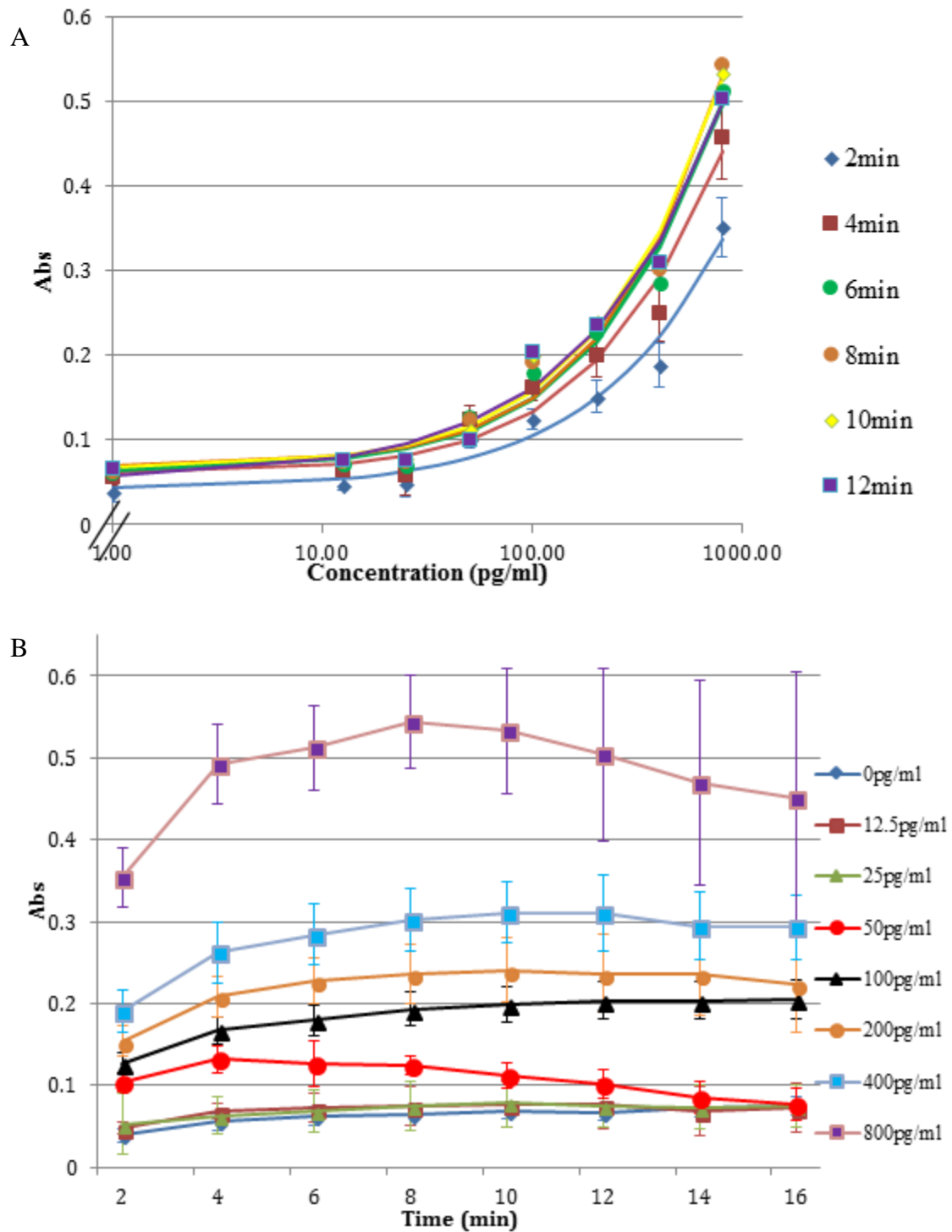
Figure 37 A: IL-8 standard curves showing the effect of OPD incubation time on sensitivity. The respective observed values (coloured markers) and 4PL (solid line) model predicated values are shown. The experimental parameters were 10µg/ml capture antibody, 5µg/ml detection antibody, 4µg/ml HRP, 4mg/ml OPD, the standards were reconstituted in fresh hMSC cell culture medium. Error bars are

representative of a minimum of 6 replicates. B: Absorbance values of data in A displayed over time. Repeated images were scanned every 2mins (n=3-10)

Table 9: Summary of LOD and r^2 values in Figure 37A. LOD was calculated from the absorbance value of the blank plus the 3 times the standard deviation

Time (min)	LOD (pg/ml)	r^2
2	132.15	98.3%
4	38.08	98.4%
6	43.24	98.8%
8	40.75	98.9%
10	44.51	99.0%
12	143.41	99.0%

Determining the optimal time to measure OPD reduction is a balance between obtaining the lowest limit of detection, therefore making the assay more sensitive, and having the closest fit to the 4PL model which makes the assay more reliable. The scanning time can take between 1-2min which is not ideal in a rapid enzymatic reaction. However, in Figure 37A and Table 9 2min post addition of OPD produces a high LOD in comparison to the 4 subsequent time points, but the r^2 of 98.3% indicates a good model fit. The LOD values are between 40pg/ml and 45pg/ml for 6-10min OPD incubation times. The LOD at 4min is below that range the r^2 value at 4min of 98.4% which indicates a good fit. After 10mins incubation the LOD steadily increases over time. An LOD of around 50pg/ml is further supported by the data in Figure 37B, the 12.5pg/ml and 25pg/ml conditions cannot be distinguished from the blank control over a 16min time period. The 50pg/ml condition can be distinguished until approximately 10mins incubation times were the standard deviation over laps with that of the lower values. In terms of establishing an optimal time point, based on the data in Figure 37 4mins produced a good curve fit an LOD of 38.06pg/ml and before the absorbance values drop in the 50pg/ml standard. One of the challenges of working with OPD without a stop solution is that in some capillaries the solution begins to fade over time (Figure 38). As shown in Chapter 3 levels of IL-8 and HGF in the T25 flask format are higher than 100pg/ml for some cell lines and this was at a relatively small scale (5ml) compared to the largescale manufacturing environments where

concentrations would be expected to be higher. Hence a LOD of ~50pg/ml is acceptable for this application, based on the Luminex data in Chapter 3.
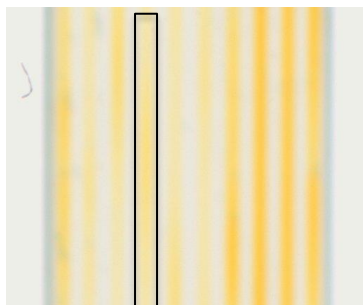
Figure 38: Example of colour fading within the same capillary. This example shows IL-8 50pg/ml with 10mins OPD incubation.

The reason for the disparity in colour within the same capillaries is unclear. In the literature nothing has been found relating this directly to OPD behaviour, though the use of OPD in a microfluidic platform with this specific set of conditions has only been done a handful of times before (Barbosa et al. 2013; Barbosa et al. 2014; Castanheira et al. 2015). Further investigation would need to be done; the possibility that the faded sections may not be as well coated with antibody would be an avenue that could be explored also.

The IL-8 MCF ELISA was also tested with samples that had previously been tested using the Luminex platform (Figure 39). The samples were from some of the conditioned medium used in Chapter 3; two freshly made solutions of Il-8 with a concentration of 200pg/ml and 400pg/ml were also run on the same MSA. The images were scanned at 4mins, 6mins, 8mins and 10mins, concentrations were calculated using the fitted curves in Figure 37A.
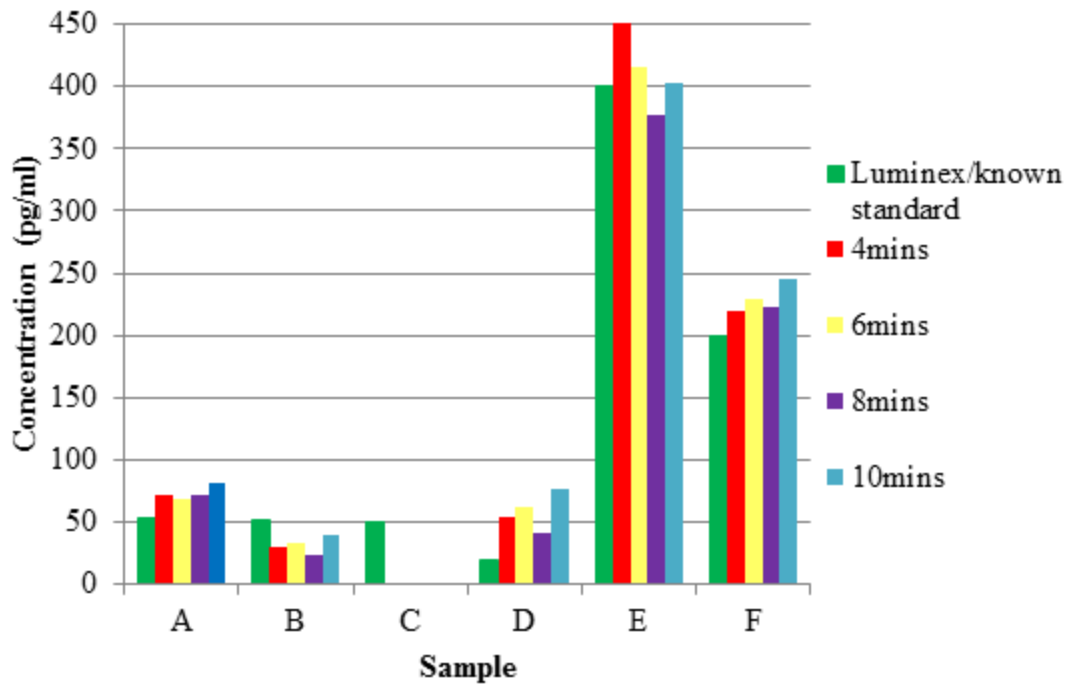
Figure 39: Comparing Luminex measurements and known standards to the MCF ELISA platform using the standard curves formulated in Figure 37. A, B, C and D are conditioned medium samples used in Chapter 3; E and F are 400pg/ml and 200pg/ml respectively of freshly made standard form recombinant IL-8 protein.

4.4.4 MCF HGF ELISA
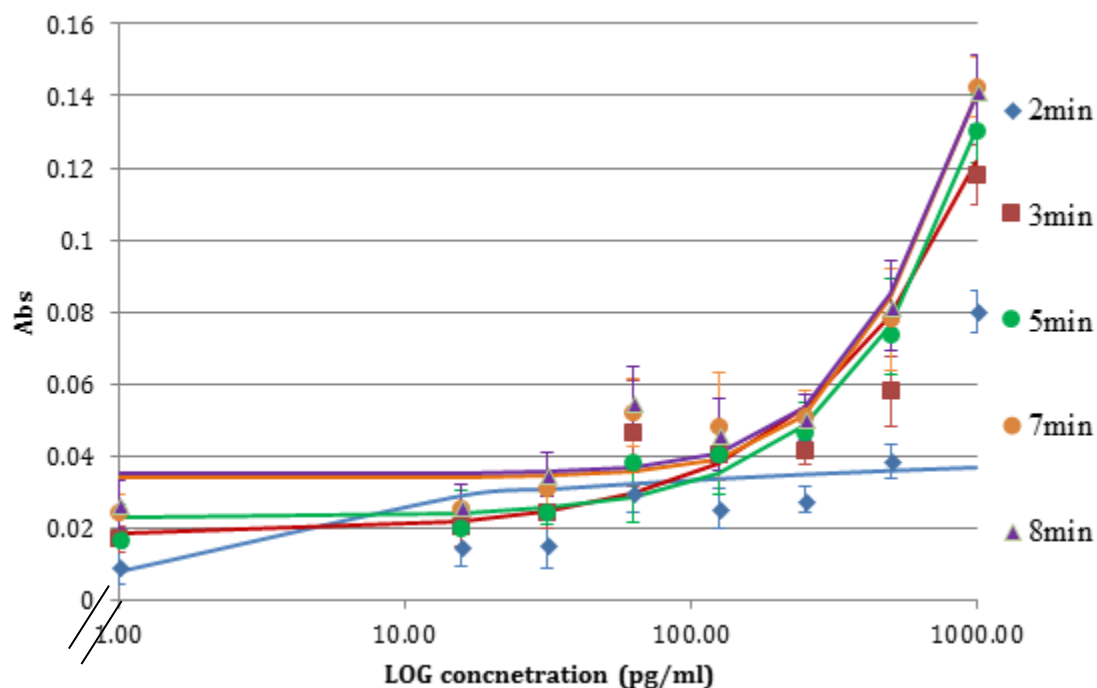
Figure 40: HGF standard curve at 2, 3, 5, 7 and 8 minutes incubation with OPD. Standards are expressed as log values, the pg/ml values are 1000, 500, 250, 125, 62.5, 31.25, 15.625 and 0. The respective observed values (coloured markers) and 4PL (solid line) model predicated values are shown.

Table 10: Summary of LOD and r^2 values based on data in Figure 40

Time (min)	LOD (pg/ml)	r2
2	1.39	56.79%
3	102.38	95.31%
5	36.42	99.08%
7	27.99	97.22%
8	3.17	97.38%

4.4.5 Improving the measurement process

In order to obtain meaningful results from the MCF ELISA the images were scanned and the processed using ImageJ software. The image processing was done manually therefore during some of the stages there is an opportunity to introduce errors or operator bias. As with any imaging process ensuring the equipment is clean and free

of artefacts is an important step. Artefacts can include liquid droplets on the outside of the MCF, dust and debris from the environment or the scanner itself having smudges on the scan surface. In plate readers and the Magpix system the optics are in an enclosed dust free environment, the flatbed scanner is more open to the environment and liquid droplets can form on the imaging surface from the end of the MCF strips. Operators must take extra care to ensure the scanning window is clean, however when scanning under a time pressure there is the risk of error and accidental spillage. When the images of the strips in full colour are split into the blue channels (Figure 41), some image quality issues can be seen but these will be discussed later. The operator must ensure that the portions of the strips selected for analysis are consistent. Issues arise as not all the capillaries may be full or have an equal distribution of colour therefore, the operator is deciding what they deem to be the best portion. This introduced variation as by nature a human operator will have a different option compared to another operator.

A

B
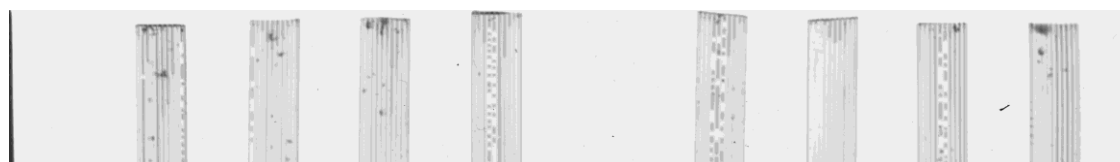
Figure 41: Scanned images of MCF ELISA strips held in the MSA of a HGF ELISA with 6mins OPD incubation. A) Original full colour scan image B) Blue channel image of A

Once a portion of the strip has been selected a grayscale profile is produced within the ImageJ software, the operator must then select a baseline at the top of the peaks and measure the height of each peak (Figure 42). Selecting a baseline is guided by the peak height, but when the peaks are not level the end placement of the baseline is on the operators' discretion. In Figure 42B it can be seen that not every peak lies directly on the selected base line. The peak heights measured are transferred into an excel

document and the average absorbance calculated using the absorbance equation in Section 4.2.4.
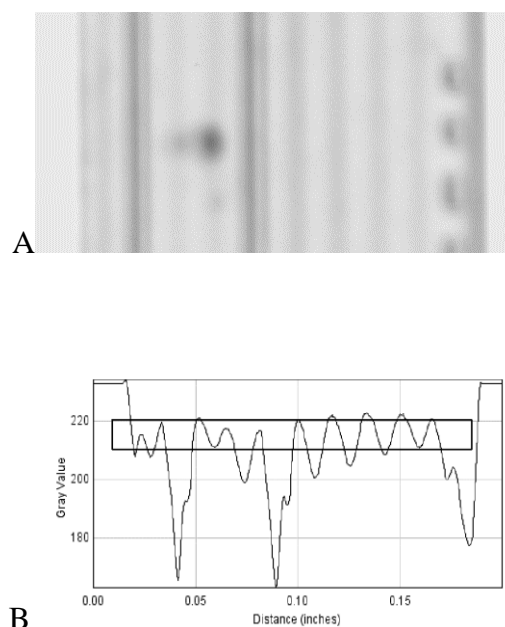
Figure 42: Analysed section of HGF MCF ELISA 1000pg/ml after 6mins incubation with OPD. A) Section of strip analysed as seen in ImageJ B) Grayscale of absorbance of image A

Images in Figure 41 and Figure 42 show one of the challenges of the MCF ELISA systems is the improvement of the fluid handling, as seen in the images a number of capillaries have failed due to the liquid emptying from the capillary or because of a number of air bubbles. This can occur as a result of weakness in the rubber holder which connects the MCF strip to the MSA (Figure 27), or the strips were removed from the well too quickly when a solution was not fully aspirated into the strips therefore introducing air bubbles. The MSA is also in a vertical position when the solutions are being aspirated into the strips, but is then moved into a horizontal position for measurement which changes the forces exerted on the capillaries and can result in geometry induced capillary emptying (Rascón et al. 2016). The total failure of a strip would in a manufacturing setting be a negative attribute of this method, with the well plate and Luminex platforms liquid handling is straightforward and therefore less prone to error. The MCF does contain 10 capillaries that act as repeats which provides some tolerance to individual capillary failure.

The issue also arises that air bubbles or uneven mixing impact on the accuracy of the measurement, while the operator, when analysing the images, should avoid including non-uniform capillaries this is not always possible. The first issue encountered was that due to the strips being inserted into the connecting rubber seals manually not all the strips were perfectly parallel. The strips were also not directly touching the glass surface of the scanner due to the MSA which increases the length of the light path (Figure 43 A) and therefor the clarity of the image, this is due to light dispersing at the source (Myers & Lee 2008). This is demonstrated in Figure 43B and C where the image of the MCF scanned in contact with the scanner and therefore has the shortest light path has sharper contrast between filled capillaries and the capillary wall.

A

B

C
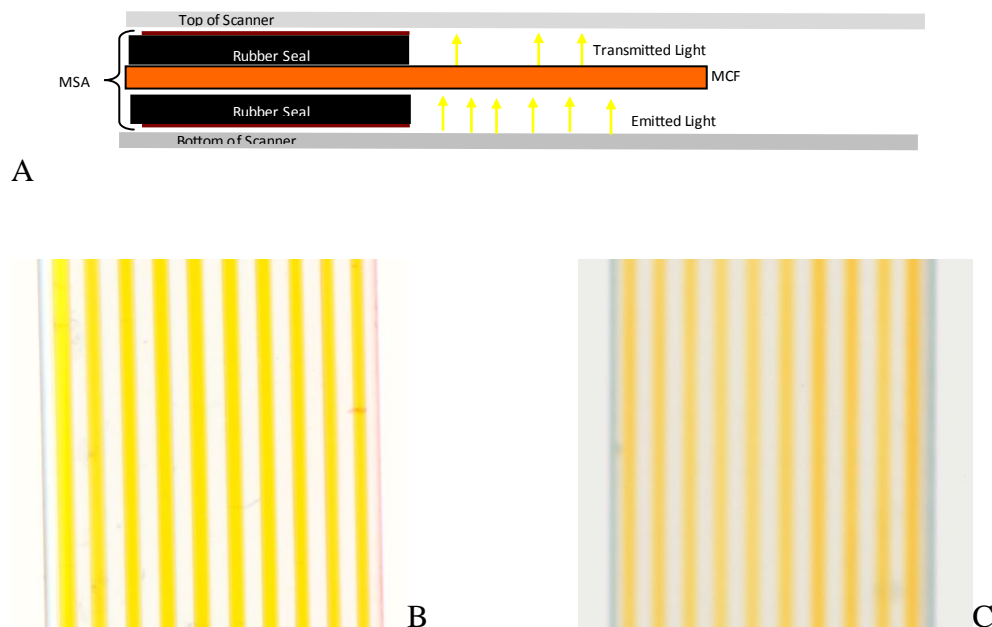
Figure 43 A) A depiction of the light pathway during imaging of the MCF ELISA using a flatbed scanner. B and C two section of MCF strip, B contains fully reduced NADP which was scan without the MSA hence the MCF was in direct contact with the flatbed scanner, image is representative of 3 scanned strips. C is a section of MCF containing 1000pg/ml HGF analyte scanned after 2min incubation with OPD, the MCF strip was scanned while being held in the MSA. Image is representative of 10 scans.

It can be argued that as long as the image quality is consistent any inherent errors will not affect the end result as the standard curve is calculated form the same quality image. The fact that the MCF strips are able to have up to 10 replicates per strip also

reduced the variability of the assay. The impact of one capillary being measured incorrectly will have less impact on the mean than if there were only 3 replicates. Usually in the 96 well plate format a standard curve is run on every plate but with the MCF the standard curve is not run at the same time as the samples. Other variable factors such as the placement of the strips in the rubber seal, and the distance between the scanner and the MCF strips must be consistent in order to negate any variation between conditions.

An image analysis software was developed to automate the image processing with the aim of removing operator biases and increasing the speed of the image processing therefore reducing the time needed to obtain a result. The Luminex platform employs a highly calibrated and optimized LED based measurement system. The 96 well- plate platform uses a plate reader which is regularly calibrated and designed to obtain optimal readings. The MCF system currently uses a standard scanner though the scanner is set to the highest resolution the quality of the image selection is not optimal as seen in Figure 42B. This presents a number of problems when developing image analysis software, as the software processes the image a pixel at a time. A lower resolution (therefore less pixels) will have an effect on the end result.
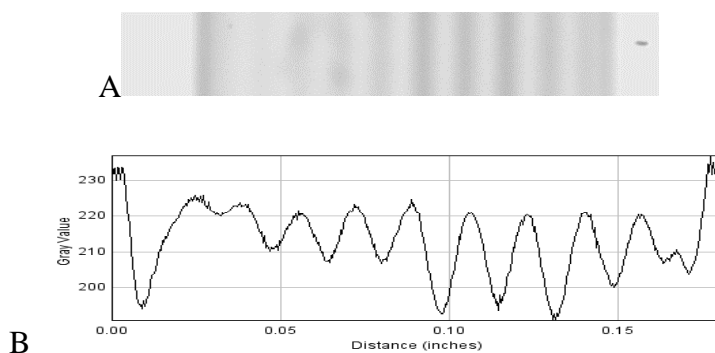
Figure 44: A) MCF strip 0pg/ml HGF 6mins OPD incubation processed using custom built software. B)

The custom built software splits the image into the blue channel, it then realigns the capillaries in order to analyse a reliable cross section. It then finds the largest consistent section within the strip, this process aims to prevent sections which contain bubbles from being analysed, however this is not always possible if no such section

exists. When this situation occurs, the software keeps the bubble size included in the section to a minimum and will omit the value from that capillary from the end analysis. As seen in Figure 44A the quality of the image when interrogated to the individual pixel level deteriorates, a grayscale profile can still be obtained but the issue with establishing a level baseline is still present.

A potential reason for the lack of a consistent baseline could be due to the 10 individual capillaries in each strip not being uniform in terms of diameter. When the MCF is filled with 2,3-diaminophenazine (DAP), which is formed when OPD has been fully converted by HRP (Hamilton et al. 1999), the baseline becomes, to the naked eye, level (Figure 45). It should be note that this image was scanned in direct contact with the scanner so any inconstancies introduced by a longer light path will not be apparent in the profile. The outer 3 capillaries on both sides of the MCF are shorter in height than the middle four peaks. As the profile is an inverse profile this would provisionally indicate that the middle four capillaries had a lower concentration of analyte.
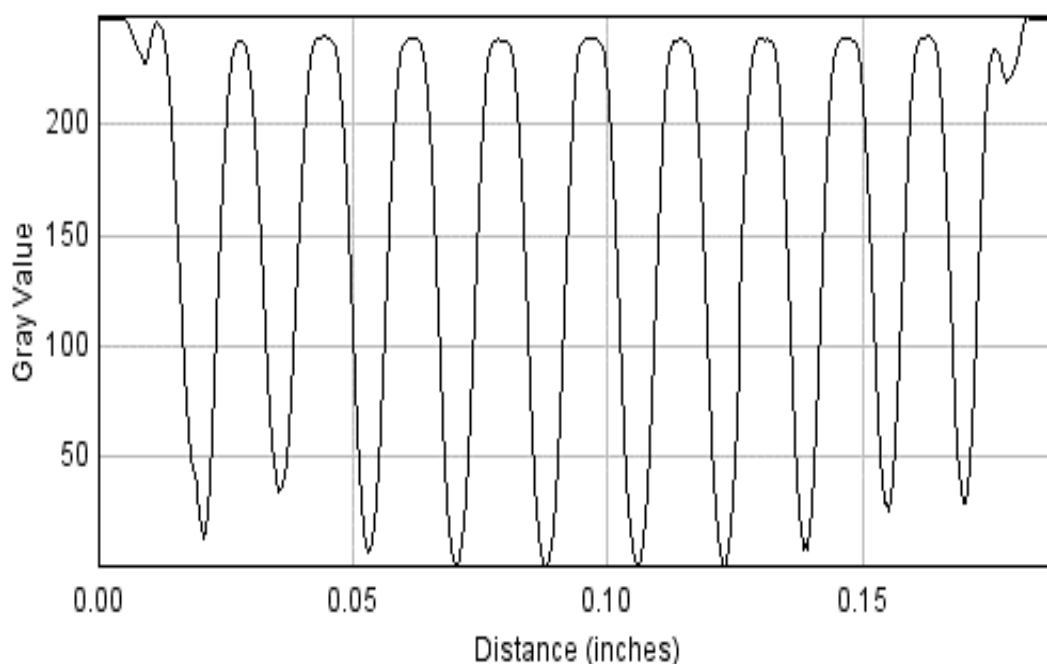
Figure 45: Grayscale profile of Figure 43B, in which the MCF is filled with fully reduced OPD

An element which has not been discussed in detail is the selection of the antibodies used in the MCF ELISA. The antibodies used for IL-8 and HGF where antibody pairs which had be validated by the manufacturer and due to time constraints it was decided that further validation was not required. When pre validated antibody pairs are not available the specificity of the antibodies and any cross reactivity must be identified and validated within the same sample matrix.

4.5 Conclusions

Translation of the IL-8 and HGF ELISAs into the MCF ELISA platform has been achieved, though the LOD is higher than the Luminex and 96-well platforms in a large scale manufacturing setting this would not be an automatic impediment of the assay. In a manufacturing setting the aim would be to achieve as high concentrations of cytokine as possible therefore a higher LOD would in some instances be acceptable. Further optimisation can be carried out to increase the sensitivity of the assays, this could include selecting a blocking buffer which reduced the signal to noise ratio. The concentration of antibodies could be further optimised, values in the HGF and IL-8 assays were based on previous work by (Barbosa et al. 2014; Barbosa et al. 2013; Edwards et al. 2011). When considering an immunoassay to be used in a near online manufacturing setting more factors need to be considered. One of the current weaknesses of the MCF ELISA format is that it is not easy to check for sample/standard pipetting errors. With the Lumiex and the 96 well plate format samples/standards are pipetted minimally in duplicate the MCF ELISA is currently in a 8 strips per device therefore running samples in duplicate would mean only 4 experimental conditions could be analysed in a single run. This could be overcome simply by increasing the capacity of the MSA. The fluid handling would also need to be improved, this is very operator dependant; the risk of losing an assay/sample due to the capillaries emptying would not be acceptable in a manufacturing setting. An automated image processing software would remove the current operator bias that can occur with the MCF ELISA image processing method. Though the custom built image processing software was not used for the analysis in this work it was shown that in order to develop a high quality image processing software, as with any imaging processing software the image quality needs to improve. There is a clear benefit to using the MCF ELISA over the Luminex and standard 96-well plate platform and that

is the reduced in time from sample addition to imaging, automated software would also reduce the time to receive a result.

There is a lot of potential for using the MCF ELISA within a manufacturing setting. The rapid sample incubation to assay completion time is a benefit to the production environment. This work has taken the first steps into identify the challenges of using the MCF platform with a cell therapy manufacturing application as the focus. Il-8 and HGF ELISA assays have been shown to work in the MCF platform though more refinement is required in improve sensitivity.

Reducing the amount of manual handling steps currently required would be a great improvement for the MCF ELISA. Barbosa et al. (2015) have shown the possibility of using fluorescently labelled antibodies, replacing the current OPD colorimetric system. This method removes the time pressure of scanning the strips within an optimal time frame and as with the Lumiex platform it also reduced the wash steps required which in turn saves time. Replacing the aspirating method to fill the capillaries with reagents would help reduce the risk of failed capillaries and improve the confidence that each capillary contains the same reagents concentration. Exploring the possibility of combing the MCF device with micro-needle injection systems would overcome a lot of the fluid handling challenges. Each capillary on the same strip could be coated with a different antibody which would increase the capacity and flexibility of the MCF ELISA. When using different fluorophores in the same strip the issue of spectral overlap needs to be taken into consideration and experimental set-ups designed with this in mind. The optical clarity of the MCF is a benefit but when trying to detect emitted fluorophores to one capillary light can bleed into the neighbouring capillaries.

The ideal system in a manufacturing setting would to be able to integrate the MCF ELISA so it would be an at line system that could provide continuous and rapid feedback as to the cytokine levels in the culture system. Overall there is a lot of promise that the MCF ELISA platform could fulfil a currently unmet need for rapid quantification of cytokines within the cell therapy manufacturing setting, supporting the hypothesis that translating a plate-based ELISA assay into an MCF based microfluidic platform reduces the time between the addition of sample to result (Chapter 3).

5 Microfluidic cell based analytics

5.1 Introduction

Improving efficiency in bioanalytic and bioassays is a major challenge both at the research laboratory level to the large-scale manufacturing scale. To be able to combine two platforms whereby the bioanalytics occur either concurrently with the cell culture or within the same unit would save time, and ideally cost. There would also be the added benefit with a closed continuous system as this would reduce the need for manual handling steps and therefore operator error, and the ability to maintain sterility within the closed system. In Chapter 3 it has been shown that hMSCs produce a cytokine secretome that vary between donors and culture conditions. There was that added challenge of ensuring the integrity of the cytokines between production from the cell and measurement time. Work in Chapter 4 has shown that using the microfluidic MCF platform it is possible to detect and analysis two of the cytokines which were also measured in Chapter 3 using the Luminex platform. The use of the ELISA MCF is of the most benefit during the scale up culture environment when it is important to be able to monitor the conditions. It is however also important to have the cytokine or protein of interest production data during the cell line or clone section phase. There is time and cost saving benefits to this within allogenic treatment systems, cell recovery post cryopreservation needs to be determined and certain factors can also indicate at an early stage how a specific vial will perform. There is also the need for miniaturisation and rapid understanding of a cell populations' behaviour in autologous treatments. Autologous treatments tend to have a limited sample size obtained from the patient and a less flexible treatment schedule. Looking towards the future of precision medicine individualised treatments require a fast turn around and a greater understanding of how the patients tissue will respond to a therapy.

The MCF has the scope to fulfil a need for continuous system analytics, it has already been demonstrated that cytokine detection can occur inside the MCF using a sandwich ELISA method. The next challenge is to determine if hMSCs can also be cultured inside the MCF with the long-term prospect of being able to culture hMSCs at one end of the MCF and detecting cytokines as they are being produced by the cells

as explained in Chapter 4. Microfluidic cell based assays have been developed using other microfluidic platforms previously, primarily with a PDMS-based channel system (Eteshola & Leckband 2001; Kim et al. 2007). These systems often require isoelectric focusing and are mostly chip-based formats (Huanchun Cui et al. 2005). The MCF has the advantage that it is easy to manufacture in long lengths and has multiple capillaries in parallel. Like most microfluidic devices which provide a highly controlled and sensitive platform it will require refinement with the fluid handling.

The first step was to determine if it was possible to culture hMSCs inside the MCF and what steps were required to improve the environment of the MCF which is made from FEP. The surface energy state of FEP has been shown to not facilitate the adhesion of cells; this is reflected in the fact cell culture bags are manufactured from FEP as cells do not adhere to the surface (Kurlander et al. 2006). Most adherent cells are cultured on standard tissue culture plastic which is made from polystyrene and is also like FEP, a hydrophobic polymer. The polystyrene surface is usually modified using either corona discharge under atmospheric conditions or gas-plasma under vacuum which produces a more hydrophilic surface (Ryan 2008). Due to the optical clarity of FEP and the use of this polymer for the MCF ELISA it was deemed unfeasible to change the polymer the MCF was fabricated from, therefore surface modification was the most appropriate step.

The surface modification of FEP methods need to be compatible with the microfluidic dimensions of the MCF. Methods such as gas plasma require the plasma stream to have physical interactions with the surface which is not possible as much of the surface is internal. Taking into account these constraints and the fact that fluoropolymers are highly chemically inert so modifying using chemical reactions would be difficult, other avenues were explored. Poly (vinyl- alcohol) (PVA) and poly-L-lysine (PLL) have been shown to functionalise the surface of fluoropolymers through adsorption and hydrophobic interactions with the surface (Shoichet & McCarthy 1991; Coupe & Chen 2001). PVA and PLL are also biocompatible (Shan et al. 2009a; Jiang et al. 2011) and can be found in a liquid solution state which can be aspirated into the MCF overcoming the physical constraints of other surface modification methods. When modifying FEP for cell attachment the surface energy must be increased but there must be the correct functional groups that are optimal for the adhesion of the cell type or types used. As previously stated in Chapter 2 the ECM

is critical for cell function and survival *in vivo*, therefore these requirements need to be well-thought-out when culturing hMSC *in vitro*. There are multiple elements that need to be considered when developing a cell culture based platform made from FEP. The desired properties of FEP such as the optical clarity and robustness of the fluoropolymer need to be maintained after functionalization. The functionalization process must produce a homogenous coating equal or better than current methods used to culture the cell type of interest; for hMSCs this is standard tissue culture plastic. The function of the cells also needs to be maintain on the modified surface, adhesion does not automatically equate to cell viability and secretome expression, therefore comparisons need to be made to the most relevant condition the cell type has been studied in. It is always desirable for the functionalization process to be as inexpensive and as easy to carry out as possible. Options have been presented that can satisfy these requirements. Once the FEP surface had been functionalised it needed to be further optimised in order for cells to adhere and proliferate but any further steps needed to comply as much as possible with these requirements.

Post-surface chemistry optimisation the MCF was coated with the solution which facilities the highest level of hMSC adhesion while maintaining viability and was the most consistent across repeats. Either prior or post seeding hMSCs were stained with one of three fluorescent stains and imaged in order to present a better understanding of the cell morphology and behaviour inside the MCF. Initial development work of the hMSCs inside the MCF was carried out.

5.2 Materials and Methods

5.2.1 Materials

Fluorinated ethylene propylene copolymer (FEP-Teflon®) 0.1mm thick films with dimensions 150mm x 150mm were purchased from Goodfellow Cambridge Ltd (Huntingdon, England). A 2.86 cm diameter little B circle medium punch was sourced from Amazon EU (Rue Plaetis, Luxembourg). Low molecular weight PVA powder (13,000-23,000 Da 99% hydrolysed), medium molecular weight PVA (37,000-50,000 Da 99% hydrolysed), high molecular weight PVA ($\sim$130,000 Da 99% hydrolysed), 2% w/w sterile gelatin, poly-L-lysine hydrobromide molecular weight 70,000-150,000 0.01% solution, 1g poly-L-lysine hydrobromide molecular weight 70,000-

150,000 by viscosity and sodium hydroxide 1M (Sigma Aldrich Company Sigmacote®, 6 well plate sterile CellCrown™ inserts and Corning® Costar® ultra-low attachment 6 well plates were sourced from Sigma Aldrich (Dorset, UK). IC fixation buffer, IC permeabilisation buffer, ethidium homodimer-1 (EthD-1), PrestoBlue, Alexa Fluor 546 phalloidin, LIVE/DEAD viability/cytotoxicity kit for mammalian cells, CellTracker™ Green 5-chloromethylfluorescein diacetate (CMFDA) dye and trypsin 0.25% (1X) Solution with 0.1% EDTA were purchased from ThermoFisher Scientific (Paisley, UK). Bone marrow derived human Mesenchymal Stem Cells (hMSCs), Dulbecco's Modified Eagle Medium (DMEM), ultra-glutamine 2nM and phosphate buffered saline were supplied by Lonza (Slough, UK). Fetal Bovine Serum (FBS) was sourced from Gibco life Technologies (Paisley, UK). Ultrapure water was sourced from a Milli-Q purifier (Millipore Corporation, Billerica, MA, USA) was used to make up solutions after sterilisation. Standard tissue culture plastic 6 well plates were purchased form Fisher Scientific (Loughborough, UK).

5.2.2 Coating of FEP with Poly-L-Lysine

Circular tokens of FEP were hand cut from a sheet with 0.1mm thickness using a standard 6 well tissue culture plate well as a template. The token size was about 9.6cm^2 as per standard 6 well plate wells. The tokens were autoclaved in deionized water for sterility and when being used for cell culture were placed in ultra-low attachment six well plates, one token per well, and dried under aseptic conditions inside a biological safety cabinet overnight. Tokens which were being used for surface characterisation were placed in standard 6 well plates and dried inside a biological safety cabinet overnight. PLL was reconstituted at room temperature with sterile deionised water to a stock concentration of 20mg/ml. The solution was stored at 2ºC-4ºC until required. Sodium hydroxide was used to adjust pH to 11 immediately before use (Table 11). To each well in a 6 well plate 2mls of solution was added and incubated for the required amount of time at room temperature, excess solution was aspirated, and the tokens left to dry for a minimum of 2hrss. Live/dead staining of the adhered cells was carried out by washing the tokens twice with PBS, 2mls of a working solution comprising of 4µM red-fluorescent ethidium homodimer-1and 2µM green-fluorescent calcein-AM was added to each well. The plate was wrapped in foil

and incubated at 37°C for 40mins; post incubation the plate was imaged using a fluorescent microscope.

Table 11 PLL and NaOH solution rations

Solution	PLL	NaOH	Final PLL concentration (mg/ml)
1.5PLL0.5pH11	1.5	0.5	15
1PLL1pH11	1	1	10
0.5PLL1.5pH11	0.5	1.5	5

When using the PLL 0.01% sterile filter solution formulated by the manufacturer 2mls of the solution was added per FEP token per well in a 6well in a 6 well plate. The adjusting the pH of the PLL for the PLL at pH 11 conditions was carried out by adding NaOH to 9mls of PLL, the end total volume was then divided equally between three replicate wells (Figure 51).

5.2.3 Coating of FEP films with PVA and gelatin

Circular tokens with a surface area of 4.9 cm^2 were cut from 0.1mm FEP film sheets using a hole puncher (Figure 46A). For cell culture use the tokens we autoclaved in deionized water for sterility and then placed in ultra-low attachment six well plates, one token per well, and dried under aseptic conditions inside a biological safety cabinet. Tokens which were being used for surface characterisation were also autoclaved in deionised waster and placed in standard 6 well plates then dried inside a biological safety cabinet overnight. Stock solutions of low, medium and high molecular weight PVA were prepared at a concentration of 20 mg/ml by adding 10 g of PVA powder to 500ml warm sterile water then autoclaved. Post autoclave the solution was left in a water bath set at 85°C for approximately 4 hours or until the PVA powder had fully entered solution. The PVA and gelatin solutions were then mixed aseptically to the required final concentrations (Table 12) and used as indicated in the results and discussion section. Well inserts were coated with Sigmacote as per manufacturers' instructions, autoclaved for sterility and used to secure the FEP tokens in the wells of the ultra-low attachment plates. Then, 3mls of polymer solution was added to each well, and the tokens incubated for the required time. Coating of

solutions containing gelatin were incubated at 37ºC, all other solutions were incubated at room temperature.

Table 12: PVA gelatin coating mixtures tested; all values shown relate to the mixture

Sample	PVA concentration (mg/ml)	Gelatin concentration (mg/ml)
20PVA0Gel	20	0
16PVA4Gel	16	4
12PVA8Gel	12	8
8PVA12Gel	8	12
4PVA16Gel	4	16
0PVA20Gel	0	20

A   B   C
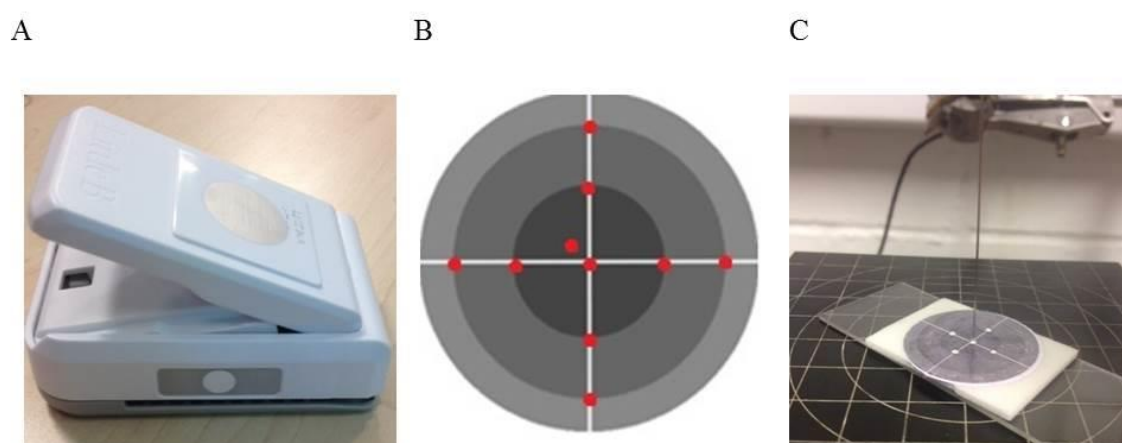
Figure 46: Hole punch used to make FEP tokens of equal size (A). The measurement grid template; the spots indicate where contact angle measurements were taken on each token for the DoE experiment (B). The contact angle measurement set up (C). FEP tokens were attached to double side sticky tap on a flat glass slide. 1µl water droplets were placed on the red spots (B) and a camera took a photo of the water droplet on the surface.

5.2.4 Surface characterization of modified FEP tokens

Contact angle measurements (Figure 46B and C) were carried out on dried tokens using the automatic DataPhysics OCA 20. Ten 1 µl sessile drop measurements were taken per film; the drops were placed either randomly or according to a set grid pattern (Figure 46B). Design Expert version 8 from Stat-Ease Inc (Minneapolis, USA)

was used to conduct a three-factor general factorial design to investigate the effect of molecular weight of PVA, concentration of PVA solution and incubation time on the final contact angle. Contact angle measurements could not be conducted on the PVA/Gelatin coating mixtures due to the need for the surface to be dry in order for the measurements to be carried out. Dried gelatin rapidly absorbs moisture, attempts to place a 1 µl resulted in the drop instantly being absorbed.

Atomic force microscopy (AFM) was undertaken using Veeco Explorer from Veeco (Cambridge, UK). On each film an area of 2 μm^2 was measured in contactless (tapping) mode.
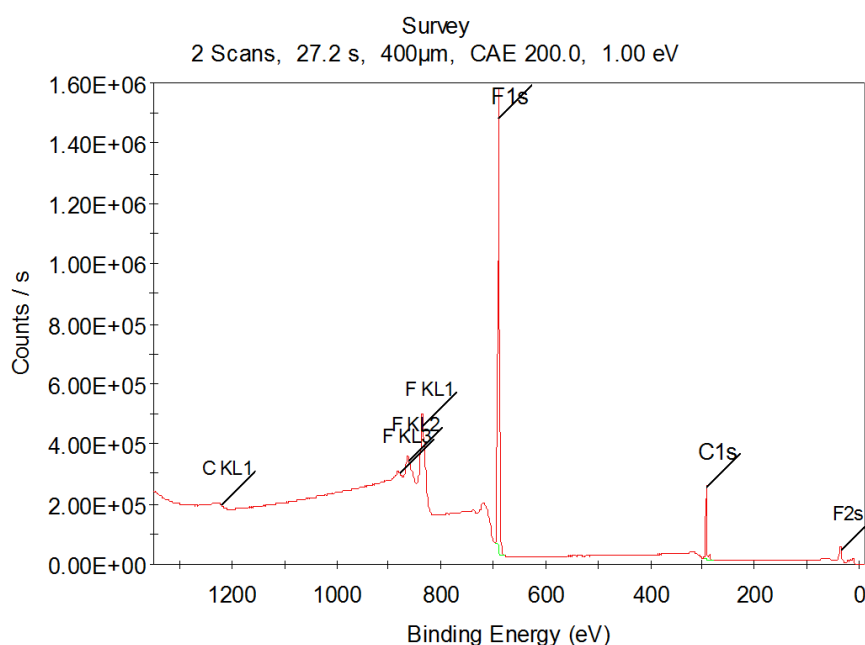
Figure 47: Example of an XPS survey scan of FEP

X-ray photoelectron spectroscopy (XPS) was conducted using K-Alpha X-ray photoelectron spectrometer from ThermoFisher Scientific (Paisley, UK). This technique was carried out within the Loughborough Materials Characterisation Centre at Loughborough university and with support from Pat Cropper. On each token a 400 µm x 400 µm array was scanned at 16 different spots per array. The tokens were scanned for the presence of the elements fluorine (F1s), oxygen (O1s), nitrogen (N1s),

organic carbon (C1s) and carbon bound to fluorine (C1s C-F), an example of the survey scan can be seen in Figure 47.

5.2.5 Culturing of hMSCs

Human MSCs were cultured in Dulbecco's Modified Eagle Medium (DMEM) supplemented with 2nM ultra-glutamine and 10v/v Fetal Bovine Serum (FBS). Unless otherwise stated cells were cultured for six days with a medium change on day three, cell culture incubation occurred at 37°C, 5% carbon dioxide with 95% humidity. In normal culturing conditions cell passage was undertaken on day six. Cells were detached using trypsin 0.25v/v (1X) solution with 0.1% v/v EDTA. Cells were seeded at a density of $5x10^3$ cell/cm^2 unless otherwise stated with a culture medium volume of 0.2 ml/cm^2. Cell counting as conducted using a NucleoCounter® NC-3000™ machine and the Via1-Cassette.

5.2.6 Analysis of hMSCs attachment and growth on modified FEP token

Cells were cultured as per Section 5.2.5. After 6 days of culture cells were passaged and seeded on to FEP on day six of cell culture the culture medium was aspirated and the tokens washed twice with 3mls PBS cells were then fixed on the tokens in 3mls of IC fixation buffer for 10 minutes at 4 °C. Fixation buffer was aspirated, and cells washed three times with PBS and then incubated with IC permeablisation buffer at room temperature for 40 min, after which the buffer was aspirated, and tokens washed twice with 3msl PBS. The tokens were then incubated with 3mls of a 4 mM ethidium homodimer solution at 37 °C for 40 mins. Ethidium homodimer is a nucleic acid stain, when bound to DNA it emits fluorescence in the red channel. The ethidium homodimer solution was aspirated and 3mls of PBS added to each well. The plates were then placed in a Biostation CT (Nikon, Europe), and each well scanned in full with phase contrast and with wavelengths excitation 540 nm, emission 600 nm. Images were then processed using CL Quant 3.10 software (Nikon, Europe), the individual nuclei of each cell were counted. The modified tokens were compared to the same number of cells seeded in standard tissue culture plastic 6 well plates as a control.

PrestoBlue assay was carried out to access the viability of the hMSCs over time. PrestoBlue contains resazurin which is reduced by the mitochondria in living cells, the reduction results in a colour change the shifts the fluorescent emission spectrum (Boncler et al. 2014). Cells were seeded onto FEP tokens in ultra-low attachment 6 well plates or into standard tissue culture plastic 6 well plates for the control. At time intervals stated in the result 300µl of culture medium was removed and replaced with 300µl of PrestoBlue solution. The plates were wrapped in foil and incubated at 37°C for 40mins. After incubation 3x100µl samples were taken from each well and pipetted into a 96 well plate. The plate was read on a ELx800 micro plate reader at an excitation of 544nm and emission of 590nm; the gains were adjusted based of fully reduced PrestoBlue.

5.2.7 Coating MCF and hMSC analysis in the MCF

The addition and removal of solutions in the MCF was carried out by inserting the ends of the MCF into a rubber connector which was inserted into a piece of rubber tubing enabling a seal to form between the tubing and the connector. The set up was sterilised by autoclaving and a sterile 1 ml syringe was inserted into the unsealed end of the rubber tubing creating a closed and sterile system.
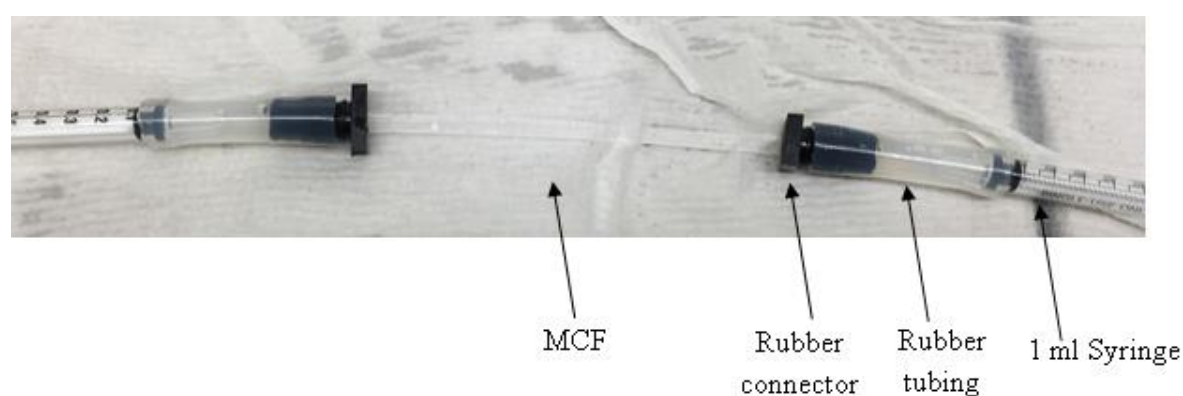
Figure 48: Set up of MCF strip to meet the fluid handling and sterility requirements in order to fictionalise the surface and seed cells inside the MCF. The MCF was held between two rubber connectors which was then inserted into two pieces of rubber tubing. Liquid can be added or aspirated using the 1 ml syringes connected to the other end of the rubber tubing.

The MCF was flushed with sterile PBS to remove any debris, and the required coating solution added ensuring the capillaries were completely full. After coating for the required about of time the MCF was washed with PBS to remove the coating solution. The MCF was then seeded with hMSCs at a concentration of 1.5×10^6 per ml. The MCF set up (

Figure 48) was placed in the incubator and imaged periodically. Imaging was carried out either phase contrast or by fluorescently labelling the cells and imaged using the Nikon inverted eclipse ti fluorescent microscope. A number of fluorescent cell staining methods were investigated; these were alexa fluor 546 phalloidin labelling of the actin filaments, a green cell tracker dye and the live/dead cytotoxic staining also used in Section 5.2.6.

5.2.7.1 Alexa Fluor 546 phalloidin labelling

Post culture the MCF was flushed twice with PBS and filled with fixation buffer for 15mins at room temperature. The MCF was flushed twice with PBS, filled with permeablisation buffer and incubated at room temperature for 40mins. Post incubation the MCF was flushed twice with PBS as filled with 5 units per ml solution of Alexa Fluor 546 phalloidin. The solution was incubated in the dark for 20mins and then imaged using the fluorescent microscope red channel.

5.2.7.2 Live/Dead viability stain

Post culture the MCF containing cells was flushed twice with PBS, and was then filled with a working solution of 4µM red-fluorescent ethidium homodimer-1and 2µM green-fluorescent calcein-AM. The MCF was wrapped in foil and incubated at 37°C for 40mins; post incubation the MCF was imaged using a fluorescent microscope.

5.2.7.3 CellTracker™ green CMFDA dye

Prior to seeding the MCF hMSCs were stained with green CMFDA dye, the dye us able to pass through the cell membrane and is retained in the cytoplasm. The cell suspension was incubated with 0.5µM dye for 30mins at 37°C, the cells were centrifuged at 220g for 5mins. The working dye solutions was aspirated and the cells resuspended in culture medium, the cell culture was then administered into the MCF.

5.3 Results and Discussion

As hMSCs are adherent and therefore long term cell survival and function is dependent on the cells ability to adhere to a surface it is important to establish the level of cell adhesion to FEP in comparisons to standard tissue culture plastic. FEP is a known hydrophobic material which is demonstrated by contact angle measurements of over 100° when measured using ultra-pure water (Figure 49 A). The surface energy and chemistry are thought to be why hMSCs will not adhere to the material as much when compared to standard tissue culture plastic, this is clearly demonstrated in Figure 49 B and C. After 6 days in culture the hMSCs seeded onto tissue culture plastic are more confluent and display morphology consistent with hMCSs in culture, a small number of cells can be seen on the FEP surface which have minimal or no contact to each other. This establishes the need to modify FEP so it provides a functional surface for hMSCs to adhere to. FEP is classed as a super hydrophobic material, hydrophobicity or hydrophilicity of a surface is related to the surface energy, hydrophobic surfaces have a low surface energy and vice versa (Lampin et al. 1997). Understanding the relationship between cell adhesion and functionality to surfaces properties including surface energy is one of the big challenges within the field of tissue engineering (Dewez et al. 1998).
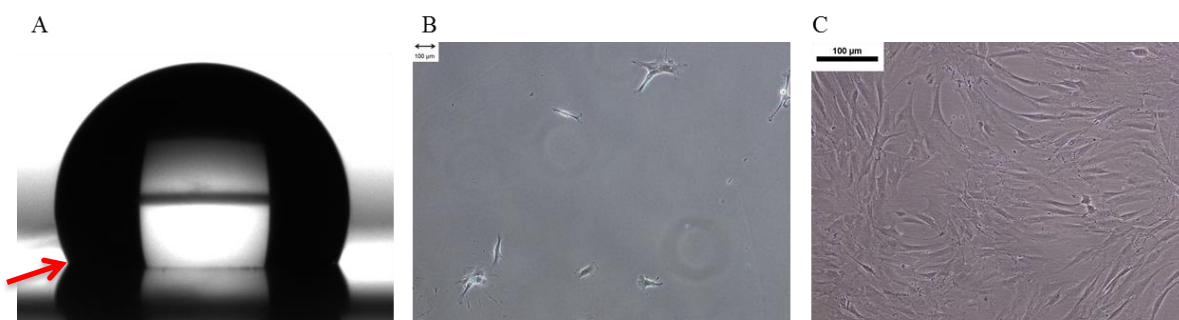
Figure 49: A) 1µl water droplet on unmodified FEP, the arrow indicates the point of water contact with the surface. B) hMSCs seeded on unmodified FEP at a density of 5000cells/cm^2 after 6 days in culture. C) hMSCs on standard tissue culture plastic at a density of 5000cells/cm^2 after 6 days in culture, image in representative of 3 images per condition and three replicates per condition.

Based on the literature two absorption methods using PVA and PLL were investigated to modify the surface of FEP for cell adhesion. Work by Shoichet & McCarthy (1991)

explored the use of PLL as a modification substrate of FEP, though the aim of this work was not to subsequently adhere cells to the surface. Findings by Shoichet & McCarthy (1991) determined that the molecular weight of PLL and the pH of the solution were factors in driving adsorption. When using this approach 3 solutions (Table 11) of PLL with a molecular weight of 70,000-150,000 mixed with a pH 11 NaOH based buffer were initially investigated. FEP tokens were incubated with the PLL solutions for 72hrss, washed and seeded with hMSCs. The tokens were imaged initially after a 24hrss attachment period (Figure 50A-D) and 72hrss (Figure 50 E-H) at which point it is expected that hMSCs would have undergone at least 1 population doubling as shown in Chapter 3.

Coating Condition	Imaged at 24hrs	Imaged at 72hrs
1.5PLL0.5pH11		
1PLL1ph11		
0.5PLL1.5pH11		
ontrol (Tissue culture plastic)		
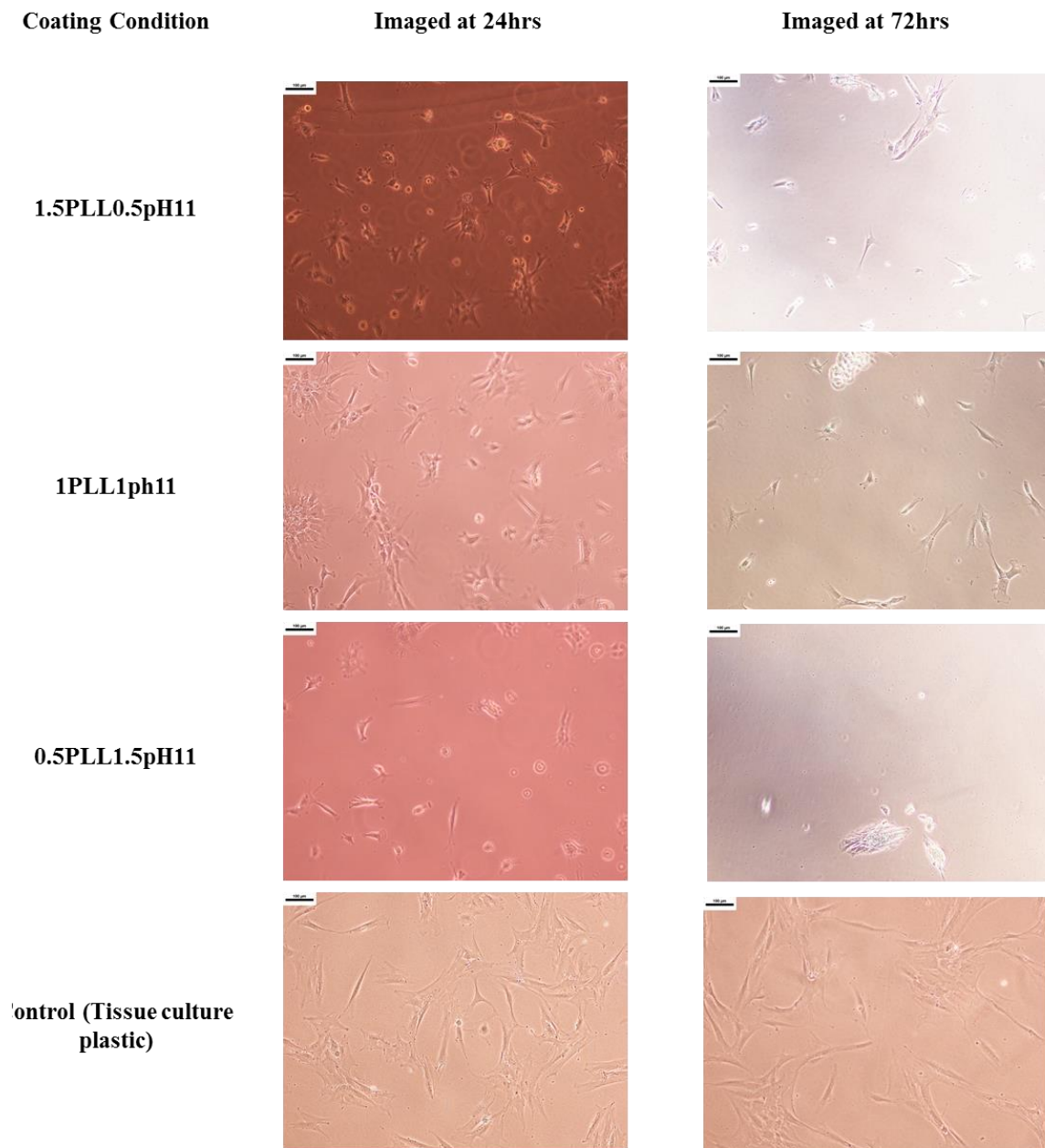
Figure 50: Attachment of hMSCs seeded at a density of 7.5×10^5 cells/cm^2 after 24hrss in culture. A) 1.5PLL0.5pH11 B) 1PLL1ph11 C) 0.5PLL1.5pH11 D) hMSC attachment control on standard tissue culture plastic. The same tokens were imaged after 72hrss in culture, the hMSC attachment control was carried out on standard tissue culture plastic Images are representative of 3 images per token or tissue culture plastic surface and each modification condition was carried out in duplicate. A 100µm scale bar present in each image.

In Figure 50 after 24hrss in culture hMSCs can be seen in all images, in C the hMSC appear sparser and seem to be mostly individual cells compared to A, B and D taken

at the same time point. This could be due to a lower concentration of PLL in coating solution which results in a limited percentage of the surface being modified, or the conditions were not optimal to drive the adsorption of PLL. While more grouped areas of hMSC can be seen A and B the cells are more compact in the areas where adhesion as occurred as opposed to the tissue culture plastic control. Under standard culturing conditions the hMSC have spread and elongated more, forming connections between regions. After 72hrss in culture very few cells were observed on the 0.5PLL1.5pH11 coating condition token, and reduction in cell number compared to the 24hrs images was observed on the 1PLL1pH11 and 1.5PLLpH110.5 coatings. Part of the challenge with using the method of Shoichet & McCarthy (1991) is that the modification was not carried out for the purpose of culturing cells. Subsequently the method has not been tested under cell culture conditions such as being in cell culture medium at higher temperatures for up to 6 days. Previous work has shown that after hMSCs adhere they produce their own cellular matrix within 24hrss which enables the cells to spread and grow (Li et al. 2013). What may have been seen in Figure 50 after 24hrss is the initial focal adhesion of the cells, but the cells may not have been functional enough to spread and alter. In the control images, it shows that the hMSC should be more spread and do sustain the morphology at 72hrss.

PLL is a substrate the is used to coat well plates and other tissue culture plastic to enable the culturing of cell types which require specific surface properties such as neurons (Khademhosseini et al. 2004; Shan et al. 2009a). The previous incubation time of 72hrss was been based on literature which indicated that over a longer duration (approximately 3 days) more PLL was absorbed onto an FEP surface (Shoichet & McCarthy 1991). It should be noted that much of the literature relating to the modification of FEP is dated, though still relevant analytical techniques and knowledge of material science have developed a lot since these publications. PLL is commercially available as a method to coat polystyrene cell culture plastic. To coat polystyrene, which is also a hydrophobic polymer, manufactures guidelines state that the PLL should be incubated on the surface for 5mins, and includes a drying step after washing. This protocol was followed when modifying the FEP surface in Figure 50.
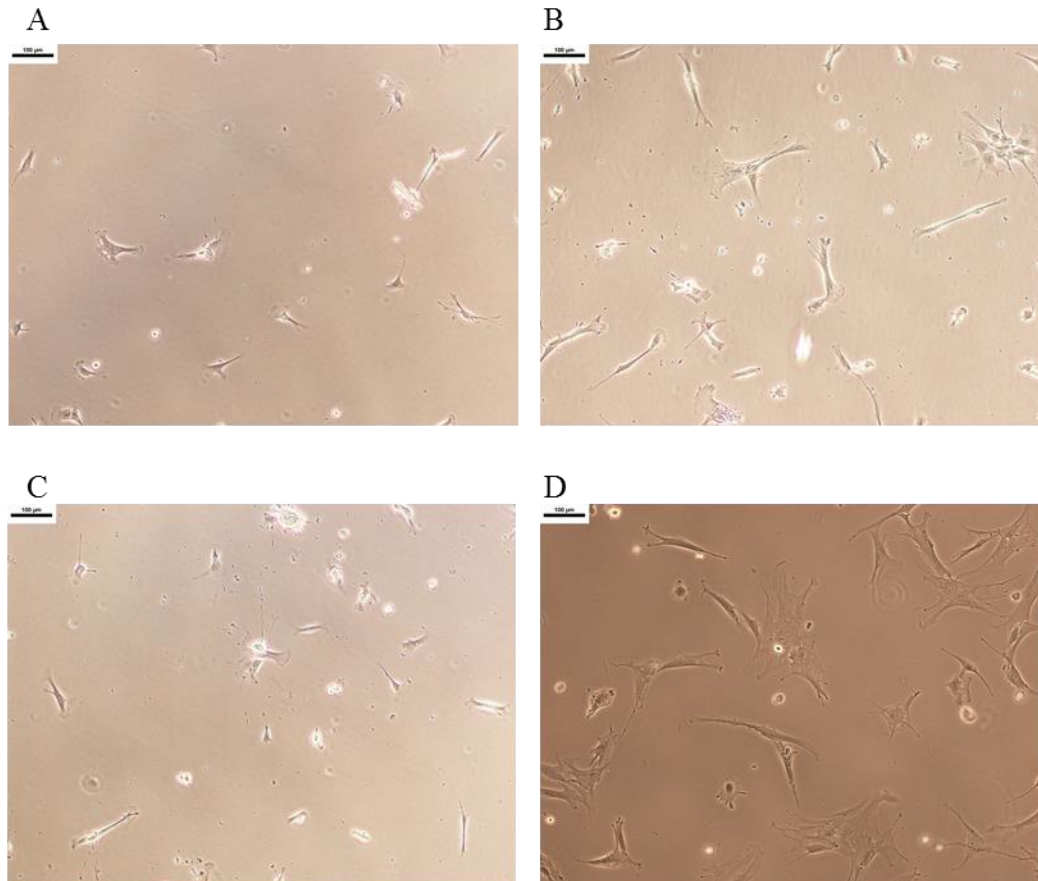
Figure 51: Attachment of hMSCs seeded at a density of $5x10^5$cells/cm^2 after 24hrss in culture to FEP tokens incubated for 5mins in 0.01% PLL (A), 0.01% PLL at pH 11 for 5mins (B) and 0.01% PLL at pH 11 for 2hrss (C), standard tissue culture plastic control (D) as the control condition. Images are representative of 3 images per token and two tokens per condition with a 100µm scale bar.

After 24hrs adhered cells were observed on all 3 FEP coatings (Figure 51) and displayed anticipated hMSC morphology that is consistent with the control (Figure 50). To gain more information regarding cell the viability of the adhered cells the coating conditions were repeated and after 6 days of total cell culture time the cells were stain using a live dead stain (Figure 52). Cells which produced red fluorescent were considered non-viable as the ethidium homodimer-1 was able to bind to DNA due to permeability in the cell membrane. Viable cells fluorescent in the green channel due to calcine-AM indicating esterase activity in the integral cell membrane.
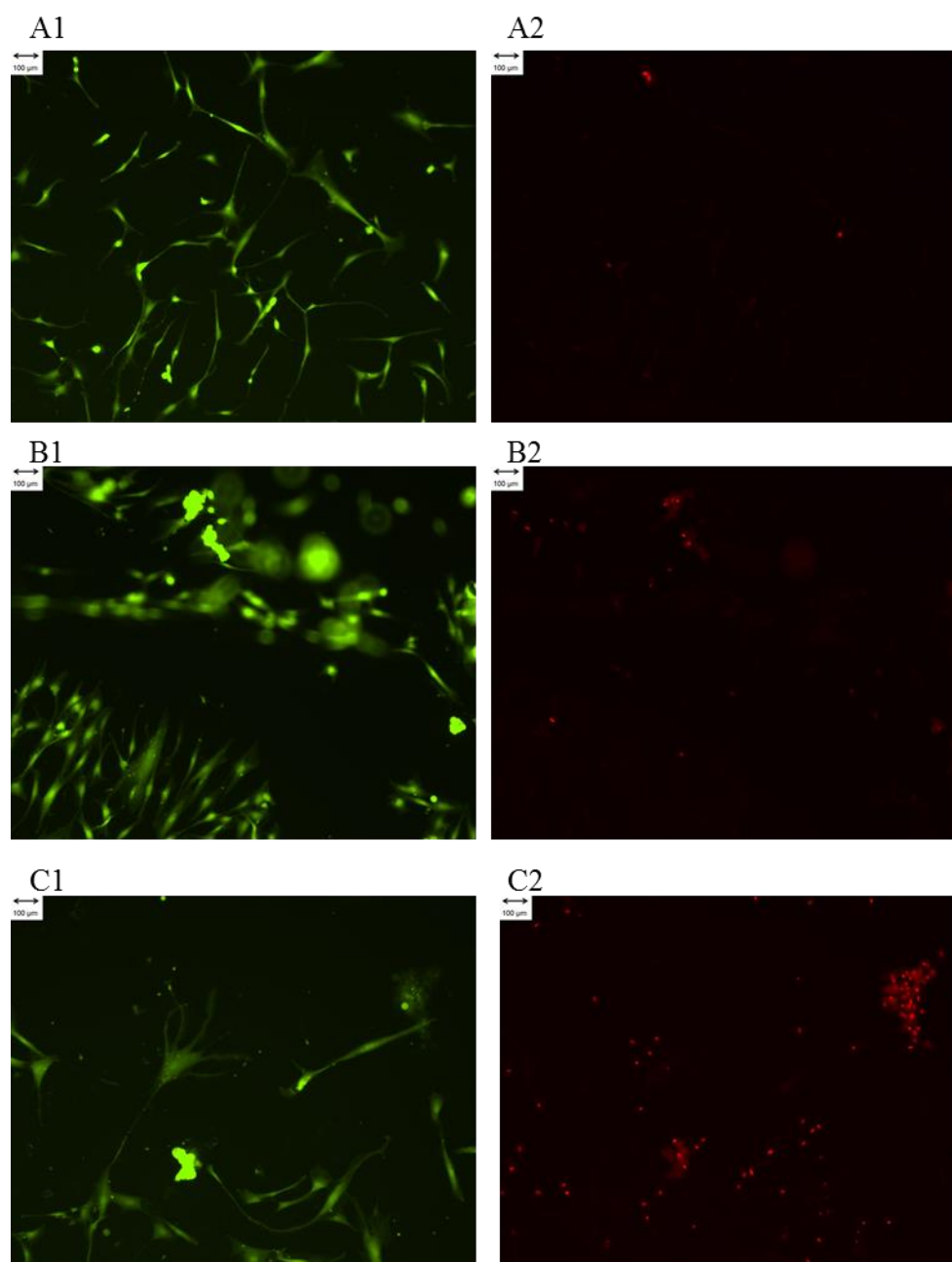
Figure 52: Live/dead imaging of hMSC cultured for 6 days on FEP tokens modified with PLL. hMSCs were seeded at a density of 5×10^5cells/cm^2 after 6 days in culture to FEP tokens incubated for 5mins in 0.01% PLL (A), 0.01% PLL at pH 11 for 5mins (B) and 0.01% PLL at pH 11 for 2hrss. Calcine-AM fluorescence (live stain) can been seen on the left with the exact imaging area in the ethidium homodimer-1 red channel on the right. Images are representative of 5 images per token and the coating conditions were carried out in duplicate.

Through using the manufacturers method of PLL coating of FEP improvement in cell attachment can be seen (Figure 51), and the cells which do attach are viable after 6 days in culture (Figure 52).

One of the challenges when developing a modification method for a cell culture application is maintaining sterility. Due to this issue the use of readymade PLL solutions with the same molecular weight range that were develop specifically for cell culture applications was explored as the manufacturer guarantees sterility. Both PLL solutions (the readymade and user reconstituted) used in Figure 50, Figure 51 and Figure 52 were added in excess, manufacturer recommendation was 1.0 ml/25 cm^2, and 2mls was added per 〜9.6cm^2 therefore disparity of concentration were not considered to be an issue as only a maximum amount of PLL can be absorbed onto FEP. Though PLL absorption onto FEP is not fully understood it is thought that hydrophobic interactions drive the absorption therefor once a portion of the FEP surface has been coated the FEP surface is no longer hydrophobic and more PLL can no longer be absorbed (K et al. 2007). The solutions were of the same molecular weight which has been reported to be the more critical factor with PLL as the longer chains provide more active amino acid binding sights for the cells to adhere to (Shan et al. 2009b). As cell attachment also occurs on FEP tokens modified with readymade PLL (Figure 51 and Figure 52), this modification method was further investigated with contact angle and AFM measurements and compared to FEP surface modification using PVA (Figure 53 and Figure 54).
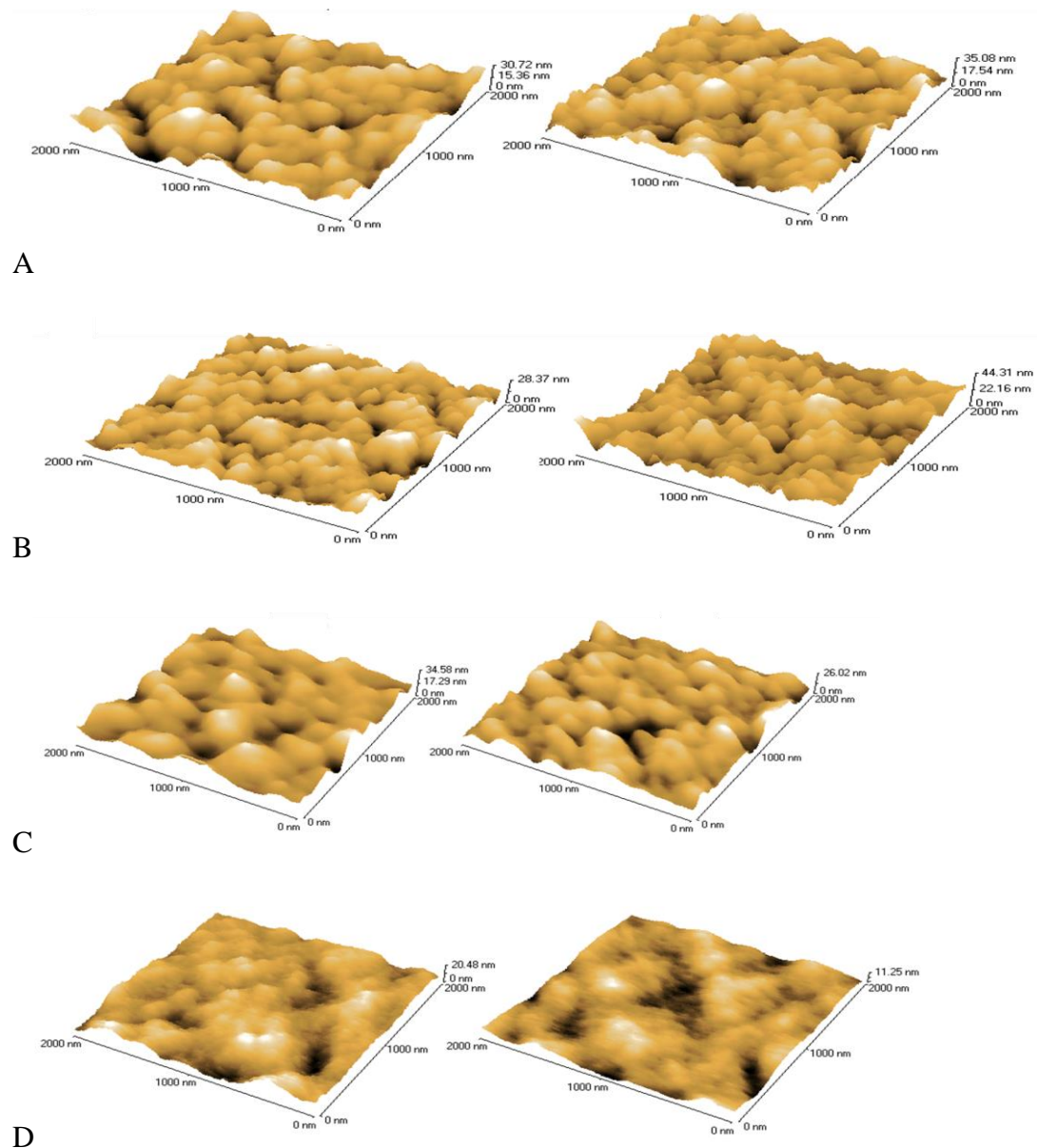
Figure 53: AFM images A) plain FEP, B) 0.01% PLL incubated for 5min C) 0.01% PLL pH incubated for 5mins D) FEP modified with 20mg/ml PVA 130,000 MWt incubated for 24hrss. The colour intensity scale (▬▬▬) corresponds to the surface height with black represented the lowest height through to white indicating the higher areas. Measurements were carried out in duplicate on a single token for each coating condition.

AFM results (Figure 53) shows FEP based on two measurements had a mean surface roughness (Ra) of 4.6 ±0.3, the Ra mean value for the 0.01% PLL incubated for 5min

(Figure 53B) and 0.01% PLL pH11 incubated for 5mins (Figure 53C) coating conditions were 4.75±0.8and 4.7±2.1, the lower the RA value the smoother the surface. The PVA coating produced the lowest Ra value of 2.2±0.7, which is out of the standard deviation range of the uncoated FEP indicating that PVA is present and reduced the surface roughness of FEP. The reduction of FEP surface roughness through the adsorption of PVA is consistent with work carried out by Kozlov et al. (2003). The PLL Ra values cannot be distinguished from the uncoated FEP results, this could indicate that PLL has not been absorbed in the regions measured using AFM. It could also indicate that PLL absorbed in a thinner layer therefore the contour of the FEP surface in maintained. A similar trend is also seen in the contact angle measurement results (Figure 54), FEP is shown to have a contact angle of over 100°. While the mean contact angle is reduced after token incubation with PLL to between 80° and 100° error bars place the coating within the plain FEP range. Previous work has shown that when plastic is coated with PLL a contact angle of 63.2° was measured showing that PLL usually has a lower contact angle when coating plastic compared to FEP (Medina Benavente et al. 2014). As with the AFM the large error bars could be reflective of PLL not being present on the surface for some of the measurements. The PLL coating could be very thin and there for the surface energy of the FEP could be influencing the contact angle measurements, or PLL is not as hydrophilic as PVA. The standard deviation on the plain FEP within the same token is relatively small, however there was a significant difference between token measurements in the same condition.
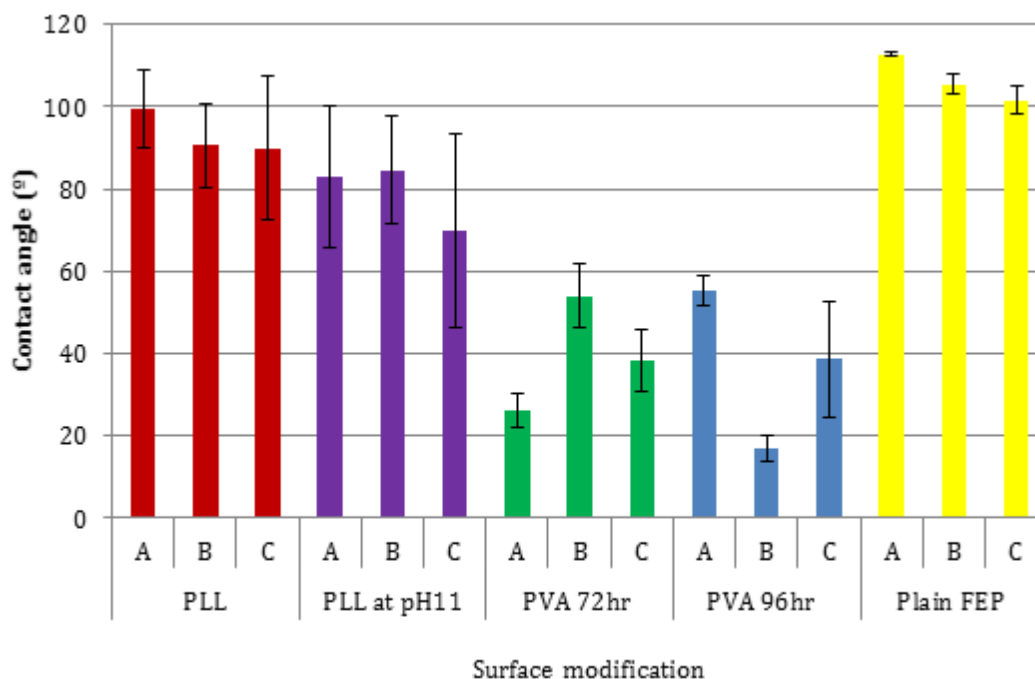
Figure 54: Contact angle measurements carried out on modified or unmodified hand cut FEP tokens. 10 1µl drops were placed randomly and two contact angles per drop were measured (n=20 per token). 3 replicates were made per coating condition; PLL coatings were carried out with 0.01% PLL at a total PLL volume of 2mls and incubated for 48hrss. A total of 2mls of PVA solution was added per token, 20mg/ml PVA solution with molecular weight of 130,000 incubated for 72hrss or 96hrs.

One of the challenges in surface modification is understanding the level of homogeneity of the modified surface. For example, AFM measures $2µm^2$ area of a $9.6cm^2$ token which is 0.02% of the total surface area. Due to the time intensiveness and challenges obtaining AFM images and data these measurements were conducted in duplicate, it would be an extensive effort to comprehensively characterise such a large surface using AFM. Though in Figure 53 difference can be seen particularly in the PVA coating condition the small areas tested do not provide insight into the homogeneity of the coating over a larger surface area. However valuable insight into the surface roughness of the coatings was obtained using AFM as the significant difference between coating conditions in Figure 54 merits further consideration, the source of the variation needs to be determined or overcome with a more robust surface modification method. Consequently, after using the AFM data to focus the

coating methods to be investigated further a more detailed approach surface characterisation was developed and a consistent coating methodology. The methodology was improved by making tokens of the same size using a whole punch (Figure 46A) as opposed to manually cutting tokens using a stencil which could physically damage the surface. Based on previous data using PVA as the surface modification method was explored further, PVA was shown to have a greater impact on reducing surface hydrophobicity based on contact angle measurements (Figure 54) and surface roughness data (Figure 53). A design of experiment (DoE) approach was utilised in order to understand if the level of PVA modification could be controlled based on the molecular weight of the PVA, the incubation times and/or the concentration of the PVA in solution. Contact angle measurement was used as the method to determine the effects of the experimental conditions as it is a simple method compatible with a DoE approach and directly relates to the level of hydrophobicity/hydrophilicity of a surface (Kwok et al. 1997).
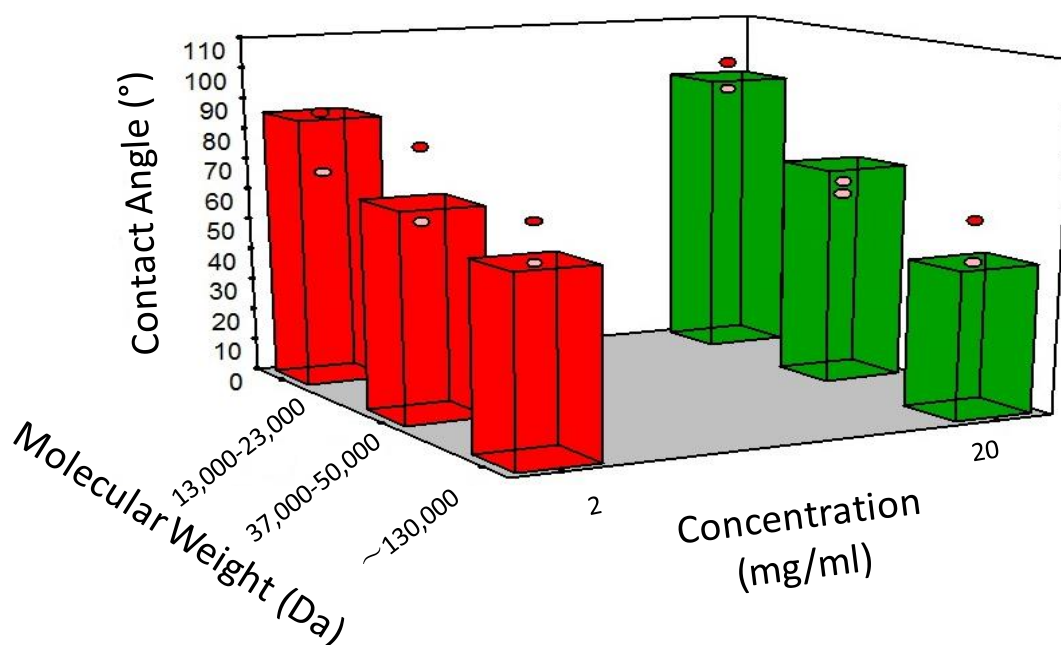
Figure 55: DoE investigating factors influencing PVA surface modification of FEP. Data shows the effect of PVA molecular weight (13,000-23,000Da, 37,000-50,000Da and ~130,000Da), and concentration of PVA at 2mg/ml and 20mg/ml on the contact angle of coated FEP. Contact angle values are associated to the surface energy and

therefore relate to hydrophilicity or hydrophobicity of the surface. Outliers are indicated by dots; 20 measurements were carried out per film with 2 replicates per coating condition.

The result of the DoE experiment shows that the hydrophobicity of FEP can be reduced in a controlled manner using different molecular weight of PVA. There is a stepwise decrease in the contact angle with increasing molecular weight of PVA, reducing the contact angle from ~85-95° to ~45°. The influence of PVA molecular weight in

Figure 55 is consistent at both concentrations of PVA (2mg/ml and 20mg/ml) this is in agreement with previous work by Kozlov et al. (2003) in relation to PVA behaviour with hydrophobic surfaces. Molecular weight has been determined to be a significant factor with a p-value of <0.0001 on modifying FEP. Individually concentration and incubation time have been determined to not be a significant factor in reducing FEP contact angle with p-values of 0.6705 and 0.6549 respectively. A relationship between molecular weight and concentration has been determined to be within the boundaries of significance with a p-value of 0.0469. Work carried out by Kozlov & McCarthy (2004) proposed that adsorption of PVA to a hydrophobic surface was a two-stage process. Firstly, hydrophobic interactions which reduce the interfacial free energy, then secondly crystallization of the PVA which results in stability of the layer. The work also proposed that the lower molecular weight produced a thicker layer of PVA due to the shorter polymer chains having the ability to crystallise more. In the work by Kozlov & McCarthy (2004) 3-5 measurements were conducted per surface and the total size of the modified token characterised is not stated so it is difficult to obtain insight into the homogeneity of the coatings.

The ability to control the surface energy of FEP means that it is possible to investigate how relevant surface energy is to hMSC attachment and function. In

Figure 56 20mg/ml PVA was used for each coating condition, though concentration was not deemed to have a significant impact on contact angle PVA is an inexpensive material so there was no draw back selecting the 20mg/ml concentration.
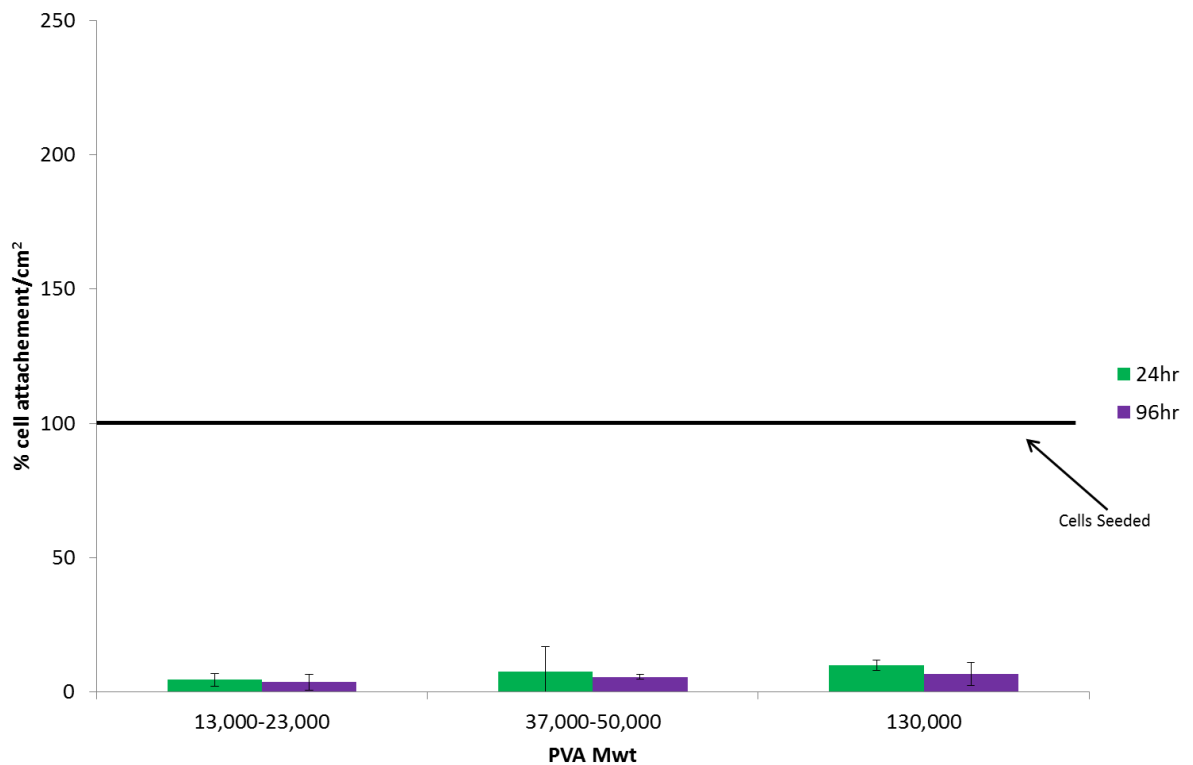
Figure 56: Attachment of hMSCs after 6 days in culture to FEP tokens modified with 20mg/ml PVA of three different molecular weights. The tokens were incubated for 24hrs or 96hrss in the respective PVA solutions. Standard deviation is representative of 3 replicates per coating condition.

Though PVA can reduce the hydrophobicity and surface roughness of FEP it is not able to effectively facilitate adhesion of hMSCs (

Figure 56). Even by producing a range of surface energies hMSCs did not adhere to the extent seen on standard tissue culture plastic.

Cell attachment data implies that surface energy and roughness are not the main reason why hMSCs do not attach to FEP. Functional groups that relate to the ECM to which the cells can attach to have been a focus of many surface modification methods (Rosso et al. 2004; Guilak et al. 2009), though PLL has previously shown to meet this requirement the coating cannot be as well controlled as PVA. Consequently, the approach of using a mixture of PVA and a protein which is commonly used for promoting cell attachment was adopted. PLL was not deemed a suitable substrate for this method as its functionality is strongly related to its physical structure and

orientation, hence using PLL in a mixture would add an extra element of unneeded complexity (Davidson & Fasman 1967; Shoichet & McCarthy 1991). Other commonly used proteins such as collagen and Matrigel (a protein mixture) were not compatible with the FEP coating method as they are temperature and time sensitive. Gelatin is a commonly used substrate for cell attachment and is denatured protein, therefore its function is not thought to be so strongly related to its structure so the functionality of gelatin is unlikely to be impeded by the presence of PVA. Gelatin has also previously been used in the hydrogel field with PVA to facilitate cell adhesion (Miao et al. 2015).

By modifying FEP with PVA and gelatin mixtures an improvement in hMSC numbers after 6 days in culture (Figure 57) compared to no gelatin (

Figure 56) being present. Though the cell number was not equal to that seen on tissue culture plastic after 6 days in culture. As expected the coating containing no gelatin in Figure 57 had the lowest number of cells attached, the coating with only gelatin performed better but did not have the highest number of cells.
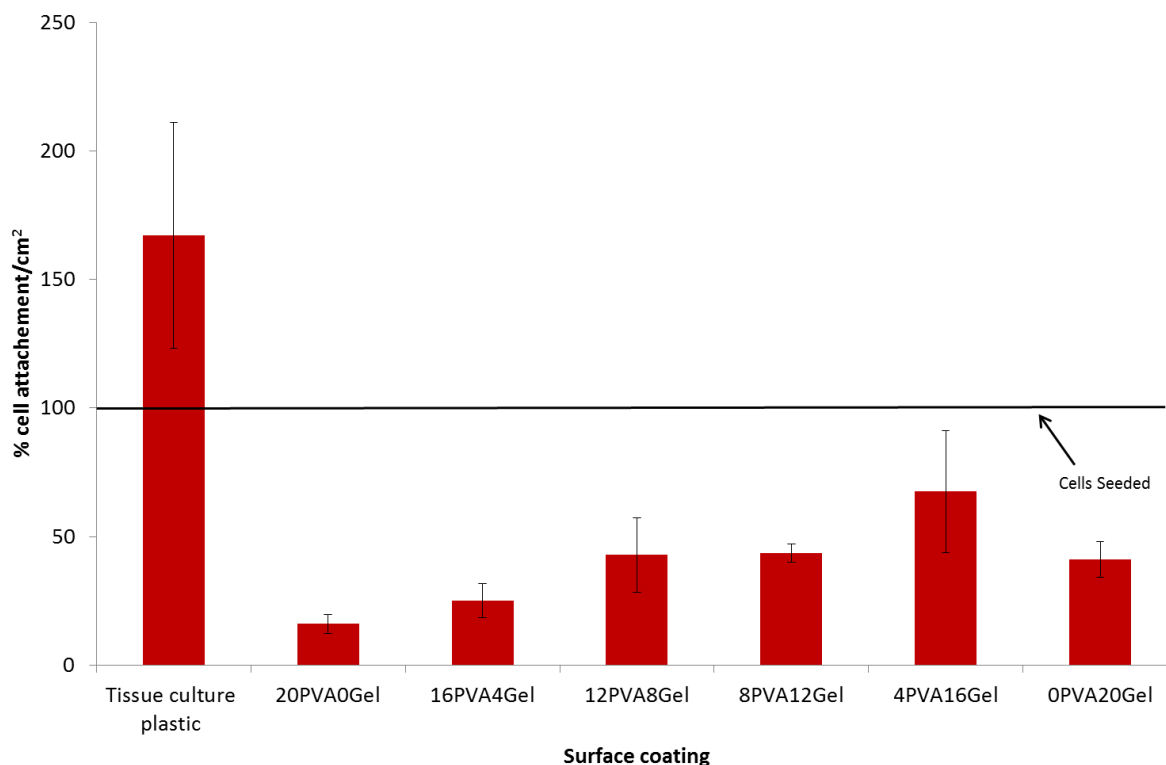
Figure 57: Cell attachment numbers to surfaces modified with PVA, gelatin or a mixture of PVA and gelatin. FEP tokens were incubated in the respective solutions for 96hrss, tissue culture plastic was used as the control surface condition. Cell count were carried on day 6 of culture, error bars are representative of 3 repeats.

Based on the standard deviation in the cell attachment data (Figure 57) 8PVA12Gel and 20PVA0Gel produced the most consistent surface for cell attachment though 4PVA16Gel had a higher percentage over all. To establish a reason behind this the coating methods were analysed using XPS. Due to the hydroscopic nature of dried gelatin contact angle analysis could not be carried out.

A

B
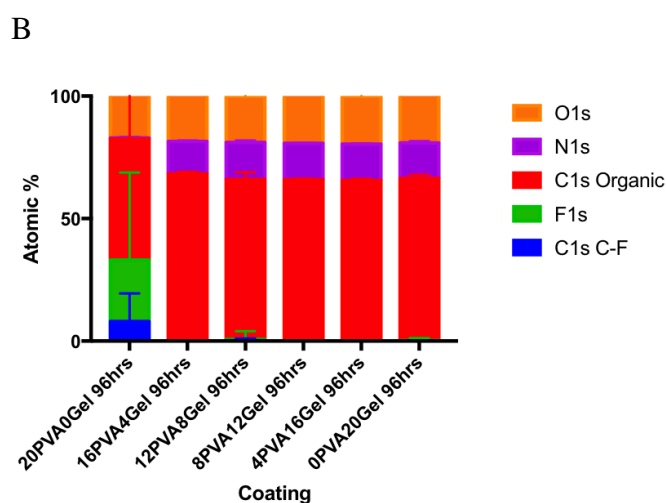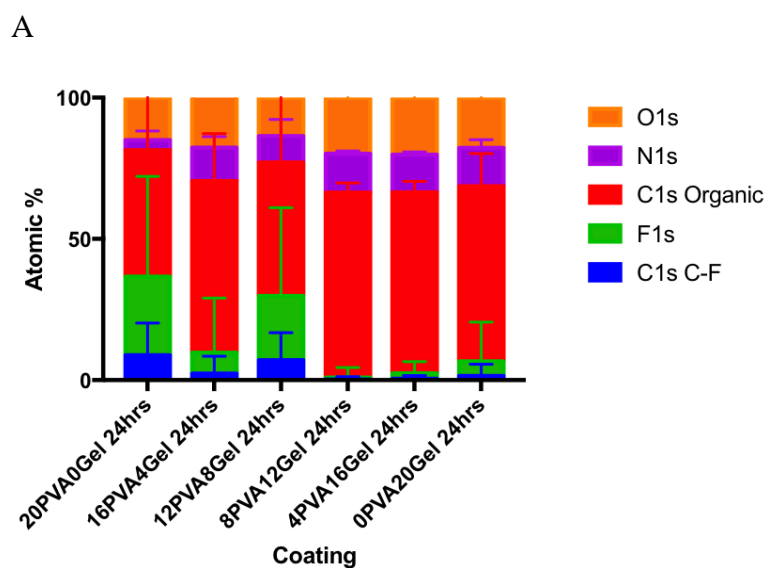
Figure 58: XPS data of FEP tokens modified with PVA, gelatin or a mixture of PVA and gelatin, incubation times of 24hrss (A) and 96hrss (B) were investigated. The surface was analysed for fluorine (F1s), oxygen (O1s), nitrogen (N1s), organic carbon (C1s) and carbon bound to fluorine (C1s C-F). Error bars are representative of mean values of 16 measurements from three replicates.

Based on the XPS data (Figure 58) for the PVA only coating in both the 24hrs coating condition (A) and the 96hrss coating (B) fluorine can still be detected. This indicates that either the coating is less than ~5 µm in thickness, and the F1s electron can be targeted or that the coating is heterogenous and regions of unmodified FEP are

exposed. With a longer incubation time in all conditions containing gelatin the F1s and C1s C-F (atoms found in FEP) atoms are barely detectable compared to the 24hrs coating. This implies that a longer coating time results in a more homogenous coating and/or a thicker coating. The 8PVA12Gel coating and the 4PVA16Gel coating show the least level of exposed fluorine after 24hrss and 96hrss incubation. In 16PVA4Gel after 96hrss F1s and C1s C-F are also not detected. Based on the cell attachment data in Figure 57 and the XPS data in Figure 58 8PVA12Gel would appear to perform more consistently as a coating and facilitating cell attachment. Gelatin does enhance cell attachment though with PVA after 24hrss the coating is more homogenous. The incubation time is an important factor from a device manufacturing perspective, being able to functionalise a surface more quickly saves time and therefore money.

Platter images of AFM data are able to show the physical location of identified atoms, this gives a greater level of insight into where specific elements were detected. Platter images of the coatings in Figure 59 concur with the XPS data (Figure 58) where FEP is (F1s) very low or undetectable components of gelatin or PVA are present (Cs1). Plain FEP (a) has the greatest amount of fluorine detected, though some organic carbon (Csl) can been seen this could be attributed to atmospheric carbon which can be difficult to eliminate in XPS machine.
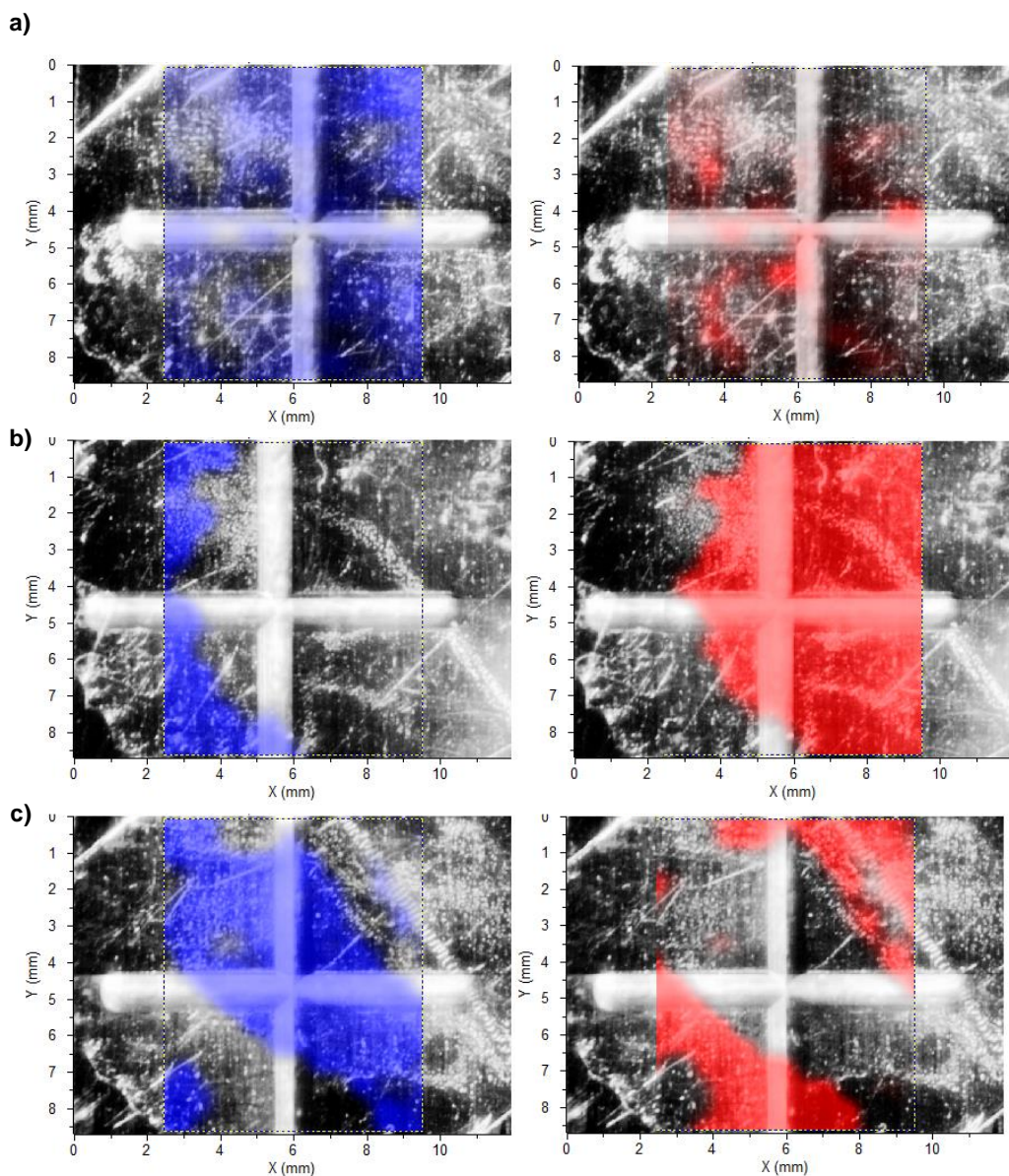
Figure 59: XPS Platter images of a) uncoated FEP, b) FEP coated with 8PVA12Gel for 96hrs and c) FEP coated with 0PVA20Gel for 96hrs. The colour represents spatial distribution of F1s (blue - left hand side images) and Cs1 organic (red – right hand side images). Images are representative of three experimental replicas.
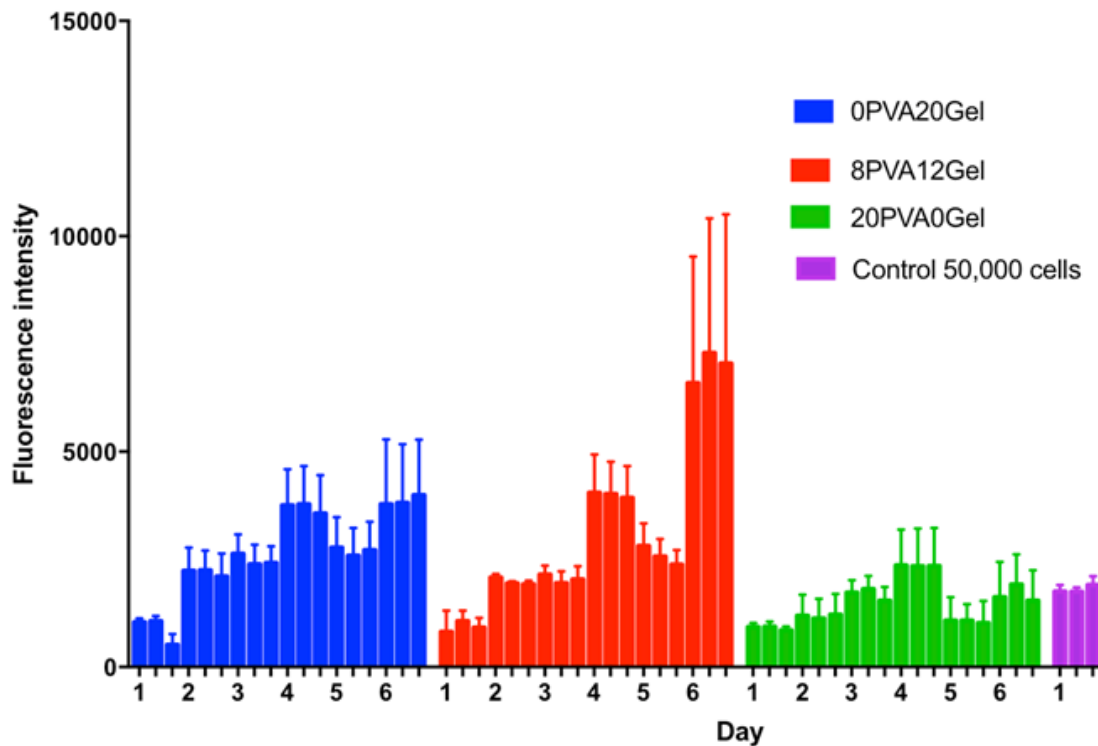
Figure 60: PrestoBlue assay during six days of incubation (n=3) of hMSCs seeded on FEP tokens coated for 96 hrs. As a control 50,000 cells on tissue culture plastic were also assayed. Error bars are representative of 3 measurements per replicate well.

While previous data has shown the number of hMSCs attached to FEP tokens after culture, attachment does not automatically equate to functional cells therefore a PrestoBlue assay was conducted to determine the level of cellular metabolic activity. PrestoBlue data shows an interesting and consistent pattern across the 3 coating conditions (0PVA20Gel, 8PVA12Gel and 20PVA0Gel). On day one all conditions had less metabolic activity compared to the tissue culture plastic control over time the level increased indicating cell growth. The 20PVA0Gel had the lowest overall level of activity indicating that the cells attached did not grow and proliferate, or that cells were detached and lost during culture. Detachment could be due to a lack of coating in the area and therefore the cells we only able to focally adhere and not able to maintain the adhesion over time. 8PVA12Gel produced the highest fluorescent intensity on day 6 of culture although initial levels were lower that the 0PVA20Gel coating on days 1,2,3 and 5. The cell line used in this experiment was the M2 cell line, it was determined in Chapter 3 that this cell line had a population doubling time of 1.5 to 2 days. The growth cycle of the cells needs to be considered when looking at

the data in Figure 60 in order to hypothesis why in all conditions the values on day 3 remain similar to day 2 and why there is a drop-in intensity in day 5. PrestoBlue is reduced in the cells mitochondria which are responsible for generating the energy for the cell to undertake all cellular functions. When a cell is proliferating, the mitochondria are more active, when the cell is at rest a lower level of activity is occurring and therefore the intensity of PrestoBlue will be less (Sonnaert et al. 2015). Based on the consistent PrestoBlue activity in the 20PVA0Gel coating the cells attached are alive but not proliferating.

The next stage was to transfer the coating work into the MCF platform and identify the challenges of seeding the MCF with hMSCs. The 8PVA12Gel coating mixture was used when coating the MCF and a higher concentration of cells equal to $50000cells/cm^2$ were seeded. Dead space such as the tube between the MCF and the syringe (

Figure 48) were taken into consideration when making the decision to administer cells in excess. Three methods of cell staining were used, as each stain provided different elements of information regarding the cell. Actin staining provides more detailed morphology of the cells. The stain can help show the level of contact or spread the cells are having inside the MCF, for example if they are adhering with direct full contact or is portions of the cell are adhered. The live/dead stain would be able to determine how viable the cells were. Initially the green cell tacker was not thought to be an appropriate stain due to auto fluorescence from the MCF. However, as cell tracker was the only stain to be administered before the cells were seeded it was unaffected by the many wash steps and administering of solutions to the MCF.
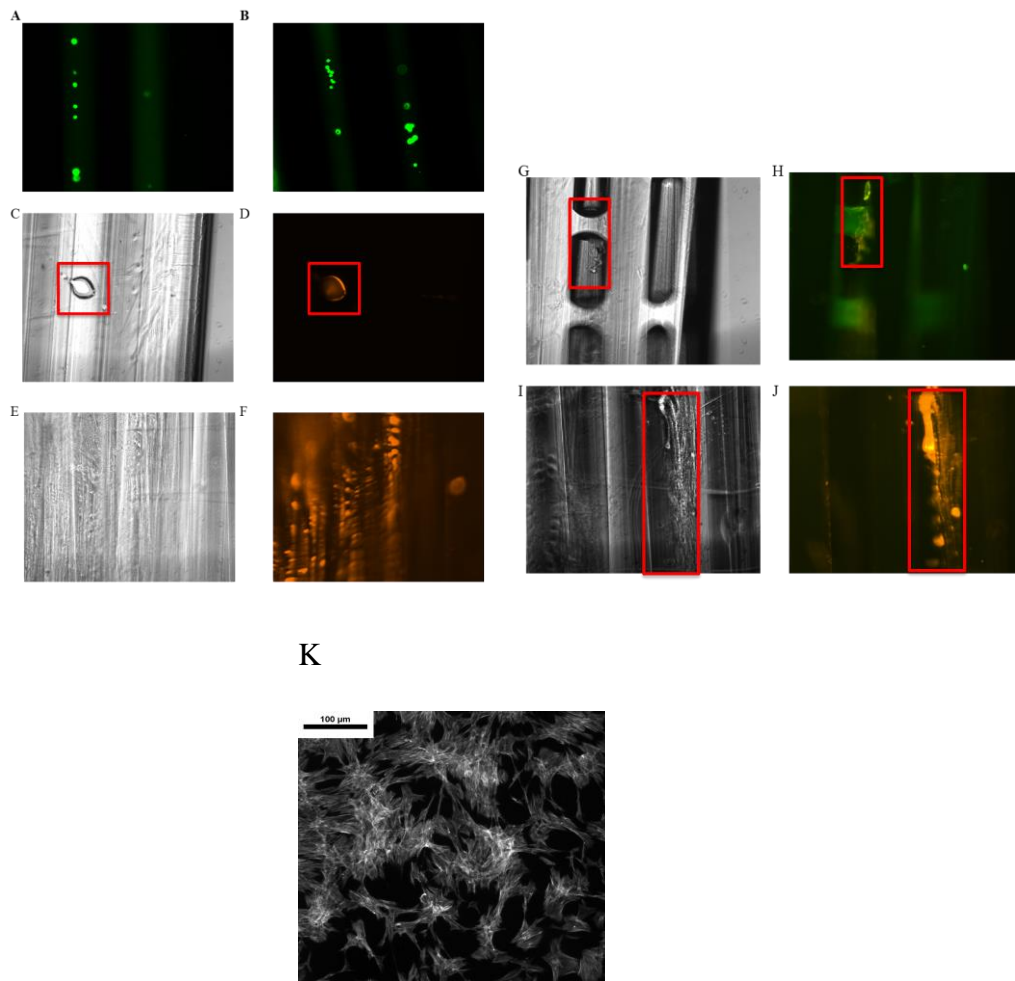
Figure 61: Fluorescent staining of hMSC inside the MCF coated with 8PVA12Gel. Green cell tracker shows cells in the MCF 2hrss post seeding (A) and after 24hrss in culture (B), cells are present in both images. Actin staining of hMSC using a phalloidin conjugated stain can be in D and F, the corresponding phase contrast image can be seen in C and E respectively. Live/dead staining of hMSCs inside the MCF was conducted 24hrss after seeding, merged images of the stains can be seen in H and J with the corresponding phase contrast images in G and I respectively. Actin of hMSCs grown on standard tissue culture plastic after 6 days in culture stained with phalloidin conjugated (K). Images are representative of a minimum of 3 MCFs.

The green cell tracker (Figure 61A and B) shows that cells are present 2hrss post seed, the cells can still be seen at 24hrss post seed however the morphology is showing the cells to be rounded rather than the hMSC elongated morphology previously seen. Actin staining was carried out inside the MCF 24hrss after cells were seeded (Figure 61 D and F) though fluorescence was detected it is difficult to

ascertain morphological information of the hMSC, image D and the corresponding phase contrast image C show a cylindrical structure which is not indicative of hMSCs but was also seen in the green cell tracker images (A and B). A region of stained actin was seen in image F however as hMSC adhered inside a transparent capillary is not a well-documented concept it is difficult to determine what adhered cells should look like within a cylinder compared to a flat surface. The image (F) shows a striated form which is consistent with the elongation of hMSC, the same stain carried out on hMSCs cultured on tissue culture plastic can be seem in image K for comparison. Imaging in a capillary also presents focusing issues and impairs image quality which compounds the identification issue, hence image K provides a higher level of morphological information and understanding into hMSC interaction. Similar striations can be seen in Image J, but this was an ethidium homodimer-1 stain which fluoresces when bound to the nucleus of the cell. Both the phase contrast images for the actin stain (E) and the ethidium homodimer-1(I) display the striations which adds to the evidence that within the capillaries cells are cells in the foreground or back ground will always be a challenge as seen in Figure 61 A and B green out of focus cells ac also been seen. Another challenging of imaging in capillaries is knowing what or were present. Ethidium homodimer-1 stains DNA which is found in the nucleus and does not have a striated form. If the cells have lysed ethidium homodimer-1 could be staining DNS debris which has attached to the capillary wall. As both staining methods require washing, fixation of the cells and addition of the staining solution to the MCF there is a possibility that hMSCs did adhere but were subsequently removed or damaged during these steps as indicated by the ethidium homodimer-1 stain. Therefore, the actin of residual cell wall could be what is stained in image F, and the cells in Image J may have had their membranes ruptured consequently only the ethidium homodimer-1 (the dead part of the live/dead stain) was positive. In images F and I the clarity of the FEP is reduced which could be due to cell presence. Imaging fluorescent stains at high resolutions in a 3D environment and parallel capillaries presents some significant challenges. Bleeding of fluoresce between capillaries is a challenge particularly as FEP is highly transparent. Being able to focus without interference from other stained morphology to look for in the hMSCs, while 2D morphology has been well documented a hMSC adhered to the side of a capillary is less well known. The actin staining seen on standard tissue culture plastic (Figure 61K) shows a high level of structural detail while the MCF actin stain (Figure 61F) it

is difficult to distinguish structural detail, though as previous mentioned this staining could be of the remanence of actin as whole hMSCs could have been removed during the staining protocol. When imaging in 3D it is common to encounter such issues and often a balance has to be found between phototoxicity, spatial resolution and when applicable temporal resolution (Gao et al. 2012). With the use of more advanced imaging equipment improvements to imaging technology can and is continuously being made which could be applicable in the future for MCF imaging (Appel et al. 2013; Jungmann et al. 2014).

The administration of solutions including the cell seeding was carried out manually therefore there was little control over the flow rates and pressure within the MCF. Other microfluidic hollow fibre cell culture platforms use more controlled flow systems, such as Huang et al. (2016) who used a flow rate of 10µl/min. Based on the evidence provided it is possible to administer hMSCs into the MCF but further work needs to be carried out on refining the administration process. Through a poorly controlled fluid handling process there is also the possibility that the PVA/gelatin coating was removed, there for fluid handling also needs to be improved for the coating process.

5.4 Conclusions

This work identifies the importance of surface homogeneity and functionality within the remit of cell based assays. Though not the primary focus this work as contributed to the understanding of critical surface characteristics for hMSC adhesion highlighting that surface energy is not the most significant factor for hMSC surface adhesion. While previous work by Shoichet & McCarthy (1991) has shown PLL to absorb onto the surface of FEP this work has progressed to show that hMSCs will subsequently adhere to the modified surface. Though morphologically differences between hMSCs on tissue culture plastic and on the PLL modified surfaces could be seen. The live/dead imaging also indicated that a high proportion of the hMSCs were dead, though this method was qualitative it did not add to the confidence in the coating method. Much of the previous literature discusses the importance of surface proteins *ex vivo* as they are *in vivo* adherent cells require an ECM for adhesion and structure, this work supports that understanding with hMSC attachment (Badylak et al. 2009; Guilak et al. 2009; Brown et al. 2010).

Through using PVA only as a coating method it was established that surface energy is not the critical factor for hMSCs adhesion. However, using different coating parameters most notably the molecular weight of PVA the surface energy, determined by contact angle measurements, could be controlled. Controlling the level of hydrophobicity is also relevant to other potential uses of the FEP and MCF for example achieving a controlled level of capillary rise in the MCF for "lab on a stick" format applications (Reis et al. 2016). While PVA alone did not facilitate cell attachment as well as tissue culture plastic, with the addition of gelatin to PVA FEP cell attachment after 6 days was improved. Based on AFM data gelatin or PVA alone indicated a heterogenic coating particularly after 24hrss coating time however as a mixture FEP was coated more homogenously and/or thicker which provided a more consistent cell attachment number. The addition of gelatin to PVA has been done before in the area of hydrogel cell scaffolds (Miao et al. 2015) however no literature has been found documenting this method for modifying the surface of FEP.

When transferring, the knowledge gained when coating flat 2D FEP tokens into the MCF format many challenges were encountered. The work on hMSC attachment in the 2D format was carried out using robust and reproducible methods, refinement of the cell seeding method (Section 5.2.7) used in Figure 61 is required for the MCF format. Using a manual injection method results in an uncontrolled and inconsistent force to which the cells inside the MCF are subjected to. Particularly when fluorescent visualisation of the cells us required it cannot be determined if the cells may have been removed or detached during the wash steps or the addition of the fluorescent stain. Improvement in the fluid handling to enable this microfluidic method to achieve the level of control seen in many commercialised microfluid platforms needs to be made (Haber 2006). In order for hMSC to attach the system would need to be static for a period of time, when seeding microcarriers for bioreactor culture hMSC are seeded to the microcarriers and the culture is static for 18hrss to allow cells to attach (Rafiq et al. 2013). Flow would then need to be introduced for the removal of waste products and the addition of fresh nutrients for the cells.

Overall it has been shown that it is viable for hMSC to attach to modified FEP proving that it is possible that the surface of FEP can be modified to improve the culture of viable hMCS (Chapter 2, Section 3.2). While there are indications this work can be translated to the MCF surface, to be able to study attachment of hMSC and

assaying of hMSC inside the MCF requires further improvements to the system as detailed in Chapter 6.

6 Conclusions

The overall objectives of this research were to identify the analytical challenges of manufacturing an hMSC based cell therapy. As a proof of concept the effect of culture conditions on the ability for hMSC to promote angiogenesis was analysed. The analytics and bioassays used to assess hMSC functionality were also evaluated from a 'use in the manufacturing environment' perspective.

By using an approach to identify the levels of 5 cytokines produced by hMSCs from four donors in three different culture environments with different oxygen levels along with secretome analysis it was determined that it was not possible to predict secretome behaviour based solely on the donor. Cytokine analysis showed that levels did vary between donor and culture environment, and the response to lower oxygen environments cannot be predicted based on the behaviour of one cell population. Consequently, this disproves hypothesis 1 (Chapter 2, Section 3.2) that hMSCs secretome profiles of VEGF-A, bFGF, HGF, PDGF-BB IL-8 /CXCL8 exhibit the same trends under three different atmospheric oxygen concentrations independent of the cell donor. While a clear trend could not be determined between the branch formation assay and analysed cytokine levels in the conditioned medium, differences could be seen between samples in the branch formation assay. In conclusion, this work indicates that the number of angiogenesis influencing factors investigated needs to be expanded to gain a more complete picture of the levels secreted by hMSCs and the influence on the branch formation assay. as noted in Chapter 2, over 120 different cytokines are produced by hMSCs (Park et al. 2009), it would be an extensive study to investigate all of these.

Based on the cytokine data in Chapter 3 IL-8 and HGF cytokines were selected for testing the feasibility of using the MCF ELISA platform for with a view to use the analytical technique away from the research bench and closer to the manufacturing floor (Chapter 4). While some improvements were suggested regarding the detection and analysis method overall it was possible to carryout HFG and IL-8 ELISAs using the MCF platform. The platform greatly reduced the assay time from addition of the sample to scanning the result, this is a great advantage in a time pressured manufacturing environment. Thus, proving hypothesis 2 (Chapter 2, Section 3.2) that

translating a plate-based ELISA assay into an MCF based microfluidic platform reduces the time between the addition of sample to result.

As a result of this the feasibility work carried out on the MCF ELISA platform to detect IL-8 and HGF the it was then determined if it was possible to develop a combine microfluidic system with a view to having both the sandwich ELISA and hMSC culture within the same microfluidic platform, the MCF. The application of the combination device was to detected cytokines relevant to the MOA of hMSC directly as the cells are secreting them. Many microfluidic devices incorporated the cell culture and analytics within one device (Toriello et al. 2008; Kamei et al. 2013), this provides more rapid results and also less error incorporated through operator handling. The most significant out come from this section of work was the successful functionalisation of FEP to improve hMSC adhesion using a PVA gelatin coating under optimised conditions. Proving hypothesis 3 that the surface of FEP can be modified to improve the culture of viable hMCS (Chapter 2, Section 3.2). This has laid the ground work and overcome a significant hurdle for the further development of an all in one microfluidic device using the MCF.

Rapid and precise analytics are much needed within many therapeutic areas not just cell therapies and manufacturing. Most notably in the area of precision medicine, where the classic "one size fits all" approach to medicine is being rejected due to the limited effectiveness of this approach (Roda et al. 2018). This work further supports the needs for precision medicine in relation to hMSC based cell therapies and demonstrates that the current criteria for defining hMSCs (Dominici et al. 2006) is limited. As discussed in Chapter 2 Section 2.6.1 applying limited characterisation criteria which doesn't fully demonstrated hMSC function for a specific therapeutic application is damaging the field. Combining cost effective cell culture (i.e. small scale) and rapid ELISA analytics is a realistic option to address these issues. It would be a powerful tool within the manufacturing setting from process development to defined production parameters and is applicable to the precision medicine field. The relationship between small-scale cell culture and large-scale cell culture would need to be determined to ensure that, functionality such as secreting factors are independent of culture scale. Should that be the case combined platforms would reduce the risk and associated cost of manufacturing cell therapies through providing more in-depth information in a timely manner without increasing the labour or finical burden.

6.1 Future works

It was shown in Chapter 3 that predicting hMSC secretome profiles under different culture conditions between donors was not possible. While this was mostly attributed to donor variation differences between the M2 and M3 controls indicating processing of the cell cultures also impacts secretome profiles. While improving process control may improve consistency within the same donor cell population, overcoming donor variation is not possible. This demonstrates the need for rapid bioanalytics when using hMSCs as a cell therapy treatment, though these lessons can be applied to any cell type.

The cell culture method used for obtaining samples analysed in Chapter 3 was the T-flask, which is the culture method used to expand hMSC populations for some clinical trials (Pérez-Simon et al. 2011) In order to provide cell numbers in the quantities required for sustainable cell therapies scale up as opposed to scale out of the cell culture needs to be carries out, and hence investigating the behaviour of hMSC in a bioreactor environment would be a future stage of this work. For allogeneic therapies where there is a selection of starting material a manufacturer needs to be able to determine which lot will perform to the required level during the scale up process. For autologous treatments gaining a fundamental understanding of the underlying causes for the variation between donors is important. Therefore, gene expression profiling would be useful in determining if the variation is genetic or if it occurs during the transcription of mRNA into proteins.

The branch formation assay analyses method used in this work is more highly automated from an imaging perspective in terms of removing operator bias when selecting the imaging area and improving the regularity of imaging. The assay produces a large volume of data per 24 well plate and with more detailed data more events need to be explained such as the behaviour of branches merging together and how that is seen within the data.

Overall the most critical part of the branch formation assay is to determine if the events seen *in vitro* are truly reflective of those events *in vivo*. This is usually carried out with animal studies, alternatively in tandem with an on-going clinical trial in order to gain more relevant data. The flatness of the Geltrex used for the branch formation assay needs to be more consistent between wells and assays, manual spreading of the

matrix introduces variation. In the assays for this work the HUVECs were from pooled donors to reduce the donor bias, there is scope to personalise the assay using the patients' own endothelial cells which would be more pertinent to determine the individual response of the treatment.

With respect to the MCF ELISA platform fluid handling an issue; prior to full assay validation in the context of cell therapy manufacturing the robustness of the assay needs to be improved. This includes removing operator bias from the imaging processing system and assembling of the MSD needs to become more dependable to prevent capillary failures. Future work should also include moving toward the use of fluorescent labelled antibodies to avoid the restrictions encountered using OPD without a stop solution.

Within an industry setting a more automated process which can be integrated into current manufacturing processes is the goal for bioanalytics (Scheper et al. 1999). Image processing software can be easily developed (Russ 2011), however the quality of the image determines the quality of the data output. Moving away from the flatbed scanner towards a more physically stable and therefore more consistent imaging platform would be a future step in improving assay robustness. Barbosa et al. (2015) have already begun to use fluorescent based assays in the MCF ELISA platform this would overcome some of the mixing issues seen in Chapter 4 which resulted in non-uniformed colour being analysed. Also using the OPD detection method means results need to be read in a defined window, and once measured cannot be re-measured. In contrast, fluorescence based assays, providing there is no photo bleaching can be re-measured. The challenge of using antibodies conjugated to fluorophores would potentially be fluorescent spectral overlap between capillaries. In the microtiter plate the well walls are black to prevent this; therefore, the MCF may require interposed optical blockers in every other capillary to overcome this.

In Chapter 5 it was shown that the surface chemistry of the MCF would need to be modified in order to facilitate the adhesion of hMSC with a view to produce an all in one device similar to Figure 62.
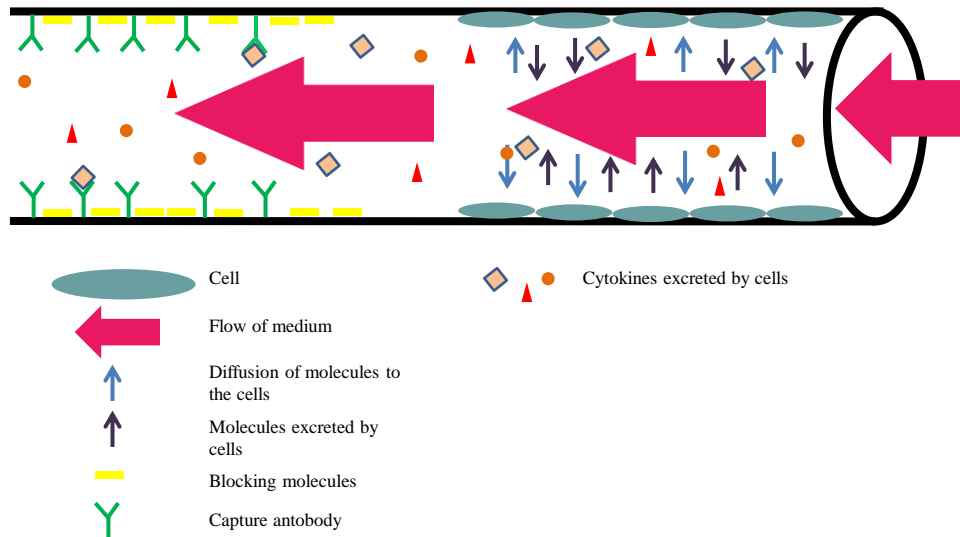
Figure 62: Schematic of an MCF microfluidic combination device for cell culture and serial detection of cytokines secreted by the cells.

The use of gelatine and PVA mixture to modify the surface of FEP proved successful and repeatable on a flat surface. It was also easily administered to the internal surface of the MCF which was a recognised limitation of other FEP surface modification methods. As with the MCF ELISA some of the challenges in adapting the MCF for a combination platform related to the fluid handling. While aspirating the PVA/gelatine coating mixture into the MCF was straightforward, using equipment which maintained sterility, enabled replacement of fluids inside the MCF and control of fluid speed and pressure were not achieved within the time frame of this work. Other microfluidic platforms utilise micro pumps to deliver fluids with precision to the device (Haeberle & Zengerle 2007). The use of pumps has not previously been a requirement for the MCF as the uses have included a dip stick style test (Reis et al. 2016), and syringe based aspiration (Barbosa et al. 2014; Barbosa et al. 2015) which did not require the level of control at low rates needed in human cell work. Being able to provide an appropriate and consistent flow rate inside the MCF is the next step for the combination device development work, mechanical stresses such as shear stress needs to be at an acceptable level for the cell type being used, in this incidence hMSCs (Shah et al. 2014). As the device would also be detecting proteins, shear stress in also an important factor to prevent unwanted protein aggregation which would result in inaccurate lower levels of analyte being detected (Cromwell et al. 2006).

Designing a controlled automated fluid handling system would also overcome some of the limitations of other microfluidic devices which rely on multiple inlet and ports that reduces the through put of the device and makes using the device more complex (Haeberle & Zengerle 2007; Gupta et al. 2010). Some lab on a chip devices also require cell seeding and culture prior to assembly of the analytical devices, over handling of the devices can risk damage to the cells (Fernandes et al. 2009). An all in one, fully controlled microfluidic cell culture and analysis system would be the end goal for this platform.

The behaviour of the cells, in this work hMSCs, will need to be compared to other culture platforms, and determine if the culture of cells at this scale causes adverse effects. It is a common concern when studying cell behaviour *in vitro* that it is not truly reflective of *in vivo* cell behaviour (Huh et al. 2011). Microfluidic devices are thought to be able to mimic the *in vivo* cellular microenvironment which would make the platform more relevant than standard tissue culture plastic. Therefore, culturing cells inside the MCF has the potential to be an improvement on current methods.

Overall this work has identified challenges in manufacturing hMSCs and has made progress in addressing some of these challenges. Using hMSC as a mainstream treatment for many conditions is becoming a realisation. However, in the pressure to fulfil the potential of these applications a need to for rapid bioanalytics has grown rapidly.

References

Abad, M. et al., 2013. Reprogramming in vivo produces teratomas and iPS cells with totipotency features. *Nature*, advance on. Available at: http://dx.doi.org/10.1038/nature12586 [Accessed September 16, 2013].

Addison, W.N. et al., 2007. Pyrophosphate inhibits mineralization of osteoblast cultures by binding to mineral, up-regulating osteopontin, and inhibiting alkaline phosphatase activity. *The Journal of biological chemistry*, 282(21), pp.15872–83. Available at: http://www.ncbi.nlm.nih.gov/pubmed/17383965 [Accessed May 13, 2018].

Ahmed, Z. & Bicknell, R., 2009. Angiogenic signalling pathways. *Methods in molecular biology (Clifton, N.J.)*, 467, pp.3–24. Available at: http://www.ncbi.nlm.nih.gov/pubmed/19301662 [Accessed August 6, 2014].

Andersen, M.N. et al., 2016. Elimination of erroneous results in flow cytometry caused by antibody binding to Fc receptors on human monocytes and macrophages. *Cytometry Part A*, 89(11), pp.1001–1009. Available at: http://doi.wiley.com/10.1002/cyto.a.22995 [Accessed April 30, 2018].

Anderson, J.D. et al., 2016. Mesenchymal stem cell-based therapy for ischemic stroke. *Chinese Neurosurgical Journal*, 2(1), p.36. Available at: http://cnjournal.biomedcentral.com/articles/10.1186/s41016-016-0053-4 [Accessed November 2, 2016].

Andreasson, U. et al., 2015. A Practical Guide to Immunoassay Method Validation. *Frontiers in neurology*, 6, p.179. Available at: http://www.ncbi.nlm.nih.gov/pubmed/26347708 [Accessed December 28, 2016].

Appel, A.A. et al., 2013. Imaging challenges in biomaterials and tissue engineering. *Biomaterials*, 34(28), pp.6615–6630.

Arnaoutova, I. et al., 2009. The endothelial cell tube formation assay on basement membrane turns 20: state of the science and the art. *Angiogenesis*, 12(3), pp.267–74. Available at: http://www.ncbi.nlm.nih.gov/pubmed/19399631 [Accessed December 17, 2014].

Astori, G. et al., 2010. Bone marrow derived stem cells in regenerative medicine as advanced therapy medicinal products. *American journal of translational research*, 2(3), pp.285–95. Available at:

http://www.pubmedcentral.nih.gov/articlerender.fcgi?artid=2892405&tool=pmce
ntrez&rendertype=abstract [Accessed September 4, 2015].

Atala, A. et al., 2006. Tissue-engineered autologous bladders for patients needing cystoplasty. *Lancet (London, England)*, 367(9518), pp.1241–6. Available at: http://www.ncbi.nlm.nih.gov/pubmed/16631879 [Accessed April 8, 2017].

Badylak, S. & Rosenthal, N., 2017. Regenerative medicine: are we there yet? *npj Regenerative Medicine*, 2(1), p.2. Available at: http://www.nature.com/articles/s41536-016-0005-9 [Accessed February 25, 2017].

Badylak, S.F., Freytes, D.O. & Gilbert, T.W., 2009. Extracellular matrix as a biological scaffold material: Structure and function. *Acta biomaterialia*, 5(1), pp.1–13. Available at: http://www.sciencedirect.com/science/article/pii/S1742706108002821 [Accessed May 23, 2014].

Baharvand, H., Hashemi, S.M. & Shahsavani, M., 2008. Differentiation of human embryonic stem cells into functional hepatocyte-like cells in a serum-free adherent culture condition. *Differentiation; research in biological diversity*, 76(5), pp.465–77. Available at: http://dx.doi.org/10.1111/j.1432-0436.2007.00252.x [Accessed November 1, 2012].

Baker, H.N. et al., 2012. Conversion of a Capture ELISA to a Luminex xMAP Assay using a Multiplex Antibody Screening Method. *Journal of Visualized Experiments*, (65), pp.e4084–e4084. Available at: http://www.jove.com/video/4084/ [Accessed March 5, 2017].

Bang, O.Y. et al., 2005. Autologous mesenchymal stem cell transplantation in stroke patients. *Annals of neurology*, 57(6), pp.874–82. Available at: http://www.ncbi.nlm.nih.gov/pubmed/15929052 [Accessed June 9, 2014].

Baraniak, P.R. & McDevitt, T.C., 2010. Stem cell paracrine actions and tissue regeneration. *Regenerative medicine*, 5(1), pp.121–43. Available at: http://www.ncbi.nlm.nih.gov/pubmed/20017699 [Accessed December 4, 2016].

Barbosa, A.I. et al., 2014. A lab-in-a-briefcase for rapid prostate specific antigen (PSA) screening from whole blood. *Lab on a chip*, 14(16), pp.2918–28. Available at: http://pubs.rsc.org/en/content/articlehtml/2014/lc/c4lc00464g [Accessed June 8, 2015].

Barbosa, A.I. et al., 2015. Portable smartphone quantitation of prostate specific

antigen (PSA) in a fluoropolymer microfluidic device. *Biosensors & bioelectronics*, 70, pp.5–14. Available at: http://www.sciencedirect.com/science/article/pii/S0956566315001499 [Accessed March 19, 2015].

Barbosa, A.I., Edwards, A. & Reis, N.M., 2013. Application of a disposable multiplex microfluidic device to rapid biomolecule quantitation. *Current Opinion in Biotechnology*, 24(24), p.S66. Available at: https://www.infona.pl//resource/bwmeta1.element.elsevier-e92eec89-655a-3b91-9dd2-5b3404d8726b [Accessed June 8, 2015].

Barbulovic-Nad, I. et al., 2008. Digital microfluidics for cell-based assays. *Lab on a chip*, 8(4), pp.519–26. Available at: http://pubs.rsc.org/en/Content/ArticleHTML/2008/LC/B717759C [Accessed June 6, 2015].

Barry, F.P. & Murphy, J.M., 2004. Mesenchymal stem cells: clinical applications and biological characterization. *The international journal of biochemistry & cell biology*, 36(4), pp.568–84. Available at: http://www.sciencedirect.com/science/article/pii/S1357272503003625 [Accessed July 12, 2014].

Bartosh, T.J. et al., 2010. Aggregation of human mesenchymal stromal cells (MSCs) into 3D spheroids enhances their antiinflammatory properties. *Proceedings of the National Academy of Sciences of the United States of America*, 107(31), pp.13724–9. Available at: http://www.ncbi.nlm.nih.gov/pubmed/20643923 [Accessed May 28, 2017].

Bengtsson, N.E. et al., 2016. Progress and prospects of gene therapy clinical trials for the muscular dystrophies. *Human molecular genetics*, 25(R1), pp.R9-17. Available at: http://www.ncbi.nlm.nih.gov/pubmed/26450518 [Accessed November 28, 2016].

Bhatia, S.N. & Ingber, D.E., 2014. Microfluidic organs-on-chips. *Nature biotechnology*, 32(8), pp.760–772. Available at: http://dx.doi.org/10.1038/nbt.2989 [Accessed August 7, 2014].

Bhosale, A.M. et al., 2007. Combined autologous chondrocyte implantation and allogenic meniscus transplantation: a biological knee replacement. *The Knee*, 14(5), pp.361–8. Available at: http://dx.doi.org/10.1016/j.knee.2007.07.002 [Accessed March 19, 2013].

Bischel, L.L. et al., 2013. Tubeless microfluidic angiogenesis assay with three-dimensional endothelial-lined microvessels. *Biomaterials*, 34(5), pp.1471–1477. Available at: http://linkinghub.elsevier.com/retrieve/pii/S0142961212012495 [Accessed March 5, 2017].

Boncler, M. et al., 2014. Comparison of PrestoBlue and MTT assays of cellular viability in the assessment of anti-proliferative effects of plant extracts on human endothelial cells. *Journal of pharmacological and toxicological methods*, 69(1), pp.9–16. Available at: http://www.sciencedirect.com/science/article/pii/S1056871913003006 [Accessed May 2, 2016].

Bonyadi, S. & Mackley, M., 2012. The development of novel micro-capillary film membranes. *Journal of Membrane Science*, 389, pp.137–147. Available at: http://www.sciencedirect.com/science/article/pii/S0376738811007733 [Accessed October 30, 2013].

Boomsma, R.A. & Geenen, D.L., 2012. Mesenchymal stem cells secrete multiple cytokines that promote angiogenesis and have contrasting effects on chemotaxis and apoptosis. T. G. Hofmann, ed. *PloS one*, 7(4), p.e35685. Available at: http://dx.plos.org/10.1371/journal.pone.0035685 [Accessed July 17, 2014].

Brandwein, H. et al., 2012. Meeting Lot-Size Challenges of Manufacturing Adherent Cells for Therapy - BioProcess InternationalBioProcess International. *Bioprocess International*, 10(3), pp.16–22. Available at: http://www.bioprocessintl.com/manufacturing/cell-therapies/meeting-lot-size-challenges-of-manufacturing-adherent-cells-for-therapy-328093/.

Bravery, C.A. et al., 2013. Potency assay development for cellular therapy products: an ISCT review of the requirements and experiences in the industry. *Cytotherapy*, 15(1), pp.9–19. Available at: http://www.ncbi.nlm.nih.gov/pubmed/23260082 [Accessed May 26, 2014].

Brindley, D.A. et al., 2011. The Impact of Market Volatility on the Cell Therapy Industry. *Cell Stem Cell*, 9(5), pp.397–401. Available at: http://linkinghub.elsevier.com/retrieve/pii/S1934590911004905 [Accessed March 4, 2017].

British Standards Institution, 2011. *Characterization of human cells for clinical applications Guide*,

Bronckaers, A. et al., 2014. Mesenchymal stem/stromal cells as a pharmacological

and therapeutic approach to accelerate angiogenesis. *Pharmacology & therapeutics*, 143(2), pp.181–96. Available at: http://www.sciencedirect.com/science/article/pii/S0163725814000527 [Accessed August 27, 2014].

Brown, B.N. et al., 2010. Surface characterization of extracellular matrix scaffolds. *Biomaterials*, 31(3), pp.428–37. Available at: http://www.sciencedirect.com/science/article/pii/S0142961209009934 [Accessed May 28, 2014].

Butler, J.E. et al., 1992. The physical and functional behavior of capture antibodies adsorbed on polystyrene. *Journal of Immunological Methods*, 150(1–2), pp.77–90.

Caplan, A.I. & Bruder, S.P., 2001. Mesenchymal stem cells: building blocks for molecular medicine in the 21st century. *Trends in Molecular Medicine*, 7(6), pp.259–264. Available at: http://www.sciencedirect.com/science/article/pii/S1471491401020160 [Accessed July 17, 2014].

Carlos Polanco, J. et al., 2013. Identification of Unsafe Human Induced Pluripotent Stem Cell Lines Using a Robust Surrogate Assay for Pluripotency. *Stem cells (Dayton, Ohio)*. Available at: http://www.ncbi.nlm.nih.gov/pubmed/23728894 [Accessed August 16, 2013].

Carmen, J. et al., 2012. Developing assays to address identity, potency, purity and safety: cell characterization in cell therapy process development. *Regenerative medicine*, 7(1), pp.85–100. Available at: http://www.ncbi.nlm.nih.gov/pubmed/22168500 [Accessed May 22, 2014].

Carpenter, M.K., Frey-Vasconcells, J. & Rao, M.S., 2009. Developing safe therapies from human pluripotent stem cells. *Nature Biotechnology*, 27(7), pp.606–613. Available at: http://www.nature.com/doifinder/10.1038/nbt0709-606 [Accessed February 26, 2017].

Carreau, A. et al., 2011. Why is the partial oxygen pressure of human tissues a crucial parameter? Small molecules and hypoxia. *Journal of cellular and molecular medicine*, 15(6), pp.1239–53. Available at: http://www.ncbi.nlm.nih.gov/pubmed/21251211 [Accessed December 5, 2016].

Castanheira, A.P. et al., 2015. Multiplexed femtomolar quantitation of human cytokines in a fluoropolymer microcapillary film. *The Analyst*, 140(16),

pp.5609–5618. Available at: http://xlink.rsc.org/?DOI=C5AN00238A [Accessed January 9, 2017].

Center for Biologics Evaluation and Research, 1998. *Guidance for Industry: Guidance for Human Somatic Cell Therapy and Gene Therapy*,

Chan, A.K.C., 2016. Development of characterisation and quality potency assays for human mesenchymal stem cells. Available at: https://dspace.lboro.ac.uk/dspace-jspui/handle/2134/22977 [Accessed May 13, 2018].

Chan, A.K.C. et al., 2013. Multiparameter flow cytometry for the characterisation of extracellular markers on human mesenchymal stem cells. *Biotechnology letters*. Available at: http://www.ncbi.nlm.nih.gov/pubmed/24322774 [Accessed January 21, 2014].

Chang, Y.-H. et al., 2006. Integrated polymerase chain reaction chips utilizing digital microfluidics. *Biomedical Microdevices*, 8(3), pp.215–225. Available at: http://link.springer.com/10.1007/s10544-006-8171-y [Accessed April 15, 2017].

Chen, G. et al., 2015. Comparison of biological characteristics of mesenchymal stem cells derived from maternal-origin placenta and Wharton's jelly. *Stem Cell Research & Therapy*, 6(1), p.228. Available at: http://stemcellres.com/content/6/1/228 [Accessed November 26, 2015].

Chen, G.J. & Forough, R., 2006. Fibroblast growth factors, fibroblast growth factor receptors, diseases, and drugs. *Recent patents on cardiovascular drug discovery*, 1(2), pp.211–24. Available at: http://www.ncbi.nlm.nih.gov/pubmed/18221087 [Accessed October 25, 2016].

Chen, K.G. et al., 2014. Human Pluripotent Stem Cell Culture: Considerations for Maintenance, Expansion, and Therapeutics. *Cell Stem Cell*, 14(1), pp.13–26.

Chi, E.Y. et al., 2003. Physical Stability of Proteins in Aqueous Solution: Mechanism and Driving Forces in Nonnative Protein Aggregation. *Pharmaceutical Research*, 20(9), pp.1325–1336. Available at: http://link.springer.com/10.1023/A:1025771421906 [Accessed May 1, 2017].

Chuang, C.-H. et al., 2014. Suppression of alpha-tocopherol ether-linked acetic acid in VEGF-induced angiogenesis and the possible mechanisms in human umbilical vein endothelial cells. *Toxicology and applied pharmacology*, 281(3), pp.310–6. Available at: http://www.sciencedirect.com/science/article/pii/S0041008X14003871 [Accessed February 18, 2015].

ClinicalTrials.gov, 2017. Mesenchymal stem cell - List Results. Available at: https://clinicaltrials.gov/ct2/results?term=Mesenchymal+stem+cell&brwse-force=true [Accessed March 4, 2017].

Cohn, C. et al., 2015. *Comparative study of antibody immobilization mediated by lipid and polymer fibers*,

Collart-Dutilleul, P.-Y. et al., 2014. Adhesion and Proliferation of Human Mesenchymal Stem Cells from Dental Pulp on Porous Silicon Scaffolds. *ACS Applied Materials & Interfaces*, 6(3), pp.1719–1728. Available at: http://pubs.acs.org/doi/abs/10.1021/am4046316 [Accessed November 30, 2016].

Collins, F.S. & Varmus, H., 2015. A New Initiative on Precision Medicine. *New England Journal of Medicine*, 372(9), pp.793–795. Available at: http://www.nejm.org/doi/abs/10.1056/NEJMp1500523 [Accessed December 5, 2016].

Coopman, K. & Medcalf, N., 2014. *From production to patient: challenges and approaches for delivering cell therapies*, Harvard Stem Cell Institute. Available at: http://www.ncbi.nlm.nih.gov/pubmed/24945057 [Accessed April 9, 2017].

Corcione, A. et al., 2006. Human mesenchymal stem cells modulate B-cell functions. *Blood*, 107(1), pp.367–72. Available at: http://bloodjournal.hematologylibrary.org/content/107/1/367?variant=short&sso-checked=1 [Accessed May 26, 2014].

Corey, S. et al., 2017. An update on stem cell therapy for neurological disorders: cell death pathways as therapeutic targets. *Chinese Neurosurgical Journal*, 3(1), p.4. Available at: http://cnjournal.biomedcentral.com/articles/10.1186/s41016-016-0071-2 [Accessed February 15, 2017].

Coupe, B. & Chen, W., 2001. A New Approach to Surface Functionalization of Fluoropolymers. *Macromolecules*, 34(6), pp.1533–1535. Available at: http://adsabs.harvard.edu/abs/2001MaMol..34.1533C [Accessed July 25, 2013].

Cox, K.L. et al., 2004. *Immunoassay Methods*, Eli Lilly & Company and the National Center for Advancing Translational Sciences. Available at: http://www.ncbi.nlm.nih.gov/pubmed/22553884 [Accessed October 20, 2016].

Cromwell, M.E.M., Hilario, E. & Jacobson, F., 2006. Protein aggregation and bioprocessing. *The AAPS Journal*, 8(3), pp.E572–E579. Available at: http://www.springerlink.com/index/10.1208/aapsj080366 [Accessed March 12, 2017].

Cross, M.J. & Claesson-Welsh, L., 2001. FGF and VEGF function in angiogenesis: signalling pathways, biological responses and therapeutic inhibition. *Trends in pharmacological sciences*, 22(4), pp.201–7. Available at: http://www.ncbi.nlm.nih.gov/pubmed/11282421 [Accessed October 25, 2016].

Curran, J.M., Chen, R. & Hunt, J.A., 2005. Controlling the phenotype and function of mesenchymal stem cells in vitro by adhesion to silane-modified clean glass surfaces. *Biomaterials*, 26(34), pp.7057–7067. Available at: http://www.sciencedirect.com/science/article/pii/S0142961205003893 [Accessed January 29, 2014].

Davidson, B. & Fasman, G.D., 1967. The Conformational Transitions of Uncharged Poly-L-lysine. α Helix-Random Coil-β Structure *. *Biochemistry*, 6(6), pp.1616–1629. Available at: http://dx.doi.org/10.1021/bi00858a008 [Accessed July 2, 2014].

Dewez, J.-L. et al., 1998. Adhesion of mammalian cells to polymer surfaces: from physical chemistry of surfaces to selective adhesion on defined patterns. *Biomaterials*, 19(16), pp.1441–1445. Available at: http://www.sciencedirect.com/science/article/pii/S0142961298000556 [Accessed May 7, 2014].

Diaz-Romero, J. et al., 2005. Immunophenotypic analysis of human articular chondrocytes: changes in surface markers associated with cell expansion in monolayer culture. *Journal of cellular physiology*, 202(3), pp.731–42. Available at: http://www.ncbi.nlm.nih.gov/pubmed/15389573 [Accessed November 23, 2012].

Dmitriev, A.D. et al., 2013. MONOCLONAL ANTIBODIES REQUIRING COATING BUFFER WITH LOW PH FOR EFFICIENT ANTIGEN CAPTURE IN SANDWICH ELISA: THE RARITIES OR PRACTICALLY IMPORTANT PHENOMENA? *Journal of Immunoassay and Immunochemistry*, 34(4), pp.414–437. Available at: http://www.tandfonline.com/doi/abs/10.1080/15321819.2013.764894 [Accessed January 11, 2017].

Dominici, M. et al., 2006. Minimal criteria for defining multipotent mesenchymal stromal cells. The International Society for Cellular Therapy position statement. *Cytotherapy*, 8(4), pp.315–7. Available at: http://www.ncbi.nlm.nih.gov/pubmed/16923606 [Accessed May 21, 2013].

Donovan, D. et al., 2001. Comparison of three in vitro human "angiogenesis" assays with capillaries formed in vivo. *Angiogenesis*, 4(2), pp.113–121. Available at: http://link.springer.com/10.1023/A:1012218401036 [Accessed October 24, 2016].

Doorn, J. et al., 2012. Therapeutic Applications of Mesenchymal Stromal Cells: Paracrine Effects and Potential Improvements. *http://dx.doi.org/10.1089/ten.teb.2011.0488*.

Dorronsoro, A. et al., 2013. Immunoregulation : Mechanisms of Action and Clinical Applications. *Bone Marrow Research*, 2013.

Duffy, A.M., Bouchier-Hayes, D.J. & Harmey, J.H., 2013. Vascular Endothelial Growth Factor (VEGF) and Its Role in Non-Endothelial Cells: Autocrine Signalling by VEGF. Available at: https://www.ncbi.nlm.nih.gov/books/NBK6482/?report=reader [Accessed March 5, 2017].

Duijvestein, M. et al., 2010. Autologous bone marrow-derived mesenchymal stromal cell treatment for refractory luminal Crohn's disease: results of a phase I study. *Gut*, 59(12), pp.1662–9. Available at: http://www.ncbi.nlm.nih.gov/pubmed/20921206 [Accessed May 27, 2017].

Dutkowski, P. et al., 2015. Challenges to Liver Transplantation and Strategies to Improve Outcomes. *Gastroenterology*, 148(2), pp.307–323.

Eaves, C.J., 2015. Hematopoietic stem cells: concepts, definitions, and the new reality. *Blood*, 125(17).

Edwards, Alexander, D. et al., 2011. IMMUNOASSAYS, METHODS FOR CARRYING OUT IMMUNOASSAYS, IMMUNOASSAY KITS AND METHOD FOR MANUFACTURING IMMUNOASSAY KITS.

Edwards, A.D. et al., 2011. A simple device for multiplex ELISA made from melt-extruded plastic microcapillary film. *Lab on a chip*, 11(24), pp.4267–73. Available at: http://www.ncbi.nlm.nih.gov/pubmed/22030675 [Accessed February 10, 2013].

Ellinas, K. et al., 2017. Micro-bead immunoassays for the detection of IL6 and PDGF-2 proteins on a microfluidic platform, incorporating superhydrophobic passive valves. *Microelectronic Engineering*, 175, pp.73–80. Available at: http://linkinghub.elsevier.com/retrieve/pii/S0167931717300710 [Accessed March 5, 2017].

Engvall, E. & Perlmann, P., 1971. Enzyme-linked immunosorbent assay (ELISA) quantitative assay of immunoglobulin G. *Immunochemistry*, 8(9), pp.871–874. Available at: http://linkinghub.elsevier.com/retrieve/pii/001927917190454X [Accessed March 5, 2017].

Estrada, J.C. et al., 2012. Culture of human mesenchymal stem cells at low oxygen tension improves growth and genetic stability by activating glycolysis. *Cell death and differentiation*, 19(5), pp.743–55. Available at: http://www.nature.com/doifinder/10.1038/cdd.2011.172 [Accessed December 4, 2016].

Eteshola, E. & Leckband, D., 2001a. Development and characterization of an ELISA assay in PDMS microfluidic channels. *Sensors and Actuators B: Chemical*, 72(2), pp.129–133. Available at: http://linkinghub.elsevier.com/retrieve/pii/S0925400500006407 [Accessed March 4, 2017].

Eteshola, E. & Leckband, D., 2001b. Development and characterization of an ELISA assay in PDMS microfluidic channels. *Sensors and Actuators B: Chemical*, 72(2), pp.129–133.

European Medicines Agency, 2017. Clinical Trials Register. Available at: https://www.clinicaltrialsregister.eu/ctr-search/search [Accessed March 4, 2017].

European Medicines Agency, 2008. Guideline on human cell-based medicinal products. , EMA(May), p.EMEA/CHMP/410869/2006.

Fan, Y. et al., 2008. Interleukin-6 stimulates circulating blood-derived endothelial progenitor cell angiogenesis in vitro. *Journal of cerebral blood flow and metabolism : official journal of the International Society of Cerebral Blood Flow and Metabolism*, 28(1), pp.90–8. Available at: http://www.pubmedcentral.nih.gov/articlerender.fcgi?artid=2581498&tool=pmcentrez&rendertype=abstract [Accessed November 17, 2014].

FDA, 2014. Drug Innovation - Novel Drug Approvals for 2014.

FDA, 2015. Drug Innovation - Novel Drug Approvals for 2015.

FDA, 2016. Drug Innovation - Novel Drug Approvals for 2016.

FDA, 2004. *Guidance for Industry PAT: A Framework for Innovative Pharmaceutical Development, Manufacuring, and Quality Assurance*,

Fernandes, T.G. et al., 2009. High-throughput cellular microarray platforms: applications in drug discovery, toxicology and stem cell research. *Trends in*

biotechnology, 27(6), pp.342–9. Available at: http://dx.doi.org/10.1016/j.tibtech.2009.02.009 [Accessed March 2, 2013].

Findlay, J.W.A. et al., 2000. Validation of immunoassays for bioanalysis: a pharmaceutical industry perspective. *Journal of Pharmaceutical and Biomedical Analysis*, 21(6), pp.1249–1273. Available at: http://www.sciencedirect.com/science/article/pii/S0731708599002447 [Accessed September 15, 2015].

Findlay, J.W.A. & Dillard, R.F., 2007. Appropriate calibration curve fitting in ligand binding assays. *The AAPS Journal*, 9(2), pp.E260–E267. Available at: http://www.springerlink.com/index/10.1208/aapsj0902029 [Accessed January 12, 2017].

Fodor, W.L. et al., 2003. Tissue engineering and cell based therapies, from the bench to the clinic: The potential to replace, repair and regenerate. *Reproductive Biology and Endocrinology*, 1(1), p.102. Available at: http://rbej.biomedcentral.com/articles/10.1186/1477-7827-1-102 [Accessed November 27, 2016].

Food and Drug Administration, 2008. Cellular & Gene Therapy Guidances - Draft Guidance for Industry: Potency Tests for Cellular and Gene Therapy Products. Available at: http://www.fda.gov/BiologicsBloodVaccines/GuidanceComplianceRegulatoryInformation/Guidances/CellularandGeneTherapy/ucm072571.htm [Accessed June 25, 2014].

Food and Drug Administration, 2013. *Guidance for Industry Bioanalytical Method Validation*, Available at: http://google2.fda.gov/search?q=cache:oi26OHHs1qYJ:www.fda.gov/downloads/drugs/guidancecomplianceregulatoryinformation/guidances/ucm368107.pdf+bioanalytical&client=FDAgov&site=FDAgov&lr=&proxystylesheet=FDAgov&output=xml_no_dtd&access=p&ie=UTF-8&oe=UTF-8 [Accessed May 10, 2016].

Food and Drug Administration, HHS, 2005. Definition of primary mode of action of a combination product. Final rule. *Federal register*, 70(164), pp.49848–62. Available at: http://www.ncbi.nlm.nih.gov/pubmed/16121446 [Accessed December 9, 2016].

Fox, J.L., 2008. FDA scrutinizes human stem cell therapies. *Nature Biotechnology*, 26(6), pp.598–599. Available at:

http://www.nature.com/doifinder/10.1038/nbt0608-598 [Accessed December 16, 2016].

Francavilla, C., Maddaluno, L. & Cavallaro, U., 2009. The functional role of cell adhesion molecules in tumor angiogenesis. *Seminars in Cancer Biology*, 19(5), pp.298–309. Available at: http://linkinghub.elsevier.com/retrieve/pii/S1044579X09000674 [Accessed May 1, 2017].

Galipeau, J. et al., 2016. International Society for Cellular Therapy perspective on immune functional assays for mesenchymal stromal cells as potency release criterion for advanced phase clinical trials. *Cytotherapy*, 18(2), pp.151–159. Available at: http://linkinghub.elsevier.com/retrieve/pii/S1465324915011226 [Accessed October 18, 2016].

Gao, D. et al., 2012. Recent developments in microfluidic devices for in vitro cell culture for cell-biology research. *TrAC Trends in Analytical Chemistry*, 35, pp.150–164.

Gao, L. et al., 2012. Noninvasive imaging beyond the diffraction limit of 3D dynamics in thickly fluorescent specimens. *Cell*, 151(6), pp.1370–1385. Available at: http://dx.doi.org/10.1016/j.cell.2012.10.008.

Gardner, J. & Webster, A., 2017. Accelerating Innovation in the Creation of Biovalue. *Science, Technology, & Human Values*, 42(5), pp.925–946. Available at: http://journals.sagepub.com/doi/10.1177/0162243917702720 [Accessed May 14, 2018].

Gebhardt, R. et al., 2003. New hepatocyte in vitro systems for drug metabolism: metabolic capacity and recommendations for application in basic research and drug development, standard operation procedures. *Drug metabolism reviews*, 35(2–3), pp.145–213. Available at: http://www.ncbi.nlm.nih.gov/pubmed/12959414 [Accessed November 18, 2012].

George, B., 2011. Regulations and guidelines governing stem cell based products: Clinical considerations. *Perspectives in clinical research*, 2(3), pp.94–9. Available at: http://www.pubmedcentral.nih.gov/articlerender.fcgi?artid=3159216&tool=pmcentrez&rendertype=abstract [Accessed September 4, 2015].

Gerhardt, H. et al., 2003. VEGF guides angiogenic sprouting utilizing endothelial tip cell filopodia. *The Journal of Cell Biology*, 161(6).

Gerritsen, M.E., 2005. HGF and VEGF: A Dynamic Duo. *Circulation Research*, 96(3).

Gerritsen, M.E. et al., 2003. Using gene expression profiling to identify the molecular basis of the synergistic actions of hepatocyte growth factor and vascular endothelial growth factor in human endothelial cells. *British Journal of Pharmacology*, 140(4), pp.595–610. Available at: http://doi.wiley.com/10.1038/sj.bjp.0705494 [Accessed October 28, 2016].

Gieseke, F. et al., 2010. Human multipotent mesenchymal stromal cells use galectin-1 to inhibit immune effector cells. *Blood*, 116(19), pp.3770–9. Available at: http://bloodjournal.hematologylibrary.org/content/116/19/3770?variant=short&sso-checked=1 [Accessed July 15, 2014].

Goldring, C.E.P. et al., 2011. Assessing the Safety of Stem Cell Therapeutics. *Cell Stem Cell*, 8(6), pp.618–628.

Gottschalk, P.G. & Dunn, J.R., 2005. The five-parameter logistic: A characterization and comparison with the four-parameter logistic. *Analytical Biochemistry*, 343(1), pp.54–65.

Gronthos, S., 2003. Molecular and cellular characterisation of highly purified stromal stem cells derived from human bone marrow. *Journal of Cell Science*, 116(9), pp.1827–1835. Available at: http://jcs.biologists.org/content/116/9/1827.short [Accessed May 26, 2014].

Guilak, F. et al., 2009. Control of stem cell fate by physical interactions with the extracellular matrix. *Cell stem cell*, 5(1), pp.17–26. Available at: http://www.sciencedirect.com/science/article/pii/S1934590909002938 [Accessed May 23, 2014].

Guo, S. & Dipietro, L.A., 2010. Factors affecting wound healing. *Journal of dental research*, 89(3), pp.219–29. Available at: http://www.ncbi.nlm.nih.gov/pubmed/20139336 [Accessed December 5, 2016].

Gupta, K. et al., 2010. Lab-on-a-chip devices as an emerging platform for stem cell biology. *Lab on a chip*, 10(16), pp.2019–31. Available at: http://pubs.rsc.org/en/Content/ArticleHTML/2010/LC/C004689B [Accessed May 2, 2013].

Haber, C., 2006. Microfluidics in commercial applications; an industry perspective. *Lab on a Chip*, 6(9), p.1118. Available at: http://www.ncbi.nlm.nih.gov/pubmed/16929389 [Accessed February 12, 2017].

Haeberle, S. & Zengerle, R., 2007. Microfluidic platforms for lab-on-a-chip applications. *Lab on a chip*, 7(9), pp.1094–110. Available at: http://pubs.rsc.org/en/Content/ArticleHTML/2007/LC/B706364B [Accessed June 23, 2014].

Hallmark, B., Mackley, M.R. & Gadala-Maria, F., 2005. Hollow Microcapillary Arrays in Thin Plastic Films. *Advanced Engineering Materials*, 7(6), pp.545–547. Available at: http://doi.wiley.com/10.1002/adem.200400154 [Accessed May 2, 2013].

Halme, D.G. & Kessler, D. a, 2006. FDA regulation of stem-cell-based therapies. *The New England journal of medicine*, 355(16), pp.1730–5. Available at: http://www.ncbi.nlm.nih.gov/pubmed/22842860.

Hambor J.E, 2012. Bioreactor Design and Bioprocess Controls for Industrialized Cell Processing - BioProcess InternationalBioProcess International. *Bioprocess International*, 10(6), pp.22–30. Available at: http://www.bioprocessintl.com/upstream-processing/upstream-single-use-technologies/bioreactor-design-and-bioprocess-controls-for-industrialized-cell-processing-331147/.

Hamilton, T.M., Dobie-Galuska, A.A. & Wietstock, S.M., 1999. The o-Phenylenediamine-Horseradish Peroxidase System: Enzyme Kinetics in the General Chemistry Laboratory. *Journal of Chemical Education*, 76(5), p.642. Available at: http://pubs.acs.org/doi/abs/10.1021/ed076p642 [Accessed November 25, 2016].

Harkness, L. et al., 2008. Identification of a membrane proteomic signature for human embryonic stem cells independent of culture conditions. *Stem cell research*, 1(3), pp.219–27. Available at: http://dx.doi.org/10.1016/j.scr.2008.06.001 [Accessed February 10, 2013].

Harnett, E.M., Alderman, J. & Wood, T., 2007. The surface energy of various biomaterials coated with adhesion molecules used in cell culture. *Colloids and surfaces. B, Biointerfaces*, 55(1), pp.90–7. Available at: http://www.sciencedirect.com/science/article/pii/S0927776506003870 [Accessed May 1, 2014].

Heathman, T.R.J. et al., 2016. Characterization of human mesenchymal stem cells from multiple donors and the implications for large scale bioprocess development. *Biochemical Engineering Journal*, 108, pp.14–23. Available at:

https://www.sciencedirect.com/science/article/pii/S1369703X15300073 [Accessed May 13, 2018].

Heathman, T.R.J. et al., 2016. Scalability and process transfer of mesenchymal stromal cell production from monolayer to microcarrier culture using human platelet lysate. *Cytotherapy*, 18(4), pp.523–535.

Heidemann, J. et al., 2003a. Angiogenic effects of interleukin 8 (CXCL8) in human intestinal microvascular endothelial cells are mediated by CXCR2. *The Journal of biological chemistry*, 278(10), pp.8508–15. Available at: http://www.ncbi.nlm.nih.gov/pubmed/12496258 [Accessed October 28, 2016].

Heidemann, J. et al., 2003b. Angiogenic effects of interleukin 8 (CXCL8) in human intestinal microvascular endothelial cells are mediated by CXCR2. *The Journal of biological chemistry*, 278(10), pp.8508–15. Available at: http://www.ncbi.nlm.nih.gov/pubmed/12496258 [Accessed October 17, 2014].

Heinzelmann, E., 2016. Thematic Platform <I>in vitro</I> Diagnostics Technological Progress with a Powerful Network. *CHIMIA International Journal for Chemistry*, 70(9), pp.662–665. Available at: http://openurl.ingenta.com/content/xref?genre=article&issn=0009-4293&volume=70&issue=9&spage=662 [Accessed November 25, 2016].

Hematti, P. & Keating, A., 2013. *Mesenchymal stromal cells : biology and clinical applications*, Humana Press.

Herbert, S.P. & Stainier, D.Y.R., 2011. Molecular control of endothelial cell behaviour during blood vessel morphogenesis. *Nature reviews. Molecular cell biology*, 12(9), pp.551–64. Available at: http://www.ncbi.nlm.nih.gov/pubmed/21860391 [Accessed October 27, 2016].

Herman, R.A., Scherer, P.N. & Shan, G., 2008. Evaluation of logistic and polynomial models for fitting sandwich-ELISA calibration curves. *Journal of Immunological Methods*, 339(2), pp.245–258.

Herron, G.S. et al., 1986. Secretion of metalloproteinases by stimulated capillary endothelial cells. II. Expression of collagenase and stromelysin activities is regulated by endogenous inhibitors. *The Journal of biological chemistry*, 261(6), pp.2814–8. Available at: http://www.ncbi.nlm.nih.gov/pubmed/3005266 [Accessed May 14, 2018].

Holmes, A., Brown, R. & Shakesheff, K., 2009. Engineering tissue alternatives to animals: applying tissue engineering to basic research and safety testing.

Regenerative medicine, 4, pp.579–92. Available at: http://www.ncbi.nlm.nih.gov/pubmed/19580406.

Hornung, Christian H., † et al., 2007. A Microcapillary Flow Disc Reactor for Organic Synthesis. Available at: http://pubs.acs.org/doi/abs/10.1021/op700015f [Accessed March 5, 2017].

Hourd, P. et al., 2014. Manufacturing models permitting roll out/scale out of clinically led autologous cell therapies: regulatory and scientific challenges for comparability. *Cytotherapy*, 16(8), pp.1033–1047.

Hu, W., Berdugo, C. & Chalmers, J.J., 2011. The potential of hydrodynamic damage to animal cells of industrial relevance: current understanding. *Cytotechnology*, 63(5), pp.445–460. Available at: http://link.springer.com/10.1007/s10616-011-9368-3 [Accessed February 28, 2017].

Huanchun Cui, † et al., 2005. Isoelectric Focusing in a Poly(dimethylsiloxane) Microfluidic Chip.

Huang, J.-H. et al., 2016. Hollow fiber integrated microfluidic platforms for in vitro Co-culture of multiple cell types. *Biomedical Microdevices*, 18(5), p.88. Available at: http://link.springer.com/10.1007/s10544-016-0102-y [Accessed June 25, 2017].

Huh, D. et al., 2012. Microengineered physiological biomimicry: Organs-on-Chips. *Lab on a Chip*, 12(12), p.2156. Available at: http://xlink.rsc.org/?DOI=c2lc40089h [Accessed February 28, 2017].

Huh, D., Hamilton, G.A. & Ingber, D.E., 2011. From 3D cell culture to organs-on-chips. *Trends in Cell Biology*, 21(12), pp.745–754. Available at: http://linkinghub.elsevier.com/retrieve/pii/S0962892411001954 [Accessed March 12, 2017].

Ich, 2009. Q8(R2) Pharmaceutical Development. *Food and Drug Administration*, 8(November), pp.1–29.

Ishak, S.A. et al., 2014. Angiogenesis in tissue engineering: from concept to the vascularization of scaffold construct. *IOP Conference Series: Materials Science and Engineering*, 58(1), p.12015. Available at: http://stacks.iop.org/1757-899X/58/i=1/a=012015?key=crossref.9450e2a4b8b110fe001971151d5d4b6c [Accessed October 24, 2016].

Jiang, S., Liu, S. & Feng, W., 2011. PVA hydrogel properties for biomedical application. *Journal of the mechanical behavior of biomedical materials*, 4(7),

pp.1228–33. Available at: http://www.sciencedirect.com/science/article/pii/S1751616111000786 [Accessed September 2, 2014].

Jin, K. et al., 2002. Vascular endothelial growth factor (VEGF) stimulates neurogenesis in vitro and in vivo. *Proceedings of the National Academy of Sciences of the United States of America*, 99(18), pp.11946–50. Available at: http://www.pnas.org/content/99/18/11946.full [Accessed July 24, 2014].

Jones, D., Mckee, S. & Levine, H.L., 2012. Emerging Challenges in Cell Therapy Manufacturing. *BioProcess International 10(3)*, 10(3), pp.4–7.

Jones, R.N., Fritsche, T.R. & Moet, G.J., 2008. In vitro potency evaluations of various piperacillin/tazobactam generic products compared with the contemporary branded (Zosyn®, Wyeth) formulation. *Diagnostic Microbiology and Infectious Disease*, 61(1), pp.76–79. Available at: http://linkinghub.elsevier.com/retrieve/pii/S0732889307005986 [Accessed March 4, 2017].

Jonsson, B., 1998. The Economic Impact of Diabetes. *Diabetes Care*, 21(Supplement 3).

Jorgensen, C. et al., 2003. Engineering mesenchymal stem cells for immunotherapy. *Gene therapy*, 10(10), pp.928–31. Available at: http://dx.doi.org/10.1038/sj.gt.3302019 [Accessed August 18, 2014].

Jungmann, R. et al., 2014. Multiplexed 3D cellular super-resolution imaging with DNA-PAINT and Exchange-PAINT. *Nature Methods*, 11(3), pp.313–318. Available at: http://www.nature.com/doifinder/10.1038/nmeth.2835 [Accessed February 12, 2017].

K, J., Hsu, S.L. & McCarthy, T.J., 2007. Versatile multilayer thin film preparation using hydrophobic interactions, crystallization, and chemical modification of poly(vinyl alcohol). *Langmuir : the ACS journal of surfaces and colloids*, 23(6), pp.3260–4. Available at: http://www.ncbi.nlm.nih.gov/pubmed/17261054 [Accessed August 20, 2013].

Kaga, T. et al., 2012. Hepatocyte growth factor stimulated angiogenesis without inflammation: differential actions between hepatocyte growth factor, vascular endothelial growth factor and basic fibroblast growth factor. *Vascular pharmacology*, 57(1), pp.3–9. Available at: http://www.sciencedirect.com/science/article/pii/S1537189112000353 [Accessed

October 29, 2014].

Kagawa, Y. et al., 2016. System for measuring oxygen consumption rates of mammalian cells in static culture under hypoxic conditions. *Biotechnology Progress*, 32(1), pp.189–197. Available at: http://doi.wiley.com/10.1002/btpr.2202 [Accessed December 21, 2016].

Kagiwada, H. et al., 2008. Human mesenchymal stem cells as a stabte source of VEGF-producing cells. *Journal of tissue engineering and regenerative medicine*, 2(4), pp.184–9. Available at: http://www.ncbi.nlm.nih.gov/pubmed/18452238 [Accessed October 29, 2014].

Kamei, K. et al., 2013. An integrated microfluidic culture device for quantitative analysis of human embryonic stem cells †. , (i), pp.555–563.

Karle, M. et al., 2016. Microfluidic solutions enabling continuous processing and monitoring of biological samples: A review. *Analytica Chimica Acta*, 929, pp.1–22.

Kellathur, S.N. & Lou, H.-X., 2012. Cell and tissue therapy regulation: worldwide status and harmonization. *Biologicals : journal of the International Association of Biological Standardization*, 40(3), pp.222–4. Available at: http://dx.doi.org/10.1016/j.biologicals.2012.01.004 [Accessed March 19, 2013].

Khademhosseini, A. et al., 2004. Layer-by-layer deposition of hyaluronic acid and poly-L-lysine for patterned cell co-cultures. *Biomaterials*, 25(17), pp.3583–92. Available at: http://www.sciencedirect.com/science/article/pii/S0142961203009475 [Accessed May 14, 2014].

Kiel, M.J. et al., 2005. *SLAM Family Receptors Distinguish Hematopoietic Stem and Progenitor Cells and Reveal Endothelial Niches for Stem Cells*,

Kim, M. et al., 2013. Mesenchymal stem cells for treatment of neurological disorders: a paracrine effect. *Tissue Engineering and Regenerative Medicine*, 10(5), pp.234–245. Available at: http://www.scopus.com/inward/record.url?eid=2-s2.0-84896701313&partnerID=tZOtx3y1 [Accessed October 28, 2014].

Kim, M.S., Yeon, J.H. & Park, J.-K., 2007. A microfluidic platform for 3-dimensional cell culture and cell-based assays. *Biomedical microdevices*, 9(1), pp.25–34. Available at: http://www.ncbi.nlm.nih.gov/pubmed/17103048 [Accessed May 27, 2014].

Kinnaird, T. et al., 2004. Marrow-Derived Stromal Cells Express Genes Encoding a

Broad Spectrum of Arteriogenic Cytokines and Promote In Vitro and In Vivo Arteriogenesis Through Paracrine Mechanisms. *Circulation Research*, 94(5).

Kirouac, D.C. & Zandstra, P.W., 2008. The systematic production of cells for cell therapies. *Cell stem cell*, 3(4), pp.369–81. Available at: http://dx.doi.org/10.1016/j.stem.2008.09.001 [Accessed February 27, 2013].

Kleinman, H.K. & Martin, G.R., 2005. Matrigel: Basement membrane matrix with biological activity. *Seminars in Cancer Biology*, 15(5), pp.378–386. Available at: http://linkinghub.elsevier.com/retrieve/pii/S1044579X05000313 [Accessed March 5, 2017].

Knoepfler, P.S., 2009. Deconstructing stem cell tumorigenicity: a roadmap to safe regenerative medicine. *Stem cells (Dayton, Ohio)*, 27(5), pp.1050–6. Available at: http://www.ncbi.nlm.nih.gov/pubmed/19415771 [Accessed December 5, 2016].

Knoepfler, P.S., 2015. From bench to FDA to bedside: US regulatory trends for new stem cell therapies. *Advanced Drug Delivery Reviews*, 82, pp.192–196.

Kong, F. et al., 2012. Automatic Liquid Handling for Life Science. *Journal of Laboratory Automation*, 17(3), pp.169–185. Available at: http://journals.sagepub.com/doi/10.1177/2211068211435302 [Accessed January 11, 2017].

Konstantinidis, S., Kong, S. & Titchener-Hooker, N., 2013. Identifying analytics for high throughput bioprocess development studies. *Biotechnology and Bioengineering*, 110(7), pp.1924–1935. Available at: http://doi.wiley.com/10.1002/bit.24850 [Accessed November 25, 2016].

Kozlov, M. et al., 2003. Adsorption of poly(vinyl alcohol) onto hydrophobic substrates. A general approach for hydrophilizing and chemically activating surfaces. *Macromolecules*, 36(16). Available at: http://scholarworks.umass.edu/pse_faculty_pubs/705 [Accessed July 25, 2013].

Kozlov, M. & McCarthy, T.J., 2004. Adsorption of poly(vinyl alcohol) from water to a hydrophobic surface: effects of molecular weight, degree of hydrolysis, salt, and temperature. *Langmuir : the ACS journal of surfaces and colloids*, 20(21), pp.9170–6. Available at: http://dx.doi.org/10.1021/la0492299 [Accessed August 20, 2013].

Krampera, M. et al., 2013. Immunological characterization of multipotent mesenchymal stromal cells--The International Society for Cellular Therapy

(ISCT) working proposal. *Cytotherapy*, 15(9), pp.1054–61. Available at: http://www.ncbi.nlm.nih.gov/pubmed/23602578 [Accessed January 30, 2014].

Krock, B.L., Skuli, N. & Simon, M.C., 2011. Hypoxia-induced angiogenesis: good and evil. *Genes & cancer*, 2(12), pp.1117–33. Available at: http://gan.sagepub.com/content/2/12/1117.full [Accessed October 1, 2014].

Kurlander, R.J. et al., 2006. A functional comparison of mature human dendritic cells prepared in fluorinated ethylene-propylene bags or polystyrene flasks. *Transfusion*, 46(9), pp.1494–504. Available at: http://www.ncbi.nlm.nih.gov/pubmed/16965575 [Accessed June 21, 2014].

Kwok, D.Y. et al., 1997. Contact Angle Measurements and Contact Angle Interpretation. 1. Contact Angle Measurements by Axisymmetric Drop Shape Analysis and a Goniometer Sessile Drop Technique. *Langmuir*, 13(10), pp.2880–2894. Available at: http://dx.doi.org/10.1021/la9608021 [Accessed October 7, 2013].

Kwon, H.M. et al., 2014a. Multiple paracrine factors secreted by mesenchymal stem cells contribute to angiogenesis. *Vascular Pharmacology*, 63(1), pp.19–28.

Kwon, H.M. et al., 2014b. Multiple paracrine factors secreted by mesenchymal stem cells contribute to angiogenesis. *Vascular pharmacology*, 63(1), pp.19–28. Available at: http://www.sciencedirect.com/science/article/pii/S1537189114001104 [Accessed October 29, 2014].

Lampin, M. et al., 1997. Correlation between substratum roughness and wettability, cell adhesion, and cell migration. *Journal of biomedical materials research*, 36(1), pp.99–108. Available at: http://www.ncbi.nlm.nih.gov/pubmed/9212394 [Accessed October 14, 2013].

Ledford, H., 2016. Boom in unproven cell therapies intensifies regulatory debate. *Nature*, 537(7619), pp.148–148. Available at: http://www.nature.com/doifinder/10.1038/537148a [Accessed December 6, 2016].

Lee, A.S. et al., 2013. Tumorigenicity as a clinical hurdle for pluripotent stem cell therapies. *Nature Medicine*, 19(8), pp.998–1004. Available at: http://www.nature.com/doifinder/10.1038/nm.3267 [Accessed February 25, 2017].

Lehman, N. et al., 2012. Development of a surrogate angiogenic potency assay for

clinical-grade stem cell production. *Cytotherapy*, 14(8), pp.994–1004. Available at: http://www.ncbi.nlm.nih.gov/pubmed/22687190 [Accessed November 17, 2014].

Levy, N., 2012. The Use of Animal as Models: Ethical Considerations. *International Journal of Stroke*, 7(5), pp.440–442. Available at: http://www.ncbi.nlm.nih.gov/pubmed/22712743 [Accessed May 14, 2018].

Li, A. et al., 2003. IL-8 directly enhanced endothelial cell survival, proliferation, and matrix metalloproteinases production and regulated angiogenesis. *Journal of immunology (Baltimore, Md. : 1950)*, 170(6), pp.3369–76. Available at: http://www.ncbi.nlm.nih.gov/pubmed/12626597 [Accessed October 27, 2016].

Li, B. et al., 2013. Mesenchymal stem cells exploit extracellular matrix as mechanotransducer. *Scientific reports*, 3, p.2425. Available at: http://www.nature.com/srep/2013/130813/srep02425/full/srep02425.html [Accessed May 12, 2015].

Li, F. et al., 2010. Cell culture processes for monoclonal antibody production. *mAbs*, 2(5), pp.466–479. Available at: http://www.tandfonline.com/doi/abs/10.4161/mabs.2.5.12720 [Accessed February 26, 2017].

Li, H. et al., 2008. Mesenchymal Stem Cells Alter Migratory Property of T and Dendritic Cells to Delay the Development of Murine Lethal Acute Graft-Versus-Host Disease. *STEM CELLS*, 26(10), pp.2531–2541. Available at: http://doi.wiley.com/10.1634/stemcells.2008-0146 [Accessed March 4, 2017].

Liang, X. et al., 2014. Paracrine mechanisms of mesenchymal stem cell-based therapy: current status and perspectives. *Cell transplantation*, 23(9), pp.1045–59. Available at: http://www.ncbi.nlm.nih.gov/pubmed/23676629 [Accessed April 20, 2016].

Lieu, C., Heymach, J. & Overman, M., 2011. Beyond VEGF : Inhibition of the Fibroblast Growth Factor Pathway and Antiangiogenesis Beyond VEGF : Inhibition of the Fibroblast Growth Factor Pathway and Antiangiogenesis. *Clinical Cancer Research*, 17(19), pp.6130–6139.

Lim, M. et al., 2007. Intelligent bioprocessing for haemotopoietic cell cultures using monitoring and design of experiments. *Biotechnology advances*, 25(4), pp.353–68. Available at: http://dx.doi.org/10.1016/j.biotechadv.2007.02.002 [Accessed March 10, 2013].

Lindvall, O., Kokaia, Z. & Martinez-Serrano, A., 2004. Stem cell therapy for human neurodegenerative disorders–how to make it work. *Nature Medicine*, 10(7), pp.S42–S50. Available at: http://www.nature.com/doifinder/10.1038/nm1064 [Accessed December 1, 2016].

Lipowska-Bhalla, G. et al., 2012. Targeted immunotherapy of cancer with CAR T cells: achievements and challenges. *Cancer Immunology, Immunotherapy*, 61(7), pp.953–962. Available at: http://link.springer.com/10.1007/s00262-012-1254-0 [Accessed December 1, 2016].

Liu Tsang, V. et al., 2007. Fabrication of 3D hepatic tissues by additive photopatterning of cellular hydrogels. *FASEB journal : official publication of the Federation of American Societies for Experimental Biology*, 21(3), pp.790–801. Available at: http://www.fasebj.org/content/21/3/790.short [Accessed November 27, 2012].

Lu, L.-L. et al., 2006. Isolation and characterization of human umbilical cord mesenchymal stem cells with hematopoiesis-supportive function and other potentials. *Haematologica*, 91(8), pp.1017–26. Available at: http://www.ncbi.nlm.nih.gov/pubmed/16870554 [Accessed April 8, 2017].

Ma, M., Tudan, C. & Koltchev, D., 2015. The 10th Annual Bioassays and Bioanalytical Method Development Conference. *Bioanalysis*, 7(5), pp.569–72. Available at: http://www.future-science.com/doi/full/10.4155/bio.14.319 [Accessed May 10, 2016].

Ma, Q. et al., 1998. Impaired B-lymphopoiesis, myelopoiesis, and derailed cerebellar neuron migration in CXCR4- and SDF-1-deficient mice. *Proceedings of the National Academy of Sciences of the United States of America*, 95(16), pp.9448–53. Available at: http://www.ncbi.nlm.nih.gov/pubmed/9689100 [Accessed March 4, 2017].

Maciulaitis, R. et al., 2012. Clinical Development of Advanced Therapy Medicinal Products in Europe: Edidence That Regulators Must Be Proactive. *The American Society of Gene & Cell Therapy*, 20(3), pp.479–482.

Mallinger, R., Geleff, S. & Böck, P., 1986. Histochemistry of glycosaminoglycans in cartilage ground substance. Alcian-blue staining and lectin-binding affinities in semithin Epon sections. *Histochemistry*, 85(2), pp.121–7. Available at: http://www.ncbi.nlm.nih.gov/pubmed/3744895 [Accessed May 13, 2018].

Martinez, A.W., 2011. Microfluidic paper-based analytical devices: from POCKET to

paper-based ELISA. *Bioanalysis*, 3(23), pp.2589–2592. Available at: http://www.future-science.com/doi/10.4155/bio.11.258 [Accessed March 4, 2017].

Mason, C. et al., 2011. Cell therapy industry: billion dollar global business with unlimited potential. *Regenerative medicine*, 6(3), pp.265–72. Available at: http://www.futuremedicine.com/doi/abs/10.2217/rme.11.28 [Accessed April 4, 2016].

Mason, C. & Dunnill, P., 2008. A brief definition of regenerative medicine. *Regenerative medicine*, 3(1), pp.1–5. Available at: http://www.futuremedicine.com/doi/full/10.2217/17460751.3.1.1 [Accessed July 3, 2014].

Mattila, P.K. & Lappalainen, P., 2008. Filopodia: molecular architecture and cellular functions. *Nature Reviews Molecular Cell Biology*, 9(6), pp.446–454. Available at: http://www.nature.com/doifinder/10.1038/nrm2406 [Accessed October 27, 2016].

Medina Benavente, J.J. et al., 2014. Evaluation of Silicon Nitride as a Substrate for Culture of PC12 Cells: An Interfacial Model for Functional Studies in Neurons W. Lam, ed. *PLoS ONE*, 9(2), p.e90189. Available at: http://dx.plos.org/10.1371/journal.pone.0090189 [Accessed June 25, 2017].

Mendicino, M. et al., 2014. MSC-based product characterization for clinical trials: an FDA perspective. *Cell stem cell*, 14(2), pp.141–5. Available at: http://www.ncbi.nlm.nih.gov/pubmed/24506881 [Accessed May 14, 2018].

Miao, T. et al., 2015. Physically crosslinked polyvinyl alcohol and gelatin interpenetrating polymer network theta-gels for cartilage regeneration. *J. Mater. Chem. B*, 3(48), pp.9242–9249. Available at: http://xlink.rsc.org/?DOI=C5TB00989H [Accessed July 18, 2016].

Mirotsou, M. et al., 2011. Paracrine mechanisms of stem cell reparative and regenerative actions in the heart. *Journal of Molecular and Cellular Cardiology*, 50(2), pp.280–289. Available at: http://linkinghub.elsevier.com/retrieve/pii/S0022282810002920 [Accessed June 25, 2017].

Mogensen, K.B. & Kutter, J.P., 2009. Optical detection in microfluidic systems. *ELECTROPHORESIS*, 30(S1), pp.S92–S100. Available at: http://doi.wiley.com/10.1002/elps.200900101 [Accessed November 25, 2016].

Moises, S.S. & Schäferling, M., 2009. Toxin immunosensors and sensor arrays for food quality control. *Bioanalytical Reviews*, 1(1), pp.73–104. Available at: http://link.springer.com/10.1007/s12566-009-0006-x [Accessed March 5, 2017].

Morgenstern, D.A. et al., 2017. Developing quality assurance for pediatric autologous stem cell transplants in England: results of a 3-year national audit of activity and engraftment by treatment centre. *Bone Marrow Transplantation*. Available at: http://www.nature.com/doifinder/10.1038/bmt.2017.32 [Accessed April 29, 2017].

Morgenstern, D.A. et al., 2016. Post-thaw viability of cryopreserved peripheral blood stem cells (PBSC) does not guarantee functional activity: important implications for quality assurance of stem cell transplant programmes. *British Journal of Haematology*, 174(6), pp.942–951. Available at: http://doi.wiley.com/10.1111/bjh.14160 [Accessed May 1, 2017].

Murakami, M. et al., 2011. FGF-dependent regulation of VEGF receptor 2 expression in mice. *The Journal of clinical investigation*, 121(7), pp.2668–78. Available at: http://www.ncbi.nlm.nih.gov/pubmed/21633168 [Accessed October 28, 2016].

Myers, F.B. & Lee, L.P., 2008. Innovations in optical microfluidic technologies for point-of-care diagnostics. *Lab on a Chip*, 8(12), p.2015. Available at: http://xlink.rsc.org/?DOI=b812343h [Accessed November 25, 2016].

N.L.Davie, C.Mason, D.A.Brindley, E.J.C.-S., 2012. Streamlining Cell Therapy Manufacture - Cell Therapies - BioProcess International. *BioProcess International*, 10(3), pp.24–28. Available at: http://www.bioprocessintl.com/journal/supplements/2012/March/Streamlining-Cell-Therapy-Manufacture-328083 [Accessed April 29, 2013].

Nakatsu, M.N. et al., 2003. Angiogenic sprouting and capillary lumen formation modeled by human umbilical vein endothelial cells (HUVEC) in fibrin gels: the role of fibroblasts and Angiopoietin-1☆. *Microvascular Research*, 66(2), pp.102–112. Available at: http://www.sciencedirect.com/science/article/pii/S0026286203000451 [Accessed September 25, 2014].

Neufeld, G. & Kessler, O., 2006. Pro-angiogenic cytokines and their role in tumor angiogenesis. *Cancer metastasis reviews*, 25(3), pp.373–85. Available at: http://www.ncbi.nlm.nih.gov/pubmed/17006765 [Accessed October 31, 2014].

Novo, P., Chu, V. & Conde, J.P., 2014. Integrated optical detection of autonomous capillary microfluidic immunoassays:a hand-held point-of-care prototype. *Biosensors and Bioelectronics*, 57, pp.284–291.

Nunnari, J.J. et al., 1989. Quantitation of oil red O staining of the aorta in hypercholesterolemic rats. *Experimental and Molecular Pathology*, 51(1), pp.1–8. Available at: https://www.sciencedirect.com/science/article/abs/pii/0014480089900026 [Accessed May 13, 2018].

Ocampo, A., Lum, S. & Chow, F., 2007. Current challenges for FDA-regulated bioanalytical laboratories for human (BA/BE) studies. Part I: defining the appropriate compliance standards – application of the principles of FDA GLP and FDA GMP to bioanalytical laboratories. *The Quality Assurance Journal*, 11(1), pp.3–15. Available at: http://doi.wiley.com/10.1002/qaj.399 [Accessed May 10, 2016].

Oh, S.K.W. & Choo, A.B.H., 2006. Human embryonic stem cells: technological challenges towards therapy. *Clinical and experimental pharmacology & physiology*, 33(5–6), pp.489–95. Available at: http://www.ncbi.nlm.nih.gov/pubmed/16700884 [Accessed April 28, 2013].

Ohno, K., Tachikawa, K. & Manz, A., 2008. Microfluidics: Applications for analytical purposes in chemistry and biochemistry. *ELECTROPHORESIS*, 29(22), pp.4443–4453. Available at: http://doi.wiley.com/10.1002/elps.200800121 [Accessed June 15, 2016].

Ornitz, D.M. et al., 1996. Receptor specificity of the fibroblast growth factor family. *The Journal of biological chemistry*, 271(25), pp.15292–7. Available at: http://www.ncbi.nlm.nih.gov/pubmed/8663044 [Accessed October 25, 2016].

Ornitz, D.M. & Itoh, N., 2015. The Fibroblast Growth Factor signaling pathway. *Wiley interdisciplinary reviews. Developmental biology*, 4(3), pp.215–66. Available at: http://www.ncbi.nlm.nih.gov/pubmed/25772309 [Accessed October 25, 2016].

Paguirigan, A.L. et al., 2010. Expanding the available assays: adapting and validating In-Cell Westerns in microfluidic devices for cell-based assays. *Assay and drug development technologies*, 8(5), pp.591–601. Available at: http://www.pubmedcentral.nih.gov/articlerender.fcgi?artid=2957247&tool=pmcentrez&rendertype=abstract [Accessed July 23, 2015].

Pal, R. et al., 2012. Comparative analysis of cardiomyocyte differentiation from human embryonic stem cells under 3-D and 2-D culture conditions. *Journal of bioscience and bioengineering*, null(null). Available at: http://dx.doi.org/10.1016/j.jbiosc.2012.08.018 [Accessed November 10, 2012].

Palomares, L.A. & Ramírez, O.T., 2009. Bioreactor Scale-Up. In *Encyclopedia of Industrial Biotechnology*. Hoboken, NJ, USA: John Wiley & Sons, Inc. Available at: http://doi.wiley.com/10.1002/9780470054581.eib143 [Accessed December 21, 2016].

Park, C.W. et al., 2009. Cytokine secretion profiling of human mesenchymal stem cells by antibody array. *International journal of stem cells*, 2(1), pp.59–68. Available at: http://www.pubmedcentral.nih.gov/articlerender.fcgi?artid=4021795&tool=pmcentrez&rendertype=abstract [Accessed November 12, 2014].

Pearce, K.F. et al., 2014. Regulation of advanced therapy medicinal products in Europe and the role of academia. *Cytotherapy*, 16(3), pp.289–97. Available at: http://linkinghub.elsevier.com/retrieve/pii/S1465324913006713 [Accessed December 6, 2016].

Pellegrini, G. et al., 2014. Concise Review: Hurdles in a Successful Example of Limbal Stem Cell-based Regenerative Medicine. *STEM CELLS*, 32(1), pp.26–34. Available at: http://doi.wiley.com/10.1002/stem.1517 [Accessed February 25, 2017].

Pérez-Simon, J.A. et al., 2011. Mesenchymal stem cells expanded in vitro with human serum for the treatment of acute and chronic graft-versus-host disease: results of a phase I/II clinical trial. *Haematologica*, 96(7), pp.1072–6. Available at: http://www.ncbi.nlm.nih.gov/pubmed/21393326 [Accessed March 4, 2017].

Petzelbauer, P. et al., 1995. IL-8 and angiogenesis: evidence that human endothelial cells lack receptors and do not respond to IL-8 in vitro. *Cytokine*, 7(3), pp.267–72. Available at: http://www.sciencedirect.com/science/article/pii/S1043466685700312 [Accessed November 17, 2014].

Pfeifer, A. & Verma, I.M., 2003. GENE THERAPY: Promises and Problems. Available at: http://www.annualreviews.org/doi/abs/10.1146/annurev.genom.2.1.177 [Accessed July 3, 2014].

Pham, C.D. et al., 2014. Development of a Luminex-based multiplex assay for detection of mutations conferring resistance to Echinocandins in Candida glabrata. *Journal of clinical microbiology*, 52(3), pp.790–5. Available at: http://www.ncbi.nlm.nih.gov/pubmed/24353003 [Accessed March 5, 2017].

Pihl, J. et al., 2005. Microfluidics for cell-based assays. *Materials Today*, 8(12), pp.46–51. Available at: http://www.sciencedirect.com/science/article/pii/S1369702105712244 [Accessed June 21, 2014].

Pittenger, M.F., 1999. Multilineage Potential of Adult Human Mesenchymal Stem Cells. *Science*, 284(5411), pp.143–147. Available at: http://www.sciencemag.org/content/284/5411/143.abstract [Accessed May 23, 2013].

Plagnol, A.C. et al., 2009. Industry perceptions of barriers to commercialization of regenerative medicine products in the UK. *Regenerative medicine*, 4(4), pp.549–59. Available at: http://www.futuremedicine.com/doi/abs/10.2217/rme.09.21 [Accessed June 23, 2014].

Potier, E. et al., 2007. Hypoxia affects mesenchymal stromal cell osteogenic differentiation and angiogenic factor expression. *Bone*, 40(4), pp.1078–87. Available at: http://www.sciencedirect.com/science/article/pii/S8756328206008520 [Accessed October 22, 2014].

Presta, M. et al., 2005. Fibroblast growth factor/fibroblast growth factor receptor system in angiogenesis. *Cytokine & growth factor reviews*, 16(2), pp.159–78. Available at: http://www.ncbi.nlm.nih.gov/pubmed/15863032 [Accessed October 25, 2016].

Preti, R.A., 2005. Bringing safe and effective cell therapies to the bedside. *Nature Biotechnology*, 23(7), pp.801–804. Available at: http://www.nature.com/doifinder/10.1038/nbt0705-801 [Accessed May 28, 2017].

Pruszak, J. et al., 2007. Markers and methods for cell sorting of human embryonic stem cell-derived neural cell populations. *Stem cells (Dayton, Ohio)*, 25(9), pp.2257–68. Available at: http://www.pubmedcentral.nih.gov/articlerender.fcgi?artid=2238728&tool=pmcentrez&rendertype=abstract [Accessed May 21, 2013].

Rafiq, Q.A., Coopman, K., et al., 2013. A quantitative approach for understanding small-scale human mesenchymal stem cell culture - implications for large-scale bioprocess development. *Biotechnology journal*, 8(4), pp.459–71. Available at: http://www.ncbi.nlm.nih.gov/pubmed/23447369 [Accessed September 16, 2014].

Rafiq, Q.A., Brosnan, K.M., et al., 2013. Culture of human mesenchymal stem cells on microcarriers in a 5 l stirred-tank bioreactor. *Biotechnology letters*, 35(8), pp.1233–45. Available at: http://www.ncbi.nlm.nih.gov/pubmed/23609232 [Accessed January 20, 2014].

Rafiq, Q.A. et al., 2018. Qualitative and quantitative demonstration of bead-to-bead transfer with bone marrow-derived human mesenchymal stem cells on microcarriers: Utilising the phenomenon to improve culture performance. *Biochemical Engineering Journal*, 135, pp.11–21. Available at: http://linkinghub.elsevier.com/retrieve/pii/S1369703X17303121 [Accessed May 13, 2018].

Raica, M. & Cimpean, A.M., 2010. Platelet-Derived Growth Factor (PDGF)/PDGF Receptors (PDGFR) Axis as Target for Antitumor and Antiangiogenic Therapy. *Pharmaceuticals*, 3(3), pp.572–599. Available at: http://www.mdpi.com/1424-8247/3/3/572/ [Accessed October 28, 2016].

Ranganath, S.H. et al., 2012. Harnessing the Mesenchymal Stem Cell Secretome for the Treatment of Cardiovascular Disease. *Cell Stem Cell*, 10(3), pp.244–258.

Ranganath, S.H. et al., 2012. Harnessing the mesenchymal stem cell secretome for the treatment of cardiovascular disease. *Cell stem cell*, 10(3), pp.244–58. Available at: http://www.sciencedirect.com/science/article/pii/S193459091200063X [Accessed July 11, 2014].

Rascón, C., Parry, A.O. & Aarts, D.G.A.L., 2016. Geometry-induced capillary emptying. *Proceedings of the National Academy of Sciences*, 113(45), pp.12633–12636. Available at: http://www.pnas.org/lookup/doi/10.1073/pnas.1606217113 [Accessed January 17, 2017].

Rasini, V. et al., 2013. Mesenchymal stromal/stem cells markers in the human bone marrow. *Cytotherapy*, 15(3), pp.292–306. Available at: http://www.ncbi.nlm.nih.gov/pubmed/23312449 [Accessed January 30, 2014].

Ratcliffe, E., Thomas, R.J. & Williams, D.J., 2011. Current understanding and challenges in bioprocessing of stem cell-based therapies for regenerative

medicine. *British medical bulletin*, 100(1), pp.137–55. Available at: http://www.researchgate.net/publication/51581405_Current_understanding_and_ challenges_in_bioprocessing_of_stem_cell-

based_therapies_for_regenerative_medicine [Accessed October 13, 2015].

Rayment, E.A. & Williams, D.J., 2010. Mind the Gap: Challenges in Characterising and Quantifying Cell- and Tissue-Based Therapies for Clinical Translation. *STEM CELLS*, 28(5), p.N/A-N/A. Available at: http://doi.wiley.com/10.1002/stem.416 [Accessed December 23, 2016].

Read, E.K. et al., 2010. Process analytical technology (PAT) for biopharmaceutical products: Part I. concepts and applications. *Biotechnology and Bioengineering*, 105(2), pp.276–284. Available at: http://doi.wiley.com/10.1002/bit.22528 [Accessed December 20, 2016].

Rehman, A.O. & Wang, C.-Y., 2006. Notch signaling in the regulation of tumor angiogenesis. *Trends in Cell Biology*, 16(6), pp.293–300. Available at: https://www.sciencedirect.com/science/article/pii/S0962892406001164 [Accessed May 14, 2018].

Reilly, G.C., 2010. Intrinsic extracellular matrix properties regulate stem cell differentiation. *Journal of Biomechanics*, 43(1), pp.55–62.

Reis, N.M. et al., 2016. Lab on a Stick: Multi-Analyte Cellular Assays in a Microfluidic Dipstick. *Lab Chip*. Available at: http://pubs.rsc.org/en/Content/ArticleLanding/2016/LC/C6LC00332J [Accessed June 30, 2016].

Reisman, M. & Adams, K.T., 2014. Stem cell therapy: a look at current research, regulations, and remaining hurdles. *P & T : a peer-reviewed journal for formulary management*, 39(12), pp.846–57. Available at: http://www.ncbi.nlm.nih.gov/pubmed/25516694 [Accessed December 6, 2016].

Richarz, N.A., Boada, A. & Carrascosa, J.M., 2017. Angiogenesis in Dermatology – Insights of Molecular Mechanisms and Latest Developments. *Actas Dermo-Sifiliográficas*. Available at: http://linkinghub.elsevier.com/retrieve/pii/S0001731017300108 [Accessed March 5, 2017].

Ritter, N.M., 2011. Distinctions Between Analytical and Bioanalytical Test Methods. *Bioprocess International*. Available at: http://www.bioprocessintl.com/analytical/downstream-validation/distinctions-

between-analytical-and-bioanalytical-test-methods-312823/ [Accessed December 14, 2016].

Roda, A. et al., 2018. Advanced bioanalytics for precision medicine. *Analytical and Bioanalytical Chemistry*, 410(3), pp.669–677. Available at: http://link.springer.com/10.1007/s00216-017-0660-8 [Accessed May 13, 2018].

Romanyshyn, L., Tiller, P.R. & Hop, C.E.C.A., 2000. Bioanalytical applications of ?fast chromatography? to high-throughput liquid chromatography/tandem mass spectrometric quantitation. *Rapid Communications in Mass Spectrometry*, 14(18), pp.1662–1668. Available at: http://doi.wiley.com/10.1002/1097-0231%2820000930%2914%3A18%3C1662%3A%3AAID-RCM77%3E3.0.CO%3B2-N [Accessed February 26, 2017].

Rosano, J.M. et al., 2012. Targeted Delivery of VEGF after a Myocardial Infarction Reduces Collagen Deposition and Improves Cardiac Function. *Cardiovascular engineering and technology*, 3(2), pp.237–247. Available at: http://www.pubmedcentral.nih.gov/articlerender.fcgi?artid=3405981&tool=pmcentrez&rendertype=abstract [Accessed October 29, 2014].

Rosová, I. et al., 2008. Hypoxic preconditioning results in increased motility and improved therapeutic potential of human mesenchymal stem cells. *Stem cells (Dayton, Ohio)*, 26(8), pp.2173–82. Available at: http://www.pubmedcentral.nih.gov/articlerender.fcgi?artid=3017477&tool=pmcentrez&rendertype=abstract [Accessed October 14, 2014].

Rosset, P., Deschaseaux, F. & Layrolle, P., 2014. Cell therapy for bone repair. *Orthopaedics & Traumatology: Surgery & Research*, 100(1), pp.S107–S112.

Rosso, F. et al., 2004. From cell-ECM interactions to tissue engineering. *Journal of cellular physiology*, 199(2), pp.174–80. Available at: http://www.ncbi.nlm.nih.gov/pubmed/15039999 [Accessed April 28, 2014].

Russ, J.C., 2011. *The image processing handbook*, CRC Press. Available at: https://www.crcpress.com/The-Image-Processing-Handbook-Sixth-Edition/Russ/p/book/9781439840450 [Accessed March 12, 2017].

Russo, V. et al., 2014. Mesenchymal stem cell delivery strategies to promote cardiac regeneration following ischemic injury. *Biomaterials*, 35(13), pp.3956–74. Available at: http://www.sciencedirect.com/science/article/pii/S0142961214001197 [Accessed September 12, 2014].

Ryan, J.A., 2008. Evolution of Cell Culture Surfaces. *BioFiles*, pp.8–11.

Scheper, T. et al., 1999. Bioanalytics: detailed insight into bioprocesses. *Analytica Chimica Acta*, 400(1–3), pp.121–134. Available at: http://www.sciencedirect.com/science/article/pii/S0003267099006121 [Accessed September 21, 2015].

Schmitt, S.C. et al., 2008. Comparative in vitro study of the proliferation and growth of ovine osteoblast-like cells on various alloplastic biomaterials manufactured for augmentation and reconstruction of tissue or bone defects. *Journal of Materials Science: Materials in Medicine*, 19(3), pp.1441–1450. Available at: http://www.ncbi.nlm.nih.gov/pubmed/17914632 [Accessed May 13, 2018].

Schneider, F. et al., 2009. Process and material properties of polydimethylsiloxane (PDMS) for Optical MEMS. *Sensors and Actuators A: Physical*, 151(2), pp.95–99.

Shah, N., Morsi, Y. & Manasseh, R., 2014. From mechanical stimulation to biological pathways in the regulation of stem cell fate. *Cell biochemistry and function*, 32(4), pp.309–25. Available at: http://www.ncbi.nlm.nih.gov/pubmed/24574137 [Accessed June 22, 2015].

Shan, C. et al., 2009a. Water-Soluble Graphene Covalently Functionalized by Biocompatible Poly- l -lysine. *Langmuir*, 25(20), pp.12030–12033.

Shan, C. et al., 2009b. Water-Soluble Graphene Covalently Functionalized by Biocompatible Poly- l -lysine. *Langmuir*, 25(20), pp.12030–12033. Available at: http://pubs.acs.org/doi/abs/10.1021/la903265p [Accessed January 29, 2017].

Sharma, R. et al., 2010. Three-dimensional culture of human embryonic stem cell derived hepatic endoderm and its role in bioartificial liver construction. *Journal of biomedicine & biotechnology*, 2010, p.236147. Available at: http://www.hindawi.com/journals/jbb/2010/236147/abs/ [Accessed November 24, 2012].

Shibuya, M., 2009. Unique signal transduction of the VEGF family members VEGF-A and VEGF-E. *Biochemical Society Transactions*, 37(6).

Shibuya, M., 2011. Vascular Endothelial Growth Factor (VEGF) and Its Receptor (VEGFR) Signaling in Angiogenesis: A Crucial Target for Anti- and Pro-Angiogenic Therapies. *Genes & cancer*, 2(12), pp.1097–105. Available at: http://www.ncbi.nlm.nih.gov/pubmed/22866201 [Accessed October 28, 2016].

Shikada, Y. et al., 2005. Platelet-Derived Growth Factor-AA Is an Essential and

Autocrine Regulator of Vascular Endothelial Growth Factor Expression in Non–Small Cell Lung Carcinomas. *Cancer Research*, 65(16).

Shin, T.-H. et al., 2017. Mesenchymal Stem Cell Therapy for Inflammatory Skin Diseases: Clinical Potential and Mode of Action. *International Journal of Molecular Sciences*, 18(2), p.244. Available at: http://www.mdpi.com/1422-0067/18/2/244 [Accessed February 15, 2017].

Shoichet, M.S. & McCarthy, T.J., 1991. Surface modification of poly(tetrafluoroethylene-co-hexafluoropropylene) film by adsorption of poly(L-lysine) from aqueous solution. *Macromolecules*, 24(6), pp.1441–1442. Available at: http://dx.doi.org/10.1021/ma00006a041 [Accessed March 20, 2014].

Simaria, A.S. et al., 2014. Allogeneic cell therapy bioprocess economics and optimization: single-use cell expansion technologies. *Biotechnology and bioengineering*, 111(1), pp.69–83. Available at: http://www.ncbi.nlm.nih.gov/pubmed/23893544 [Accessed December 21, 2016].

Song, W.K. et al., 2015. Treatment of macular degeneration using embryonic stem cell-derived retinal pigment epithelium: preliminary results in Asian patients. *Stem cell reports*, 4(5), pp.860–72. Available at: http://www.ncbi.nlm.nih.gov/pubmed/25937371 [Accessed February 26, 2017].

Sonnaert, M. et al., 2015. Quantitative Validation of the Presto Blue[TM] Metabolic Assay for Online Monitoring of Cell Proliferation in a 3D Perfusion Bioreactor System. *Tissue Engineering Part C: Methods*, 21(6), pp.519–529.

Spellman, S. et al., 2011. Guidelines for the development and validation of new potency assays for the evaluation of umbilical cord blood. *Cytotherapy*, 13(7), pp.848–855. Available at: http://linkinghub.elsevier.com/retrieve/pii/S1465324911705655 [Accessed March 4, 2017].

Strafford, N., 1936. Colorimetric analysis by the photo-electric cell. *The Analyst*, 61(720), p.170. Available at: http://xlink.rsc.org/?DOI=an9366100170 [Accessed May 1, 2018].

Suna Wang, Y.Z. et al., 2015. Clinical Trials Using Cell-based Therapy in Ischemic Heart Diseases - A Decade's Efforts. *Journal of Vascular Medicine & Surgery*, 3(1), p. Available at: http://www.esciencecentral.org/journals/clinical-trials-using-cellbased-therapy-in-ischemic-heart-diseases-a-decades-efforts-2329-6925.1000174.php?aid=40497 [Accessed December 5, 2016].

T.Dall, S.Edge Mann, Y. Zhang, J.Martin, Y.Chen, and P. & Hogan, 2008. Economic Costs of Diabetes in the U.S. in 2007. *Diabetes Care*, 31(3).

Takahashi, K. et al., 2007. Induction of pluripotent stem cells from adult human fibroblasts by defined factors. *Cell*, 131(5), pp.861–72. Available at: http://www.cell.com/fulltext/S0092-8674(07)01471-7 [Accessed September 16, 2013].

Tarakanova, Y.N. et al., 2015. Effect of pH of adsorption buffers on the number and antigen-binding activity of monoclonal antibodies immobilized on the surface of polystyrene microplates. *Applied Biochemistry and Microbiology*, 51(4), pp.462–469. Available at: http://link.springer.com/10.1134/S0003683815040158 [Accessed January 11, 2017].

Thomas, R.J. et al., 2007. Manufacture of a human mesenchymal stem cell population using an automated cell culture platform. *Cytotechnology*, 55(1), pp.31–9. Available at: http://www.ncbi.nlm.nih.gov/pubmed/19002992 [Accessed December 4, 2016].

Titmarsh, D.M. et al., 2014. Concise review: microfluidic technology platforms: poised to accelerate development and translation of stem cell-derived therapies. *Stem cells translational medicine*, 3(1), pp.81–90. Available at: http://stemcellstm.alphamedpress.org/content/3/1/81.full [Accessed March 21, 2016].

Toma, J.G. et al., 2001. Isolation of multipotent adult stem cells from the dermis of mammalian skin. *Nature cell biology*, 3(9), pp.778–84. Available at: http://dx.doi.org/10.1038/ncb0901-778 [Accessed May 7, 2014].

Toriello, N.M. et al., 2008. Integrated microfluidic bioprocessor for single-cell gene expression analysis. *Proceedings of the National Academy of Sciences of the United States of America*, 105(51), pp.20173–8. Available at: http://www.ncbi.nlm.nih.gov/pubmed/19075237 [Accessed March 5, 2017].

Tran, C. & Damaser, M.S., 2014. Stem cells as drug delivery methods: Application of stem cell secretome for regeneration. *Advanced Drug Delivery Reviews*. Available at: http://www.sciencedirect.com/science/article/pii/S0169409X14002154 [Accessed October 29, 2014].

Trappmann, B. et al., 2012. Extracellular-matrix tethering regulates stem-cell fate. *Nature materials*, 11(7), pp.642–9. Available at:

http://dx.doi.org/10.1038/nmat3339 [Accessed February 19, 2015].

Trounson, A. et al., 2011. Clinical trials for stem cell therapies. *BMC medicine*, 9(1), p.52. Available at: http://www.biomedcentral.com/1741-7015/9/52 [Accessed June 16, 2014].

Tunceli, K. et al., 2005. The Impact of Diabetes on Employment and Work Productivity. *Diabetes Care*, 28(11).

Turner, L., 2015. US stem cell clinics, patient safety, and the FDA. *Trends in Molecular Medicine*, 21(5), pp.271–273.

Turner, M.D. et al., 2014. Cytokines and chemokines: At the crossroads of cell signalling and inflammatory disease. *Biochimica et Biophysica Acta (BBA) - Molecular Cell Research*, 1843(11), pp.2563–2582.

Uccelli, A., Moretta, L. & Pistoia, V., 2008. Mesenchymal stem cells in health and disease. *Nature reviews. Immunology*, 8(9), pp.726–36. Available at: http://dx.doi.org/10.1038/nri2395 [Accessed July 13, 2014].

Ullah, M. et al., 2012. A reliable protocol for the isolation of viable, chondrogenically differentiated human mesenchymal stem cells from high-density pellet cultures. *BioResearch open access*, 1(6), pp.297–305. Available at: http://www.ncbi.nlm.nih.gov/pubmed/23514965 [Accessed October 6, 2016].

Ullah, M. et al., 2013. Mesenchymal stem cells and their chondrogenic differentiated and dedifferentiated progeny express chemokine receptor CCR9 and chemotactically migrate toward CCL25 or serum. *Stem Cell Research & Therapy*, 4(4), p.99. Available at: http://stemcellres.com/content/4/4/99 [Accessed October 6, 2016].

Unger, C. et al., 2008. Good manufacturing practice and clinical-grade human embryonic stem cell lines. *Human molecular genetics*, 17(R1), pp.R48-53. Available at: http://hmg.oxfordjournals.org/content/17/R1/R48.short [Accessed August 29, 2013].

Verdoy, D. et al., 2012. A novel Real Time micro PCR based Point-of-Care device for Salmonella detection in human clinical samples. *Biosensors and Bioelectronics*, 32(1), pp.259–265. Available at: http://www.sciencedirect.com/science/article/pii/S0956566311008542 [Accessed April 15, 2017].

Vernetti, L.A. et al., 2017. Evolution of Experimental Models of the Liver to Predict Human Drug Hepatotoxicity and Efficacy. *Clinics in Liver Disease*, 21(1),

pp.197–214. Available at: http://linkinghub.elsevier.com/retrieve/pii/S1089326116300733 [Accessed March 4, 2017].

Vertelov, G. et al., 2013. High targeted migration of human mesenchymal stem cells grown in hypoxia is associated with enhanced activation of RhoA. *Stem cell research & therapy*, 4(1), p.5. Available at: http://stemcellres.com/content/4/1/5 [Accessed September 16, 2014].

Viateau, V. et al., 2014. PERFUSION BIOREACTOR FOR ENGINEERING BONE CONSTRUCTS: BONE REGENERATION IN SHEEP USING CORAL SCAFFOLD AND AUTOLOGOUS MESENCHYMAL STEM CELLS. *Orthopaedic Proceedings*, 96–B(SUPP 11).

Vila-Planas, J. et al., 2011. Cell analysis using a multiple internal reflection photonic lab-on-a-chip. *Nature Protocols*, 6(10), pp.1642–1655. Available at: http://www.nature.com/doifinder/10.1038/nprot.2011.383 [Accessed February 28, 2017].

Vogenberg, F.R., Isaacson Barash, C. & Pursel, M., 2010. Personalized medicine: part 1: evolution and development into theranostics. *P & T : a peer-reviewed journal for formulary management*, 35(10), pp.560–76. Available at: http://www.ncbi.nlm.nih.gov/pubmed/21037908 [Accessed May 14, 2018].

Vojinović, V., Cabral, J.M.S. & Fonseca, L.P., 2006. Real-time bioprocess monitoring. *Sensors and Actuators B: Chemical*, 114(2), pp.1083–1091. Available at: http://www.sciencedirect.com/science/article/pii/S0925400505007434 [Accessed May 21, 2015].

Walsh, D.A., 2007. Pathophysiological Mechanisms of Angiogenesis. *Advances in Clinical Chemistry*, 44, pp.187–221.

Wang, T., Zhang, M., Dreher, D.D. & Zeng, Y., 2013. Ultrasensitive microfluidic solid-phase ELISA using an actuatable microwell-patterned PDMS chip. *Lab on a Chip*, 13(21), p.4190. Available at: http://xlink.rsc.org/?DOI=c3lc50783a [Accessed March 5, 2017].

Wang, T., Zhang, M., Dreher, D.D., Zeng, Y., et al., 2013. Ultrasensitive microfluidic solid-phase ELISA using an actuatable microwell-patterned PDMS chip. *Lab on a Chip*, 13(21), p.4190. Available at: http://xlink.rsc.org/?DOI=c3lc50783a [Accessed March 4, 2017].

Van Weemen, B.K. & Schuurs, A.H.W.M., 1971. Immunoassay using antigen-enzyme conjugates. *FEBS Letters*, 15(3), pp.232–236. Available at: http://doi.wiley.com/10.1016/0014-5793%2871%2980319-8 [Accessed March 5, 2017].

Whitesides, G.M., 2006. The origins and the future of microfluidics. *Nature*, 442(7101), pp.368–73. Available at: http://dx.doi.org/10.1038/nature05058 [Accessed October 17, 2013].

Whiting, P. et al., 2015. Progressing a human embryonic stem-cell-based regenerative medicine therapy towards the clinic. *Philosophical Transactions of the Royal Society of London B: Biological Sciences*, 370(1680).

Whitmire, M. et al., 2011. LC-MS/MS Bioanalysis Method Development, Validation, and Sample Analysis: Points to Consider When Conducting Nonclinical and Clinical Studies in Accordance with Current Regulatory Guidances. *Journal of Analytical & Bioanalytical Techniques*, 1(1). Available at: http://www.omicsonline.org/2155-9872/2155-9872-S4-001.digital/2155-9872-S4-001.html [Accessed June 16, 2016].

Wild, D., 2013. *The Immunoassay Handbook: Theory and Applications of Ligand Binding, ELISA and Related Techniques*, Available at: https://books.google.at/books?hl=en&lr=&id=xuYf6tcVdqYC&oi=fnd&pg=PA157&dq=luminex&ots=kDdkfGD2IO&sig=DOFBDR0-FFxrvt3z2nNOsdRWf8E#v=onepage&q=luminex&f=false.

Wild, E.J. & Tabrizi, S.J., 2014. Targets for future clinical trials in Huntington's disease: What's in the pipeline? *Movement Disorders*, 29(11), pp.1434–1445. Available at: http://doi.wiley.com/10.1002/mds.26007 [Accessed November 28, 2016].

Windmolders, S. et al., 2014. Mesenchymal stem cell secreted platelet derived growth factor exerts a pro-migratory effect on resident Cardiac Atrial appendage Stem Cells. *Journal of molecular and cellular cardiology*, 66, pp.177–88. Available at: http://www.sciencedirect.com/science/article/pii/S0022282813003489 [Accessed November 9, 2014].

Wirth, T., Parker, N. & Ylä-Herttuala, S., 2013. History of gene therapy. *Gene*, 525(2), pp.162–169.

World Health Organization, 2015. *World report on ageing and health*,

Xiong, B. et al., 2014. Recent developments in microfluidics for cell studies.

Advanced materials (Deerfield Beach, Fla.), 26(31), pp.5525–32. Available at: http://www.ncbi.nlm.nih.gov/pubmed/24536032 [Accessed January 13, 2015].

Xu, F. et al., 2011. Microengineering methods for cell-based microarrays and high-throughput drug-screening applications. *Biofabrication*, 3(3), p.34101. Available at: http://stacks.iop.org/1758-5090/3/i=3/a=034101?key=crossref.3c06e7354f79f949ef5f55010e89e3ef [Accessed February 28, 2017].

Xu, J.J. et al., 2008. Cellular Imaging Predictions of Clinical Drug-Induced Liver Injury. *Toxicological Sciences*, 105(1), pp.97–105. Available at: https://academic.oup.com/toxsci/article-lookup/doi/10.1093/toxsci/kfn109 [Accessed March 4, 2017].

Xu, X. et al., 2012. Effects of osmotic and cold shock on adherent human mesenchymal stem cells during cryopreservation. *Journal of Biotechnology*, 162(2), pp.224–231.

Xu, X. & Wang, X., 2010. DERIVATION OF WENZEL'S AND CASSIE'S EQUATIONS FROM A PHASE FIELD MODEL FOR TWO PHASE FLOW ON ROUGH SURFACE *. *SIAM Journal on Applied Mathematics*, 20(8), pp.2929–2941. Available at: http://lsec.cc.ac.cn/~xmxu/publication/wetting-siam-final.pdf [Accessed May 13, 2018].

Yancopoulos, G.D. et al., 2000. Vascular-specific growth factors and blood vessel formation. *Nature*, 407(6801), pp.242–8. Available at: http://dx.doi.org/10.1038/35025215 [Accessed October 27, 2014].

Yañez, R. et al., 2006. Adipose tissue-derived mesenchymal stem cells have in vivo immunosuppressive properties applicable for the control of the graft-versus-host disease. *Stem cells (Dayton, Ohio)*, 24(11), pp.2582–91. Available at: http://www.ncbi.nlm.nih.gov/pubmed/16873762 [Accessed May 27, 2014].

Yi, Y., Hahm, S. & Lee, K., 2005. Retroviral Gene Therapy: Safety Issues and Possible Solutions. *Current Gene Therapy*, 5(1), pp.25–35. Available at: http://www.eurekaselect.com/openurl/content.php?genre=article&issn=1566-5232&volume=5&issue=1&spage=25 [Accessed November 28, 2016].

Young, E.W.K. & Beebe, D.J., 2010. Fundamentals of microfluidic cell culture in controlled microenvironments. *Chemical Society Reviews*, 39(3), p.1036. Available at: http://xlink.rsc.org/?DOI=b909900j [Accessed February 28, 2017].

Yu, Y. et al., 2012. Hepatocyte-like cells differentiated from human induced

pluripotent stem cells: Relevance to cellular therapies. *Stem cell research*, 9(3), pp.196–207. Available at: http://dx.doi.org/10.1016/j.scr.2012.06.004 [Accessed November 1, 2012].

Zhan, X. et al., 2014. A novel superhydrophobic hybrid nanocomposite material prepared by surface-initiated AGET ATRP and its anti-icing properties. *J. Mater. Chem. A*, 2(24), pp.9390–9399. Available at: http://xlink.rsc.org/?DOI=C4TA00634H [Accessed May 13, 2018].

Zhang, Y.J., Luo, L. & Desai, D.D., 2016. Overview on biotherapeutic proteins: impact on bioanalysis. *Bioanalysis*, 8(1), pp.1–9. Available at: http://www.future-science.com/doi/abs/10.4155/bio.15.224 [Accessed May 10, 2016].

Zhao, D. et al., 2012. Treatment of early stage osteonecrosis of the femoral head with autologous implantation of bone marrow-derived and cultured mesenchymal stem cells. *Bone*, 50(1), pp.325–330. Available at: http://www.sciencedirect.com/science/article/pii/S8756328211013391 [Accessed May 27, 2017].

Appendices

Appendices 1

EXPT A 2% O2 Nodes
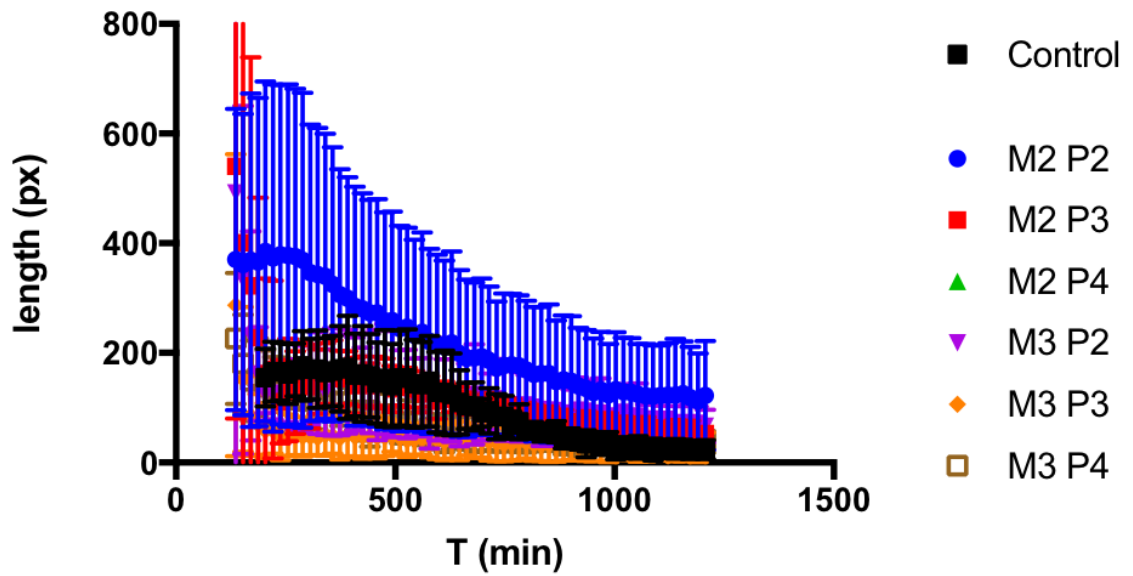
EXPT A 2% O2 Tube Length

Appendices 2
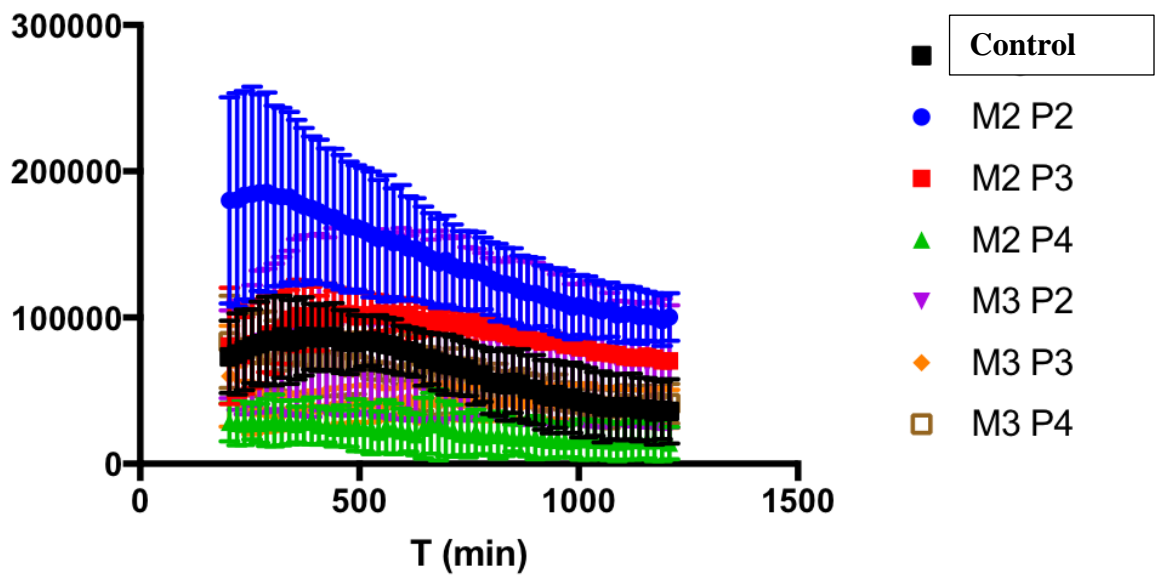
CFT Capillary Film Technology	Singleplex Sandwich ELISA Standard Curve	Issue No. 1	Prepared by: A. Castanheira
No. of pages 6	Microcapillary film operational procedure – Multi-Syringe Device	Issue Date: 27Feb2014	Reviewed by: N.M. Reis

1 PURPOSE

1.1 To assemble MCF for assay completion

1.2 To perform singleplex sandwich ELISA in MCF

2 SCOPE

2.1 This procedure is designed to perform singleplex sandwich ELISAs in MCF strips

3 DEFINITIONS AND ABBREVIATIONS

3.1 MCF: Microcapillary film

3.2 MSD: Multi-syringe device

3.3 BSA: Bovine serum albumin

3.4 PBS: Phosphate buffered saline solution

3.5 HRP: Horseradish peroxidase

3.6 OPD: o-Phenylenediamine dihydrochloride

4 REAGENTS, CHEMICALS AND SOLUTIONS

4.1 1xPBS

4.2 Wash buffer (1xPBS, 0.05% Tween 20)

4.3 Block buffer (Superblock blocking buffer)

4.4 OPD

5 INSTRUMENTS AND EQUIPMENT

5.1 MCF

5.2 Micro-centrifuge tubes

5.3 Centrifuge tubes

5.4 Micropipettes

5.5 Micropipette tips

5.6 Silicon rubber tubing 3.0 mm

5.7 1 mL Terumo syringes

5.8 Flatbed scanner

5.9 Straight-edge blade

5.10 96-well flat bottom microtitre plate

5.11 MSD, composed of plastic frame, SLA cartridge, 8 disposable syringes, 8 plungers, 1 push-fit seal rubber

6 PROCEDURE

6.1 MCF coating – *Figure 1*

6.1.1   Prepare the purified antibody coating solution with the required concentration to a volume of 250 µl in a micro-centrifuge tube

6.1.2   Cut a strip of MCF approximately 30 cm in length

6.1.3   Attach 2 cm of rubber tubing to one end of MCF strip

6.1.4   Attach syringe to rubber tubing (Step 1)

6.1.5   Place the opposite end of MCF into coating solution applying pressure at the interface of MCF and rubber tubing (finger tips or clamp works best – Step 2)

6.1.6   Gently release the syringe plunger allowing fluid to be taken up through the entire width (capillaries 1-10) and length of MCF strip

6.1.7   Place MCF coil in a moist environment (Step 3) at room temperature for a minimum of 2h.
Do not dis-assemble MCF coil attached to rubber tubing
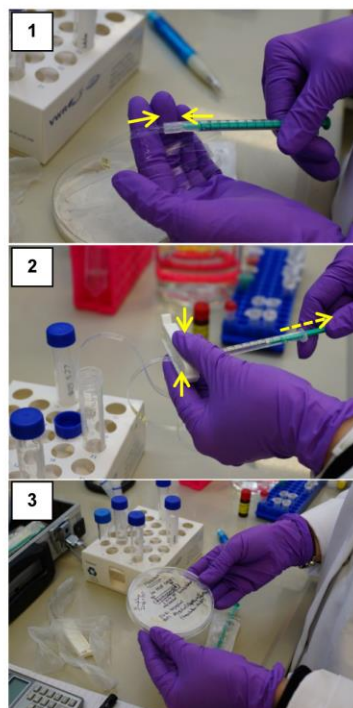
Figure 1 Manual handling aspiration. **1.** Attach 2 cm of rubber tubing to one end of MCF and to the syringe; **2.** Gently release the syringe plunger; **3.** Store the MCF coil in a moist environment at room temperature.

6.2 MCF blocking – *Figure 1*

6.2.1   Prepare blocking solution (Superblock Blocking buffer) to a volume of 1 ml in a centrifuge tube

6.2.2   Place MCF coil, assembled with rubber tubing and syringe, into blocking solution and release the syringe plunger, allowing the uptake of fluid (Step 2)

6.2.3   Remove the syringe

6.2.4   Place MCF coil in a humidified environment at room temperature for 1-2 hours (Step 3).

6.3 MCF washing – *Figure 1*

6.3.1   Prepare washing solution to a volume of 1 ml in a centrifuge tube

6.3.2   Place MCF coil, assembled with rubber tubing and syringe, into washing solution and release the syringe plunger, allowing the uptake of fluid (Step 2)

6.3.3   Remove the syringe

6.3.4   Place MCF coil in a humidified environment and store it in the fridge until using (Step 3).

6.4 MCF assembly in the MSD – *Figure 2*

6.4.1   Cut 8 strips with 30 mm in length from the pre-coated, blocked and washed MCF coil prepared in 6.1, 6.2 and 6.3 (Step 1 and 2)

6.4.2   Put films into the rubber, making sure it is about 1 mm above edge of the push-fit seal rubber seal and assemble it into the Multi Syringe Device (Steps 3 and 4).

6.4.3   Use Wash buffer or PBS to fill up the syringes (Step 6) and rotate the knob until all the syringes are full and with no bubbles (Step 6).

6.4.4   Assemble the push-fit seal rubber into the MSD (Step 7).

6.4.5   Turn the knob to empty the syringes and make sure that all the capillaries are full with solution before start the assay.
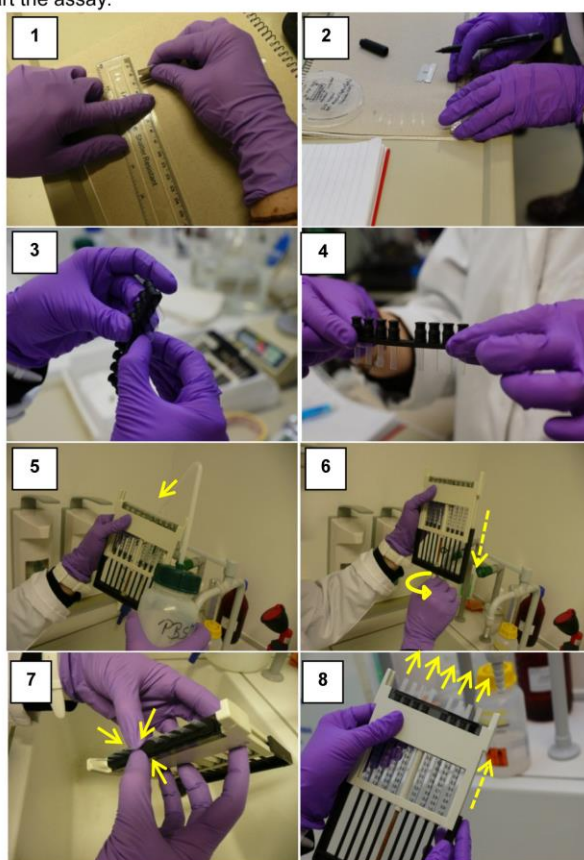
Figure 2 MCF assembly in the MSD. **1.** Cut 8 strips with 30mm in length; **2.** Make sure all the strip are in the same orientation; **3.** Put the strips into the seal rubber; **4.** All strips fitted and with 1mm above the edge; **5.** Fill the syringes with wash buffer or PBS; **6.** Rotate the knob until all the syringes are full with solution; **7.** Assemble the seal rubber into the MSD; **8.** Turn the knob to empty the syringes and fill up all the capillaries with solution before starting the assay.

6.5 Addition of recombinant protein – *Figure 3*

6.5.1 Prepare serial dilutions of recombinant protein to a total volume of 150 µl for MCF strip

6.5.2 Transfer 150 µl of each concentration of recombinant protein to individual wells of the plate corresponding to each MCF strip (Step 1)

6.5.3 Assemble the MSD on the plate, making sure it is in the right orientation (Step 2)

6.5.4 Rotate the knob 6x (6 complete turns) to aspirate de solutions into de capillaries (Step 3)– this will aspirate 78 µl of solution from each well

6.5.5 Incubate for 30 min (long version) or 5 min (short version) at room temperature (Step 3)

6.5.6 Fill 150 µl of wash buffer to each MCF corresponding well in the plate

6.5.7 Perform steps 6.5.3 and 6.5.4.

6.6 Detection Antibody – *Figure 3*

6.6.1 Prepare a stock solution of biotinylated detection antibody to the required concentration

6.6.2 Transfer 150 µl from stock solution to each MCF corresponding well of the plate (Step1)

6.6.3 Perform steps 6.5.3 and 6.5.4 (Step 2–4)

6.6.4 Incubate for 10 min (long version) or 5 min (short version) at room temperature

6.6.5 Fill 150 µl of wash buffer to each MCF corresponding well in the plate

6.6.6 Perform steps 6.5.3 and 6.5.4.

6.7 Addition of enzyme – *Figure 3*

6.7.1 Prepare a stock solution of High Sensitivity Streptavidin-HRP to a concentration of 1 µg/ml

6.7.2 Transfer 150 µl from stock solution to each MCF corresponding well of the plate (Step1)

6.7.3 Perform steps 6.5.3 and 6.5.4 (Step 2–4)

6.7.4 Incubate for 10 min (long version) or 5min (short version) at room temperature

6.7.5 Fill 150 µl of wash buffer to each MCF corresponding well in the plate
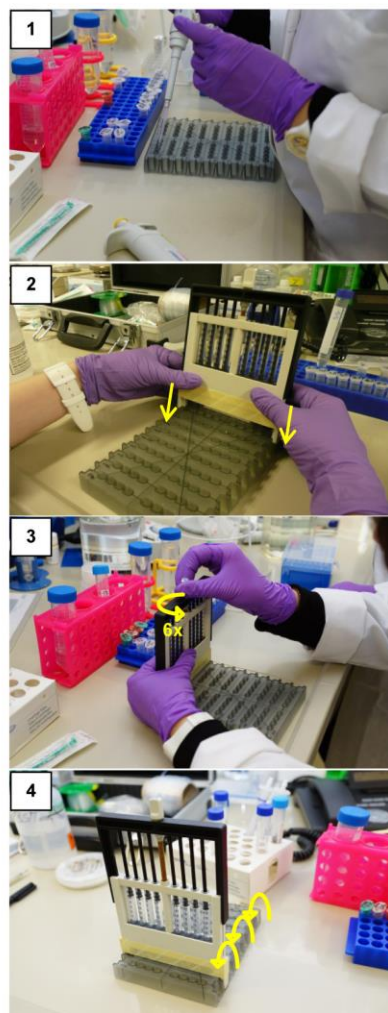
Figure 3 Addition of the reagents and incubation. **1.** Transfer 150 µl 150 µl from stock solution to each MCF corresponding well of the plate; **2.** Assemble the MSD on the plate; **3.** Rotate the knob 6x to aspirate the solutions into the capillaries; **4.** Incubate at room temperature. Repeat the procedure for each reagent.

6.7.6   Perform steps 6.5.3 and 6.5.4

6.7.7   Repeat 6.7.5 and 6.7.6 two times.

6.8 Preparation of OPD substrate at a concentration of 4 mg/ml

6.8.1   <u>Substrate should be made up no more than 1 hour prior to use and protected from the light</u>

6.8.2   Transfer 1x OPD tablet to 1 ml distilled water in a 1 ml centrifuge tube

6.8.3   Cover with foil to protect from the light

6.8.4   Transfer 1x H_2O_2 tablet to 4 ml distilled water in a 15 ml centrifuge tube

6.8.5   Vortex until both tablets have fully dissolved

6.8.6   Transfer 1 ml of H_2O_2 solution to the OPD centrifuge tube and mix

6.8.7   Store at 4 ^{o}C until ready to use.

6.9 Addition of OPD substrate – *Figure 3*

6.9.1   Transfer 150 µl from stock OPD solution to each MCF corresponding well of the plate (Step 1)

6.9.2   Perform steps 6.5.3 and 6.5.4 (Step 2–4).

7   DATA ANALYSIS

7.1 MCF strips scanning – HP Scanjet 4050 scanner – *Figure 4*

7.1.1   Place the device on the flatbed scanner, making sure it is well aligned (Step 2)

7.1.2   Scan RGB images in TIF format (Step 3)

7.1.3   Set resolution to 2,400 dpi (Step 3)

7.1.4   Select ONLY the area of the strips after the preview image (Step 3)

7.1.5   Click cutting tool and tick option "manual" and change the colour settings to: highlights -70; gamma 1.2 (lighter/darker) (Step 3)

7.1.6   Go to 'Adjust colours' and enter 'optimize values' (Step 3)

7.1.7   Enter 'finish' and save the picture.

7.2 Data analyse using ImageJ software – *Figure 4*

7.2.1   Split each RGB image into Red, Green and Blue channels and analyse ONLY blue channel (Step 4 (a))

7.2.2   Confirm the strips are well aligned and use selection tool to select a 6*6 mm^2 area in the middle of the strip (Step 4 (b))

7.2.3   Select "profile plot" (or CTR+K) and measure the peak height in terms of grey scale intensity for each capillary and save the values into excel spreadsheet (Step 4 (c))

7.2.4   Calculate the Absorbance for each capillary using the equation: $Abs = -\log (I/I_0)$, by setting I_0 as the grey scale pixel intensity of the baseline and I as I_0 minus the peak height (in grey scale units) (Step 4 (d)).
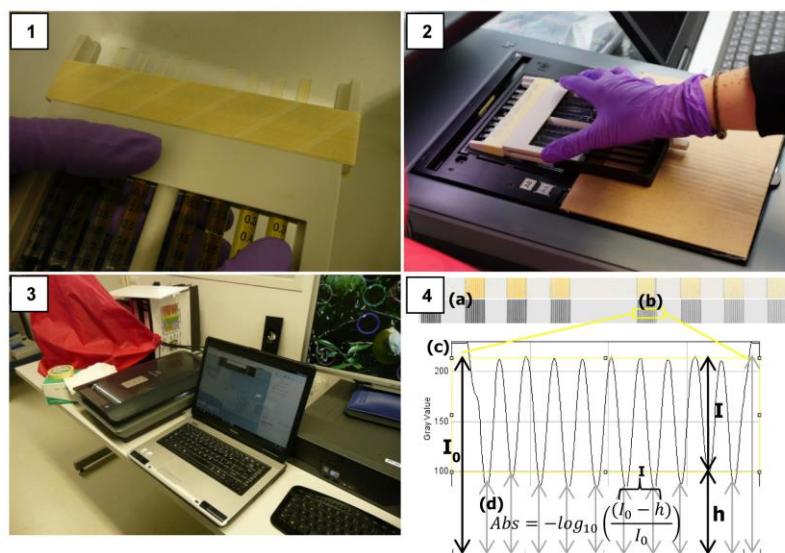
Figure 4 Data Analysis. **1.** Colour gradient visible in the strips after OPD addition; **2.** Place the MSD in the flatbed scanner; **3.** Set the right settings using the HP scanner software and save the pictures in .tiff format; **4.** ImageJ analysis **(a)** RGB colour and blue channel pictures; **(b)** Square section to analyse the peak high of each capillary; **(c)** Grey scale plot to measure the high of the peaks; **(d)** Formula to calculate the Abs using the peak high.

The formula shown in (d):

$$Abs = -log_{10}\left(\frac{(I_0 - h)}{I_0}\right)$$